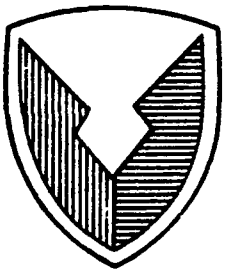

US ARMY
MATERIEL COMMAND

METEOROLOGICAL INFLUENCES ON SMOKE/OBSCURANT EFFECTIVENESS PHASE II

Volume I

by

Steven R. Hanna, David G. Strimaitis
Joseph C. Chang and Sharon M. McCarthy

Sigma Research Corporation
234 Littleton Road, Suite 2E
Westford, Massachusetts 01886

Contract DAAD09-89-C-0039

November 1991

Prepared for

METEOROLOGY DIVISION
MATERIEL TEST DIRECTORATE
U.S. ARMY DUGWAY PROVING GROUND
DUGWAY, UTAH 84022-5000

Disposition Instructions

Destroy this report when no longer needed. Do not return to the originator.

Disclaimer Statement

The views, opinions, and/or findings in this report are those of the authors and should not be construed as an official Department of the Army position, unless so designed by other official documentation.

Trade Names Statement

The use of trade names in this report does not constitute an official endorsement or approval of the use of such commercial hardware or software. This report may not be cited for purpose of advertisement.

REPORT DOCUMENTATION PAGE

Form Approved
OMB No. 0704-0188

1a. REPORT SECURITY CLASSIFICATION: UNCLASSIFIED	1b. RESTRICTIVE MARKINGS
2a. SECURITY CLASSIFICATION AUTHORITY: N/A	3. DISTRIBUTION/AVAILABILITY OF REPORT: Approved for public release; distribution unlimited
2b. DECLASSIFICATION/DOWNGRADING SCHEDULE	
4. PERFORMING ORGANIZATION REPORT NUMBER(S)	5. MONITORING ORGANIZATION REPORT NUMBER(S): DPG-CR-92-902
6a. NAME OF PERFORMING ORGANIZATION: Sigma Research Corporation; 6b. OFFICE SYMBOL (If applicable)	7a. NAME OF MONITORING ORGANIZATION: Meteorology Division, Materiel Test Directorate
6c. ADDRESS (City, State, and ZIP Code): 234 Littleton Rd., Suite 2E, Westford, MA 01886	7b. ADDRESS (City, State, and ZIP Code): U.S. Army Dugway Proving Ground, Dugway, UT 84022-5000
8a. NAME OF FUNDING/SPONSORING ORGANIZATION; 8b. OFFICE SYMBOL (If applicable): STEDP-MT-M	9. PROCUREMENT INSTRUMENT IDENTIFICATION NUMBER: DAAD09-89-C-0039
8c. ADDRESS (City, State, and ZIP Code): Dugway, UT 84022-5000	10. SOURCE OF FUNDING NUMBERS: PROGRAM ELEMENT NO. W67HY8; PROJECT NO. 9024; TASK NO. 4006; WORK UNIT ACCESSION NO.

11. TITLE (Include Security Classification)
Meteorological Influences on Smoke/Obscurant Effectiveness Phase II, Volumes I and II

12. PERSONAL AUTHOR(S)
Hanna, Steven R.; Strimaitis, David G.; Chang, Joseph C.; and McCarthy, Sharon M.

13a. TYPE OF REPORT	13b. TIME COVERED	14. DATE OF REPORT (Year, Month, Day)	15. PAGE COUNT
Final Report	FROM Aug 89 TO Nov 91	1991 November	

16. SUPPLEMENTARY NOTATION

17. COSATI CODES			18. SUBJECT TERMS (Continue on reverse if necessary and identify by block number)
FIELD	GROUP	SUB-GROUP	Air Pollution; Smoke/Obscurants; Dispersion Models; Uncertainties; Meteorology
04	02		

19. ABSTRACT (Continue on reverse if necessary and identify by block number)

Uncertainties in modeling meteorological influences on smoke/obscurant concentrations are evaluated. Three components of modeling uncertainty are identified--input data uncertainties, random or stochastic uncertainties, and uncertainties due to model formulation. A method is proposed for analyzing smoke/obscurant field tests in order to determine whether there is a significant difference in source emissions between groups of tests. The method is tested using measurements from several field experiments, including U.S. Army smoke/obscurant tests. This scheme may also be applicable to other scientific endeavors where confidence limits on measured and predicted data must be assessed.

20. DISTRIBUTION/AVAILABILITY OF ABSTRACT	21. ABSTRACT SECURITY CLASSIFICATION
☐ UNCLASSIFIED/UNLIMITED ☒ SAME AS RPT ☐ DTIC USERS	UNCLASSIFIED
22a. NAME OF RESPONSIBLE INDIVIDUAL: James F. Bowers	22b. TELEPHONE (Include Area Code): (801)831-5101; 22c. OFFICE SYMBOL: STEDP-MT-M

DD Form 1473, JUN 86 *Previous editions are obsolete.*

SUMMARY

A computer code was developed that permits the meteorological influences on smoke/obscurant effectiveness to be quantitatively assessed. A typical problem to be addressed would be whether there is a significant difference in the effectiveness of two types of smoke/obscurant munitions. If there are a sufficient number of field data available, the problem would be analyzed using standard statistical procedures. If there are few or no field data, then the uncertainties are estimated based on previous knowledge on the magnitudes of stochastic fluctuations and data input uncertainties.

The code is tested using field data from many dispersion experiments, including four standard tracer gas experiments (Prairie Grass, Ocean Breeze, Dry Gulch, and Green Glow) and ten special-purpose smoke/obscurant experiments. It is found that for experiments with simple source emission scenarios and about 20 to 30 independent trials, differences in source emission rates of about 20% or more can be discerned using observed concentrations and meteorological variables, and back-calculations of emission rates using scaling relations or dispersion formulas.

When the code is applied to the data from smoke/obscurant experiments, where there are two to seven independent trials, it is usually not possible to discern significant differences between source emission rates of munitions which have similar designs. Factor of two differences in emission rates are necessary before they can be detected by the statistical procedures.

Very little information on source emissions observations has been found in the literature on smoke/obscurant munitions, despite the fact that several empirical factors must be used to estimate effective smoke emissions based on munition mass. It is recommended that further field experiments be conducted to better assess the uncertainties in these empirical factors.

The statistical procedures coded in the software can be applied to any type of problem in which the uncertainties in observed and predicted data must be assessed.

TABLE OF CONTENTS

TABLE OF CONTENTS (Continued)

PREFACE

The work in this report was authorized under Contract No. DAAD09-89-C-0039. Work was started in August, 1989 and was completed in August, 1991.

The use of trade names in this report does not constitute an official endorsement or approval of the use of such commercial hardware or software. This report may not be cited for purposes of advertisement.

SECTION I

INTRODUCTION AND OBJECTIVES

The U.S. Army conducts numerous field tests of smoke/obscurant materials to determine the relative effectiveness of different materials or to determine the possible degradation over time of a single material. Detailed observations of the smoke/obscurants are made using a variety of instruments, including line-averaging photo-optical devices and human observers. Supporting meteorological data are also taken, such as wind speed and turbulence. The problem is that it is not well-known whether the difference in performance of the smoke/obscurant from one test to another is due to variations in the munitions or to variations in the meteorological conditions. Much of the difference can be explained through proper use of scaling variables, which account for the variation in the mean concentrations as a function of averaged meteorological variables such as wind speed, stability, and turbulence intensity. However, uncertainties will always be present even after scaling by meteorological variables. These uncertainties can be caused by three components:

1. Physical errors in the scaling assumptions.
2. Errors in input data.
3. Stochastic uncertainty (i.e., random turbulence)

The purpose of the Phase II research reported here has been to develop a quantitative method for accounting for the influences of meteorological variables on smoke/obscurant effectiveness. The research has been aimed towards the ultimate goal of developing a reliable, objective and quantitative means to assess the relative effectiveness of smoke/obscurant materials. There are many new concepts that have been advanced in this area in the past few years, and this is an excellent opportunity to apply these concepts to a problem where a useful, quantitative scheme may be developed.

In any objective method of quantifying the meteorological influences on apparent smoke/obscurant effectiveness, the problem reduces to answering the following statistical question:

Is the difference in source emission rates, Q(1)-Q(2), or concentrations, C(1)-C(2), significantly different from zero, after allowances for meteorological influences are made?

where Q is a measure of source strength estimated by observations, C, of the smoke effectiveness (e.g., line-integrated concentration) and the numbers 1 and 2 refer to different experiments or materials.

The following sections in this report provide detailed descriptions of the results of the Phase II work. The quantitative method is described in detail and examples of applications to a variety of field experiments are given, including several U. S. Army smoke/obscurant tests. Formulas are also suggested for the contribution to the total variance or uncertainty due to data input errors and stochastic or random variability.

SECTION II
OVERVIEW OF PROCEDURES

A. Basic Statistical Question

The problem addressed by this research project always involves two or more sets of field observations of point concentrations, C, or line-averaged concentrations, C_y. The question is then asked whether there is a difference between the observations from the two sets of field experiments. If the observations from the first and second sets are indicated by subscripts 1 and 2, respectively, then the following data are available for analysis:

Set 1: $C_{11}, C_{12}, C_{13}, \cdots C_{1n}$
Set 2: $C_{21}, C_{22}, C_{23}, \cdots C_{2m}$

where the second subscript indicates an individual field experiment, and there are n experiments in Set 1 and m experiments in Set 2. It is assumed that all of these data are independent; i.e., no one piece of data is correlated with any other piece.

Before carrying out any analysis, it is necessary to make a hypothesis, which will then be tested using statistical methods. The "null hypothesis" is usually made that the averages $\overline{C_1}$ and $\overline{C_2}$ are equal. In our procedure, we test this hypothesis by estimating the probability that, when $\overline{C_1}$ and $\overline{C_2}$ are drawn from the same population, then the observed value of $\overline{C_1} - \overline{C_2}$ is found.

The main difficulty in this procedure is the determination of the shape of the "population," or the probability density function (pdf) of C. This pdf would be easy to define if the number of experiments, n and m, were in the range of 100 or more. However, because of the high costs of field programs, n and m are more likely to be on the order of 10 or less. For n and m less than about 5, the pdf of C cannot be reliably calculated from the observations and it must be estimated by means of parameterization of $\overline{C}$ and σ_c.

Assuming for the moment that the pdf of the underlying population of C is known, and that it has mean, $\overline{C}_p$, and standard deviation, σ_{pc}, then the central limit theorem states that a sample mean, $\overline{C}_1$, taken over n points, has a normal

or Gaussian distribution, with mean $\overline{C}_p$ and standard deviation $\sigma_{pc}/\sqrt{n}$. Similarly, if C_1 and C_2 are from the same population, then the distribution of the difference $\overline{C_1} - \overline{C_2}$ will be normal with standard deviation $\sigma_{C_1-C_2}$ equal to $\sigma_{pc}\,(n^{-1} + m^{-1})^{1/2}$ assuming that the two samples are independent of each other (Panofsky and Brier, 1958). In practical applications the standard deviation $\sigma_{C_1-C_2}$ is calculated from the formula:

$$\sigma^2_{C_1-C_2} = \frac{n\sigma_1^2 + m\sigma_2^2}{n + m - 2}\,(n^{-1} + m^{-1}) \qquad (2\text{-}1)$$

Then the ratio

$$t = \frac{\overline{C_1}-\overline{C_2}}{\sigma_{C_1-C_2}} \qquad (2\text{-}2)$$

follows the "student-t" distribution with $n + m - 2$ degrees of freedom. For $n + m - 2$ greater than about 10, the student-t is very close to a normal distribution. For example, when $n + m - 2 > 10$, then the difference $\overline{C_1} - \overline{C_2}$ is significant at the 95% confidence level if t exceeds about 2.0. Thus the null hypothesis could be rejected with 95% confidence in this example.

B. Estimate of PDF

As shown in Section A, an estimate of the pdf of C_1 and C_2 must be available, either from observations or from a theoretical formula. For $n \gtrsim 5$ or 10, the pdf (or at least the mean and variance) can be estimated from the data. However, for $n < 5$ or 10 an analytical formula for the pdf must be specified. Most commonly, a normal or Gaussian pdf is chosen, which is completely specified by a mean, $\overline{C}$, and a standard deviation, σ_c. Other pdf formulas can be selected, such as a log-normal or an exponential formula, but these are more difficult to analyze. The selected mean could be the average over the available C observations, and the selected standard deviation can be based on estimated of variations due to data input errors and stochastic variations. Based on observations over a great number of datasets, the following rough approximation can be made:

$$\sigma_c/\overline{C} \approx 0.5, \qquad (2\text{-}3)$$

which allows a pdf to be defined.

C. Normalization of Observed C

The title of this report indicates that it is expected that variations in meteorological variables can influence the observed concentrations. Consequently, even if $\overline{C_1}$ and $\overline{C_2}$ are significantly different, that difference may be solely due to a difference in say, wind speed. If it is known that $C \propto u^{-1}$, then, for everything else constant, the product Cu should also be constant. In this case C is "normalized" by 1/u.

To <u>remove</u> the effects of meteorological variations, the observed data should first be normalized, using known relations. According to the Gaussian dispersion model, for near-ground continuous point releases:

$$C \propto Q/(u\sigma_y\sigma_z) \tag{2-4}$$

$$C_y \propto Q/(u\sigma_z) \tag{2-5}$$

where Q is source emission rate and σ_y and σ_z are lateral and vertical dispersion coefficients. It is known that $\sigma_y \propto \sigma_\theta x$ and $\sigma_z \propto \sigma_\phi x$, where x is downwind distance, and σ_θ and σ_ϕ are the standard deviations (in radians) of lateral and vertical wind direction fluctuations. Therefore Equations (4) and (5) can be written:

$$C \propto Q/(u\sigma_\theta\sigma_\phi x^2) \tag{2-4a}$$

$$C_y \propto Q/(u\sigma_\phi x) \tag{2-5a}$$

These simple results indicate that, if measurements are taken at different x, then C should be normalized by $1/x^2$ and C_y should be normalized by 1/x. Similarly, both C and C_y should be normalized by 1/u. Hypothetical pdf's for the un-normalized and the normalized C's are shown in Figure 2-1. Note that the normalized pdf's are much narrower (i.e., the variance has been reduced), thus allowing the null hypothesis to be better tested. However, the pdf's for tests 1 and 2 could shift together or apart after the data are normalized - we have no way of knowing which direction they will move.

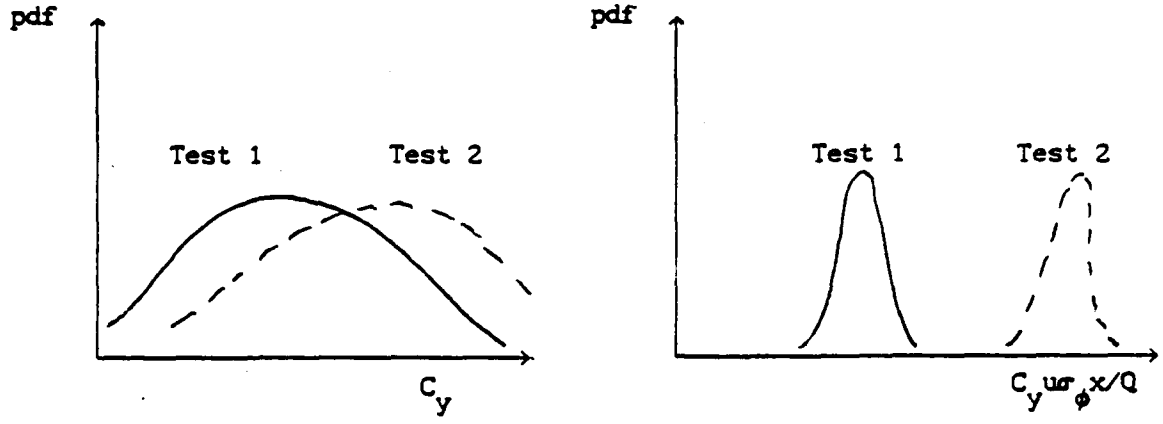

Figure 2-1. Schematic examples of pdf's for un-normalized (left) and normalized (right) concentration observations for Test 1 and Test 2.

SECTION III

BACKGROUND OF PREVIOUS RELATED WORK

A. Concentration Normalization Studies by DPG

A preliminary assessment of the use of normalization procedures to compare the results of smoke tests at DPG was published by Rafferty and Dumbauld (1983). They divide (or normalize) the observed CLID (cross-wind line-integrated dosages) values by predicted CLID values using a dispersion model closely related to the VSDM model. The normalized variable is called Q', which has a mean of unity and a variance of 0.0 if the normalization procedure accounts for all of the variance in CLID observations.

Four lots of single grenades were tested, and Q' means of 0.99, 1.34, 1.36, and 1.24 were calculated for the four lots. It was determined that these means were not significantly different at the 95% confidence level (i.e., the null hypothesis could not be rejected, since the 95% confidence range on Q' was estimated to be between 0.93 and 1.41).

Eight trials with multiple grenades were also analyzed, with the result that the geometric mean $\overline{Q'}$ of 1.85 was significantly different from the mean $\overline{Q'}$ of the single grenade tests, at the 95% confidence level. However, it is expected that the normalization procedure would not work so well for multiple grenades because of the difficulties in specifying the source emission term.

Saterlie and Dumbauld (1982) earlier carried out a similar analysis for L8A1 and reworked L8A1 grenades, yielding values of $\overline{Q'}$ of 0.88 and 1.14, respectively. These means are not significantly different at the 95% confidence level.

B. Studies of Components of Uncertainty

Much work has been done on the subject of uncertainty of observations in field studies by researchers in other areas, including economics, ecology, and health sciences. These persons must also deal with widely scattered data,

incomplete input data, non-normal distributions, and wide confidence bounds. The following discussion summarizes the general approach to uncertainty that has been adopted for this research (Hanna, 1986).

If major decisions are to be made based on observations, it is important to have the best possible information on our confidence in the physical assumptions that are made and the data that are being collected. It may even be possible to build the confidence intervals (uncertainty) into the decision-making process. There are three components of total error or uncertainty:

Errors caused by imprecise formulation of physical relationships
Random variability (turbulence)
Errors generated by input data errors

These components have not yet been studied in any comprehensive way. Our general understanding of the relationship between the components of uncertainties is shown in Figure 3-1, where the three components of uncertainty are plotted as a function of the number of parameters in the model system. The positions of these curves will shift depending on the problem and the particular application. Note that the total uncertainty can be large for systems with a large number of parameters, due to the combined effect of data input errors. It is desirable to design your analysis such that the total uncertainty on the figure is at its lowest point. It is seen that a complex system is not always the best in a given application. In many instances a simple relationship provides the lowest uncertainty. The truth of this statement will be shown by the applications shown in Section X.

C. Overview of Meteorological Requirements of DOD Dispersion Models

Ohmstede (1984) recently prepared a unique review of DOD applied dispersion models, tracing the "family tree" of most DOD models. He showed that most could be traced back to five fundamental models:

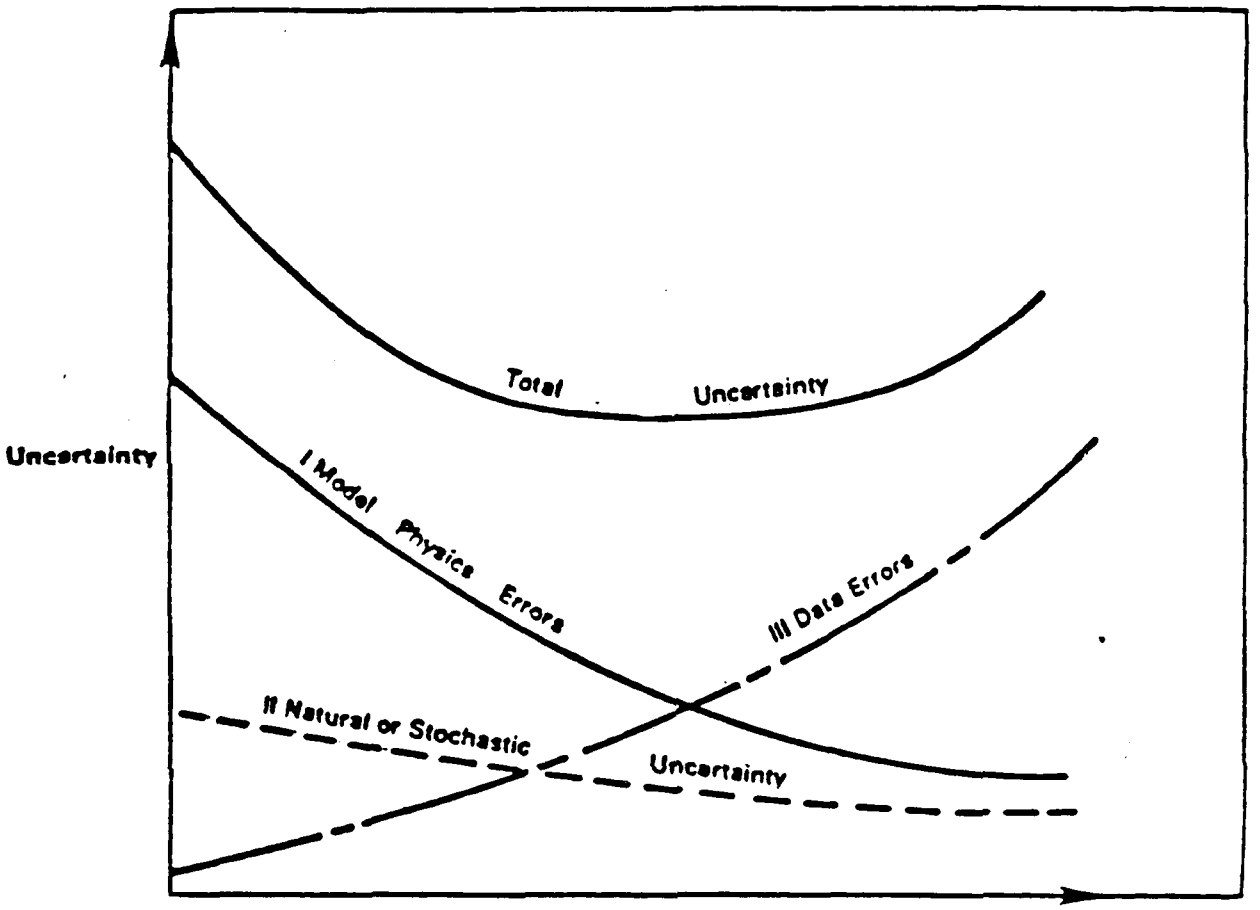

Figure 3-1. Illustration of the variation of uncertainty components with the number of parameters in an analysis system.

1) ORG-17 (Milly 1958). This is the bible for munitions expenditures calculations. It contains a variety of solutions (cross-wind integrals, dosages, etc.) to the Gaussian equation, and generally directly accounts for mean wind speed and indirectly accounts for turbulence intensity.

2) OB/DG (Haugen and Fuquay 1963). This is an empirical equation best fit to dispersion experiments at Vandenberg and Cape Kennedy. It includes the wind speed, the standard deviation of wind direction fluctuations, and the vertical temperature gradient.

3) Cramer (1957). The Cramer model uses turbulence measurements to directly calculate the dispersion parameters σ_x, σ_y, and σ_z. It also uses the wind speed to account for dilution.

4) Pasquill Stability Class (PSC) (Smith 1972, Hansen 1979). This procedure uses definitions of Pasquill stability class altered to account for surface roughness. By this method the turbulence intensity is parameterized. The wind speed is also included in this class of models.

5) EVAP (Pennsyle 1979). This model developed at CRDC has a weak link to ORG-17 but has special algorithms for the evaporation of aerosols. It requires as input the wind speed and a parameterization of the turbulence intensity.

The Cramer family of dispersion models is in widest use at DPG (H. E. Cramer Co. 1983). The Volume Source Diffusion Model (VSDM) is possibly the most representative of the Cramer concept (Bjorklund and Dumbauld 1981) and has been used extensively in this project. This model can calculate dosage, concentration, and deposition from a variety of sources. The model is based on the Gaussian equation, but the equations appear quite complicated due to inclusion of many diverse factors such as reflection, gravitational settling, wind shear, and so on. The models were developed for use at DPG, where turbulence observations are routinely made. Since turbulence data are generally not available at other locations where emissions may occur, it is

necessary to include algorithms to parameterize these data in the event that they are not measured.

This brief review suggests that the following meteorological observations are required by DOD dispersion models:

Wind speed u - required by all models and directly measured

Turbulence parameters σ_v and σ_w - required by all models, either directly measured or parameterized through measurements of stability and roughness.

Vertical stability - required in some form by all models; determined from cloudiness, time of day, and wind speed; or from vertical temperature gradient and wind speed.

In order to relate concentrations to meteorological variables, some knowledge of the source emission term Q is required. DPG has models for Q for a variety of munitions based on field and laboratory tests. In some cases when the effectiveness of two munitions is compared, the fundamental question is whether Q has changed. To answer this question, we invert the dispersion equation and use it to predict emission rate through the formula $Q = C_o/(C_p/Q)$, where C_p/Q is the prediction for unit emission rate.

D. Meteorological Requirements for New Dispersion Scaling Approaches

In order to calculate transport and diffusion in the planetary boundary layer (pbl), it is first necessary to understand the structure of the pbl, including vertical profiles of wind velocity, turbulence, and temperature, and the height, h, of the top of the pbl. There has been a "revolution" in pbl modeling during the past decade (Wyngaard 1985). Before this happened, for example, Kaimal et al. (1976) could not find proper scaling parameters for vertical velocity spectra in the convective pbl. But once convective scaling concepts were discovered, it became apparent that these spectra scaled with w_* and h, where the convective scaling velocity, w_*, is defined by

$$w_* = (H_o h)^{1/3} \qquad (3\text{-}1)$$

where H_o is the surface heat flux. Similarly, understanding of the stable pbl has greatly increased, thanks to research by Nieuwstadt (1981) and others, who now recognize that "z-less" scaling applies over much of the stable pbl; i.e., the distance to the ground no longer influences the turbulence. Using this new understanding of the convective and stable pbl, we can parameterize the neutral pbl with asymptotic solutions to the formulas for the convective and stable pbl. Of course, it is necessary to make sure that the stable and convective formulas match as neutral conditions are approached.

A good summary of these new meteorological scaling concepts is given in Figure 3-2, from Holtslag and Nieuwstadt (1986). In both portions of the figure the applicable scaling parameters are given as functions of z/h and h/L. It is important to note that for z/h > 1 or for large h/L, the atmosphere can be intermittent and no good formulas for turbulence, winds, or temperatures are known.

In an operational dispersion model, it is often necessary to generate meteorological profiles using a minimum of information. The concepts outlined above have been included in meteorological preprocessors for the Offshore and Coastal Dispersion (OCD) model (Hanna et al. 1985) and the Hybrid Plume Dispersion Model (HPDM, Hanna et al. 1986 and 1987). In both models the primary goal is to properly parameterize the surface heat and momentum fluxes, H_o and u_*^2, using simple measurements such as the wind speed at a height of 10m, the solar elevation and cloudiness, and a measure of ground moisture. It is found that diffusion models that use turbulence parameterizations based on these models give predictions that agree with observations almost as well as models that use observed turbulence.

A major potential problem with pbl formulas is that they are often not robust; i.e., they sometimes give predictions that are unreasonable for input conditions that are outside of the range of conditions used for initial development and testing. In the above applications it was necessary to define limits or bounds to the formulas to ensure that they would be robust.

E. DPG Dispersions Tests Available for Analysis

Many field tests of the effectiveness of various methods of producing

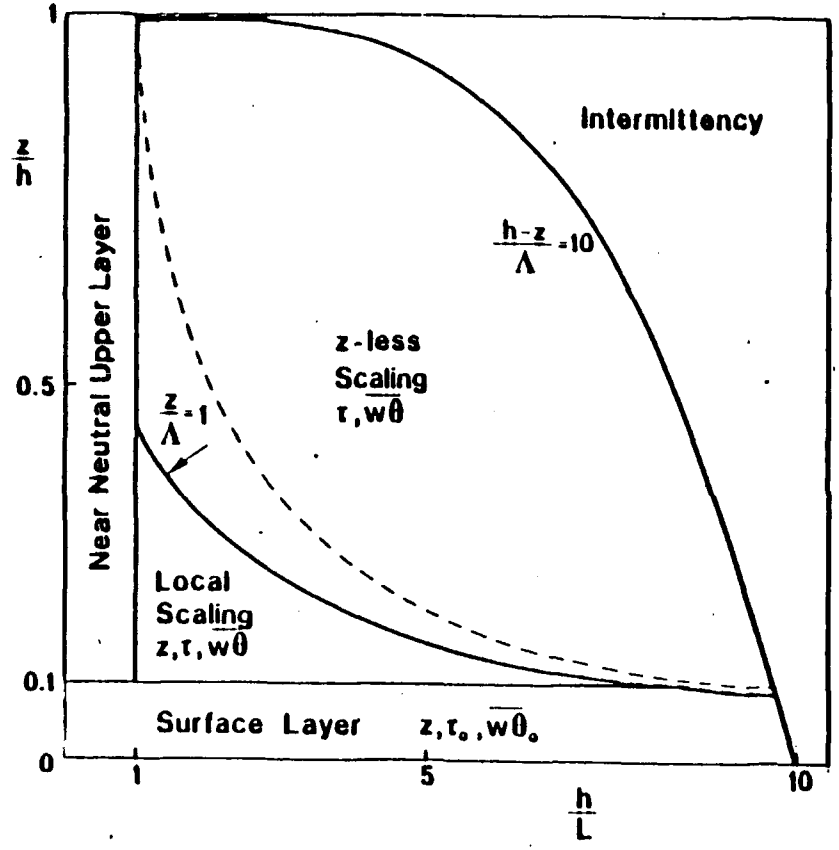

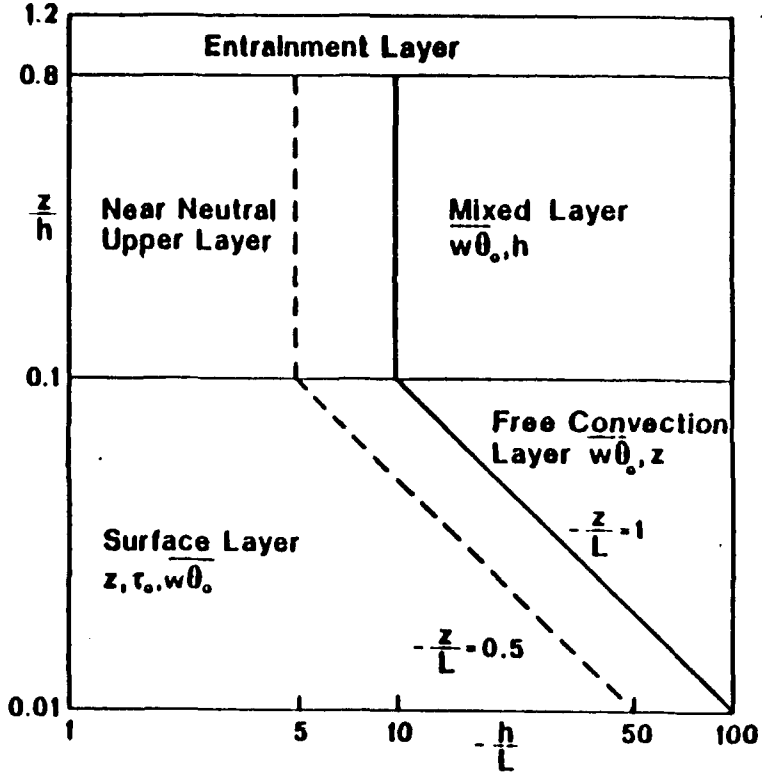

Figure 3-2. Scaling laws in the stable (left hand figure) and unstable (right hand figure) PBL (from Holtslag and Nieuwstadt 1986).

obscurants have been carried out at DPG. These tests generally include the following elements:

target area for the source(s)
transmissometer array
32-m meteorological tower(s)

The target area for the source may either be the location of a fog-generator, or the zone at which projectiles (e.g., smoke grenades) are aimed. The array of transmissometers is set up to record line-of-sight measurements of the obscurant clouds as they develop within approximately the first 300 m of travel from the target area. There are generally at least two lines-of-sight. Depending upon the range of wind directions that are anticipated, additional lines-of-sight may be instrumented, some at right angles to others. Meteorological data are obtained from one or two towers located within the test grid. These towers are typically instrumented at 2, 4, 8, 16, and 32 m, and obtain measurements of mean wind speed and direction, and temperature difference (between instrument levels). The data collector computes the standard deviation of wind-vane fluctuations (a bivane) to obtain σ_θ and σ_ϕ. The σ_ϕ data are frequently discounted in the earlier tests, although DPG scientists have improved the instruments so that σ_ϕ data are more reliable after about 1989.

The transmissometer data are recorded once a second along each line-of-sight producing a time-series showing the passage of the obscurant. A typical example from Dumbauld et al. 1981 is shown in Figure 3-3 along with the output of the HECSO dispersion model. These time-series are integrated to provide line-of-site integrated dosage (CLID) measurements:

$$CLID = \frac{-1}{\alpha(\lambda)} \int_{t=0}^{t=\tau} \ln [T(t)]\, dt \qquad (3\text{-}2)$$

where τ = total time that data were collected during the trial
$\alpha(\lambda)$ = extinction coefficient at wavelength λ for the obscurant
$T(t)$ = transmittance at time t.

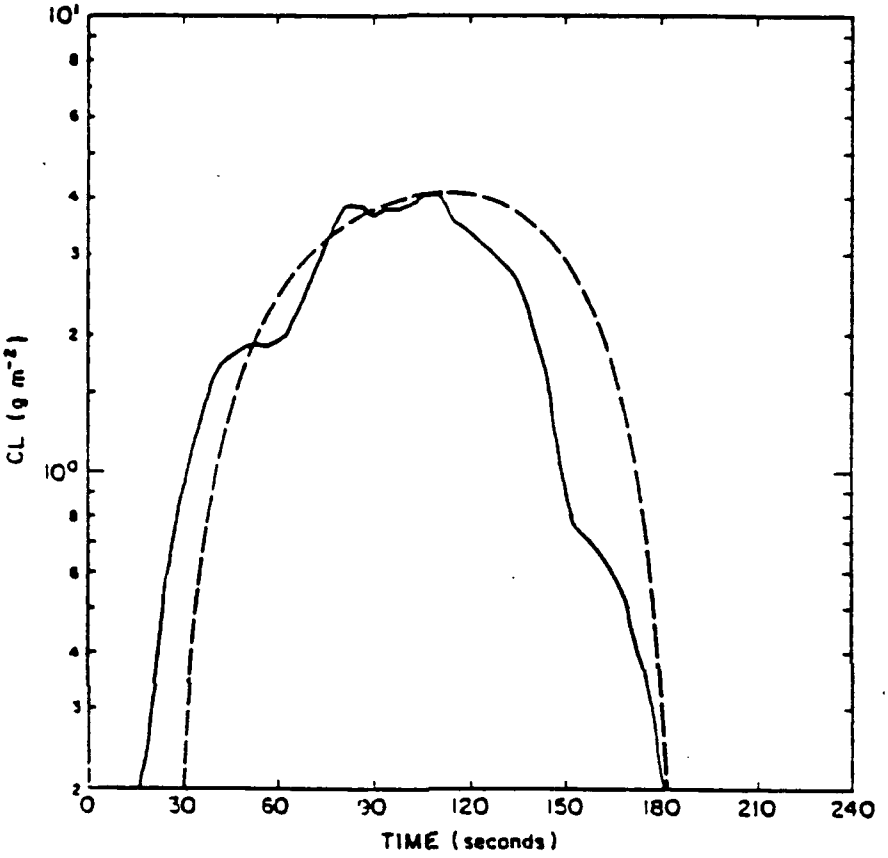

Figure 3-3. Measured (solid line) and modeled (dashed line) line-of-sight integrated concentration values for row 0, trial 33 (Dumbauld et al. 1981).

Hence each trial provides one CLID for each line-of-sight, for each wavelength. Usually two wavelengths are used, one in the visible range (0.4 - 0.7 μm) and one in another (e.g., 3.4 μm or 1.06 μm).

Major DPG obscurant datasets include:

o	M116 Smoke Projectile	Carter et al. 1979
o	M116A1 Smoke Projectile	Bowman et al. 1982
o	XM825 Smoke Projectile	Carter et al. 1979 Bowman et al. 1982
o	XM819, M375A2 Smoke Projectiles	Saterlie et al. 1981a
o	XM803 Smoke Projectile	Carter et al. 1979
o	L8A1 Smoke Grenade	Rafferty and Dumbauld 1983
o	L8A1, L8A1 (reworked), L8A3 Smoke Grenade	Saterlie and Dumbauld 1982a
o	XM49 Fog Generator	Saterlie et al. 1981b
o	M3A3 Fog Generator	Saterlie et al. 1981b
o	105 HC, 155 HC M1, M2 Smoke Canisters	Carter et al. 1979
o	Foreign Smoke Pots	Saterlie and Dumbauld 1982b

The M116 and M116A1 munitions produce a smoke screen by burning canisters of a zinc oxide-aluminum-hexachloroethane (HC) mixture. The XM825 munition produces a smoke screen by burning 116 wedge-shaped pieces of felt saturated with white phosphorous (WP). The XM803 munition contains wedges of red phosphorous (RP) rather than WP. Carter et al. (1979) noted that the RP wedges exhibit a burn rate which is far more uneven than that exhibited by the WP wedges. The XM819 munition is also of an RP wedge design, but the M375A2 contains bulk WP. The L8 series of grenades are air-burst smoke grenades filled with RP mixed with 5% butyl rubber. The XM49 and M3A3 generators create an obscurant fog by evaporating either fog oil, diesel oil, or infrared (IR) obscurant. All of the foreign smoke pots tested contained the HC mixture.

The test sites in general offer several complications relative to an ideal, flat setting. There are usually an array of instrument shelters and

visual targets (e.g., tank silhouettes) within a few hundred meters of the test area, or frequently within the test area. Other miscellaneous characteristics of the surface can include raised roadbeds, vehicle tracks, and munitions debris.

Dumbauld et al. (1986) review results of dispersion model verification studies performed for DPG regarding the ability of HECSO to simulate line-of-sight integrated dosages (CLID) inferred from transmissometer measurements. They found "reasonable" model performance for all munitions except XM803, the foreign smoke pots, and the XM49 fog generator dispensing IR material. In fact, the results for the XM825 and LA83 smoke munitions show model estimates to be well within a factor of two of the observed CLID values. This good agreement suggests that the model includes a sufficient set of meteorological parameters.

In the case of the IR material, the evidence suggests that significant deposition of the material on the ground had occurred. A more recent study by Bowers et al. (1985) also suggests that deposition of IR material on the ground could be important.

F. Smoke Week Tests

Policastro et al. (1984) evaluated the Smoke Week 3 and Smoke Week 4 data sets against what they defined as a minimum set of measured parameters that are necessary to define dispersion model performance and to isolate causes for poor dispersion model performance. They concluded that the Smoke Week data are of largely unknown quality, since there was little QA in the field and no one has evaluated the internal consistency of the data. Furthermore, no measurements were made beyond 100m from any source, and the emission rates from the smoke generators used for Smoke Week 3 were not measured. Nonetheless, they used data from both studies to compare four dispersion models: COMBIC, ACT II, MAD PUFF, and Ludwig (1977).

Given the limited time-of-travel for these experiments, differences in plume/puff formulations among these dispersion models were found to be slight. All of the predicted concentrations were within a factor of two to three of the observed concentrations, although plume growth in the lateral direction

tended to be underestimated in all cases. Comparisons with the Smoke Week 4 concentration observations were found to be more successful, since the emission rates were measured during that experiment.

SECTION IV

ARCHIVAL OF DATASETS

The datasets that have been investigated under this project have been divided into two types: historical studies of the dispersion of tracer gases, and specific studies of the dispersion of smoke obscurants. The historical datasets include some of the classical tracer experiments such as the Prairie Grass studies in which concentrations were measured at a number of discrete receptors employed along some concentric arcs. Point sources can be assumed for these historical datasets and the source emission rate was well-defined.

The smoke/obscurant datasets include a host of smoke munition tests conducted at U.S. Army Dugway Proving Ground, Utah, between the late 1970's and early 1980's, in which the effectiveness of various smoke grenades, smoke projectiles, smoke pots, and smoke generators was tested. Cross-wind integrated concentrations were observed along many lines-of-sight (LOS) during these experiments using transmissometers. It was generally necessary to assume finite volume sources for the DPG experiments, since significant initial source dimensions were usually observed. Source information such as emission rate, total mass emitted, source location, and source dimensions were usually not well-defined. In some cases, the munitions were dynamically fired, and the mass emitted was not directly measured but derived from some empirical formulas.

In the following, we will first discuss the archival of the historical and smoke datasets. The creation of the computerized Dugway Data Archive (DDA), which converts the data to a common format, will then be described.

A. Archival of Historical Datasets

Table 4-1 summarizes the historical datasets that have been archived. Detailed descriptions of each dataset are in the following paragraphs.

Prairie Grass Field Study (Barad, 1958)

The Prairie Grass tests were conducted at O'Neill, Nebraska, during July

Table 4-1

A Brief Summary of the Historical Datasets Included in This Study

DATABASE/REFERENCE	NO. OF ARCS	TRACER TYPE	ATTRIBUTES	NO. OF TRIALS	DDA NAME
Prairie Grass	5	SO2	All trials	44	PG
Barad, 1958			Daytime trials	22	PGDY
			Nighttime trials	22	PGNH
Ocean Breeze	3	Fluorescent	All trials	69	OB
Haugen and Fuquay, 1963		Particles	10 highest Q trials	10	OBHI
			10 lowest Q trials	10	OBLO
Dry Gulch / Course B	2	Fluorescent	All trials	55	DGB
Haugen and Fuquay, 1963		Particles	10 highest Q trials	10	DGBHI
			10 lowest Q trials	10	DGBLO
Dry Gulch / Course D	3	Fluorescent	All trials	51	DGD
Haugen and Fuquay, 1963		Particles	10 highest Q trials	10	DGDHI
			10 lowest Q trials	10	DGDLO
Green Glow	6	Fluorescent	All trials	24	GG
Barad and Fuquay, 1962		Particles	10 highest Q trials	10	GGHI
			10 lowest Q trials	10	GGLO

and August, 1956. SO_2 tracer gas was released over periods of about ten minutes from a point source located at an elevation of 0.45 m. Ten minute averaged tracer concentrations were obtained from observations at an elevation of 1.5 m along five concentric arcs at distances of 50, 100, 200, 400, and 800 m from the source. Figure 4-1 displays the sampling used in the Prairie Grass experiments. Values of crosswind integrated concentrations were published in papers by van Ulden (1978) and Nieuwstadt (1980).

Data from 44 trials were included in the archive. The experiments were conducted in such a way that the emission rates of the daytime releases were about twice the emission rates of the nighttime releases. Supporting meteorological observations were made from a nearby tower, located in a flat area representative of the site. The average surface roughness was determined to be 0.6 cm.

Ocean Breeze Field Study (Haugen and Fuquay, 1963)

The Ocean Breeze tests were conducted at Cape Canaveral, Florida, during May and June, 1961, and January through March, 1962. Fluorescent particles were released continuously from ground level for 30 minute periods using aerosol fog generators. Tracer particle dosages were measured at concentric arcs located 1200, 2400, and 4800 m downwind at a height of 4.57 m above ground level. Figure 4-2 displays the Ocean Breeze diffusion course layout.

A total of 69 trials were included in the archive. Many of the trials were conducted under sea breeze conditions. The test site was characterized by 10-20 feet tall rolling sand dunes. In addition, much of the diffusion course was covered with brushwood and palmetto growth. A roughness length of 10 cm is estimated by Kunkel (1988).

Dry Gulch Field Study (Haugen and Fuquay, 1963)

The Dry Gulch tests were conducted at Vandenberg Air Force Base, California, during June through August, 1961, and February, March, and June, 1962. Fluorescent particles were released continuously from ground level over 30 minute periods using aerosol fog generators. Tracer particle dosages were measured with membrane filters on concentric arcs located 2301 and 5665 m downwind on Course B, and 853, 1500, and 4715 m downwind on Course D, at a height of 4.57 m above ground level. Figure 4-3 displays the Dry Gulch diffusion course layout.

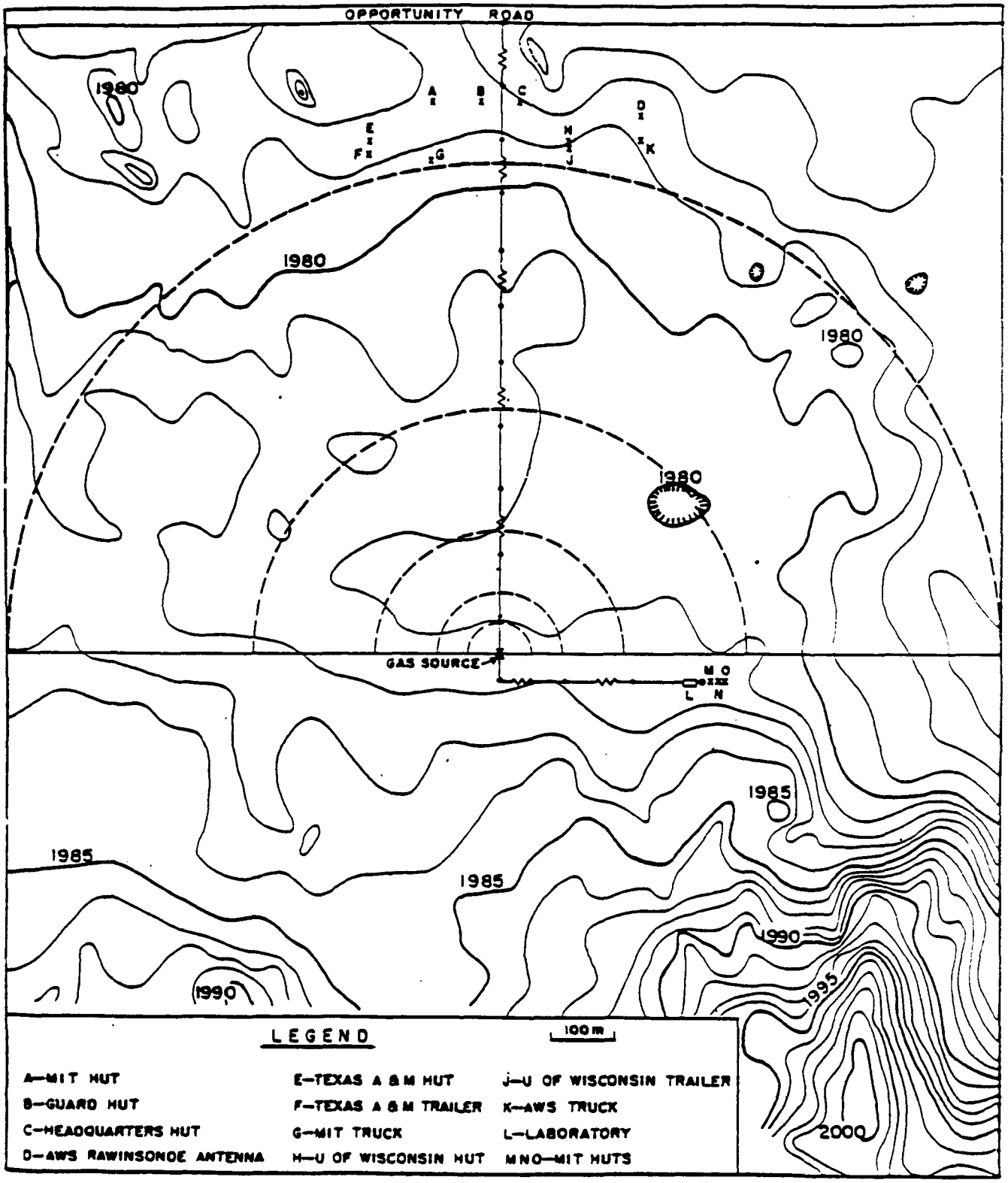

Figure 4-1. Sampling grid used in the Prairie Grass experiments, from Barad (1958).

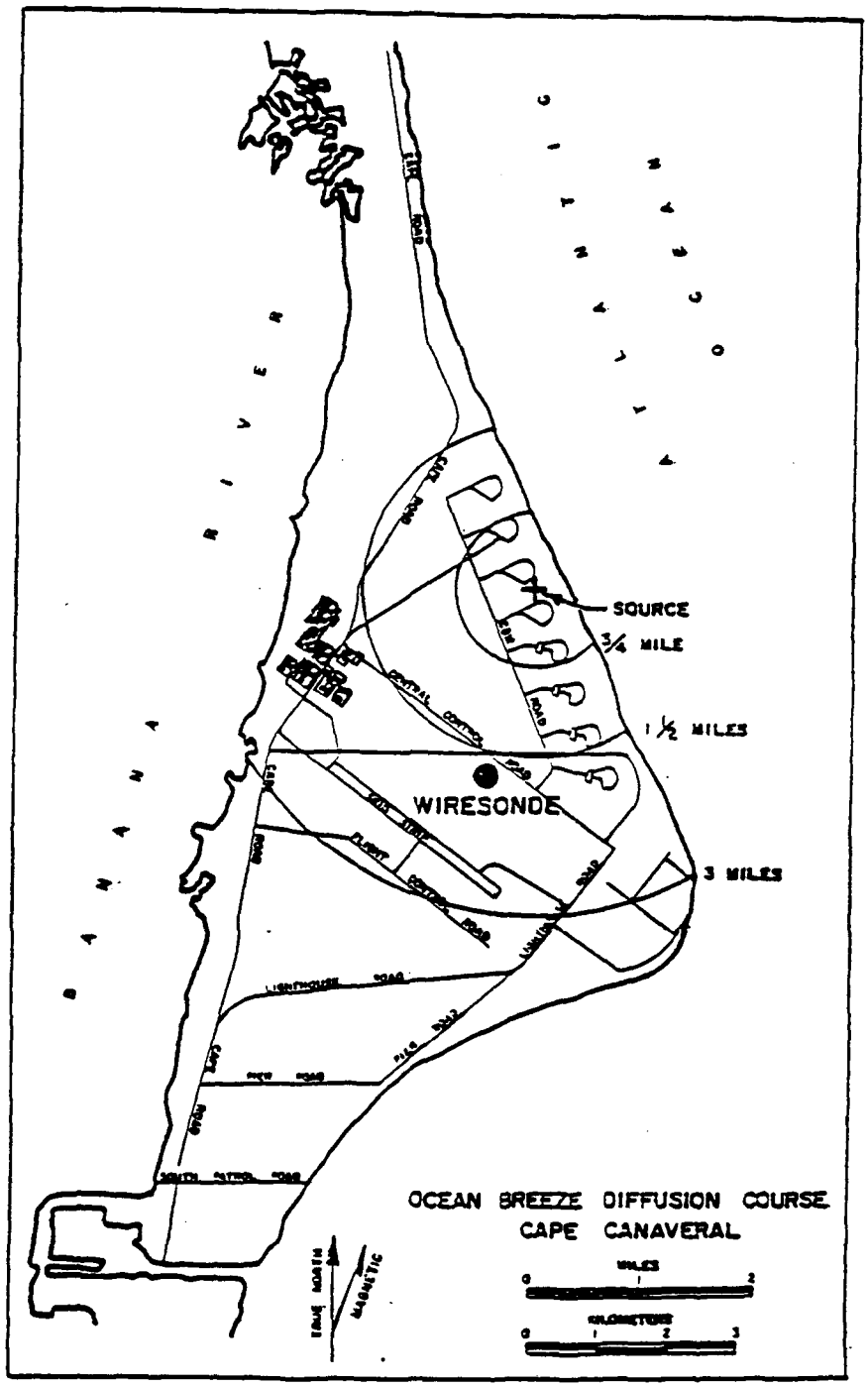

Figure 4-2. Ocean Breeze diffusion course layout, from Haugen and Fuquay (1963).

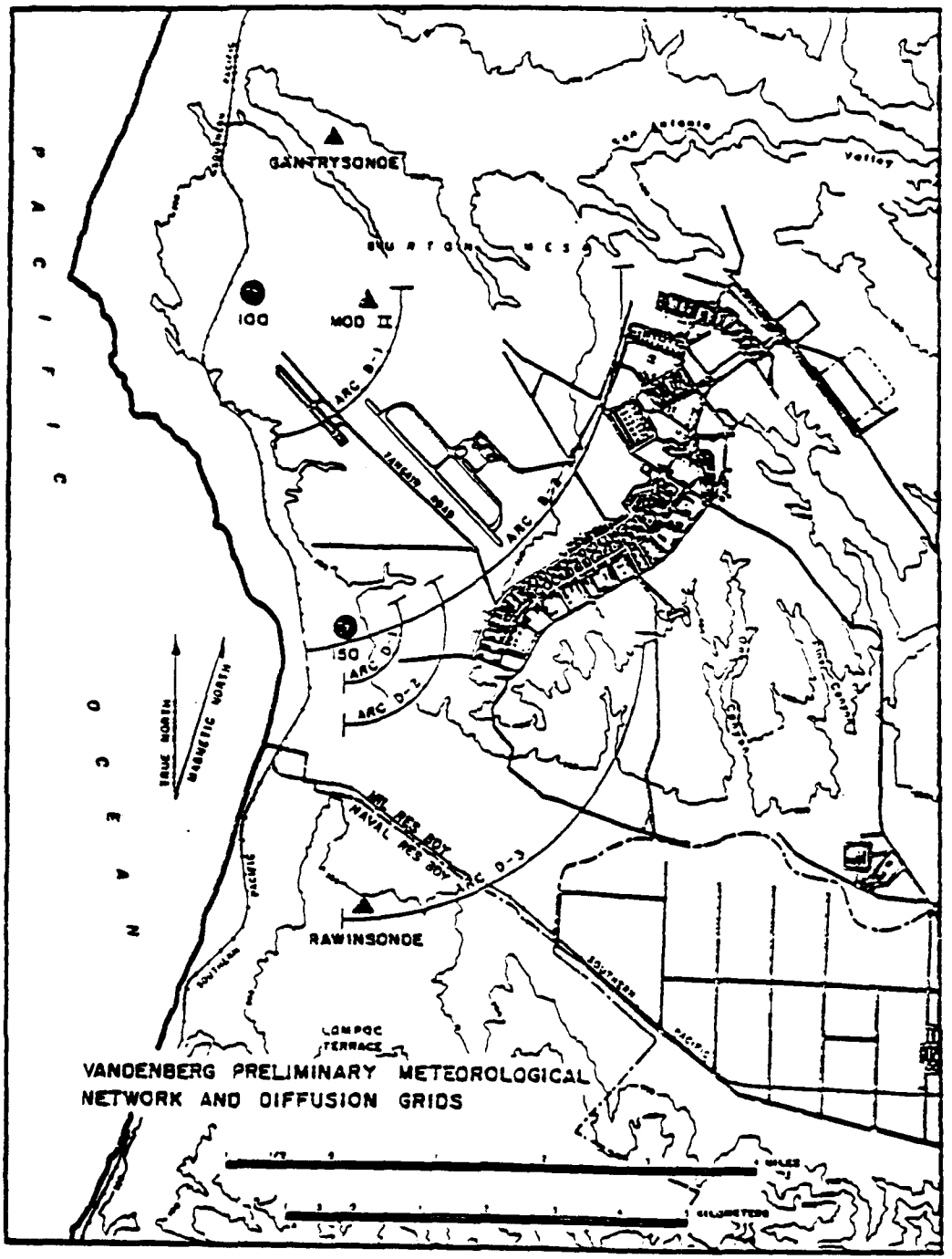

Figure 4-3. Dry Gulch diffusion courses, from Haugen and Fuquay (1963).

Data from 55 trials for Course B and 51 trials for Course D were included in the archive. The terrain of the test site was quite complex, with numerous nearby mountains and valleys. Near the source location, the roughness length is assumed to be 20 cm for Course B and 50 cm for Course D (Kunkel, 1988).

Green Glow Field Study (Barad and Fuquay, 1962)

The Green Glow tests were conducted at Hanford, Washington, during June through August, 1959. Fluorescent particles (which gave off a green glow under ultraviolet light; hence the project name) were released continuously over 30 minute periods using aerosol fog generator. Tracer particle dosages were measured using membrane filters at concentric arcs located at 200, 800, 1600, 3200, 12800, and 25600 m downwind, at a height of 1.5 m above ground level. Figure 4-4 displays the sampling grid used in the Green Glow program.

Data from 24 trials were included in the archive. All trials were conducted during nighttime stable conditions. The site was relatively flat, but was surrounded by elevated terrain at a distance of several kilometers and drainage flows were common. The surface vegetation consisted of desert grasses interspersed with sagebrush 1 to 2 m in height. The roughness length is estimated to be 10 cm (Kunkel, 1988).

B. Archival of Smoke/Obscurant Datasets

Table 4-2 summarizes the smoke/obscurant datasets that have been archived. Detailed descriptions of each dataset are in the following paragraphs.

Inventory Smoke Munition Test, Phase IIa and Smoke Week I (Carter et al., 1979)

The tests were conducted at US Army Dugway Proving Ground, Utah, in October and November, 1977, where the HC (hexachloroethane) munitions were ignited statically. A total of six trials were included in the archive, four from the Phase IIa trials, and two from the Smoke Week I trials. All trials were conducted in the early afternoon. The number of munitions ignited during the trials ranged from 2 to 36. Values of light transmittance were measured at four wavelengths (visible, 1.06, 3.4, and 9.75 μm) along three

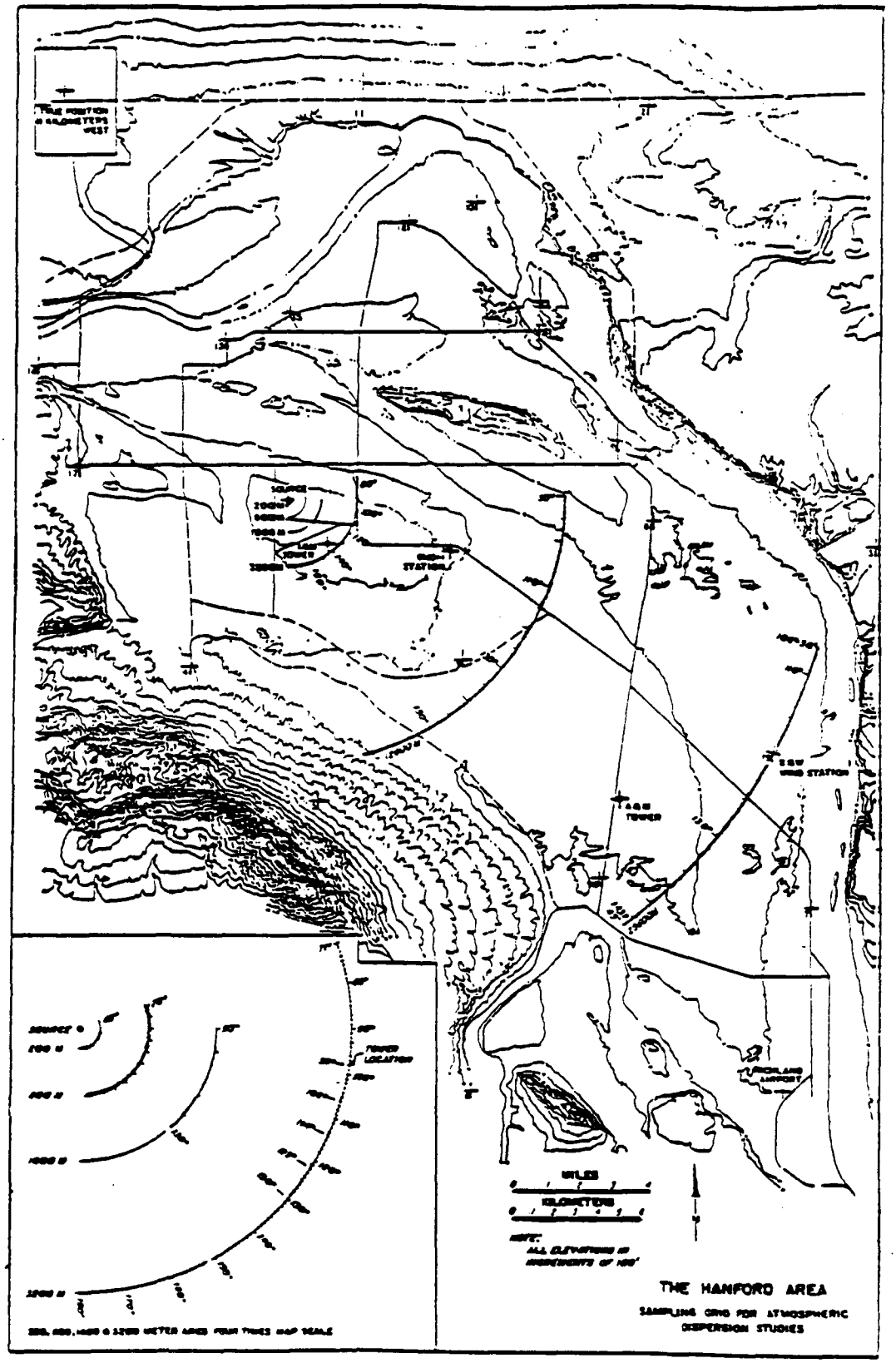

Figure 4-4. Sampling grid used in the Green Glow program, from Barad and Fuquay (1962).

Table 4-2

A Brief Summary of the Smoke/Obscurant Datasets Included in This Study

DATABASE/REFERENCE	NO. OF LOS's[2]	MUNITION TYPE[1]	ATTRIBUTES	NO. OF TRIALS	DDA NAME
Inventory Smoke Munition Test	3	HC canisters	Phase IIa, 2- 36 munitios used	4	INVHC
Phase IIa and Smoke Week I, Carter et al., 1979		HC canisters	Smoke Week I, 3 and 18 munitions used	2	INVHC
Development Test I of 155 mm	1	M116 (HC)	1 round, 4 canisters/round	16	DT1HC
Smoke Projectiles,		XM803 (RP)	1 round, 228 wedges/round	17	DT1RP
Carter et al., 1979		XM825 (WP)	1 round, 98 wedges/round	17	DT1WP
Development Test II of 155 mm	6	XM825 (WP)	1 round, 116 wedges/round	17	DT2W1
Smoke Projecctiles,			2 rounds, 116 wedges/round	9	DT2W2
Bowman et al., 1982		M116A1 (HC)	1 round, 4 canisters/round	11	DT2H1
			2 rounds, 4 canisters/round	4	DT2H2
Development Test I of 81 mm	5	XM819 (RP)	1 round, 28 wedges/round	15	DT1X1
Smoke Projectiles,			3 rounds, 28 wedges/round	7	DT1X3
Saterlie et al., 1981		M375A2 (WP)	1 round, bulk	16	DT1M1
			3 rounds, bulk	10	DT1M3
Comparison Test of L8A1	2	L8A1 (RP)	1 round (lot A)	7	L81A1
Screeing Smoke Grenades,			1 round (lot B)	6	L81B1
Ratterty and Dumbauld, 1983;			1 round (lot C)	6	L81C1
Sutton, 1981			1 round (lot D)	5	L81D1
			12 rounds (lot A, B, C, or D)	6	L8112
Evaluation of Reworked L8A1	5	L8A1 (RP)	6 rounds (3 cond. temp.)	5	L81E6
and Product Improved L8A3			8 rounds (3 cond. temp.)	6	L81E8
Screening Smoke Grenades,			12 rounds (3 cond. temp.)	6	L81E2
Saterlie and Dumbauld, 1982a			low cond. temp. (6, 8, or 12 rounds)	5	L81EL
			med. cond. temp. (6, 8, or 12 rounds)	6	L81EM
			high cond. temp. (6, 8, or 12 rounds)	6	L81EH
		Reworked	6 rounds (3 cond. temp.)	6	L81R6
		L8A1 (RP)	8 rounds (3 cond. temp.)	6	L81R8
			12 rounds (3 cond. temp.)	6	L81R2
			low cond. temp. (6, 8, or 12 rounds)	6	L81RL
			med. cond. temp. (6, 8, or 12 rounds)	6	L81RM
			high cond. temp. (6, 8, or 12 rounds)	6	L81RH
		L8A3	6 rounds (3 cond. temp.)	6	L836
			8 rounds (3 cond. temp.)	4	L838
			12 rounds (3 cond. temp.)	6	L832
			low cond. temp. (6, 8, or 12 rounds)	5	L83L
			med. cond. temp. (6, 8, or 12 rounds)	6	L83M
			high cond. temp. (6, 8, or 12 rounds)	5	L83H

1 HC: hexachloroethane.
RP: red phosphorus
WP: white phosphorus
FO: fog oil
DO: diesel oil
IR: infrared obscurant

2 This is the number of LOS's whose data were actually used, not the number of LOS's employed during the experiments.

Table 4-2 (Concluded)

A Brief Summary of the Smoke/Obscurant Datasets Included in This Study

DATABASE/REFERENCE	NO. OF LOS'S[4]	MUNITION TYPE[3]	ATTRIBUTES	NO. OF TRIALS	DDA NAME
Evaluation of Foreign Smoke Pots, Saterlie and Dumabuld, 1982b	1	ABC-M5 (HC)	1 round, U.S.	17	INTUS
		No. 24 MK5 (HC)	1 round, British	18	INTBR
		Type 3-00 (HC)	1 round, Japanese	7	INTJA
		No. 24-SCI-SC 39	1 round, Canadian	17	INTCA
Developement Test I of Man-Portable Smoke Generator, Saterlie et al., 1981	3	XM49 (FO)	FO only (1 generator)	12	POXF
		M3A3 (FO)	FO only (1 generator)	6	POMF
		XM49 (DO)	DO only (1 generator)	4	POXD
			DO part of DO+IR (multiple generators)	2	POXD[5]
		XM49 (IR)	IR only (1 generator)	4	POXI
			IR part of DO+IR (multiple generators)	2	POXI[6]
		XM49 (FO)	FO part of FO+IR (multile generators)	10	POXFC[7]
		XM49 (IR)	IR part of FO+IR (multiple generators)	10	POXIC[8]
Atterbury-87 Field Study, Liljegren et al., 1989; DeVaull et al., 1989	4	M3A4 (FO)	1 generator	4	ATFOG
		M5 (HC)	18 - 20 rounds	5	ATHC

3 HC: hexachloroethane.
RP: red phosphorus
WP: white phosphorus
FO: fog oil
DO: diesel oil
IR: infrared obscurant

4 This is the number of LOS's whose data were actually used, not the number of LOS's employed during the experiments.

5 The contribution due to DO only whereas both DO and IR were released during the trials.

6 The contribution due to IR only whereas both DO and IR were released during the trials.

7 The contribution due to FO only whereas both FO and IR were released during the trials.

8 The contribution due to IR only whereas both FO and IR were released during the trials.

lines-of-sight (LOS). Moreover, 100 chemical impinger samplers and 20 aerosol photometer samplers were located at regular intervals along one of the LOS's. Transmittance measurements for the 3.4 μm wavelength were used for the calculation of cross-wind line integrated dosage (CLID). The heights of the sampling instruments were not mentioned in Carter et al. (1979); a value of 1.5 m is assumed because the instrument heights for other similar smoke trials were between 1 and 2 m. Figure 4-5 displays the test grid configuration for this set of experiments.

The test site was characterized by flat clay soil with widely spaced low shrubs and grasses not exceeding 0.5m in height. The surface roughness length is estimated at 2 to 4 cm, and 3 cm is used in the model applications.

Although the HC munitions were ignited statically and the munition locations should have been well-defined, detailed information regarding the munition locations is not contained in Carter et al. (1979). This report states that all munitions were placed along a certain LOS for southerly winds and along another LOS for northerly winds. In the subsequent analysis of this dataset, all munitions ignited during each trial are assumed to be one volume source located at the center of the appropriate LOS. Sensitivity of the model-predicted cross-wind line-integrated dosage (CLID) to the assumption of the source location should be minimized as long as the LOS's are long enough to cover most of the width of the cloud.

Standard deviations of the fluctuations in azimuth wind angle, σ_θ, and the fluctuations in elevation wind angle, σ_ϕ, were both measured during the trials. However, the data for many of the trials indicated that there were instrument problems which affected the accuracy of the σ_ϕ measurements. Therefore, σ_ϕ values were estimated from observed σ_θ values based on the following empirical relationship:

$$\sigma_\phi = \sigma_\theta(T_a)\ (2.5/T_a)^{0.2} \qquad (4\text{-}1)$$

where T_a is the averaging time for σ_θ in seconds.

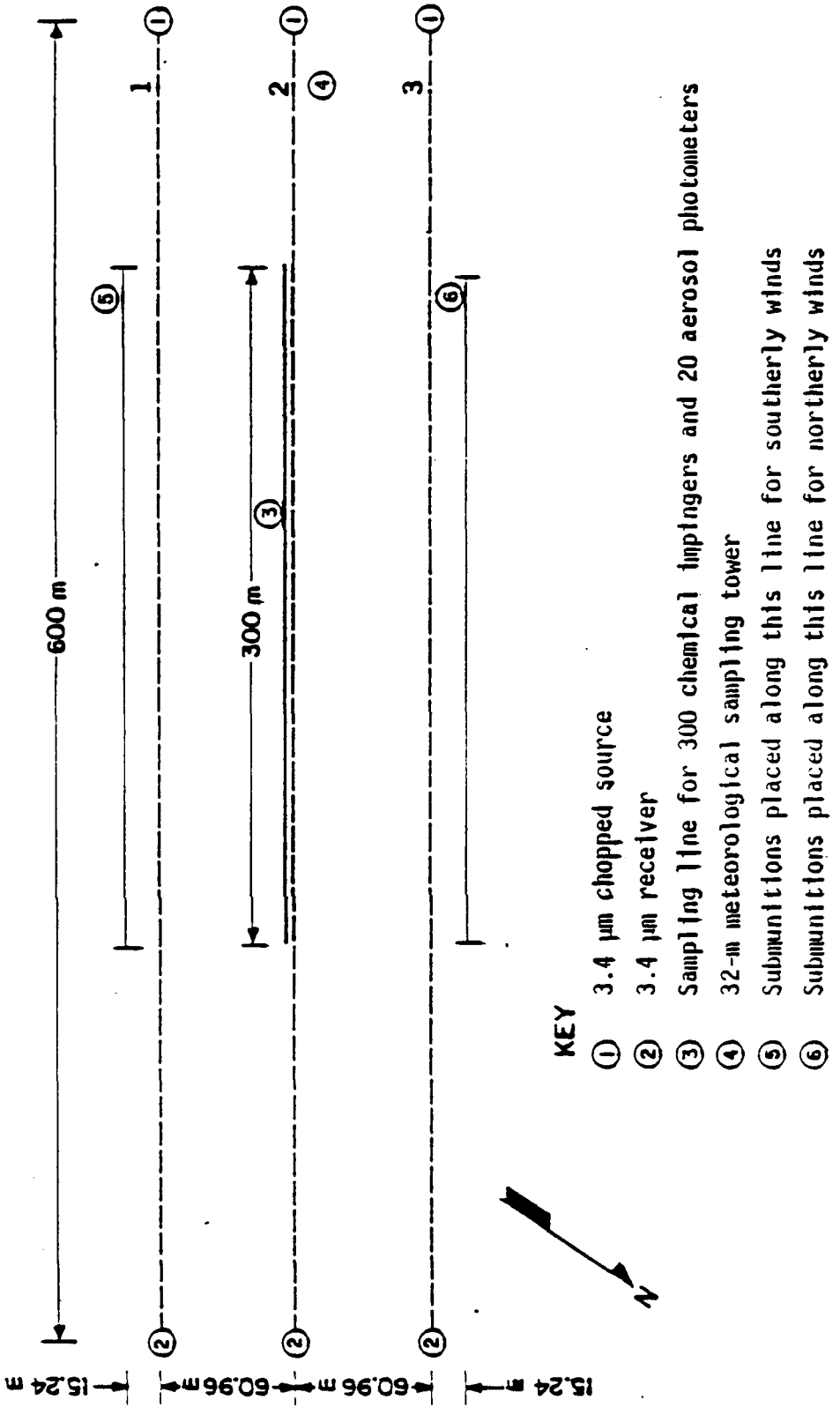

Figure 4-5. Test grid configuration for the inventory smoke munition tests, from Carter et al. 1979. Large numerical values designate LOS's whose data were used in the calculation.

Development Test I of 155mm Smoke Projectiles (Carter et al., 1979):

The tests were conducted at the US Army Dugway Proving Ground, Utah, in August, 1978. Three types of munitions were used: M116 (HC), XM803 (red phosphorus, RP) and XM825 (white phosphorus, WP). The M116 projectile consists of four HC canisters, the XM803 projectile consists of 228 RP wedges, and the XM825 projectile consists of 98 WP wedges. The total fill weights for the M116, XM803, and XM825 projectiles are 12.4, 8.8, and 9.1 kg, respectively. Single rounds were fired during all trials. There were 16 M116 trials, 17 XM803 trials, and 17 XM825 trials. All trials were conducted during daytime.

All munitions were dynamically fired, and the geometrical position of submunition patterns upon ground impact were measured only for a limited number of trials. Characteristic or average patterns for each type of munition were determined from all the trials in which the pattern was measured. In the subsequent analysis of this dataset, it is assumed that the total source emission during each trial can be represented by one volume source and that all trials using the same munition have an identical ground impact pattern with respect to the center location. Because the elliptical ground impact pattern generally does not agree with the wind direction, the known orientation of the pattern assumed for each trial was reoriented with the wind direction. The alongwind and crosswind source dimensions, σ_{x0} and σ_{y0}, were obtained by dividing the alongwind and crosswind pattern dimensions, respectively, by 4.3. The value of 4.3 is based on the assumption that the alongwind and crosswind distributions of smoke are Gaussian and that the smoke concentration at the edge is one-tenth the concentration at the center.

Values of light transmittance at two wavelengths (1.06 and 3.4 μm) were measured along one LOS. Transmittance measurements for the 1.06 μm wavelength were used in computing CLID. The height at which the sampling instruments were located was not mentioned in Carter et al. (1979); a value of 1.5 m is assumed because the instrument heights for other similar smoke trials were between 1 and 2 m. Figure 4-6 displays the test grid configuration for these experiments.

σ_θ values were measured. σ_ϕ values were also measured but deemed unreliable, and were therefore derived from observations of σ_θ based on Equation (4-1).

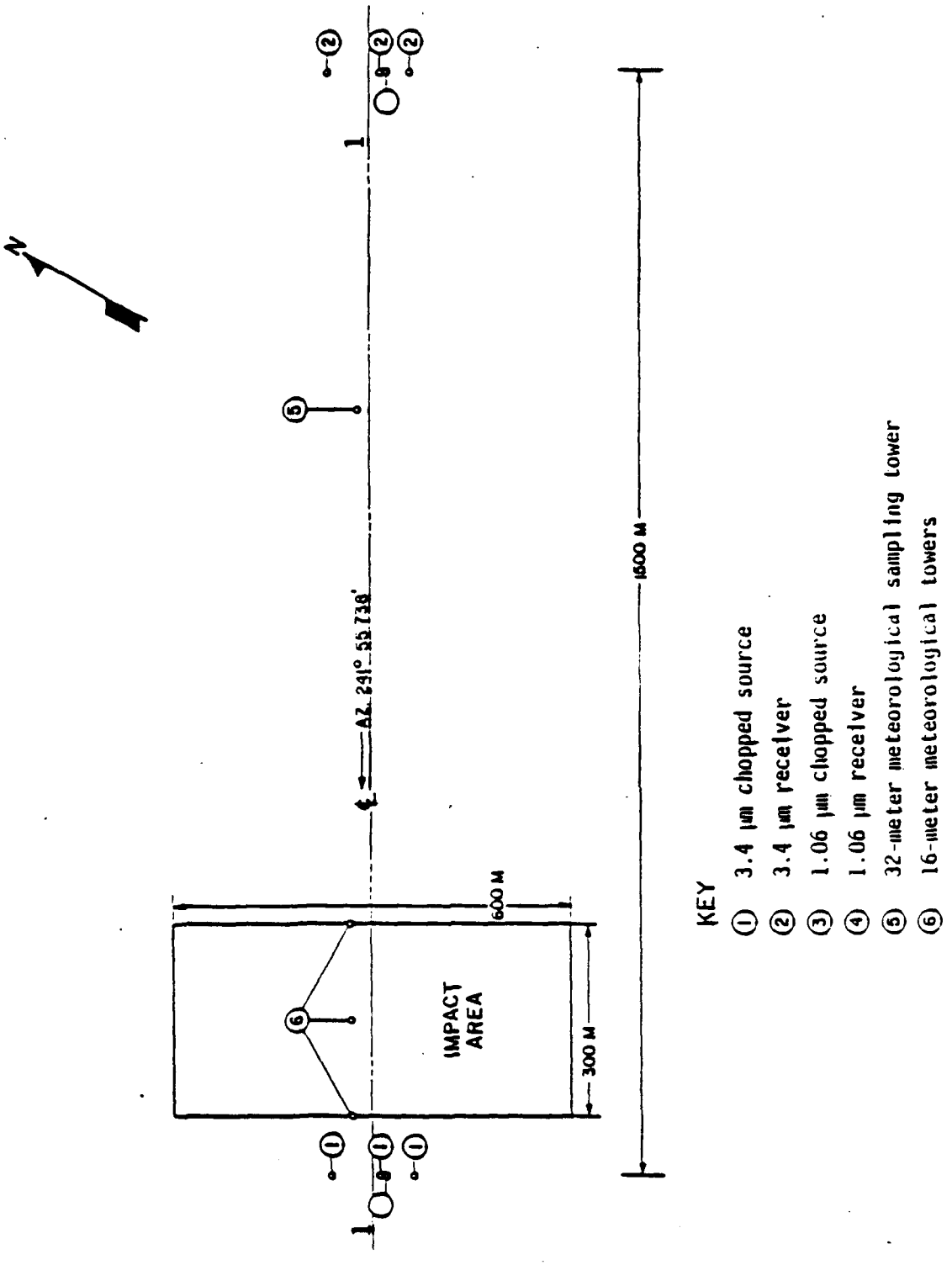

Figure 4-6. Test grid for the development test I of 155 mm smoke projectiles, from Carter et al., 1979. Large numerical values designate LOS's whose data were used in the calculation.

Development Test II of 155mm Smoke Projectiles (Bowman et al., 1982):

The tests were conducted at US Army Dugway Proving Ground, Utah, during July to September, 1981. Two types of munitions were used: M116A1 (HC) and XM825 (WP). The M116A1 projectile consists of four HC canisters and the XM825 projectile consists of 116 WP wedges. Fifteen M116A1 trials were included in the archive, where four were two-round trials and the remainder were single-round trials. Twenty six XM825 trials were included in the archive, where nine were two-round trials and the remainder were single-round trials. The fill weight is 7.5 kg for a single XM825 round. Because the fill weight of a single M116A1 round is not mentioned in Bowman et al. (1982), the value of 12.4 kg listed in Carter et al. (1979) is assumed. All trials were conducted between 1500 and 2200 local time.

Values of transmittance were measured at one-second intervals at two wavelengths (visible and 3.4 μm) along eight LOS's at a height of 1.5 m. An analysis of the transmittance data showed sharply-defined reductions in transmittance that was assumed to be due to dust raised by the impact of the projectile. An attempt was made to remove from the data the effects of dust in reducing the transmittance. Figure 4-7 displays the test grid configuration for these experiments.

Detailed information about the position of each HC canister and WP wedge is available for all trials. For the M116A1 trials, each canister is modeled as one volume source. For the XM825 trials, because of the very large number of smoke sources released, it is not feasible to model each of the 116 wedges with a volume source. According to Bowman et al. (1982), the impact grid area was subdivided into many 30-m squares. In the subsequent model application, a volume source was assigned to each 30-m square with a source strength equivalent to the total source strength of the wedges contained in that square. However, this still leads to roughly 20 and 30 equivalent volume sources for the one-round and two-round XM825 trials, respectively. For each 30-m square, the alongwind and crosswind source dimensions, σ_{x0} and σ_{y0}, are assumed to be 30/4.3 = 6.98 m.

σ_θ values were measured. σ_ϕ values were also measured but deemed unreliable, and were therefore derived from observations of σ_θ based on Equation (4-1).

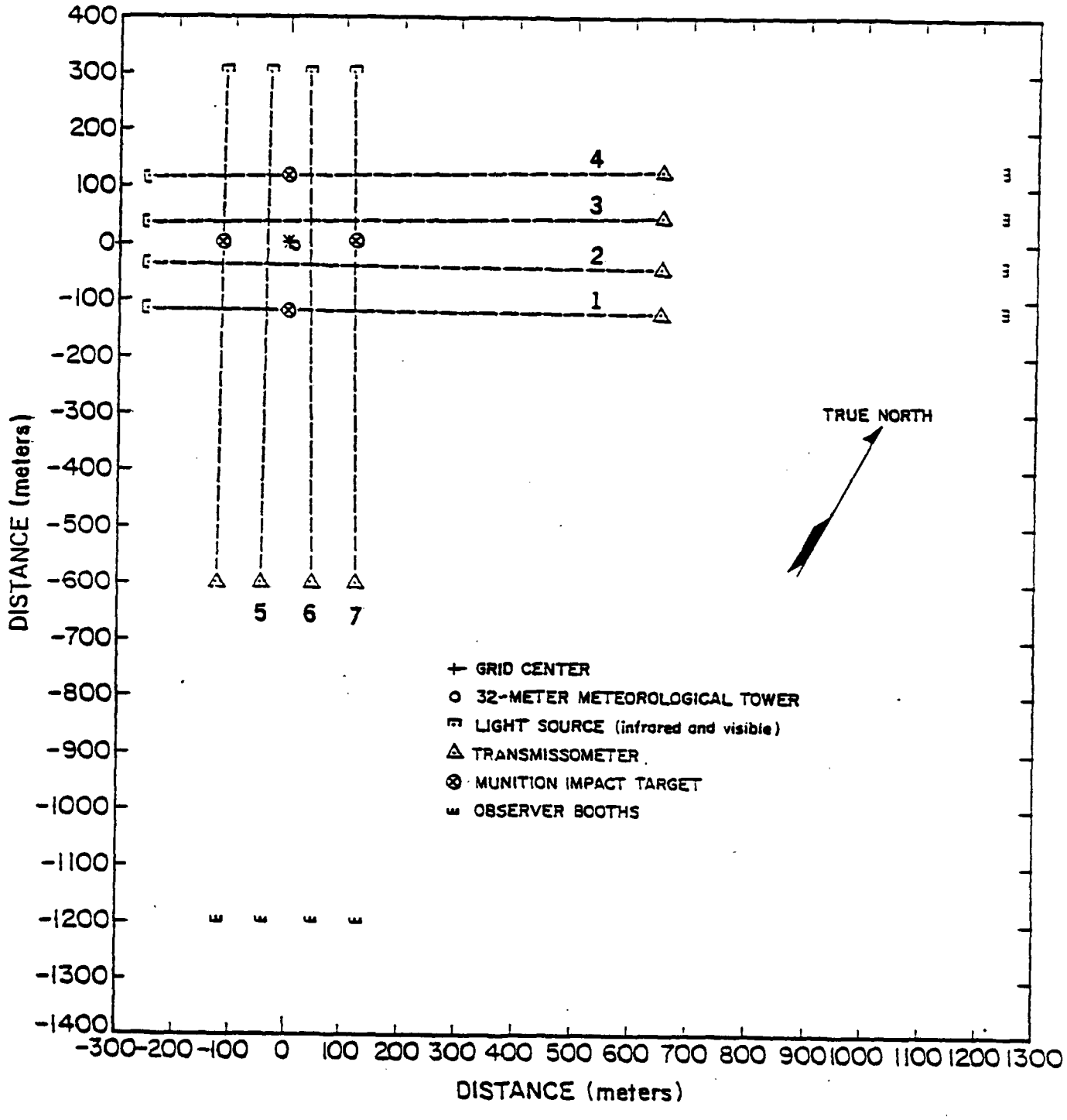

Figure 4-7. Measurement grid for the development test II of 155 mm smoke projectiles, from Bowman et al., 1982. Large numerical values designate LOS's whose data were used in the calculation.

Development Test I of 81mm Smoke Cartridges (Saterlie et al., 1981):

The tests were conducted at US Army Dugway Proving Ground, Utah, during December, 1980, to March, 1981. Two types of munitions were used: XM819 (RP) and M375A2 (WP). The XM819 projectile consists of 28 RP wedges, whereas M375A2 is a bulk WP projectile. Information regarding the fill weights for both munitions is not available in Saterlie et al. (1981). Twenty six M375A2 trials were included in the archive, where ten were three-round trials and the remainder were single-round trials. Twenty two XM819 trials were included in the archive, where seven were three-round trials and the remainder were single-round trials. All trials were conducted during daytime.

Values of transmittance were measured at one-second intervals at 3.4 μm along five LOS's at a height of 1.5 m. Some LOS measurements of transmittance exhibited a drift due to an incorrect baseline measurement of the transmissometer, indicated by the failure of the transmittance measurement to return to unity after the cloud had passed through the LOS. An attempt was made to remove the drift from the data. Figure 4-8 displays the measurement grid for the test.

The impact points for the XM819 RP wedges and the M375A2 projectile were known from survey data. However, for the XM819 trials, Saterlie et al. (1981) suggest that a circular pattern be drawn to enclose the impact points, and that a single volume source be used to represent the wedge pattern from a single XM819 projectile. The alongwind and crosswind source dimensions, σ_{x0} and σ_{y0}, are assumed to be D/4.3, where D is the diameter of the circular pattern. For the XM819 trials when three projectiles were fired, the impact patterns from the wedges for two or more projectiles were often superimposed. Under these circumstances, one to three circles were drawn to enclose the wedge patterns depending on their separation.

As done with the other studies, σ_ϕ values were derived from observations of σ_θ values based on Equation (4-1).

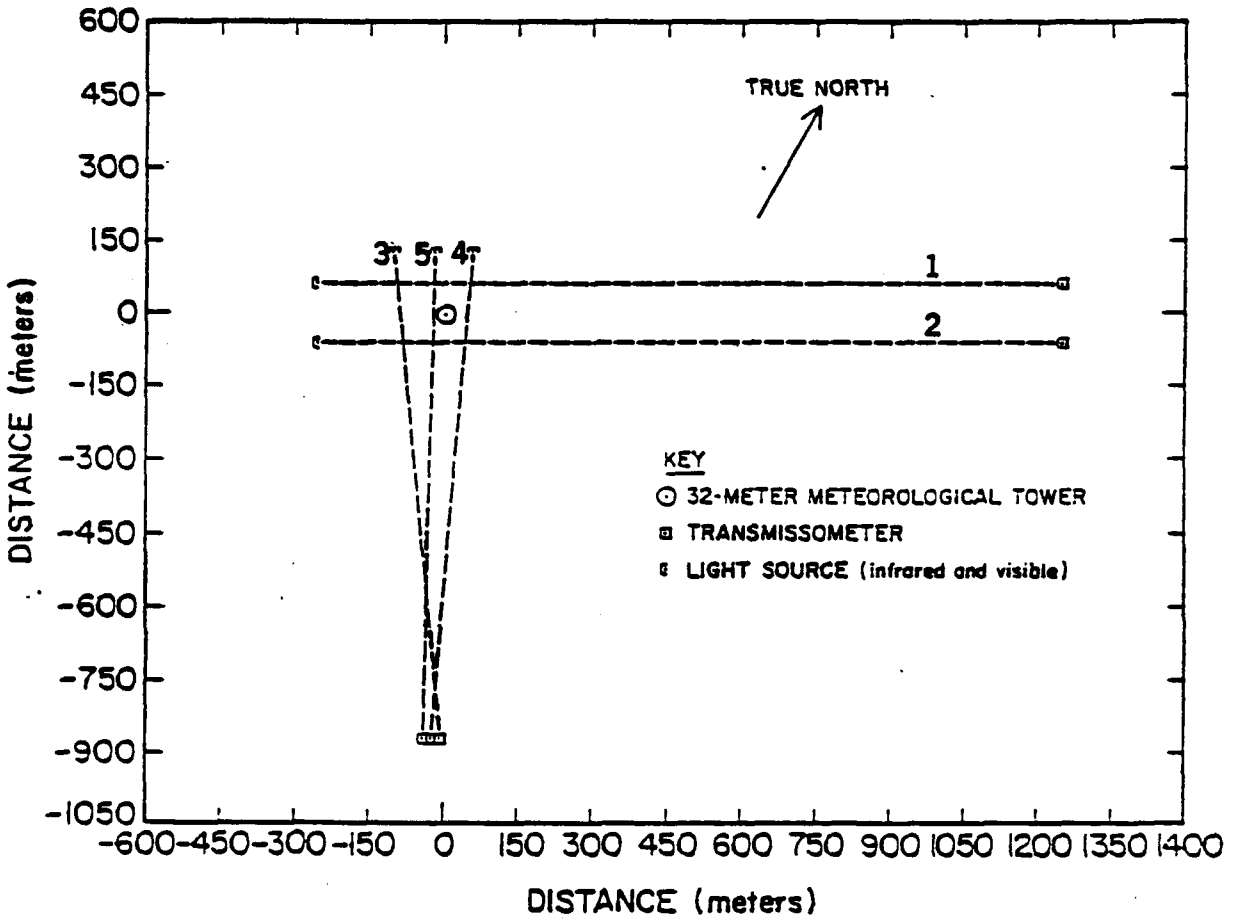

Figure 4-8. Measurement grid for the development test I of 81 mm smoke cartridges, from Saterlie et al., 1981. Large numerical values designate LOS's whose data were used in the calculation.

Comparison Test of L8A1 Screening Smoke Grenades (Rafferty and Dumbauld, 1983; Sutton, 1981):

The tests were conduced at US Army Dugway Proving Ground, Utah, in June, 1981. The L8A1 grenade is an airburst grenade filled with RP pellets mixed with 5% butyl rubber. The fill weight of each grenade is 360 g. Thirty trials were included in the archive. All trials were conducted during daytime. The first 24 trials were single grenade trials, and the remaining six trials were multiple grenade trials where salvos of 12 grenades were fired simultaneously. The grenades used in each trial were taken from one of the four grenade lots.

The grenades were fired from one or both of two M239 (6-tube) grenade launchers mounted on either side of a launch vehicle. The exact grenade impact locations were not measured during the Phase B trials (namely, the 30 trials included in the archive). In the Phase A trials conducted prior to the Phase B trials, a single grenade was fired on each trial to obtain the average range, pattern dimensions and burn time for each of the four grenade lots. In the subsequent model application for the Phase B trials, the average pattern dimensions and ranges produced in the Phase A trials for the four grenade lots were used. Because the elliptical pattern of the grenade generally does not agree with the wind direction, the known orientation of the pattern for each trial was translated according to the wind direction. The alongwind and crosswind source dimensions, σ_{x0} and σ_{y0}, were obtained by dividing the alongwind and crosswind pattern dimensions, respectively, by 4.3. The source height was assumed to be zero because the bulk of the smoke is released by the pellets burning on the ground.

Values of transmittance were measured at one-second intervals at two wavelengths (visible and 3.4 μm) along four LOS's at a height of 1.0 m. However, transmittance data from two LOS's were not used. Only measurements of transmittance at the visible wavelengths were used in the CLID calculation. Figure 4-9 displays the measuring grid for the test.

σ_ϕ values were derived from observations of σ_θ values based on Equation (4-1).

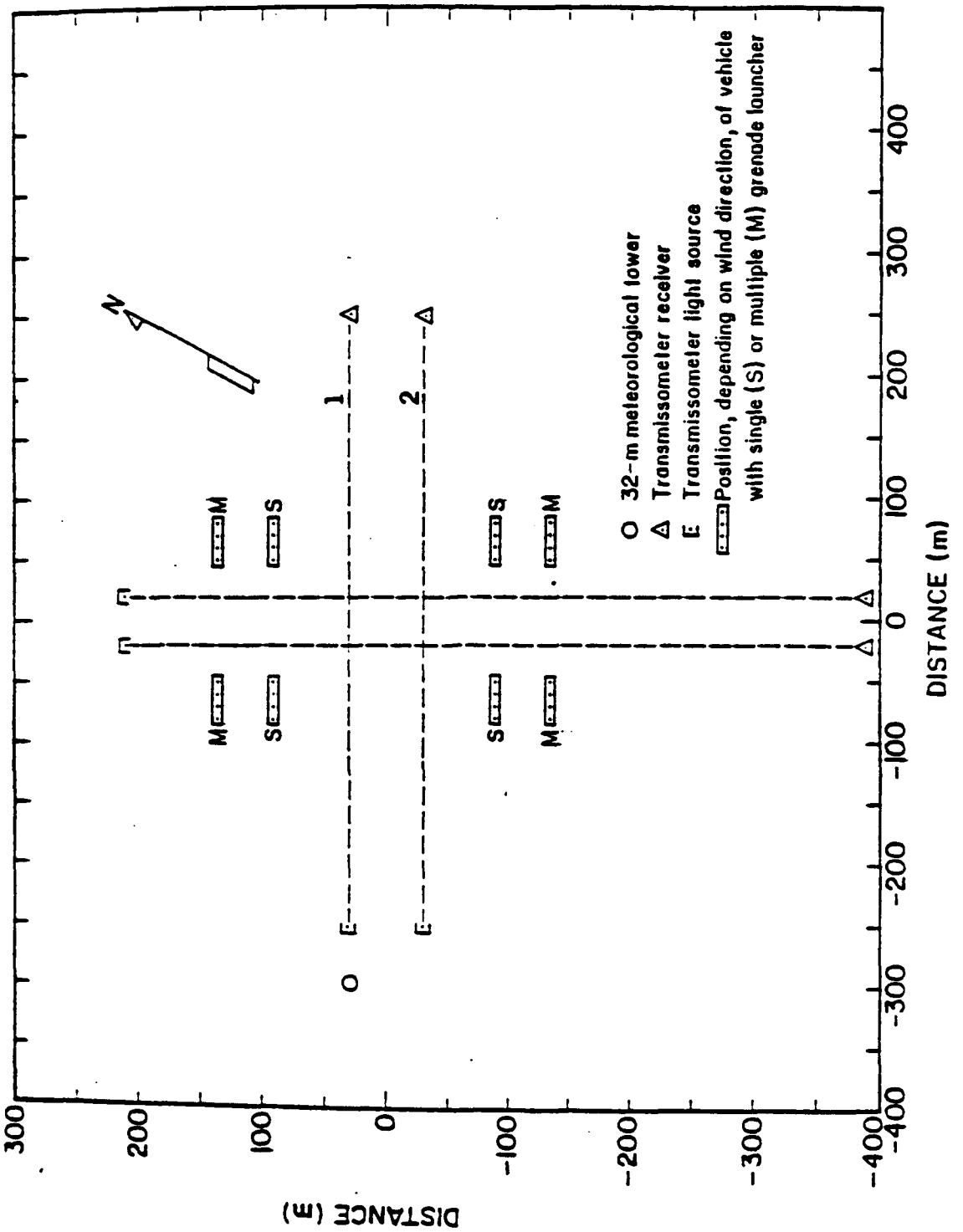

Figure 4-9. Measurement grid for the comparison test of L8A1 smoke grenades from Rafferty and Dumbauld, 1983. Large numerical values designate LOS's whose data were used in the calculation.

Evaluation of Reworked L8A1 and Product Improved L8A3 Screening Smoke Grenades (Saterlie and Dumbauld, 1982a):

The tests were conducted at US Army Dugway Proving Ground, Utah, during May and June, 1982. Three types of grenades were tested: standard L8A1, reworked L8A1, and product improved L8A3. The L8 series smoke grenade is an airburst grenade filled with RP pellets mixed with 5% butyl rubber. The fill weight for each grenade is 360 g. Fifty one trials were included in the archive. All trials were conducted between 1400 and 0100 local time. The numbers of the L8A1, reworked L8A1, and L8A3 grenade trials are 17, 18, and 16, respectively. Various numbers of grenades (either 6, 8, or 12 grenades) were fired during each trial and, prior to firing, the grenades were conditioned at either -40°C, 21°C, or 49°C.

The grenades were fired from either two M239 (6-tube) or two M250 (4-tube) grenade launchers mounted on either side of an M557 modified track vehicle. The exact grenade impact locations were not measured during the Phase B trials (namely, the 51 trials included in the archive). In the Phase A trials conducted prior to the Phase B trials, a single grenade was fired on each trial to obtain the average range, pattern dimensions and burn time for each grenade type and condition temperature. In the subsequent model application for the Phase B trials, the average pattern dimensions and ranges produced in the Phase A trials were used. Because the elliptical pattern of the grenade generally does not agree with the wind direction, the known orientation of the pattern for each trial was reoriented with the wind direction. The alongwind and crosswind source dimensions, σ_{x0} and σ_{y0}, were obtained by dividing the alongwind and crosswind pattern dimensions, respectively, by 4.3. The source height was assumed to be zero because the bulk of the smoke is released by the pellets burning on the ground.

According to Saterlie and Dumbauld (1982a), the grenade impact pattern ranges and dimensions are not a function of condition temperature, but the grenade obscuring effectiveness is a function of condition temperature.

Values of transmittance were measured at one-second intervals at two wavelengths (visible and 3.4 μm) along seven LOS's at a height of 2.0 m. However, transmittance data from two LOS's were later found not useful. Measurements made at the visible wavelengths were primarily used in the CLID

calculation. Figure 4-10 displays the measuring grid and the representative ground pattern for a salvo of 12 grenades for the test.

Observations of vertical turbulence σ_ϕ values were listed in the report.

Evaluation of Foreign Smoke Pots (Saterlie and Dumbauld, 1982b):

The tests were conducted at US Army Dugway Proving Ground, Utah, during September to November, 1981. Smoke pots from four countries were tested: ABC-M5 (United States), No. 24 MK5 (United Kingdom), Type 3-00 (Japan), and Ground Type No. 24-SCI-SC 39 (Canada). All four types of smoke pots released HC smoke and a single pot was burned in each trial. A total of 59 trials were included in the archive, among which were 18 British, 17 Canadian, 7 Japanese, and 17 U.S. trials. All trials were conducted between 1600 and 2300 Greenwich time. The fill weights for the British, Canadian, Japanese and U.S. smoke pots are 13.02, 12.93, 12.40, and 13.61 kg, respectively. The effective source heights are 0.31 m for the British and Canadian smoke pots, 0.25 m for the Japanese smoke pot, and 0.24 m for the U.S. smoke pots.

Values of transmittance were measured at one-second intervals at four wavelengths (visible, 0.7 - 1.9, 1.06, and 3.4 μm) along a single LOS at a height of 2.0 m. Transmittance measurements made at 1.06 μm were used in the calculation of CLID. Figure 4-11 displays the measuring grid for the test.

Observations of σ_ϕ values were listed in the report.

Development Test I of Man-Portable Smoke Generators (Saterlie et al., 1981):

The tests were conducted at US Army Dugway Proving Ground, Utah, during April to June, 1981. Two types of smoke generators were tested: XM49 and M3A3. The M3A3 smoke generator released only fog oil during the trials, while the XM49 smoke generator released either fog oil, diesel oil, or infrared obscurant during the trials. A total of 38 trials were included in the archive, among which were six M3A3 trials, twelve XM49 trials with fog oil only, four XM49 trials with diesel oil only, four XM49 trials with infrared obscurant only, two XM49 trials with both diesel oil and infrared obscurant, and ten XM49 trials with both fog oil and infrared obscurant.

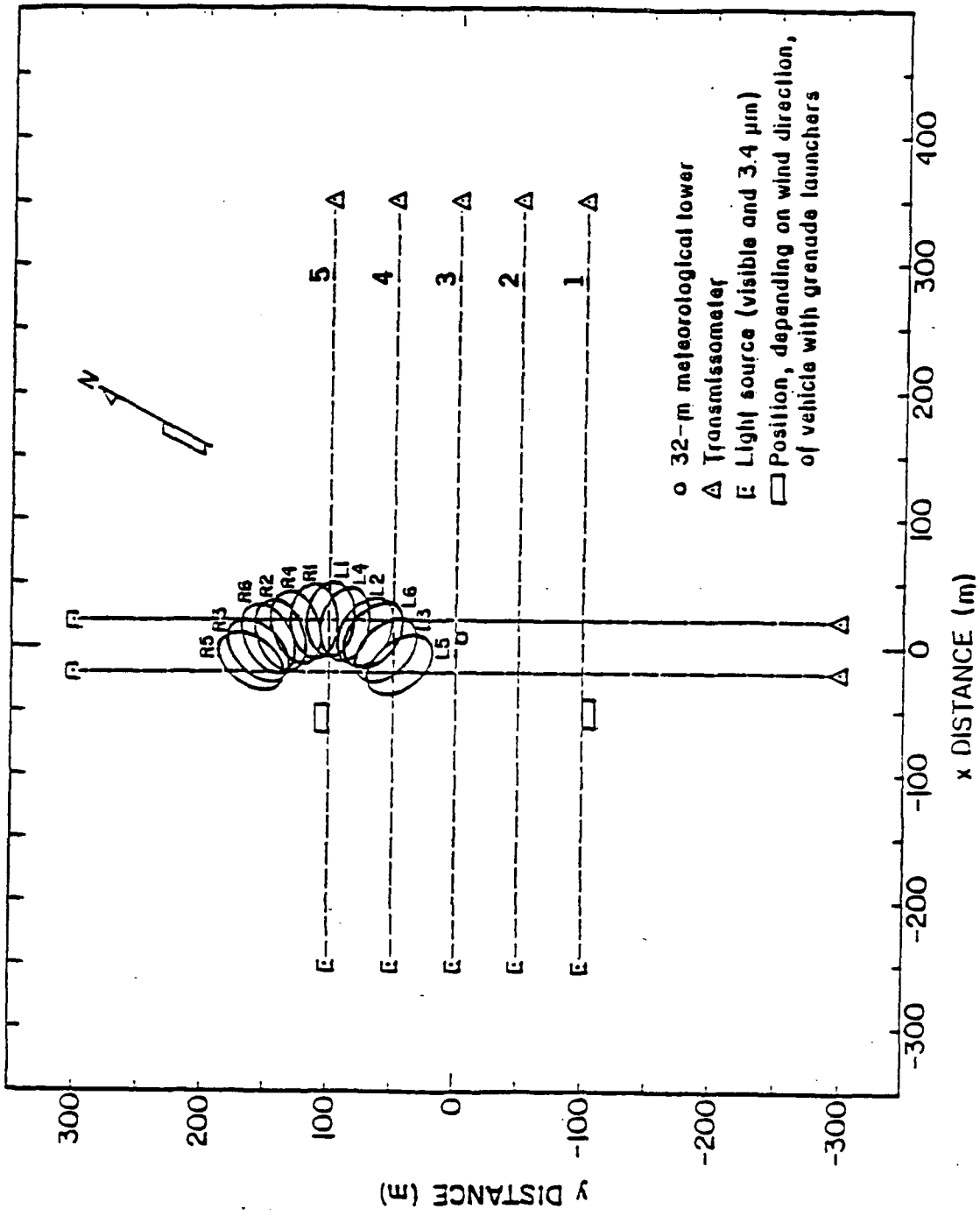

Figure 4-10. Measurement grid for the evaluation of reworked L8A1 and product improved L8A3 screening smoke grenades, from Saterlie and Dumbauld, 1982a. Also shown is the representative ground pattern of the L8A1 grenades for a salvo of 12 grenades fired from the M239 grenade launcher (alphanumeric designations of the patterns indicate the launcher tube used). Large numerical values designate LOS's whose data were used in the calculation.

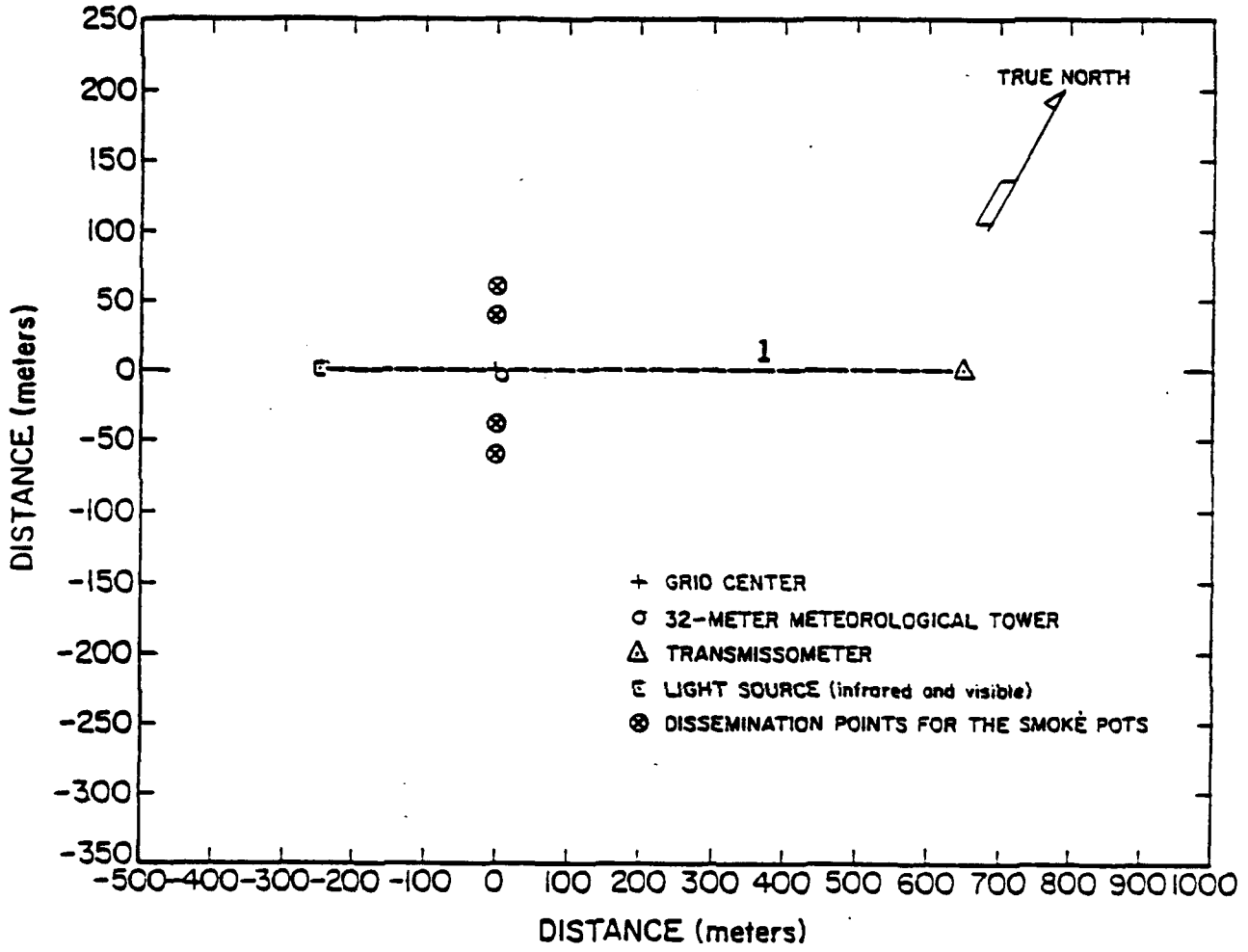

Figure 4-11. Measurement grid for the evaluation of foreign smoke pots, from Saterlie and Dumbauld, 1982b. Large numerical values designate the LOS whose data were used in the calculations.

Multiple-obscurant releases were achieved using two to four XM49 smoke generators with each generator releasing only one type of obscurant. All trials were conducted between 1500 and 2300 Greenwich time. The source strength for each smoke generator was typically from 12 to 20 kg. The effective source height is 0.38 m for the XM49 smoke generator, and 0.30 m for the M3A3 smoke generator.

A single volume source was used to represent each smoke generator. The initial source dimensions of the smoke generators required by the diffusion models were not measured. However, visual observations indicated that both the XM49 and M3A3 smoke generators emitted a smoke cloud with an approximate diameter of 1 m at a distance of 1 m downwind from the source. Therefore, it is assumed that the alongwind, crosswind and vertical source dimensions, σ_{x0}, σ_{y0}, and σ_{z0}, are 1/4.3 = 0.23 m.

Values of transmittance were measured at one-second intervals at four wavelengths (visible, 1.06, 3.4, and 8 - 12 μm) along five LOS's at a height of 2.44 m. However, transmittance data from two LOS's were not used. For multiple-obscurant releases it is possible to distinguish the contribution to the CLID data from each obscurant, because transmittance measurements were made at more than a single wavelength. Figure 4-12 displays the measurement grid for the test.

σ_ϕ values were derived from observations of σ_θ values based on Equation (4-1).

Atterbury-87 Field Study (Liljegren et al., 1989; DeVaull et al., 1989):

The tests were conducted at Camp Atterbury, Indiana, during November, 1987. The study involved four releases of fog oil smoke and five releases of HC smoke. All releases were conducted during daytime. The fog oil smoke was produced from SGF-2 fog oil using a single M3A4 smoke generator. The HC smoke was produced using 18 to 20 M5 HC smoke pots per test where the smoke pots were burned over a period of between 25 and 47 minutes. The source strengths for the fog oil trials ranged from 44 to 193 kg. Each HC smoke pot contains a charge of 13.6 kg material, and the source strengths for the HC trials were between 200 and 240 kg. The effective source heights were 1.0 m for the fog oil trials, 0.4 m for the first HC trial, and 1.5 m for the remaining HC trials.

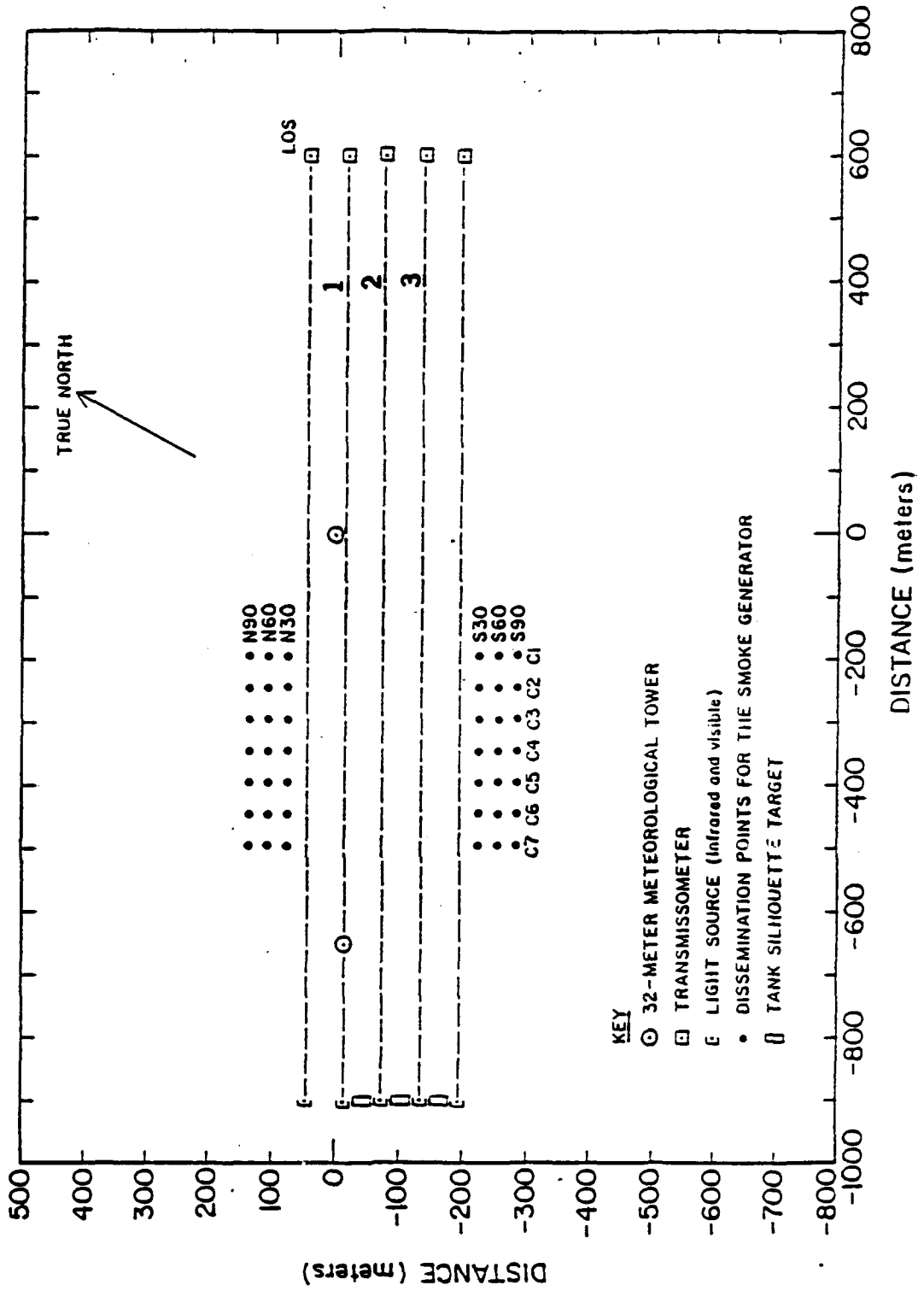

Figure 4-12. Measurement grid for development test I of XM49 man-portable smoke generator system for trials FO-01 through FO-19 (fog oil), from Saterlie, et al., 1981). Large numerical values designate LOS's whose data were used in the calculation.

The plume was mapped using 50 sampling masts organized into five linear transects at distances of 50, 100, 250, 450, and 675 m from the source. On each of the first four transects concentrations were measured at heights of 1, 2, 4, and 8 m above the ground; on the fifth transect concentrations were measured at heights of 2 and 8 m. The value of CLID along each transect was obtained by numerically integrating the maximum dosages at each sampler along that transect. The data obtained along the fifth transect were not used since only four sampling masts were employed. Figure 4-13 displays the measurement grid for the test.

Extensive high quality meteorological data were collected during the study, including σ_u, σ_v, and σ_w, the standard deviations of the fluctuations in the u-, v-, and w-components of the winds, respectively.

C. Preparation of Dugway Data Archive (DDA)

Data from the historical and smoke datasets need to be placed in a common format so that the user can efficiently conduct analyses using these datasets. The so-called Dugway Data Archive (DDA) has been developed for this purpose. The DDA contains enough information to satisfy the input requirements of all of the analysis procedures described in Section IX. It certainly does not contain all of the data from each experiment. Therefore, the DDA is a subset of the complete dataset. Tables 4-3 and 4-4 list the information contained in a DDA file. Most of the entries are self-explanatory. As described later, there are some entries that are required, and other entries that can be missing.

At the beginning of the DDA, information is given that defines the experiment and trial, such as experiment name, trial name (cannot be longer than five letters), location of the site, the number of trials included in the DDA, and date and time when the trials were conducted.

Next, the DDA contains information related to the source conditions, including the location, elevation, emission rate, total mass emitted, duration, and initial dimensions of the source. Because only one emission rate is used to characterize each source, it is implied that all sources are treated as quasi-steady state releases by the DDA. The coordinates used are such that x is positive eastward, and y is positive northward. Multiple

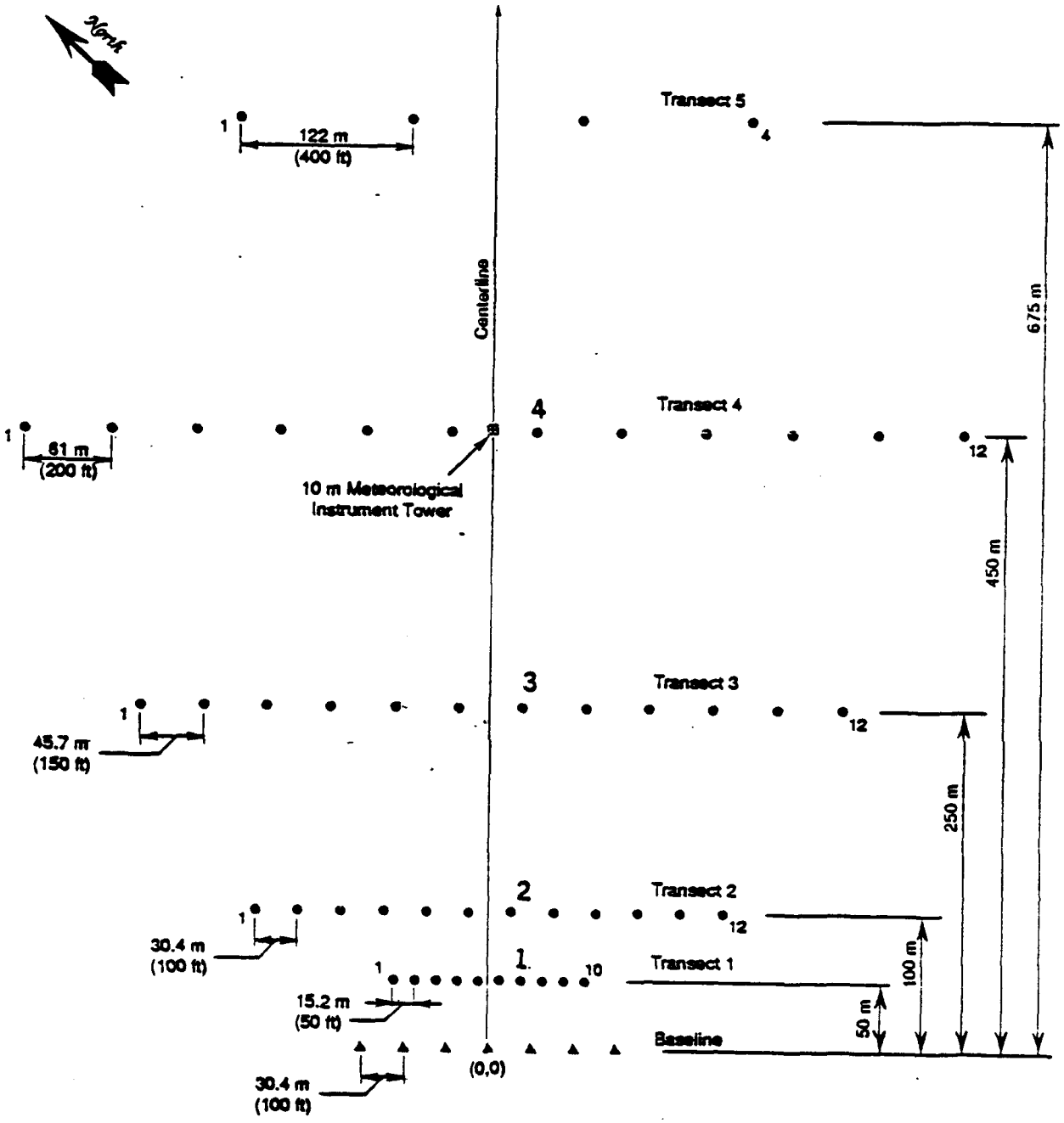

Figure 4-13. Nominal sampling network for Atterbury 87 dispersion field study, from Liljegren et al., 1989. Large numerical values designate LOS's whose data were used in the calculation. Dots are monitoring sites, and triangles are optional source locations.

Table 4-3

List of Information Contained in a DDA File. The Example Presented Here is from the PG Dataset (Prairie Grass Experiments, Barad, 1958; Only the First Trials were Listed). Note That There Were Only Concentrations Measured Along Concentric Arcs.

```
Prairie Grass
         6 : number of trials included in DDA
         6 : time zone designation
     42.30 : latitude (deg)
     98.30 : longitude (deg)
       pg7         pg8         pg9        pg10        pg13        pg15 : trial ID
         7           7           7           7           7           7 : month
        10          10          11          11          22          23 : day
      1956        1956        1956        1956        1956        1956 : year
        14          17          16          12          20           8 : hour
        15           0           0           0           0           0 : minute
         1           1           1           1           1           1 : no. of sources
       0.0         0.0         0.0         0.0         0.0         0.0 : x-coord. of source (m)
       0.0         0.0         0.0         0.0         0.0         0.0 : y-coord. of source (m)
      0.45        0.45        0.45        0.45        0.45        0.45 : source elevation (m)
    89.900      91.100      92.000      92.100      61.100      95.500 : emission rate (g/s)
     600.0       600.0       600.0       600.0       600.0       600.0 : emission duration (s)
     -99.9       -99.9       -99.9       -99.9       -99.9       -99.9 : total mass emitted (kg)
     0.000       0.000       0.000       0.000       0.000       0.000 : sigx0 at the source (m)
     0.000       0.000       0.000       0.000       0.000       0.000 : sigy0 at the source (m)
     0.000       0.000       0.000       0.000       0.000       0.000 : sigz0 at the source (m)
     -99.9       -99.9       -99.9       -99.9       -99.9       -99.9 : ambient pressure (atm)
     -99.9       -99.9       -99.9       -99.9       -99.9       -99.9 : relative humidity (%)
    305.15      305.15      301.15      304.15      293.15      295.15 : temperature at level #1 (K)
      2.00        2.00        2.00        2.00        2.00        2.00 : measuring height for temperature #1 (m)
    303.55      303.95      299.55      302.15      295.05      294.05 : temperature at level #2 (K)
     16.00       16.00       16.00       16.00       16.00       16.00 : measuring height for temperature #2 (m)
      4.20        4.90        6.90        4.60        1.30        3.40 : wind speed (m/s) at a tower
      2.00        2.00        2.00        2.00        2.00        2.00 : measuring height for wind data (m)
      4.20        4.90        6.90        4.60        1.30        3.40 : domain-averaged wind speed (m/s)
     186.0       184.0       204.0       225.0       190.0       209.0 : domain-averaged wind direction (deg)
     -99.90      -99.90      -99.90      -99.90      -99.90      -99.90 : domain-averaged sigma-u (m/s)
     25.60       10.20       10.20       16.80        3.20       12.80 : domain-averaged sigma-theta (deg)
     -99.90      -99.90      -99.90      -99.90      -99.90      -99.90 : domain-averaged sigma-phi (deg)
      2.00        2.00        2.00        2.00        2.00        2.00 : measuring ht for domain-avg wind speed (m)
     600.0       600.0       600.0       600.0       600.0       600.0 : averaging time for domain-avg data (s)
   -99.900     -99.900     -99.900     -99.900     -99.900     -99.900 : wind speed power law exponent
    0.0060      0.0060      0.0060      0.0060      0.0060      0.0060 : surface roughness (m)
     0.310       0.310       0.460       0.320       0.090       0.230 : friction velocity (m)
   -0.1020     -0.0556     -0.0323     -0.0909      0.2941     -0.1316 : inverse Monin-Obukhov length (1/m)
      0.20        0.20        0.20        0.20        0.20        0.20 : albedo
      0.50        0.50        0.50        0.50        0.50        0.50 : moisture availability
      2.00        2.00        2.00        2.00        2.00        2.00 : Bowen raio
    1539.0      1580.0       626.0      1090.0       -99.9        86.0 : mixing height (m)
       0.0         0.0        30.0        30.0        20.0         0.0 : cloud cover (%)
         2           3           3           2           6           1 : P-G stability class
     600.0       600.0       600.0       600.0       600.0       600.0 : averaging time for concentration (s)
      1.50        1.50        1.50        1.50        1.50        1.50 : suggested receptor height (m)
         5           5           5           5           5           5 : no. of distances downwind
      50.0        50.0        50.0        50.0        50.0        50.0 : distances downwind (m)
 9.260E+01   3.963E+02   1.858E+02   1.704E+02  -9.990E+01   3.887E+02 : concentration (mg/m**3)
 4.001E+03   5.102E+03   3.698E+03   4.504E+03  -9.990E+01   7.096E+03 : cross-wind integrated conc. (mg/m**2)
      6.20        6.60        9.00       12.30      -99.90        8.60 : sigma-y (m)
     100.0       100.0       100.0       100.0       100.0       100.0 : distances downwind (m)
 2.167E+01   1.066E+02   5.272E+01   4.052E+01  -9.990E+01   1.031E+02 : concentration (mg/m**3)
 2.203E+03   2.596E+03   2.199E+03   1.796E+03  -9.990E+01   3.400E+03 : cross-wind integrated conc. (mg/m**2)
     12.00       12.00       18.00       20.00      -99.90       16.00 : sigma-y (m)
     200.0       200.0       200.0       200.0       200.0       200.0 : distances downwind (m)
 4.225E+00   2.378E+01   1.306E+01   1.050E+01  -9.990E+01   2.063E+01 : concentration (mg/m**3)
 9.979E+02   1.102E+03   1.003E+03   7.101E+02  -9.990E+01   1.347E+03 : cross-wind integrated conc. (mg/m**2)
     22.30       21.30       33.00       35.00      -99.90       26.00 : sigma-y (m)
     400.0       400.0       400.0       400.0       400.0       400.0 : distances downwind (m)
 6.841E-01   3.781E+00   2.696E+00   2.487E+00   1.246E+02   4.536E+00 : concentration (mg/m**3)
 4.001E+02   3.899E+02   4.103E+02   1.999E+02  -9.990E+01   3.696E+02 : cross-wind integrated conc. (mg/m**2)
     39.00       41.00       63.00       61.00      -99.90       45.00 : sigma-y (m)
     800.0       800.0       800.0       800.0       800.0       800.0 : distances downwind (m)
 7.363E-02   6.714E-01   4.839E-01   1.584E-01   9.898E+01   5.186E-01 : concentration (mg/m**3)
 1.798E+02   1.403E+02   1.297E+02   3.223E+01   8.126E+03   1.098E+02 : cross-wind integrated conc. (mg/m**2)
     71.00       86.00      116.00       97.00      -99.90       92.00 : sigma-y (m)
         0           0           0           0           0           0 : no. of lines-of-sight
```

Table 4-4

List of Information Contained in a DDA File. The Example Presented Here is from the L81A1 Dataset (Comparison Test of L8A1 Screening Smoke Grenades, Rafferty and Dumbauld, 1983; Lot A Only). Note That There Were Only Integrated Concentrations Measured Along Lines-of-Sight (LOS).

The Evaluation of the L8 Series Grenades (L81A1)							
7							: number of trials included in DDA
6							: time zone designation
40.20							: latitude (deg)
113.00							: longitude (deg)
BB2	BB3	BB4	BB5	BB6	BB7	BB9	: trial ID
6	6	6	6	6	6	6	: month
10	10	10	10	10	15	17	: day
81	81	81	81	81	81	81	: year
10	11	12	13	14	11	11	: hour
11	51	59	51	29	22	18	: minute
1	1	1	1	1	1	1	: no. of sources
-62.9	-24.4	-24.4	-24.4	-24.4	-45.4	-24.4	: x-coord. of source (m)
68.0	89.4	89.4	89.4	89.4	77.7	89.4	: y-coord. of source (m)
0.00	0.00	0.00	0.00	0.00	0.00	0.00	: source elevation (m)
-99.9	-99.9	-99.9	-99.9	-99.9	-99.9	-99.9	: emission rate (g/s)
251.0	251.0	251.0	251.0	251.0	251.0	251.0	: emission duration (s)
0.897	0.859	0.840	0.840	0.840	0.878	0.859	: total mass emitted (kg)
9.389	4.224	6.857	8.154	0.491	11.425	2.407	: sigx0 at the source (m)
13.758	16.112	15.180	14.524	16.649	12.120	16.482	: sigy0 at the source (m)
0.120	0.120	0.120	0.120	0.120	0.120	0.120	: sigz0 at the source (m)
-99.9	-99.9	-99.9	-99.9	-99.9	-99.9	-99.9	: ambient pressure (atm)
-99.9	-99.9	-99.9	-99.9	-99.9	-99.9	-99.9	: relative humidity (%)
300.00	300.00	300.00	300.00	300.00	300.00	300.00	: temperature at level #1 (K)
2.00	2.00	2.00	2.00	2.00	2.00	2.00	: measuring height for temperature #1 (m)
-99.90	-99.90	-99.90	-99.90	-99.90	-99.90	-99.90	: temperature at level #2 (K)
-99.90	-99.90	-99.90	-99.90	-99.90	-99.90	-99.90	: measuring height for temperature #2 (m)
3.10	3.80	2.80	3.60	3.20	2.20	5.60	: wind speed (m/s) at a tower
2.00	2.00	2.00	2.00	2.00	2.00	2.00	: measuring height for wind data (m)
3.10	3.80	2.80	3.60	3.20	2.20	5.60	: domain-averaged wind speed (m/s)
335.0	24.0	345.0	340.0	11.0	326.0	1.0	: domain-averaged wind direction (deg)
-99.90	-99.90	-99.90	-99.90	-99.90	-99.90	-99.90	: domain-averaged sigma-u (m/s)
13.70	10.70	28.80	28.10	16.40	24.30	10.10	: domain-averaged sigma-theta (deg)
-99.90	-99.90	-99.90	-99.90	-99.90	-99.90	-99.90	: domain-averaged sigma-phi (deg)
2.00	2.00	2.00	2.00	2.00	2.00	2.00	: measuring ht for domain-avg wind speed (m)
267.0	252.0	245.0	255.0	287.0	600.0	211.0	: averaging time for domain-avg data (s)
0.048	0.047	0.079	0.073	0.106	0.049	0.042	: wind speed power law exponent
0.0300	0.0300	0.0300	0.0300	0.0300	0.0300	0.0300	: surface roughness (m)
-99.900	-99.900	-99.900	-99.900	-99.900	-99.900	-99.900	: friction velocity (m)
-99.9000	-99.9000	-99.9000	-99.9000	-99.9000	-99.9000	-99.9000	: inverse Monin-Obukhov length (1/m)
0.18	0.18	0.18	0.18	0.18	0.18	0.18	: albedo
0.50	0.50	0.50	0.50	0.50	0.50	0.50	: moisture availability
0.50	0.50	0.50	0.50	0.50	0.50	0.50	: Bowen ratio
-99.9	-99.9	-99.9	-99.9	-99.9	-99.9	-99.9	: mixing height (m)
-99.9	-99.9	-99.9	-99.9	-99.9	-99.9	-99.9	: cloud cover (%)
-99	-99	-99	-99	-99	-99	-99	: P-G stability class
251.0	251.0	251.0	251.0	251.0	251.0	251.0	: averaging time for concentration (s)
1.00	1.00	1.00	1.00	1.00	1.00	1.00	: suggested receptor height (m)
0	0	0	0	0	0	0	: no. of distances downwind
2	2	2	2	2	2	2	: no. of lines-of-sight
-247.7	-247.7	-247.7	-247.7	-247.7	-247.7	-247.7	: x-coord. of 1st end-point for LOSi (m)
-68.7	-68.7	-68.7	-68.7	-68.7	-68.7	-68.7	: y-coord. of 1st end-point for LOSi (m)
189.6	189.6	189.6	189.6	189.6	189.6	189.6	: x-coord. of 2nd end-point for LOSi (m)
173.7	173.7	173.7	173.7	173.7	173.7	173.7	: y-coord. of 2nd end-point for LOSi (m)
-99.9	-99.9	-99.9	-99.9	-99.9	-99.9	-99.9	: LOS integrated conc. (mg/m**2)
2.510E+04	5.300E+04	2.840E+04	3.490E+04	5.140E+04	1.700E+04	5.070E+04	: LOS integrated dosage (mg-s/m**2)
-189.6	-189.6	-189.6	-189.6	-189.6	-189.6	-189.6	: x-coord. of 1st end-point for LOSi (m)
-173.7	-173.7	-173.7	-173.7	-173.7	-173.7	-173.7	: y-coord. of 1st end-point for LOSi (m)
247.7	247.7	247.7	247.7	247.7	247.7	247.7	: x-coord. of 2nd end-point for LOSi (m)
68.7	68.7	68.7	68.7	68.7	68.7	68.7	: y-coord. of 2nd end-point for LOSi (m)
-99.9	-99.9	-99.9	-99.9	-99.9	-99.9	-99.9	: LOS integrated conc. (mg/m**2)
6.500E+03	-9.990E+01	7.600E+03	-9.990E+01	-9.990E+01	6.400E+03	2.490E+04	: LOS integrated dosage (mg-s/m**2)

sources with completely different attributes are allowed. Because the DDA has a "flat" two-dimensional structure like a table, for trials with different numbers of sources, it is necessary to insert "missing" records for those trials with less sources so that the two dimensional arrays of the DDA are all filled.

Meteorological data appear next in the DDA. These include the basic data such as ambient pressure, relative humidity, temperatures at two levels on a tower, wind speed at one level on a tower, averaged wind speed and direction, cloud cover, mixing height, and standard deviations of wind speed, wind azimuth angle, and wind elevation angle. Furthermore, there are entries for the inverse of the Monin-Obukhov length, friction velocity, surface roughness, wind speed profile power-law exponent (a measure of the distribution of wind speed with height), albedo, Bowen Ratio (a measure of the relative importance of the latent heat flux and sensible heat flux), Pasquill-Gifford stability class, and moisture availability (a measure of the wetness of the ground on a scale from 0, dry, to 1.2, saturated) Note that relative humidity, cloud cover, albedo, and moisture availability are currently not used by the program, but are included in anticipation of application of improved boundary layer analysis procedures to the dataset.

The remaining part of the DDA is related to concentrations. Receptor height and averaging time for concentrations appear first. Then all data related to concentric arcs follow, including distance downwind, highest observed point concentration, crosswind integrated concentration, and the width of the plume. All data related to lines-of-sight (LOS) appear last, including the locations of the end points of the LOS (necessary because each LOS is not necessarily perpendicular to the wind direction), and LOS-integrated concentration and dosage. The coordinates used are such that x is positive eastward, and y is positive northward. At present, it is required that all trials in the DDA have the same number of arcs and LOS's. This is mainly for the ease of processing and integrating the results later on. Moreover, the same sampling instruments were almost always used during the experiment.

It is *very important* that the concentration data be subject to careful examinations before they are included in the DDA, particularly for the data obtained from the trials similar to those in the smoke datasets described

above. For example, do not include measurements from a LOS if one of the following conditions applies: 1) the LOS intersected the location of the source pattern, 2) the LOS did not contain the major part of the plume, and 3) the LOS was not sufficiently perpendicular to the prevailing wind direction. If such precautions are not taken, the subsequent analyses of the source strength will be severely handicapped.

When preparing the DDA, the following requirements apply:

- Trial name cannot be longer than five letters.

- Temperature and measuring height at at least one level on a tower should be available.

- Domain-averaged wind speed and direction together with measuring height cannot be missing.

- Surface roughness cannot be missing.

- At least one of the following four stability parameters should be available: the inverse of the Monin-Obukhov length, temperature at two levels, Pasquill-Gifford stability class, and standard deviation of the wind azimuth angle.

- Source location cannot be missing.

- Emission rate and total mass emitted cannot be missing at the same time. Otherwise, the source strength cannot be estimated in any way.

- Total mass emitted and source duration cannot be missing at the same time. This is because there would be no way of estimating the total mass emitted.

- If only the total mass emitted is known, and both the emission rate and source duration are missing, it is arbitrarily assumed that the source duration is 600 s. This assumption is not of consequence if one is only dealing with dosages, since the time dependence will be eventually removed through the integration in time.

- The relationship of "emission rate = total mass emitted/source duration" (i.e., quasi-steady state) is always assumed by the program. In other words, when two of the variables are known, the other one is determined.

- If the standard deviation for either the wind azimuth angle or the wind elevation angle is known, then the associated averaging time also has to be known.

- Only one source is allowed if there are any concentric monitoring arcs. Otherwise, the downwind distance for each arc cannot be defined.

- Wind speed at one level on a tower, if missing, is assumed to equal the domain-averaged wind speed.

- The following default values will be assumed for the following variables, if missing:

pressure	1 atm
relative humidity	80 %
Bowen Ratio	5
mixing height	1000 m
receptor height	0
initial source dimensions	0

Other variables, such as Pasquill-Gifford stability class and the inverse of the Monin-Obukhov length, when missing, can be derived from the known variables based on physical relationships discussed in detail in Section 6.

The complete listing of all the DDA files is included in Appendix F.

Intentionally Blank

SECTION V

ACQUISITION OF SIMILARITY, STATISTICAL, AND DETERMINISTIC ANALYSIS PROCEDURES FOR RELATING CONCENTRATIONS, SOURCE EMISSIONS, AND METEOROLOGICAL CONDITIONS

Many different analysis procedures could have been selected for use in scaling concentrations in order to estimate emission strengths. We have chosen nine procedures which are representative of linear regression formulas, best fit similarity formulas, and Gaussian formulas. Several of the coefficients in these formulas are derived from the Prairie Grass dataset. In the sections that follow, we describe the methods used in developing these data analysis procedures. More information on their performance when evaluated against the Prairie Grass dataset is contained in the paper reproduced in Appendix C.

A. Methods of Analysis of Data with the Goal of the Development of Regression Formulas

The analysis procedures suggested by Box and Jenkins (1976) were applied to the Prairie Grass data set in order to derive relations among the observed variables. The three steps in this analysis are briefly described below.

1. Identification - In this step the data are analyzed using physical insights of the investigators. For example, the important functional relationships can be identified by means of dimensional analysis. Using this information, the data are studied by plotting time series, by calculating correlations, and by plotting various combinations of data versus other combinations of data.

2. Estimation - In this step, the insights gained from Step 1 are used to formulate mathematical expressions. These could be simple linear regression equations, where the parameters are "estimated" from the data by some sort of least-square minimization procedure. Or they could be based on known physical relations, such as continuity of mass, kinetic energy, and enthalpy. In the latter case, parameters required for

closure, such as entrainment rates or eddy diffusivity coefficients, must still be "estimated" from observations. A goal of this step should be that the parameters are not highly correlated with each other and that the formula is stable (i.e., relatively insensitive to errors in input data).

3. Diagnosis – In this step, the predictions and the observations should be diagnosed in order to assure that the following objectives are reached:

   - The residuals (predictions minus observations) should resemble white noise; i.e., the residuals should not be a function of any of the input variables.
   - The rmse (root mean square of residuals) should be "relatively small."
   - A paucity of terms is desired.
   - The analysis formulas should be compared with a new, independent data base.

   As another component of step 3, we add the comparative evaluation of two or more alternative procedures, where it is determined whether the differences between the performance measures (e.g., correlation coefficient) are significant at the 95% confidence level. The procedures that shall be considered include those regression formulas resulting from Step 2, plus whatever procedures have previously been suggested (e.g., Briggs, 1982).

B. Identification of Relationships Among Variables in the Prairie Grass Database

As a first step, the various meteorological data from the 44 Prairie Grass experiments listed in Table 1 of Appendix C were plotted against each other, with some of the results shown in Figure 5-1. These figures, as well as most of the analyses described in this section, were included in a journal article by Hanna et al (1990). Note that the inverse Monin-Obukhov length 1/L is used rather than L, since functions of 1/L are continuous across 0 (i.e., neutral conditions) while functions of L have a discontinuity at 0. The following ranges for the 44 points are seen:

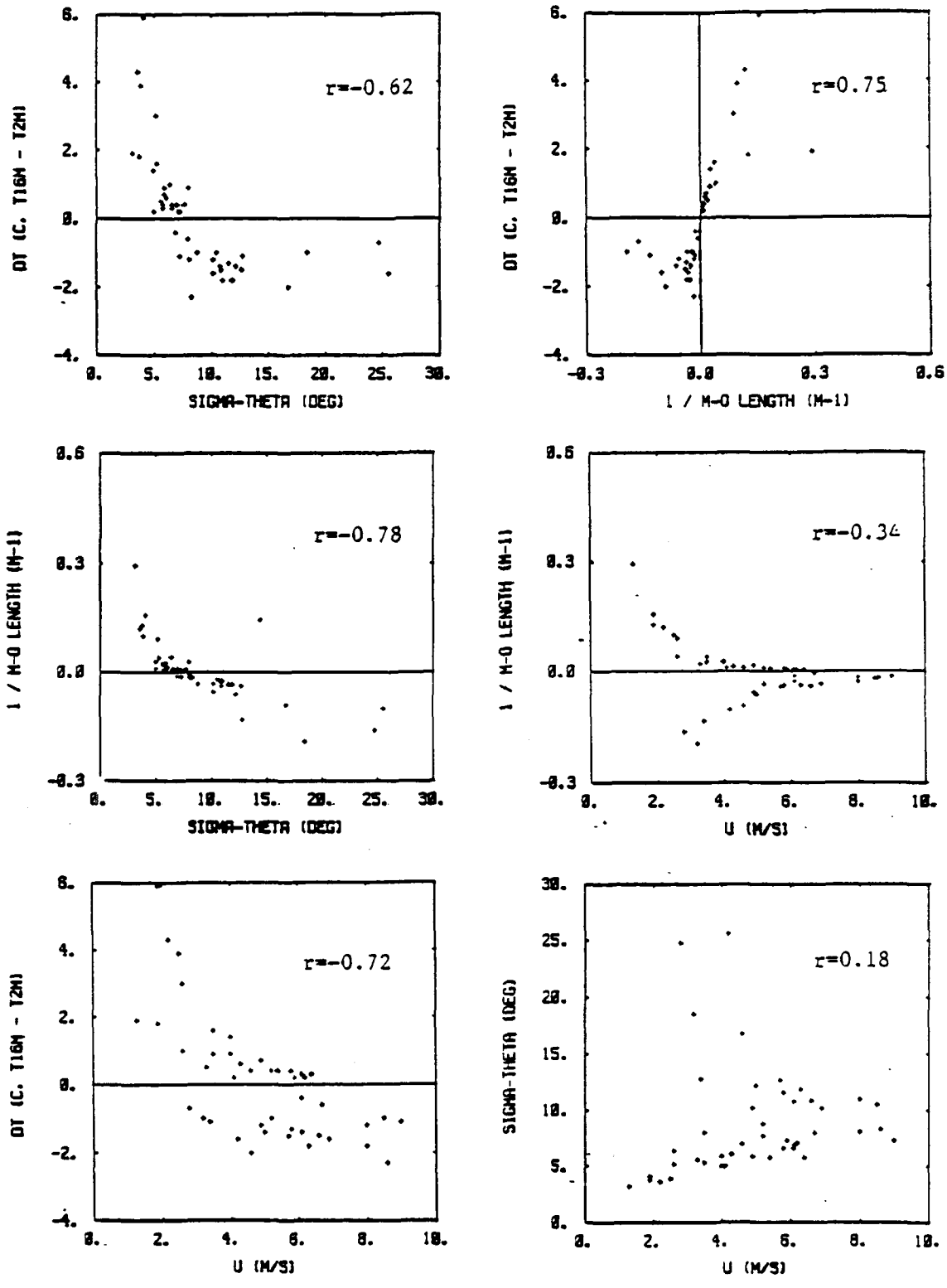

Figure 5-1. Plots of meteorological data from the 44 Prairie Grass experiments, as listed in Table 1 of Appendix C. Correlations, r, are listed on each plot.

DT (16 m - 2 m)	-2.3°C to 3.9° C
σ_θ (2 m)	4° to 26°
u (2 m)	1.9 m/s to 9.1 m/s
1/L	-0.19 m^{-1} to 0.13 m^{-1}

It is seen that the experiments are about evenly split between stable and unstable conditions. The correlations between meteorological variables, given on each figure, are good (i.e., magnitudes of about 0.6 to 0.8), except for the 1/L versus u and the σ_θ versus u plots. The poor correlations for the latter two plots are due to the fact that light winds occur during both stable and unstable periods. Consequently the plots with u contain two branches, one for stable and one for unstable conditions, which tend to cancel each other when correlations are calculated. It is also evident that DT tends to better order σ_θ, 1/L, and u during stable conditions--a conclusion reached earlier by Briggs and McDonald (1978). The good correlation among several variables suggests that a small subset of them should be able to explain most of the variance in the concentration measurements.

The observed normalized maximum concentration, C/Q, and cross-wind integrated concentration, C^y/Q, at each downwind arc are also listed in Table 1 in Appendix C. The source emission rate, Q, which is used as a normalizing factor for C or C^y, was controlled by the experimentalists, who released about twice as much tracer gas during unstable conditions than stable conditions, and showed relatively little variability (about ± 10 to 20%) within unstable or stable classes over the duration of the experiments. The source emission rates are discussed later in more detail. Examples of plots of C^y/Q versus u, σ_θ, DT, and 1/L for the 800 m arc are given in Figure 5-2. The C^y/Q versus u plot has two branches, with the lower branch for unstable conditions and the upper branch for stable conditions. The other three plots show good ordering of the points, with the C^y/Q versus 1/L plot showing a nearly-linear dependence. The agreement among these three plots is expected, however, because of the good correlation among σ_θ, DT, and 1/L evident in Figure 5-1.

Plots for the closer monitoring arcs showed similar behavior, but with less and less variability in C^y/Q across the figures as x decreased. This

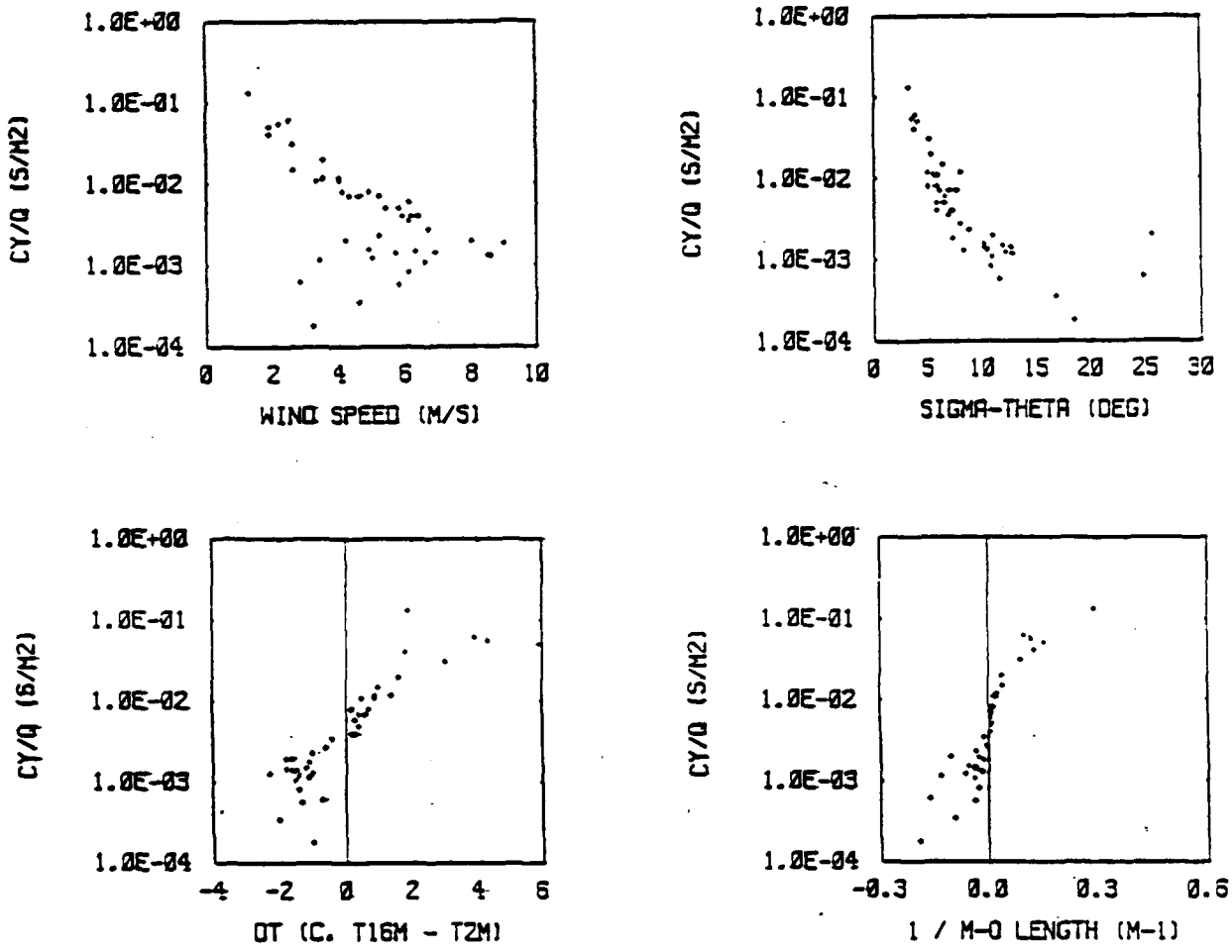

Figure 5-2. Plots of C^y/Q on the 800 m arc as functions of meteorological variables, for Prairie Grass data.

phenomenon is due to the fact that the depth of the cloud is less at smaller distances, thus assuring that diffusion is dominated by mechanical effects (i.e., wind shear).

Also, although it is not shown here, there is a strong decrease in concentration with distance, approximately following the power laws, $C/Q \propto x^{-2}$ and $C^y/Q \propto x^{-1}$. For example, the correlation coefficient between C/Q and x is -0.43, and between ℓn C/Q and ℓn x is -0.75 (the correlation is higher for the log transformation because of the -2 power law relation).

Nou (1963) applied standard multivariate general linear regression hypotheses to these data, as well as similar field data from the Ocean Breeze and Dry Gulch experiments, to derive the coefficients in a general regression equation of the form:

$$C/Q = a_1 x^{a_2} \sigma_\theta^{a_3} (DT + 10^\circ F)^{a_4} u^{a_5} \qquad (5\text{-}1)$$

Because the regression procedure works with the logarithm of the variables, the constant, 10°F, has been added to DT to avoid negative values. The units of the variables are: C/Q (s/m^3), x (m), σ_θ (deg), DT (°F), and u (m/s). The following coefficients were derived by Nou (1963) from half of the total data base:

$$C/Q = a_1 x^{a_2} \sigma_\theta^{a_3} (DT + 10^\circ F)^{a_4} u^{a_5}$$

	a_1	a_2	a_3	a_4	a_5
All variables	1.24	-2.08	-0.858	3.49	-0.503
Ignore u	0.00211	-1.96	-0.506	4.33	0
Ignore u and σ_θ	0.000175	-1.95	0	4.92	0

The formula $C/Q = 0.000175\ x^{-1.95} (DT + 10)^{4.92}$ predicts 65% of the independent C/Q observations in the other half of the data base within a factor of 2, and 94% within a factor of 4. Note that the a_1 coefficient must have a peculiar mix of dimensions in order that the dimensions of the right hand side of the equation equal s/m^3.

A commercial statistical software package, SYSTAT, was applied to the Prairie Grass data (with DT converted to the units that Nou used) in order to attempt to test Nou's approach and to derive a statistically-based regression formula. It is important to recognize that this formula has little physical insight associated with it, other than what was used in choosing the variables. The following coefficients are derived from the SYSTAT multivariate linear regression procedure for four alternate formulas.

$$C/Q = a_1 x^{a_2} \sigma_\theta^{a_3} (DT + 10^\circ F)^{a_4} u^{a_5}$$

	a_1	a_2	a_3	a_4	a_5	% variance explained
All variables	65.56	-1.83	-1.86	1.31	-0.91	95.2
Ignore u	0.175	-1.82	-1.40	2.86	0	94.0
Ignore DT	6621	-1.83	-2.34	0	-1.33	94.7
Ignore u and DT	1583	-1.80	-2.72	0	0	89.4
Ignore u and σ_θ	0.000137	-1.81	0	4.72	0	90.8

The "a" coefficients are different from those derived by Nou (1963) because he included data from two other field sites and he included only half of the Prairie Grass data. The percentage of variance explained, as listed in the last column, is approximately equal to 90% to 95% for all four choices. In all cases, the "x" term explains most of the variance.. Observations of C/Q are compared with predictions of the "ignore u" formula in Figure 5-3. There is seen to be a slight curvature in the cloud of points, with tendencies towards overpredictions at extreme high or low concentrations.

The SYSTAT package was also applied to the cross-wind integrated concentration, C^y/Q, with the following results for the coefficients:

$$C^y/Q = a_1 x^{a_2} \sigma_\theta^{a_3} (DT + 10^\circ F)^{a_4} u^{a_5}$$

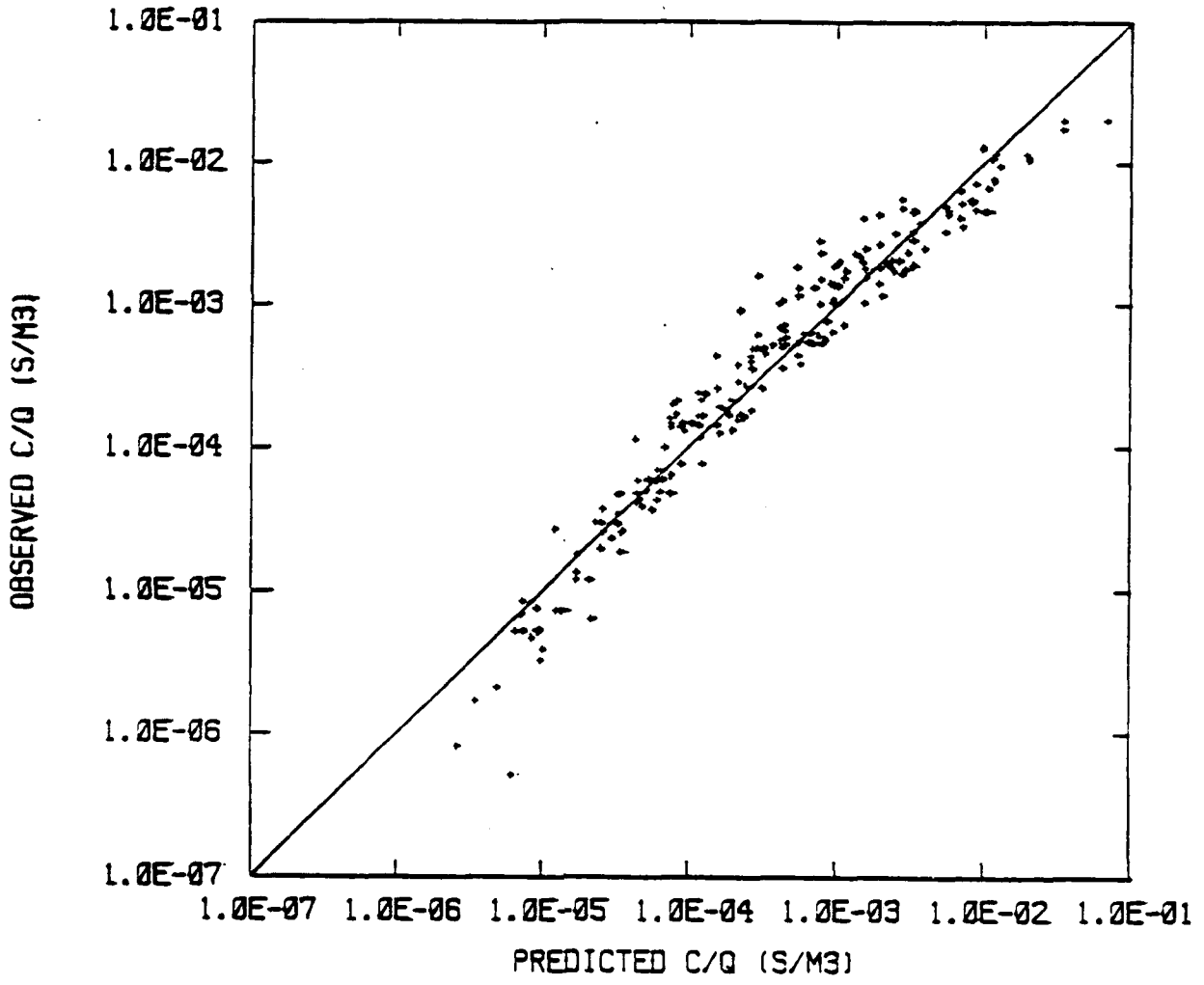

Figure 5-3. Comparison of observed C/Q at the Prairie Grass site with values predicted by $C/Q = 0.236\ x^{-1.74}\sigma_\theta^{-1.38}(\Delta T + 10)^{2.51}$, as derived by multiple linear regression procedure. 94% of the variance in the observed C/Q is accounted for by the predictions.

	a_1	a_2	a_3	a_4	a_5	% variance explained
All variables	46.8	-1.04	-1.03	0.55	-0.95	87.8
Ignore u	0.093	-1.03	-0.51	2.15	0	85.2
Ignore DT	329.6	-1.04	-1.23	0	-1.15	87.6
Ignore u and DT	0.0227	-1.04	0	2.52	-0.33	84.4
Ignore u and σ_θ	0.00666	-1.03	0	2.84	0	83.9

It was calculated that the "x" term explains about 55% of the variance, and each of the other terms explains about 10 to 20% of the variance. The reason why the regression formula can explain more of the variance in C/Q than in C^y/Q is because $C \propto x^{-2}$, while $C^y \propto x^{-1}$. Hence there is a much larger range in the C/Q observations than in the C^y/Q observations, since the range of observed x is constant in the two sets of data, ranging from 50 m to 800 m.

It must be remembered that these statistical regression formulas are valid only for the site, the source conditions, and the range of variables used in their derivation. Any extrapolation to other sites or meteorological conditions should be done very cautiously. Furthermore, because the statistical procedures use the logarithms of the variables, the average predicted C/Q does not necessarily equal the average observed C/Q.

C. Suspected Relations Based on Physical Insights

Scientists have been studying transport and dispersion for over 50 years and have conducted many detailed analyses of field data (Pasquill, 1961; Hanna et al., 1982; Draxler, 1984). They have used physical insights to derive several different dispersion formulas, which have been evaluated using the field data. In contrast to the purely statistical analysis presented in Section 4, the discussions in this section will emphasize formulas based on physical insights. The problem will be limited to the dispersion of non-buoyant inert gases released continuously near the ground surface, and will be limited to downwind distances of less than about 1 km.

Dimensional analysis can be applied to straightforward physical situations. According to the principles of dimensional analysis, if there

are n relevant variables and parameters associated with a problem (e.g., concentration, wind speed, distance, etc.) and these variables have m different dimensions (e.g., mass, speed, distance, etc.) then n - m independent dimensionless numbers can be formed. For example, the similarity theory of Monin and Obukhov (1954) would suggest that the following four variables are important in the Prairie Grass experiment:

Normalized concentration C/Q or C^y/Q	(s/m^3 or s/m^2)
Distance x	(m)
Monin-Obukhov length L	(m)
Friction velocity u_*	(m/s)

Physical insight is used to eliminate the wind speed, u, from consideration, since it is proportional to the friction velocity, u_*, which is on the list. Furthermore, it can be argued that the roughness length, z_o, is also implicitly contained in u_*, and thus does not need to be included. With 4 variables and 2 dimensions, there are then two independent dimensionless variables that can be formed, and the following functional relations can be postulated:

$$Cu_*x^2/Q = f_1(x/L) \tag{5-2}$$

$$C^y u_* x/Q = f_2(x/L) \tag{5-3}$$

where f_1 and f_2 are universal dimensionless function of x/L. The validity of this approach and the forms of these dimensionless functions can be found by plotting Cu_*x^2/Q versus x/L and $C^y u_* x/Q$ versus x/L, as is done in Figure 5-4. Note that each plot has two sections, one for positive x/L and one for negative x/L, since it is more convenient to use logarithmic scales. It is seen that the scaling methods resulting from the dimensional analysis are valid, since the points on the figures are following some monotonic curve.

Because the data in the four parts of Figure 5-4 appear to approach a constant as x/L approaches zero, the following functional relation is proposed:

$$f(x/L) = a(1 + bx/L)^c \tag{5-4}$$

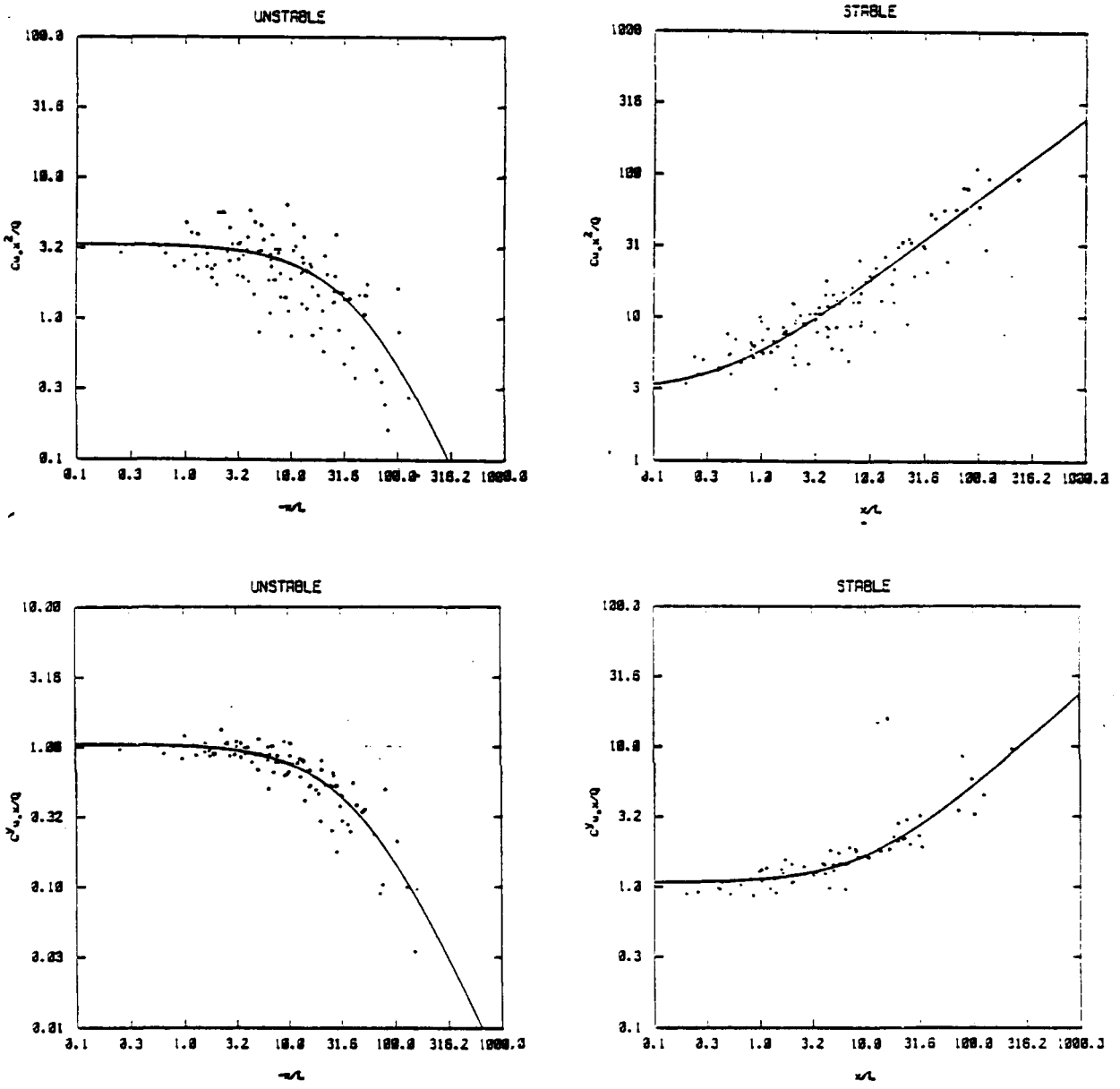

Figure 5-4. Prairie Grass data plotted in the dimensionless form suggested by equations (2) and (3). Best-fit lines of the form $a(1 + bx/L)^c$ are drawn on each figure (see equations 5-8).

A least-squares fitting algorithm was applied to each figure, with the following results:

$$f_1(x/L) = 3.37(1 - 0.019x/L)^{-1.86} \qquad x/L < 0 \qquad (5\text{-}5)$$

$$f_1(x/L) = 3.01(1 + 2.20x/L)^{0.57} \qquad x/L > 0 \qquad (5\text{-}6)$$

$$f_2(x/L) = 1.06(1 - 0.021x/L)^{-1.74} \qquad x/L < 0 \qquad (5\text{-}7)$$

$$f_2(x/L) = 1.07(1 + 0.10x/L)^{0.68} \qquad x/L > 0 \qquad (5\text{-}8)$$

These curves are drawn on the figures and appear to provide a good fit at all values of x/L. However, they have been derived with no requirements that certain physically-based asymptotic functional relationships be satisfied. For example, Briggs (1982) points out that $f_2(x/L)$ should be proportional to $(-x/L)^{1/2}$ in the limit of free convection ($-x/L \rightarrow \infty$).

As mentioned earlier, several researchers reanalyzed the Prairie Grass data from the viewpoint of either Monin-Obukhov or convective mixed layer similarity theory. Horst (1979) employs Monin-Obukhov similarity theory for diffusion from a ground-level source to derive the following relations:

$$d\bar{z}/dt = au_*G(\bar{z}/L) \qquad (5\text{-}9)$$

$$d\bar{x}/dt = u(c\bar{z}) \qquad (5\text{-}10)$$

where t is the time after emission of some diffusing material, a and c are universal constants, G is a universal dimensionless function of $\bar{z}/L$, $\bar{z}$ is the mean height of the diffusing material, and $\bar{x}$ is the mean horizontal displacement. A further assumption is made that the vertical distribution of material has the form:

$$C(z)/C(z=0) = \exp(-(z/b\bar{z})^d) \qquad (5\text{-}11)$$

where b and d are "constants". Unfortunately, there is no single equation resulting from Horst's analysis. Instead, the solution must be obtained by numerically integrating the set of governing equations with x and z. The

"constants" a, b, c, and d are determined by comparisons with data, including the Prairie Grass data, and in fact are slight functions of 1/L. Typical values are a ≈ 0.40, b ≈ 1.5, c ≈ 0.63 and d ≈ 1.5 (Hanna et al., 1982). Horst presents the graphical solution reproduced in Figure 5-5, valid for $10^2 \leq x/z_o \leq 10^7$ and $-10^{-2} \leq z_o/L \leq 10^{-2}$. Hanna et al. (1982) suggested that the curves in the figure could be approximated by power laws at each value of z_o/L; for example:

$$\text{At } z_o/L = 10^{-2} \qquad u_* z_o C^y/0.4Q = 0.75(x/z_o)^{-0.69} \tag{5-12}$$

$$\text{At } z_o/L = -10^{-2} \qquad u_* z_o C^y/0.4Q = 35(x/z_o)^{-1.54} \tag{5-13}$$

$$\text{At } z_o/L = 0 \qquad u_* z_o C^y/0.4Q = 2.4(x/z_o)^{-0.96} \tag{5-14}$$

Note that equation (5-14) is nearly equivalent to equation (5-3) with the assumption that $f_2(x/L) \approx 1$. The roughness length, z_o, which is used by Horst (1979) as a scaling distance, has little influence on the C^y curves, and can be seen to nearly cancel out of equation (5-14).

Van Ulden's (1978) analysis is very similar to Horst's, although van Ulden assumes power law profiles for wind speed and eddy diffusivity, and also discusses the effects of non-zero source elevations. He includes a table of L and u_* values for the Prairie Grass experiment and these values were used in the creation of the data base in Table 1 (Appendix C).

Nieuwstadt (1980) and Venkatram (1981) restrict themselves to the unstable and stable halves of the Prairie Grass data set, respectively. Nieuwstadt applies concepts from convective mixed layer similarity theory, which had its origins in the mid-1970's. This theory states that the characteristic convective velocity scale is w_*, which equals the cube root of the mixing depth, h, times the surface buoyancy flux, $g\overline{w'T'}/T$. The mixing depth is typically about 1000 m. Because of the relationship between the heat flux, u_*, and L, the convective velocity scale, w_*, can also be calculated from the formula:

$$w_* = u_*(h/0.4L)^{1/3} \tag{5-15}$$

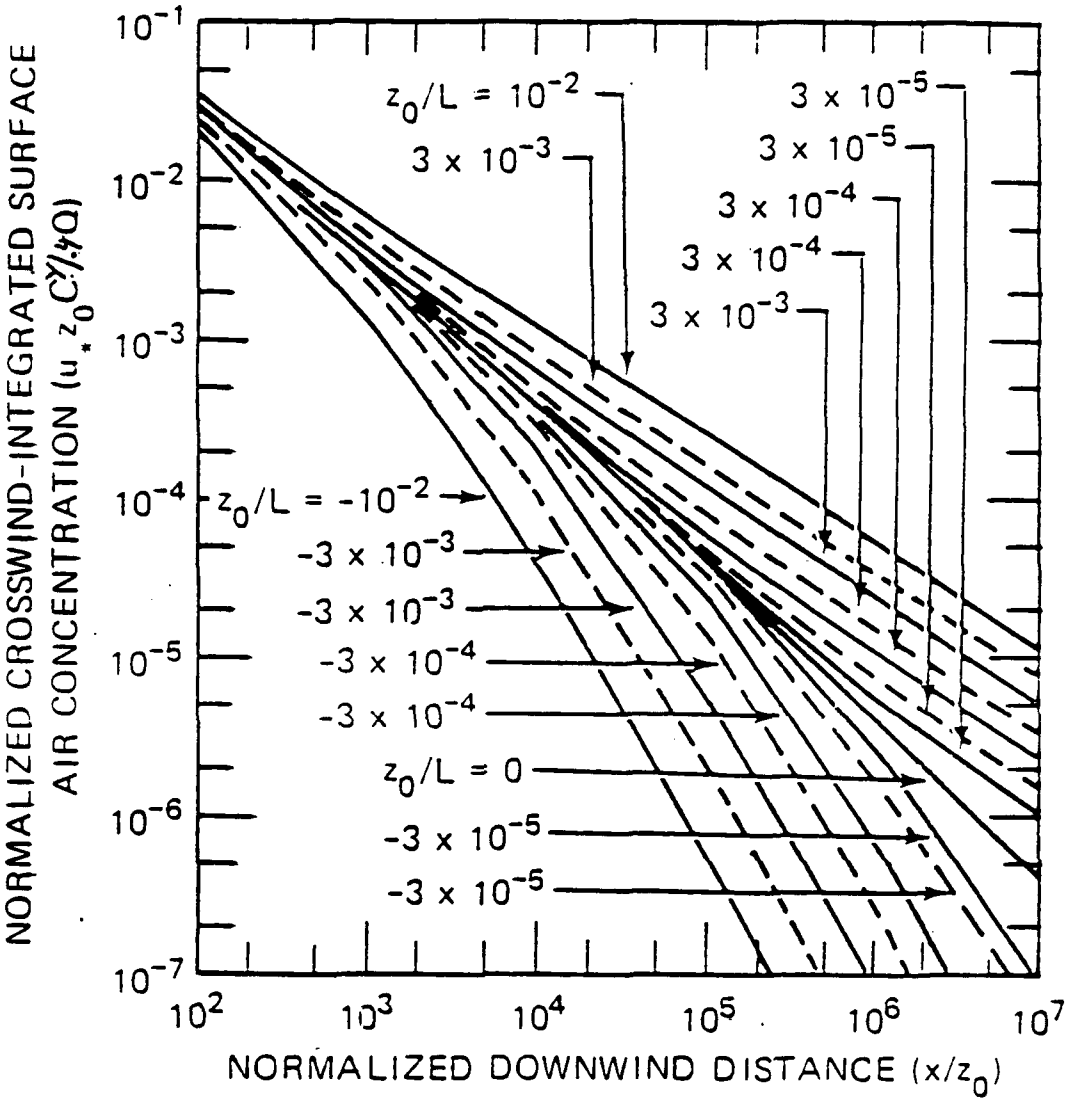

Figure 5-5. Predicted crosswind-integrated concentration at ground level as a function of downwind distance for various stability conditions (from Horst, 1979).

Convective similarity theory applies once the top of the plume diffuses out of the surface shear layer, which will occur at downwind distances of about $0.1\ uh/w_*$. Prior to that distance, Monin-Obukhov similarity will apply. Nieuwstadt (1980) presents an analysis of 20 convective Prairie Grass runs, for which $-h/L > 10$. The theory suggests that a universal curve should result if $C^y uh/Q$ is plotted as a function of xw_*/uh. Nieuwstadt (1980) suggests the following equations:

$$C^y uh/Q = 0.90(w_* x/uh)^{-3/2} \quad \text{for } 0.03 < xw_*/uh < 0.23 \qquad (5\text{-}16)$$

$$C^y uh/Q = 0.25(w_* x/uh)^{-2} \quad \text{for } 0.23 < xw_*/uh < 1.0 \qquad (5\text{-}17)$$

which have both been suggested from scaling arguments based on physical principles. At xw_*/uh greater than 1.0, $C^y uh/Q$ will approach unity, since the material will eventually be dispersed uniformly between the surface and the mixing depth, h, and mass-continuity must be satisfied. However, none of the Prairie Grass data extend into that regime.

Venkatram's (1981) analysis of stable Prairie Grass data uses Monin-Obukhov scaling to suggest functional forms for the plume depth, the wind speed, and the eddy diffusivity in order to derive the expression:

$$C^y u_* x/Q = 0.38 u_*^{-0.34} x^{0.17} \qquad (5\text{-}18)$$

An interim step in the derivation of equation (18) yields the relation $L = (1100\ s^2/m)u_*^2$. 95% of the predictions of C^y/Q made with equation (18) are within a factor of 2 of observations of C^y/Q for stable Prairie Grass runs.

Briggs (1982) investigated the entire range of Prairie Grass data from the point of view of similarity theory, but fit simple analytical functions to the data rather than following the more complicated numerical analyses of van Ulden (1978) and Horst (1979). The values of u_*, L, and so on that he is working with are slightly different than those in Table 1 of Appendix C. He suggests the formulas:

$$C^{y}u_{*}x/Q = 1.25(1 + 0.13x/L)^{1/3} \qquad x/L > 0 \qquad (5\text{-}19)$$

$$C^{y}u_{*}x/Q = 1.25(1 - 0.19x/L - 0.00014(x/L)^{3})^{-1/2} \qquad x/L < 0 \qquad (5\text{-}20)$$

where the differences in the "constant"--1.25 in the above equations versus 1.06 in equations (5-7) and (5-8)--may be due to the fact that Briggs has adjusted the constant to estimate the peak concentration in the vertical distribution, accounting for the heights of the source and the receptor. Briggs points out that the $(x/L)^{1/3}$ power law in equation (5-19) and the $(-x/L)^{-1/2}$ power law in equation (5-20) represent independent theoretical predictions based on known asymptotic solutions. The last term in equation (5-20), proportional to $(x/L)^{-3/2}$, accounts for the "sweep-out" phenomenon that has been observed for ground-level sources during convective conditions at downwind distances on the order of 0.5 to 1.0 uh/w_{*}. At these distances, large convective eddies lift parts of the plume bodily off the ground, leading to decreased ground level concentrations. Figure 5-6 contains Briggs (1982) comparison of the observations with the predictions of equations (5-19) and (5-20). Again, nearly all of the observations are within a factor of 2 of the predictions. However, equations (5-20) and (5-17) share the same problem--the data do not extend to large enough $-x/L$ or xw_{*}/uh to verify the known asymptotic relation $C^{y}uh/Q \rightarrow 1.0$. The Prairie Grass data and hence the best-fit formulas are still in the "convective sweep out" stage at large $-x/L$, and the formulas are therefore clearly not valid beyond the range of the data points.

D. Summary of Scaling Formulas

Many alternate formulas have been discussed above. For the purposes of further analyses, a few representative formulas have been chosen. These include linear regression formulas, best-fit similarity formulas, and Gaussian formulas.

Formulas for Plume Centerline C/Q:

1. OB/DG $\qquad C/Q = 0.000175 \times {}^{-1.95}(DT + 10^{\circ}F)^{4.92} \qquad (5\text{-}21)$

2. REGRESSION-C $\qquad C/Q = 0.000137 \times {}^{-1.81}(DT + 10^{\circ}F)^{4.72} \qquad (5\text{-}22)$

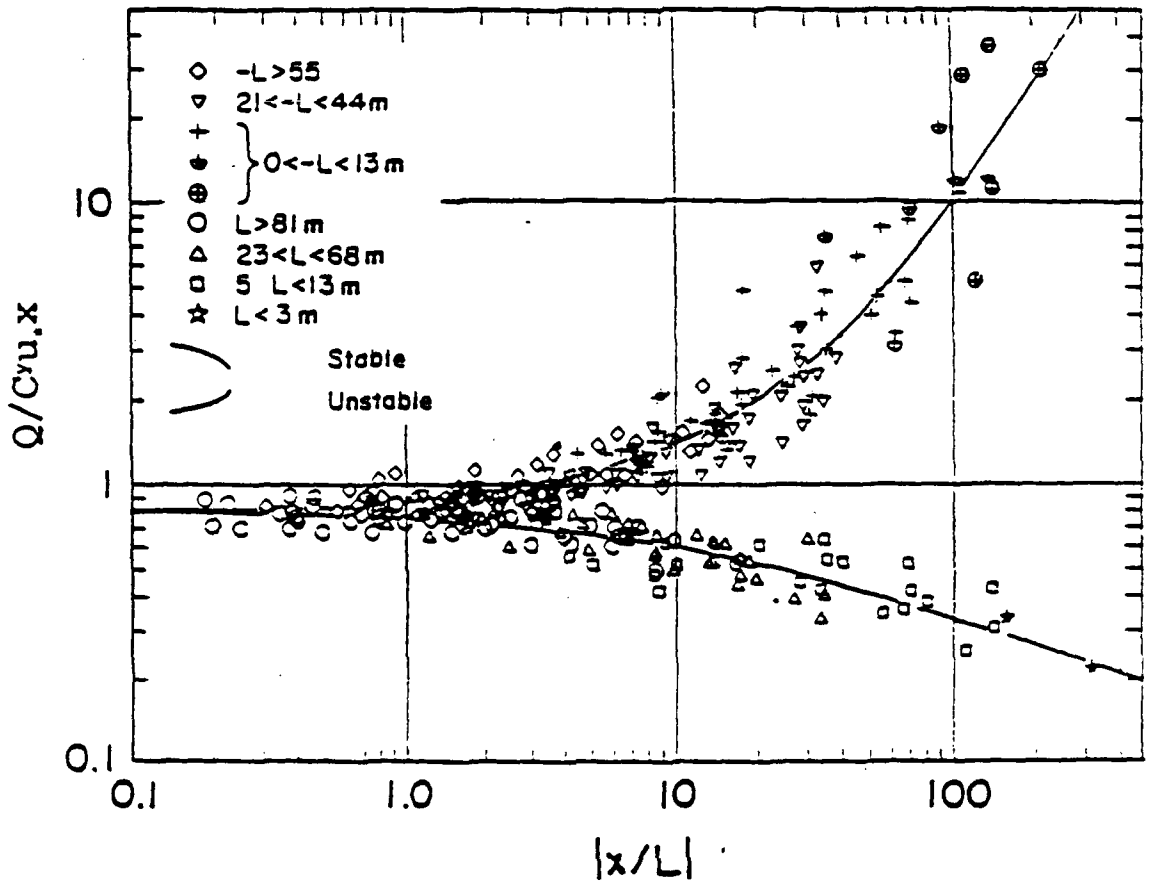

Figure 5-6. Briggs' (1982) comparison of equations (19) and (20) with Prairie Grass observations. Note that the variable used as the ordinate is inverted from that used on previous figures. The different symbols represent different L values.

3. SIMILARITY-C $C/Q = (3.37/u_* x^2)(1 - 0.019x/L)^{-1.86}$ for $x/L < 0$ (5-23)

$$C/Q = (3.01/u_* x^2)(1 + 2.20x/L)^{0.57} \quad \text{for } x/L \geq 0 \quad (5\text{-}24)$$

4. Gaussian Formula

$$C/Q = (\pi u \sigma_y \sigma_z)^{-1} \exp(-(z_s - z_r)^2/2\sigma_z^2) \quad (5\text{-}25)$$

where u is the 2 m wind speed, z_s is the source height, and z_r is the receptor height (z_s = 0.45m, z_r = 1.5m)

5. VSDM Volume Source Diffusion Model (Bjorklund and Dumbauld, 1981)

The OB/DG equation (5-21) is a regression formula taken from Nou's (1963) article. The REGRESSION-C equation (5-22) is similar to equation (21), and is also derived using linear regression procedures, but is based on a more limited database (the Prairie Grass database for equation (22) in comparison to the Ocean Breeze, Dry Gulch, and half of the Prairie Grass databases for equations (21)). The SIMILARITY-C equations (23 and 24) (given earlier as equations (5) and (6)) are based on fitting similarity equations of the form $Cu_* x^2/Q = a(1 - bx/L)^c$ to the Prairie Grass database. The symbol "C" is used here to denote point concentrations, and the symbol "C^y" will be used on the next page to denote cross-wind integrated concentrations. The Gaussian formula (equation 25) assumes complete reflection for the surface and uses the Briggs (1973) analytical formulas for the lateral and vertical dispersion coefficients, σ_y and σ_z. The VSDM model (Bjorklund and Dumbauld, 1981) is a generalized Gaussian-type model used by the U.S. Army for applications at several sites such as Dugway Proving Ground. Because VSDM requires several input variables that are not available (e.g., vertical turbulence σ_ϕ), it is necessary to parameterize these variables. The following specifications of input conditions are made in VSDM:

- No deposition (i.e., reflection parameter = 1.0)
- d(wind direction)/dz = 0.0
- z_s = 0.45 m
- z_r = 1.5 m
- distance for lateral rectilinear expansion (default XRY = 50 m)

- distance for vertical rectilinear expansion (default XRZ = 50 m)
- lateral (XLRY) and vertical (XLRZ) reference distances = 0.0 m
- standard deviations at XLRY and XLRZ = 0.0 m
- crosswind diffusion coefficient (default = 1.)
- vertical diffusion coefficient (default = 1.)
- vertical turbulence intensity σ_ϕ is calculated assuming $\sigma_\phi = \sigma_w/u$, where the following similarity formulas are used (Hanna and Chang, 1989)

$$\sigma_w = u_*(1.44 + 2.9(-z/L))^{1/3} \qquad \text{if } L \le 0 \qquad (5\text{-}26)$$

$$\sigma_w = 1.2\, u_* \qquad \text{if } L > 0 \qquad (5\text{-}27)$$

- wind profile power, p, in $u(z) = u(z_m)(z/z_m)^p$, is calculated from the Monin-Obukhov similarity wind profile formulas (Hanna and Chang, 1989).

Formulas for C^y/Q:

1. REGRESSION-C^y $C^y/Q = 0.00666\ x^{-1.03}(DT + 10°F)^{2.84}$ (5-28)

2. SIMILARITY-C^y $C^y/Q = (1.06/u_*x)(1 - 0.021x/L)^{-1.74}$ $x/L < 0$ (5-29)

$$C^y/Q = (1.07/u_*x)(1 + 0.10x/L)^{0.68} \qquad x/L \ge 0 \qquad (5\text{-}30)$$

3. Nieuwstadt/Venkatram

$$C^y/Q = (0.90/uh)(w_*x/uh)^{-3/2} \qquad 0.03 < w_*x/uh \le 0.23 \text{ and } x/L < 0 \qquad (5\text{-}31)$$

$$C^y/Q = (0.25/uh)(w_*x/uh)^{-2} \qquad 0.23 < w_*x/uh \le 1 \text{ and } x/L < 0 \qquad (5\text{-}32)$$

$$C^y/Q = (u_*x)^{-1} \qquad w_*x/uh \le 0.03 \text{ and } x/L < 0 \qquad (5\text{-}33)$$

$$C^y/Q = 0.38u_*^{-1.34}\ x^{-0.83} \qquad x/L > 0 \qquad (5\text{-}34)$$

4. Briggs $C^y/Q = (u_* x)^{-1}(1 - 0.19x/L - 0.00014(x/L)^3)^{-1/2}$ (5-35)

$x/L \leq 0$

$$C^y/Q = (u_* x)^{-1}(1 + 0.13x/L)^{1/3} \qquad x/L > 0 \qquad (5\text{-}36)$$

5. Gaussian Model

$$C/Q = \left(\sqrt{\pi/2}u\sigma_z\right)^{-1}\exp(-(z_s - z_r)^2/2\sigma_z^2) \qquad (5\text{-}37)$$

6. VSDM, assuming $C^y = \sqrt{2\pi}\sigma_y C$

The REGRESSION-C^y equation (28) is based on application of linear regression procedures. The SIMILARITY-C^y equations (29) and (30) (given earlier as equations (7) and (8)) are based on fitting equations of the form $C^y u_* x/Q = a(1 - bx/L)^c$ to the Prairie Grass database. The Nieuwstadt/Venkatram equations (31)-(34) (given earlier as equations (16)-(18)) are based on formulas suggested by Nieuwstadt (1980) for unstable conditions (with the added restriction that $C^y u_* x/Q = 1$ for $w_* x/uh < 0.03$) and by Venkatram (1981) for stable conditions. The Briggs equations (35) and (36) (given earlier as equations (19) and (20)) were suggested in his 1982 article, with the correction that the leading constant is assumed to be 1.00 rather than 1.25. The Gaussian equation (37) and VSDM use the formulas for C/Q as described above, except the C/Q values are multiplied by $\sqrt{2\pi}\sigma_y$ (valid for a Gaussian or normal distribution) in order to yield C^y/Q.

These equations are applied to the Prairie Grass data in Section X-A, in order to demonstrate the ability of the method to discern differences in source emission rates.

SECTION VI

DESCRIPTION OF SOFTWARE PACKAGE CONTAINING METHODS TO ANALYZE DUGWAY DATA ARCHIVE

A. Introduction

After the creation of the Dugway Data Archive (DDA) from the raw data, the Dugway Data Archive Monte Carlo (DDAMC) software package was written to achieve the following goals: 1) implement the application of the dispersion formulas to the DDA, and 2) estimate the source strength based on predicted and observed concentrations.

When the DDAMC software package is run, one ASCII output file is generated for the results of each analysis procedure for each DDA, containing 1) the basic information such as observed meteorological and source conditions and observed concentrations for each trial in the DDA, and 2) the values of the predicted concentrations and emission rates by the dispersion formulas.

Another software package, ASSEMBLE (to be described in detail in Section IX), then integrates all the individual ASCII files generated by the DDAMC package into one composite binary file, and allows the user to: 1) print out a summary table for all the results (e.g., centerline concentrations or emission rate), 2) generate input files that can be analyzed by the generic distribution analysis software package, ANADISTR (see Appendix D), and then plotted using the SIGPLOT plotting package (see Appendix E), and 3) perform the Student-t test for the predicted source parameters (emission rate or total mass emitted) for any two source groups available in the composite binary file. Furthermore, the DDAMC software package includes an additional feature to assess the sensitivity of the analysis procedures to input data errors using the Monte Carlo method (to be described in detail in Section IX).

Figure 6-1 graphically describes the methodology described above.

B. Formulas Included in the DDAMC Package

There are thus far a total of nine analysis methods that have been integrated into the DDAMC package. In general, they can be classified into

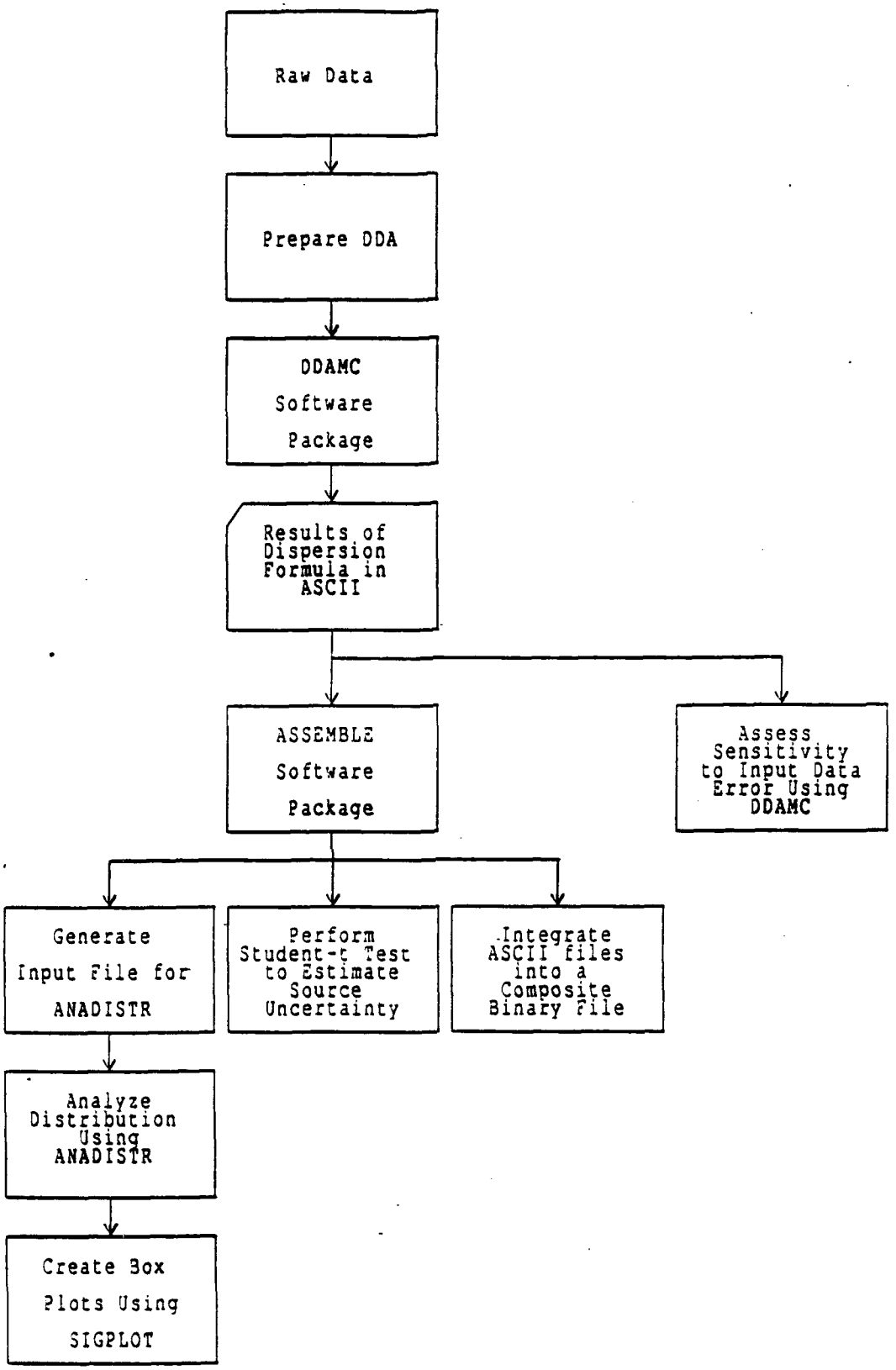

Figure 6-1. A schematic diagram of the use of various software packages developed under this project.

three types: regression, similarity, and Gaussian. The regression and similarity procedures are for quasi-steady state releases only. The Gaussian formulas can be applied to both quasi-steady state and time-varying releases; although all the experiments considered in this project were assumed to be quasi-steady state releases.

The two regression formulas, one for C/Q and one for C^y/Q, are based on an analysis by Nou (1963) of the Prairie Grass data and are assumed to have the following general form:

$$C/Q \text{ or } C^y/Q = a_1 \; x^{a_2} \; \sigma_\theta^{a_3} \; (\Delta T + 10^\circ F)^{a_4} \; u^{a_5} \qquad (6\text{-}1)$$

where a_1 through a_5 are regression coefficients, C and C^y are centerline concentration and cross-wind integrated concentration, respectively, and Q is source emission rate. The variable x is downwind distance (m), ΔT is vertical temperature difference ($^\circ F$) between two levels on a tower, u is wind speed (m/s), and σ_θ is standard deviation of the fluctuation in wind azimuth angle (deg). A simpler version of the regression formulas (i.e. letting a_3 and a_5 = 0) was implemented in the DDAMC package for the Prairie Grass, Ocean Breeze, Dry Gulch, and Green Glow datasets. The following table is a listing of the coefficients that were derived from the data for this simpler formula:

		a_1	a_2	a_4
Prairie Grass	C/Q	0.000137	-1.81	4.72
	C^y/Q	0.00666	-1.03	2.84
Ocean Breeze	C/Q	0.00526	-1.94	3.40
	C^y/Q	N/A		
Dry Gulch/Course B	C/Q	0.000894	-1.16	2.23
	C^y/Q	N/A		
Dry Gulch/Course D	C/Q	0.000301	-1.68	3.52
	C^y/Q	N/A		
Green Glow	C/Q	0.0493	-1.74	1.77
	C^y/Q	N/A		

All of the above coefficients are defined in the DEFREGR subroutine. The user should update or modify the code if the regression formulas for other datasets are to be included.

The OBDG regression formula (Nou, 1963):

$$C/Q = 0.000175\ x^{-1.95}\ (\Delta T+10^{\circ}F)^{4.92} \qquad (6\text{-}2)$$

was also implemented in the DDAMC package, where ΔT is the temperature difference in $^{\circ}F$ between 16 m and 2 m.

The following four similarity formulas, one for C/Q and three for C^y/Q, have been fit to the Prairie Grass data and were also implemented in the DDAMC package.

$$\begin{aligned} C/Q &= (3.37/u_*x^2)\ (\ 1 - 0.019x/L)^{-1.86} && \text{for } x/L < 0 \\ &= (3.01/u_*x^2)\ (\ 1 + 2.200x/L)^{0.57} && \text{for } x/L \geq 0 \end{aligned} \qquad (6\text{-}3)$$

$$\begin{aligned} C^y/Q &= (1.06/u_*x)\ (\ 1 - 0.021x/L)^{-1.74} && \text{for } x/L < 0 \\ &= (1.07/u_*x)\ (\ 1 + 0.100x/L)^{0.68} && \text{for } x/L \geq 0 \end{aligned} \qquad (6\text{-}4)$$

$$\begin{aligned} C^y/Q &= (0.90/uh)\ (w_*x/uh)^{-1.5} && \text{for } x/L < 0 \text{ and } 0.03 < w_*x/uh \leq 0.23 \\ &= (0.25/uh)\ (w_*x/uh)^{-2} && \text{for } x/L < 0 \text{ and } 0.23 < w_*x/uh \leq 1 \\ &= (u_*x)^{-1} && \text{for } x/L < 0 \text{ and } w_*x/uh \leq 0.03 \\ &= 0.38\ u_*^{-1.34}\ x^{-0.33} && \text{for } x/L > 0 \end{aligned} \qquad (6\text{-}5)$$

$$\begin{aligned} C^y/Q &= (u_*x)^{-1}\ (1 - 0.19x/L - 0.00014\ (x/L)^3)^{-1/2} && \text{for } x/L \leq 0 \\ &= (u_*x)^{-1}\ (1 + 0.13x/L)^{1/3} && \text{for } x/L \leq 0 \end{aligned} \qquad (6\text{-}6)$$

where x is the downwind distance, u_* is the friction velocity, L is the Monin-Obukhov length, h is the mixing height, and w_* is the convective velocity scale under unstable conditions. The first two sets of similarity formulas (Equations (6-3) and (6-4)) were developed for this project using data from the Prairie Grass experiments. The third set of similarity formulas (Equation (6-5)) is based on analyses of these same data by Nieuwstadt (1980)

and Venkatram (1981). The last set of similarity formulas (Equation 6-6) is based on an analysis of the data by Briggs (1982).

The above three regression formulas (Equations (6-1) and (6-2)) and four similarity formulas (Equations (6-3) through (6-6)) are implemented in the MODELS subroutine of the DDAMC package, and can be modified easily by the user. As mentioned previously, the coefficients used in the regression formulas are defined in the DEFREGR subroutine.

The DDAMC package also contains a simple Gaussian plume formula (GPM, Hanna et al., 1982):

$$\frac{C}{Q} = \frac{1}{2\pi\sigma_y\sigma_z u} e^{-y^2/2\sigma_y^2} \left[e^{-(z-z_p)^2/2\sigma_z^2} + e^{-(z+z_p)^2/2\sigma_z^2} \right] \qquad (6\text{-}7)$$

where σ_y and σ_z are the horizontal and vertical dispersion coefficients, respectively, u is the wind speed, and z_p is the height of the plume centerline. The Briggs formulas for the dispersion coefficients are used (Hanna et al., 1982). The GPM formula appears as a separate subroutine, GAUSS, in the DDAMC package. The concentration integrated along a line perpendicular to the plume axis can be derived using the following formula:

$$C^y/Q = 2\pi\sigma_y C/Q \qquad (6\text{-}8)$$

The Volume Source Diffusion Model (VSDM, Bjorklund and Dumbauld, 1981) is often used at Dugway Proving Ground and is included in our analysis. This procedure, which is also Gaussian in nature, is incorporated in the software using the "call system ('vsdm')" statement, an extension supported by the Lahey Fortran compiler. The above statement allows easy incorporation of the VSDM model into the DDAMC software package while keeping the original VSDM code intact. Like the GPM formula, the concentration integrated along a cross wind line can be derived using Equation (6-8).

The following assumptions were made when running VSDM:

- Pure steady-state release
- The cross wind dispersion parameter, α, is assumed to equal 0.9.

- The vertical dispersion parameter, β, is assumed to equal 1 when unstable, and to equal $0.32 + 0.41 \log_{10} u_{2m}$ when stable (Bowers, 1990), where u_{2m} is the wind speed (in mph) at 2m above the ground.
- Perfect reflection of the plume material from the ground.
- No variation in wind direction with height.

Because the VSDM code was incorporated without any modification, another post-processor routine, POSTVSDM, was also included in DDAMC to decipher the output file generated directly by VSDM, so that information such as values of σ_y at different downwind distances and values of concentrations at all the receptors can be easily imported back into DDAMC.

The GPM and VSDM procedures are the only two sets of formulas currently implemented in DDAMC that can calculate concentration at any given x, y, and z position. As a result, these two are the only procedures that can be used to calculate concentration integrated along any orientation of the lines-of-sight (LOS) (i.e., not necessarily cross-wind). Whenever a LOS-integrated calculation is required, the DDAMC package internally generates a large number (201) of hypothetical receptors along that LOS, runs the dispersion code, then numerically integrates the concentrations at those receptors to obtain the LOS-integrated concentration.

C. Method Used to Estimate Source Strength from Concentration Observations

The dispersion formulas mentioned in the previous sub-section can be used not only to calculate concentration values, but also to estimate the emission rate or total mass emitted. This is done by forming the ratio of observed concentration to predicted normalized concentration (i.e., assuming unit source emission rate):

$$Q_p = C_o / (C/Q)_p \qquad (6\text{-}9a)$$

where Q_p is the predicted emission rate, C_o is the observed centerline concentration, and $(C/Q)_p$ is predicted centerline concentration normalized by emission rate. In general, the centerline concentration appearing in Equation (6-9a) can be replaced by other concentration values such as cross-wind

integrated concentration (C^y), LOS-integrated concentration (CL), or LOS-integrated dosage (CLID). In other words, we also have:

$$Q_p = C^y_o/(C/Q)_p \tag{6-9b}$$

$$Q_p = CL_o/(CL/Q)_p \tag{6-9c}$$

$$Q_p = CLID_o/(CLID/Q)_p \tag{6-9d}$$

Equations (6-9a) through (6-9d) are most valid for single-source releases.

For widely separated multiple releases, the total emission rate cannot be calculated using these procedures. However, if certain assumptions can be made (e.g., all emissions are equal), it is possible to obtain an estimate of Q.

D. User's Guide for the DDAMC Package

In the following, we will discuss the use of the DDAMC package when it is used to implement the application of the dispersion formulas to the DDA, and estimate the source strength based on predicted and observed concentrations. The user is referred to Section IX for the use of the DDAMC package to assess the sensitivity of the analysis procedure to input data errors using the Monte Carlo method.

Execution of DDAMC

During the execution of the DDAMC software package, the following six points must be addressed. Refer to Figure 6-2 for a hard copy of the screen image during the execution of the DDAMC software package.

1) The user is first prompted for the name of the DDA file. It is assumed that the name of the DDA file is not longer than five letters, and that the DDA file has the extension of ".DDA". As an example, if the user has prepared a MDA file called "PG.DDA" from the raw data for the Prairie Grass experiments (refer to Section IV for the format of the DDA), then "PG" should be input at this point and there is no need to specify the extension, ".DDA".

```
D:\A135\DDAMC\PROG>ddamc

Enter key letters for the DDA (5 letters at most):
Examples:
OB_*:  Ocean Breeze,          DGB_*: Dry Gulch, Course B
DGD_*: Dry Gulch, Course D,   GG_*:  Green Glow
PG_*:  Prairie Grass,         AT*: Atterbury-87
INVHC: Inventory smoke munition test
DT1??: DT I  of 155mm projectiles
DT2??: DT II of 155mm projectiles
L81*:  Evaluation of L8A1 grenades
L83*:  Evaluation of L8A3 grenades
DT1?:  DT I of 81mm projectiles
INT??: Evaluation of international smoke pots/generators
PO*:   Evaluation of man-portable smoke generators
***** USER INPUT --->  l81a1

Enter the full path name where DDA resides
(default is \a135\ddamc\dda, a . means current directory):
***** USER INPUT --->

Choose one dispersion formula to run from the following list:
1)  VSDM
2)  GPM
Formulas for C only:
3)  OB/DG
4)  Regression (dataset specific)
5)  Similarity
Formulas for Cy only:
6)  Regression (dataset specific)
7)  Similarity
8)  Nieuwstadt/Venkatram
9)  Briggs
Enter 1-9:
***** USER INPUT --->  1

Perform Monte Carlo sensitivity analysis? (y/<N>):
***** USER INPUT --->  n

Override 1/L, if available? (y/<N>):
***** USER INPUT --->  n

Use the Dugway scheme to relate sigma-phi and sigma-theta,
if necessary? (y/<N>):
***** USER INPUT --->  n

Reading DDA...
Running dispersion formula...
W* for trial bb2 is unreliable because mixing height is missing!
W* for trial bb3 is unreliable because mixing height is missing!
W* for trial bb4 is unreliable because mixing height is missing!
W* for trial bb5 is unreliable because mixing height is missing!
W* for trial bb6 is unreliable because mixing height is missing!
W* for trial bb7 is unreliable because mixing height is missing!
W* for trial bb9 is unreliable because mixing height is missing!
Writing results...

D:\A135\DDAMC\PROG>
```

Figure 6-2. Screen image during the execution of the DDAMC software package where the VSDM dispersion formula is run for the L81A1 dataset (comparison test of L8A1 screening smoke grenades, Rafferty and Dumbauld, 1983; Lot A only).

2) The user is asked to specify the DOS-path name for the DDA file. In other words, the DDA file does not have to reside on the same directory as the DDAMC software package. The current default answer, "\a135\ddamc\dda", is specified in the main program and can be changed easily by the user. A "." means that the current working directory is assumed.

3) The user is asked the dispersion formula to be used. At present, the following nine dispersion formulas (refer to Section B for more detailed discussion) are supported,

(1) VSDM
(2) GPM
(3) OBDG (C/Q only)
(4) Regression (C/Q only)
(5) Similarity (C/Q only)
(6) Regression (C^y/Q only)
(7) Similarity (C^y/Q only)
(8) Nieuwstadt/Venkatram (C^y/Q only)
(9) Briggs (C^y/Q only)

For example, if the user decides to use the VSDM dispersion formula, then "1" (*not* the name of the dispersion formula) should be input at this point.

4) The user is asked whether to run the DDAMC software package in Monte-Carlo mode. The default answer is "n", and should be selected here, since the non-Monte Carlo mode is now being discussed.

5) The user is asked whether to override the value of the inverse Monin-Obukhov length (L^{-1}) specified in the DDA file. The DDAMC software package has the ability to calculate its own value of L^{-1} given temperature data at two levels, and wind data at one level, and this calculated value of L^{-1} is sometimes not in agreement with the value reported in the DDA. The default answer is "n".

6) The last question is related to the calculation of standard deviations of the wind azimuth and elevation angles fluctuations (σ_θ and σ_ϕ,

respectively). Two methods are available in the DDAMC software package to accomplish this goal. The first method is the one that was commonly used in the reports published by U.S. Army Dugway Proving Ground (see Section IV):

$$\sigma_\phi = \sigma_\theta(T_a)\ (2.5/T_a)^{0.2} \qquad (6\text{-}10)$$

where T_a is the averaging time in seconds. The second method, (used as a default in the DDAMC software) consists of a set of state-of-the-art turbulence formulas from the Hybrid Plume Dispersion Model (HPDM), Version 4 (Hanna and Chang, 1990).

$$\sigma_v = (4u_*^2 + 0.35w_*^2)^{1/2} \quad \text{(unstable)} \qquad (6\text{-}11a)$$

$$= \max(0.5\ \text{m/s},\ u_*) \quad \text{(stable)} \qquad (6\text{-}11b)$$

$$\sigma_w = u_*\,[1.44 + 2.9(-z/L)^{2/3}]^{1/2} \quad \text{(unstable)} \qquad (6\text{-}12a)$$

$$= 1.2u_* \quad \text{(stable)} \qquad (6\text{-}12b)$$

$$\sigma_\theta = \sigma_v/u \qquad (6\text{-}13)$$

$$\sigma_\phi = \sigma_w/u \qquad (6\text{-}14)$$

where σ_v and σ_w are standard deviations of the fluctuations of v- and w-components of the wind speeds (u), respectively, u_* is friction velocity, w_* is the convective velocity scale (valid only for unstable conditions, L is the Monin-Obukhov length, and z is the height of the plume. Equation (6-11a) is based on the study by Hicks (1985), and Equation (6-12a) is based on the study by Panofsky et al. (1977). An averaging time of one hour is assumed when either Equation (6-11) or (6-12) is used. Note that in order to use Equation (6-10), σ_θ has to be available. While we believe that Equations (6-11) through (6-14) are more scientifically sound, it is evident that they may not be able to be implemented in a given scenario because data such as mixing height and the Monin-Obukhov length may not be available.

After the answers to the above six questions are supplied, the DDAMC software package then runs the dispersion formula chosen by the user for the specified DDA file, and writes out the results to an ASCII file. The format and the naming convention of this ASCII file will be discussed later in a separate sub-section.

Derivation of Missing Variables and Internal Variables by the DDAMC Package

As mentioned at the end of Section IV, the DDAMC software package will substitute default values for some of the missing variables, such as ambient pressure, relative humidity, and mixing height. On the other hand, the DDAMC software package also has comprehensive schemes to derive some missing variables, such as σ_θ, from other parameters based on known physical relationships. Furthermore, there are some variables that are not part of the DDA file, but need to be calculated internally by the DDAMC software package. In the following, we will discuss the procedures used in the DDAMC software package to derive the values for the missing and interval variables in the DDA.

The following is a list of ten variables that DDAMC is able to derive:

Variable	Definition
L	Monin-Obukhov length
ΔT	temperature difference between two levels
σ_θ	standard deviation of the wind azimuth angle fluctuations
σ_ϕ	standard deviation of the wind elevation angle fluctuations
u_*	friction velocity
PG	Pasquill-Gifford stability class
WPL	wind speed profile power-law exponent
WS10	wind speed at 10 m above the ground
DT162	temperature difference between 16 m and 2 m
w_*	convective velocity scale

WS10, DT162, and w_* are "internal" variables calculated by the DDAMC software package, i.e., they do not appear as part of the DDA file. WS10 is used in the Irwin method (Irwin, 1980; EPA, 1987,) to estimate PG based on values of σ_θ (described later), DT162 is used in the OBDG dispersion formula (Nou, 1963; Equation (6-2)), and w_* is used in the Hicks (1985) formula (Equation (6-11a)).

Methods used by the DDAMC software package to derive the above ten variables are summarized below. More detailed discussion of each method will follow.

Method	Purpose
Profile	Calculate u_* and L based on temperature data at two levels and wind speed data at one level; calculate temperature and wind speed at any give height within the surface layer given u_* and L.
Golder	Calculate PG from z_0 (surface roughness) and L; calculate L from z_0 and PG.
Irwin	Calculate PG from σ_θ and z_0.
Dugway	Calculate σ_ϕ from σ_θ, or vice versa
Hicks	Calculate σ_θ from u_* and w_*.
Panofsky	Calculate σ_ϕ from u_* and L.

The profile method treats u_* and L as free parameters (with physical constraints imposed) that are selected to produce the best fit of the measured data to the empirical profiles. Minimum requirements are that wind speed data are available at one height above the ground, and that temperature data are available at two heights. The underlying assumptions for the validity of the estimates is that the data are measured within the surface layer, and that the flow in the surface layer is homogeneous and stationary.

The similarity profiles for wind speed and temperature are (e.g. Panofsky and Dutton, 1984):

$$u(z) = \frac{u_*}{k}\left[\ln(z/z_0) - \Psi_m(z/L)\right] \qquad (6\text{-}15)$$

$$\Theta(z)-\Theta(z_1) = \frac{T_*}{k}\left[\ln(z/z_1) - \Psi_h(z/L)\right] \qquad (6\text{-}16)$$

where u is the wind speed, Θ is the potential temperature, z_0 is the surface roughness length, z is the basic measuring height, z_1 is the lower height for

the temperature observation, k is the von Karman constant (=0.4), T_* is the temperature scale, and the Businger-Dyer equations for the dimensionless functions, ψ_m and ψ_h, are given below:

$$\Psi_m = \ln\left[\left(\frac{1+x^2}{2}\right)\left(\frac{1+x}{2}\right)^2\right] - 2\tan^{-1}(x) + \frac{\pi}{2} \qquad \text{(unstable)} \qquad (6\text{-}17)$$

where $x = (1 - 16z/L)^{1/4}$,

$$\Psi_m = -5\ z/L \qquad \text{(stable)} \qquad (6\text{-}18)$$

and

$$\Psi_h = 2\ \ln\left[\frac{1+x^2}{2}\right] \qquad \text{(unstable)} \qquad (6\text{-}19)$$

$$\Psi_h = -5\ z/L \qquad \text{(stable)} \qquad (6\text{-}20)$$

T_* and u_* are related through the Monin-Obukhov length:

$$\frac{T_*}{k} = \frac{u_*^2}{k^2}\,\frac{\Theta(z_r)}{gL(1+.07/B)} \qquad (6\text{-}21)$$

where z_r is some reference height, g is the gravitational acceleration, and B is the Bowen ratio which is equal to the ratio of the sensible heat flux to the latent heat flux.

It is clear from Equations (6-15) through (6-21) that the profile method can be used to calculate u_* and L if temperature data at two levels and wind data at one level are available. The profile method can also be used to calculate wind and temperature data at any height within the surface layer, thus permitting the calculation of variables such as ΔT, WPL, WS10, and DT162.

The Golder method is the digitized version of the Golder (1972) nomogram (Figure 6-3) that establishes a relation between PG, z_0, and 1/L. The digitization scheme used in DDAMC was obtained from Kunkel (1988).

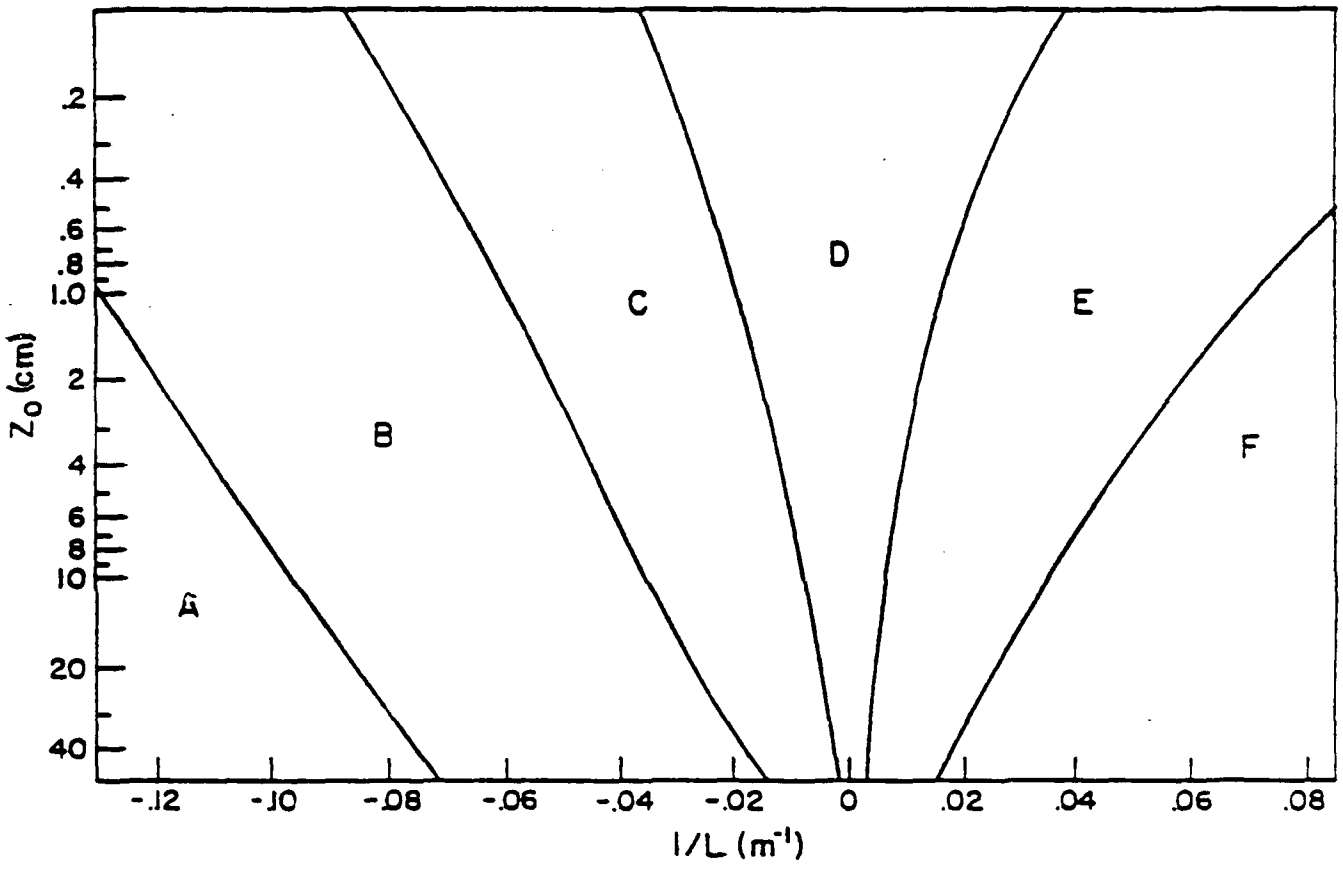

Figure 6-3. 1/L as a function of Pasquill stability classes and surface roughness z_0, from Golder (1972).

In the Irwin method (Irwin, 1980; EPA, 1987), PG is determined from the values of σ_θ. Table 6-1 describes the Irwin method. Note that the values of σ_θ and u listed in Table 6-1 are for a 10 m level, 60-min time period, and z_0 = 15 cm. The DDAMC software package can derive the wind speed at a 10 m level (WS10). The following adjustments for σ_θ are suggested for different values of the averaging time (T_a, in minutes), measuring height and z_0:

$$(\sigma_\theta(T_a=60 \text{ min})/\sigma_\theta(T_a))=(60 \text{ min}/T_a)^{0.2} \quad (6\text{-}22)$$

$$(\sigma_\theta(z=10 \text{ m})/\sigma_\theta(z))=(10 \text{ m}/z)^{0.2} \quad (6\text{-}23)$$

$$(\sigma_\theta(z_0=15 \text{ cm})/\sigma_\theta(z_0))=(15 \text{ cm}/z_0)^{0.2} \quad (6\text{-}24)$$

The user is referred to the previous sub-section for the discussion of the Dugway, Hicks, and Panofsky methods (refer to Equations (6-10) through (6-14)).

The implementation of the above methods is complicated by the many possible combinations of the variables that are available and the variables that are missing. Figure 6-4 shows the logic that is currently implemented in the DDAMC software package. Note that Figure 6-4 does not include the internal variables, WS10, DT162 and w_*. As an illustration, consider the case when ΔT and σ_θ are available, u_*, L, σ_ϕ, PG and WPL are missing, and the Panofsky method is to be used. Then from Figure 6-4, the following calculations will be performed in sequence:

- L is calculated using the profile method
- u_* is calculated using the profile method
- PG is calculated using the Golder method
- WPL is calculated using the profile method
- σ_ϕ is calculated using the Panofsky method

It is also evident from Figure 6-4 that at least one of the four variables, L, ΔT, PG, and σ_θ, must be available, as mentioned in Section IV.

Last but not least, it is clear that there are uncertainties associated with all of the above methods, even though they are all deterministic. For

Table 6-1

Wind Fluctuation Criteria for Estimating Pasquill-Gifford Stability Class*
(from Irwin, 1980)

Standard Deviation of the Horizontal Wind Direction Fluctuations, (σ_θ in Degrees)	Daytime Pasquill-Gifford Stability Class	And the Wind Speed at 10 m is m/s	Nighttime Pasquill-Gifford Stability Class
$\sigma_\theta \geq 22.5^\circ$	A	< 2.9	F
		2.9 to 3.6	E
		≥ 3.6	D
$17.5^\circ \leq \sigma_\theta < 22.5^\circ$	B	< 2.4	F
		2.4 to 3.0	E
		≥ 3.0	D
$12.5^\circ \leq \sigma_\theta < 17.5^\circ$	C	< 2.4	E
		≥ 2.4	D
$7.5^\circ \leq \sigma_\theta < 12.5^\circ$	D	wind speed not considered	D
$3.8^\circ \leq \sigma_\theta < 7.5^\circ$	E	wind speed not considered	E
$\sigma_\theta < 3.8^\circ$	F	wind speed not considered	F

*Nighttime is considered to be from 1 hour prior to sunset to 1 hour after sunrise.

*These criteria are appropriate for steady-state conditions, a measurement height of 10 m, for level terrain, and an aerodynamic surface roughness length of 15 cm. Care should be taken that the wind sensor is responsive enough for use in measuring wind direction fluctuations.

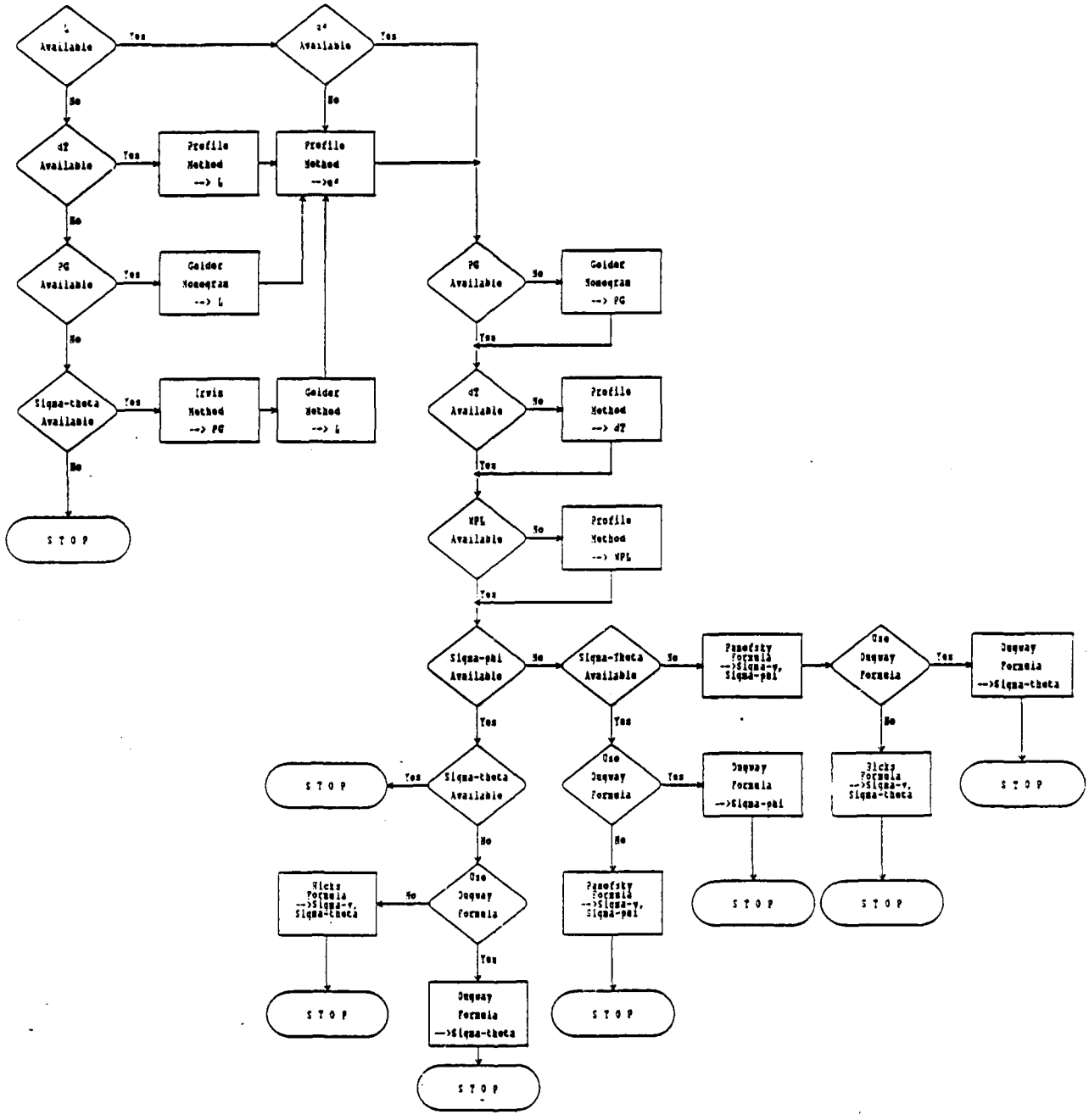

Figure 6-4. The logic that is currently implemented in the DDAMC package for the derivation of the missing variables.

example, given temperature data at two levels and wind data at one level, the values of L and u_* are uniquely determined by the profile method. However, there is a certain amount of uncertainty associated with the profile method itself which results in confidence intervals on L and u_*. Unfortunately, to the best of our knowledge, comprehensive studies on this type of uncertainty are not available. As a result, no attempts were made to incorporate uncertainties associated with various methods into the DAMC software package.

Maximum Limits to Certain Input Variables

At present, the DDAMC package has the following limits imposed:

- maximum number of trials in each DDA: 20
- maximum number of concentric arcs: 6
- maximum number of lines-of-sight (LOS): 6
- maximum number of sources in each trial: 32

All the above limits are specified in the "PARAMS.CMN" Fortran INCLUDE file. The user can easily modify the limits depending on the particular application at hand. However, the user should exercise caution so that the program will not become too large to fit in memory.

Naming Convention and Format of the ASCII Output Files Generated by DDAMC

When the DDAMC package is run, one ASCII output file will be generated for each formula and each DDA. The package automatically sets a name for these output files. The naming convention of the output file is such that the first two to three letters are used to represent the dispersion formula, the remaining letters (five at most) are used to represent the DDA, and an extension of ".OUT" will always be used. The following key letters are currently used by the DDAMC package to represent various formulas mentioned in Section B.

key letters	Formulas
VS	VSDM
GP	GPM
OB	OBDG (C/Q)
RE	Regression (C/Q)

SI	Similarity (C/Q)
REY	Regression (C^y/Q)
SIY	Similarity (C^y/Q)
NV	Nieuwstadt/Venkatram (C^y/Q)
BR	Briggs (C^y/Q)

Therefore, if "PG" is used to represent the DDA for the Prairie Grass experiments, the DDAMC package creates a file called "VSPG.OUT" to contain the VSDM dispersion formula results for the Prairie Grass experiments.

The format of the ASCII output file should be self-explanatory (see Figures 6-5 and 6-6 for examples). There are multiple sections in the output file, each section corresponding to one trial. The name of the trial appears first in each section, followed by a listing of the meteorological, source, and site conditions for that trial, including emission rate (or total emission rate for multiple-source releases), total mass emitted, wind speed, the Pasquill-Gifford stability class, inverse of the Monin-Obukhov length, surface roughness, friction velocity, standard deviation of the azimuth wind angle fluctuations, standard deviation of the elevation wind angle, wind speed power law exponent, convective velocity scale under convective conditions, and temperature difference between 16 m and 2 m. Note that some of the variables, if not directly observed, will be derived.

The output file then lists the number of concentric arcs for this trial. For each arc, values of predicted centerline concentration (C), predicted cross-wind integrated concentration (C^y), predicted plume width (σ_y), predicted emission rate (Q) based on C, predicted Q based on C^y, downwind distance of the arc from the source, observed C, observed C^y, and observed σ_y are listed. These calculations are not done if the observed concentration is not available. "-99.9" is used to indicate that the data are either missing or not applicable.

The number of lines-of-sight (LOS) for the trial is listed in the last part of each section of the output file. For each LOS, values of predicted LOS-integrated concentration (CL), predicted LOS-integrated dosage (CLID), predicted total Q based on CL, predicted total Q based on CLID, observed CL, and observed CLID are also listed. These calculations are not done if the observed

```
pg7
   qtot       masstot        u       pg     1/L          z0          u*
  8.990E+01  5.394E+01  4.200E+00  2 -1.260E-01  6.000E-03  3.185E-01
    sigd        sigp        wpl         w*         dt162
  2.560E+01  5.939E+00  9.862E-02  2.502E+00 -1.600E+00
            5
  predchi    predchiy   predsigy    predqc     predqcy     xdist      obschi     obschiy      sigy
  1.376E+02  2.752E+03  7.980E+00  6.052E+01  1.307E+02  5.000E+01  9.260E+01  4.001E+03  6.200E+00
  3.536E+01  1.411E+03  1.592E+01  5.509E+01  1.403E+02  1.000E+02  2.167E+01  2.203E+03  1.200E+01
  8.941E+00  7.101E+02  3.168E+01  4.248E+01  1.263E+02  2.000E+02  4.225E+00  9.979E+02  2.200E+01
  2.261E+00  3.556E+02  6.276E+01  2.721E+01  1.011E+02  4.000E+02  6.841E-01  4.001E+02  3.900E+01
  5.761E-01  1.779E+02  1.232E+02  1.149E+01  9.087E+01  8.000E+02  7.363E-02  1.798E+02  7.100E+01
            0
   predcl     predclid   predqcl    predqcld    obscl      obsclid
pg8
   qtot       masstot        u       pg     1/L          z0          u*
  9.110E+01  5.466E+01  4.900E+00  3 -4.999E-02  6.000E-03  3.547E-01
    sigd        sigp        wpl         w*         dt162
  1.020E+01  5.362E+00  1.128E-01  2.065E+00 -1.200E+00
            5
  predchi    predchiy   predsigy    predqc     predqcy     xdist      obschi     obschiy      sigy
  2.511E+02  3.453E+03  5.486E+00  1.438E+02  1.346E+02  5.000E+01  3.963E+02  5.102E+03  6.600E+00
  6.694E+01  1.837E+03  1.095E+01  1.451E+02  1.288E+02  1.000E+02  1.066E+02  2.596E+03  1.200E+01
  1.723E+01  9.408E+02  2.178E+01  1.257E+02  1.067E+02  2.000E+02  2.378E+01  1.102E+03  2.100E+01
  4.449E+00  4.811E+02  4.315E+01  7.743E+01  7.383E+01  4.000E+02  3.781E+00  3.899E+02  4.100E+01
  1.176E+00  2.496E+02  8.468E+01  5.202E+01  5.122E+01  8.000E+02  6.714E-01  1.403E+02  8.600E+01
            0
   predcl     predclid   predqcl    predqcld    obscl      obsclid
pg9
   qtot       masstot        u       pg     1/L          z0          u*
  9.200E+01  5.520E+01  6.900E+00  3 -3.016E-02  6.000E-03  4.913E-01
    sigd        sigp        wpl         w*         dt162
  1.020E+01  5.168E+00  1.207E-01  1.775E+00 -1.600E+00
            5
  predchi    predchiy   predsigy    predqc     predqcy     xdist      obschi     obschiy      sigy
  1.800E+02  2.476E+03  5.486E+00  9.494E+01  1.374E+02  5.000E+01  1.858E+02  3.698E+03  9.000E+00
  4.801E+01  1.317E+03  1.095E+01  1.010E+02  1.536E+02  1.000E+02  5.272E+01  2.199E+03  1.800E+01
  1.236E+01  6.747E+02  2.178E+01  9.724E+01  1.368E+02  2.000E+02  1.306E+01  1.003E+03  3.300E+01
  3.190E+00  3.450E+02  4.315E+01  7.774E+01  1.094E+02  4.000E+02  2.696E+00  4.103E+02  6.300E+01
  8.432E-01  1.790E+02  8.468E+01  5.280E+01  6.667E+01  8.000E+02  4.839E-01  1.297E+02  1.160E+02
            0
   predcl     predclid   predqcl    predqcld    obscl      obsclid
```

Figure 6-5. Partial listing of the GPPG.OUT file, a file that contains the results from the GPM dispersion for the PG (Prairie Grass) dataset.

```
wp1
   qtot       masstot        u       pg     1/L          z0          u*
 1.582E+01  1.430E+01  6.400E+00   4  0.000E+00  3.000E-02  6.096E-01
   siqd        siqp         wpl          w*         dt162
 7.200E+00  6.549E+00  9.300E-02 -9.990E+01 -1.372E-01
          0
 predchi     predchiy    predsiqy     predqc     predqcy      xdist       obschi      obschiy       siqy
          6
  predcl     predclid    predqcl     predqcld     obscl      obsclid
 1.408E+02  1.273E+05 -9.990E+01 -9.990E+01 -9.990E+01 -9.990E+01
 4.157E+02  3.758E+05 -9.990E+01 -9.990E+01 -9.990E+01 -9.990E+01
 2.851E+02  2.578E+05 -9.990E+01  2.006E+01 -9.990E+01  3.270E+05
 1.805E+02  1.632E+05 -9.990E+01 -9.990E+01 -9.990E+01 -9.990E+01
 1.974E+00  1.784E+03 -9.990E+01 -9.990E+01 -9.990E+01 -9.990E+01
 8.586E-04  7.762E-01 -9.990E+01 -9.990E+01 -9.990E+01 -9.990E+01
wp3
   qtot       masstot        u       pg     1/L          z0          u*
 1.610E+01  1.455E+01  5.600E+00   4  0.000E+00  3.000E-02  5.334E-01
   siqd        siqp         wpl          w*         dt162
 1.160E+01  6.549E+00  1.030E-01 -9.990E+01 -1.372E-01
          0
 predchi     predchiy    predsiqy     predqc     predqcy      xdist       obschi      obschiy       siqy
          6
  predcl     predclid    predqcl     predqcld     obscl      obsclid
 9.498E+02  8.586E+05 -9.990E+01 -9.990E+01 -9.990E+01 -9.990E+01
 4.026E+02  3.640E+05 -9.990E+01  8.977E+00 -9.990E+01  2.030E+05
 1.549E+02  1.400E+05 -9.990E+01  7.473E+00 -9.990E+01  6.500E+04
 3.513E+01  3.176E+04 -9.990E+01 -9.990E+01 -9.990E+01 -9.990E+01
 5.038E+02  4.554E+05 -9.990E+01 -9.990E+01 -9.990E+01 -9.990E+01
 4.009E+02  3.624E+05 -9.990E+01  1.364E+01 -9.990E+01  3.070E+05
wp6
   qtot       masstot        u       pg     1/L          z0          u*
 1.553E+01  1.404E+01  3.400E+00   4  0.000E+00  3.000E-02  3.238E-01
   siqd        siqp         wpl          w*         dt162
 1.590E+01  6.549E+00  4.400E-02 -9.990E+01 -1.372E-01
          0
 predchi     predchiy    predsiqy     predqc     predqcy      xdist       obschi      obschiy       siqy
          6
  predcl     predclid    predqcl     predqcld     obscl      obsclid
 2.800E+02  2.531E+05 -9.990E+01  4.049E+00 -9.990E+01  6.600E+04
 3.931E+02  3.553E+05 -9.990E+01  4.064E+00 -9.990E+01  9.300E+04
 7.165E+02  6.477E+05 -9.990E+01  7.000E+00 -9.990E+01  2.920E+05
 7.514E+02  6.793E+05 -9.990E+01 -9.990E+01 -9.990E+01 -9.990E+01
 2.921E+02  2.640E+05 -9.990E+01 -9.990E+01 -9.990E+01 -9.990E+01
 2.062E+03  1.864E+06 -9.990E+01 -9.990E+01 -9.990E+01 -9.990E+01
```

Figure 6-6. Partial listing of the GPDT2W1.OUT file, a file that contains the results from the GPM dispersion formula for the DT2W1 (Development Test II of 155 mm Smoke Projectiles, XM825 Munition) dataset.

concentration is not available. "-99.9" is used to indicate that the data are either missing or not applicable.

Programming Information

The DDAMC package was developed on a 80386/7-based PC using Version 4.1 of the Lahey Fortran Compiler. Because the extension "call system (...)" was used, porting the package to other platforms can be achieved only if a similar extension is also supported on that platform.

The DDAMC software package currently consists of 33 Fortran programs and 5 include files. Because a relatively large number of programs are involved, the MAKE utility, part of the Lahey Fortran program development tools, was used to develop the package. The use of the MAKE utility is not essential, but is very useful in keeping track of the updates of the programs.

The DDAMC package itself requires roughly 396 KB of memory. In addition, the stand-alone VSDM code requires about 178 KB of memory. Therefore, the user should have at least 574 KB of memory available on the system. With the proliferation of the memory management utilities for PC's, and the recent introduction of Version 5.0 of MS-DOS, allowing the operating system itself to be loaded into the memory above the conventional 640 KB limit, the memory requirement of the DDAMC package should be readily met.

SECTION VII

ASSESSMENT OF DATA UNCERTAINTIES

Data errors can make a significant contribution to uncertainties in any data analysis exercise. In some cases, these errors can be estimated based on studies of instrument errors in the field. Five approaches to solving specific aspects of this problem are discussed in the following subsections.

- References on observations of instrument uncertainty have been reviewed in order to create a summary table containing the expected uncertainties of a wide variety of instruments.

- A field study on wind data uncertainties was carried out and the data were analyzed.

- A study was made of uncertainties in source emission rates for smoke/obscurants.

- An example is given of the use of scaling parameters to reduce the variance in sets of observations.

- Papers on the use of Monte Carlo methods to estimate the sensitivity of model predictions of variation in input data were acquired and reviewed and a code that carried out Monte Carlo sensitivity tests was developed and tested.

A. Review of Instrument Uncertainties

Instrument uncertainties can be due to errors in the instruments themselves, or can be due to unrepresentative siting of the instrument. Furthermore, most instruments have a "threshold value" below which they either do not record any value, or the value that is recorded is completely unreliable.

Typical uncertainties associated with the measurement of meteorological data have been addressed in several studies. The first study reviewed is the Prairie Grass project. Although several different organizations were involved in making meteorological measurements, the project report (Barad, 1958) cites accuracy assessments for only the slow response measurements taken at an elevation of 2 meters. The second reference reviewed is the report from the workshop on on-site meteorological measurements (Strimaitis et al. 1980). Although not concerned with any one specific field program, the attendees reported on their collective experience in making meteorological measurements. The third reference is a study that was specifically designed to compare measurements obtained from five types of mechanical wind sensors, and a sonic anemometer (Kaimal et al. 1984). The test instruments were mounted on separate 10 meter tall masts, set approximately 5 meters apart (across the flow). The fourth reference assesses measurements made in support of the EPRI plume model validation study at the Kincaid and Bull Run sites (Hanna, 1988), while the fifth includes a report on measurements made at Dugway Proving Grounds (White et al. 1986). The latter report is particularly interesting in that comparisons are made between "identical" wind instruments installed 500 meters apart. The final study reviewed is a comparison of remote sounders at the Boulder Atmospheric Observatory (Chintawongvanich et al. 1989).

Table 7-1 presents information obtained from each of the references. All of the references noted that the mechanical wind sensors are not as reliable for wind speeds of less than approximately 2 m/s because of starting thresholds and response times. As stated in the workshop report (Strimaitis et al. 1980), typical thresholds attainable with cup and vane instruments are on the order of half a meter per second.

The results of the BAO study (Kaimal et al. 1984) are based on the assumption that the sonic anemometer provides the best attainable measurements of wind speed and direction, so that measurements from the mechanical systems are only compared with those from the sonic anemometer. The scatter found in wind direction measurements (4.5°), relative to the sonics, is surprisingly large.

Both the EPRI (Hanna, 1988) and DPG (White et al. 1986) reports include a measure of the effect of a support tower on wind measurements. Although this is an important consideration for general data acquisition requirements, it

TABLE 7-1. TYPICAL UNCERTAINTIES IN METEOROLOGICAL MEASUREMENTS

	u	θ	σ_θ	σ_ϕ	ΔT[1]	Ave. Time
Prairie Grass ($u > 2$ m/s)	2-5%	2°-5°	10%	-	-	10 min.
Workshop	.2 m/s + 5%	< 3°	5-10%	-	< 0.1°C	60 min.
BAO[2]	.3 m/s	4.5°	3°	1.7°	-	20 min.
BAO[3]	-	-	10%	-	-	20 min.
EPRI	.1 m/s	1.5°	13%	20%	-	60 min.
EPRI (tower shadow)	10%	10°	-	-	-	60 min.
DPG (mfg. specs).	.1 m/s + 1%	3°	1.2°	-	.4°C	-
DPG ($u > 5$ m/s)	6%[4]	-	-	30%	-	10 min.
DPG ($u < 2$ m/s)	25%[4]	-	-	48%	-	10 min.
BOA remote sounders	1 m/s	10-20°	10-20°	Large	-	10 min.

1. The temperature difference (ΔT) uncertainty applies to any height interval, since the instrument measures only a difference without regard to the location of the two points.

2. Mean bias removed (cups, props, vanes, bi-vanes relative to sonics).

3. Bias as a function of indicated σ_θ removed (vanes relative to sonics).

4. An additional uncertainty of 5-10% occurs when the wind instrument is in the tower wake.

is of limited importance for short-term experiments in which the field study can be conducted only for periods in which the instruments are properly exposed. When exposure is a problem, both studies indicate that the effect on wind speed can be as large as 10 percent (indicated speeds are lower by about 10 percent).

In general, the degree of uncertainty in wind measurements reported in the documents reviewed above is consistent. Without considering representativeness issues, well-calibrated wind speed measurements by high-quality in-situ instruments are generally within 5 percent of the "true" value, and wind directions are within 3° to 5°. The recent studies of lateral turbulence (σ_θ) also tend to confirm expectations based on experience (e.g., the workshop report and the Prairie Grass report), with an uncertainty in σ_θ of about 10 percent. But vertical turbulence (σ_ϕ) data appear to be more unreliable. It appears that σ_ϕ carries with it an uncertainty of about 20 percent, even when efforts are made to assure that the vane or prop is functioning properly. Furthermore, the uncertainty in remote sounder measurements tend to be two to three times the uncertainties in fixed (in-situ) instruments.

When representativeness is considered, the uncertainty grows appreciably (see the results of the NCAR study described below). Problems of exposure, such as tower shadows, building wakes, and nearby trees and terrain, can easily double the uncertainty in wind speed and direction. Even if the siting is excellent and the terrain open and flat, measurements taken at one point can differ substantially from measurements made using identical instrumentation located just 500 meters away. This is particularly true of turbulence measurements, and certainly wind speed measurements made under light wind speeds (less than 2 m/s). Although not documented, differences in wind direction are expected to be equally sensitive to spatial variations under light wind speed conditions.

Alternate methods for the measurement of vertical turbulence (σ_ϕ) are frequently employed, given the difficulty of obtaining reliable data on σ_ϕ from vanes and props. Stability class is sometimes used as an alternate method, inferred from observations of wind speed (near the ground), and

surrogates for the sensible heat flux. An estimate of the uncertainty in σ_ϕ that arises in the use of these methods can be obtained by assuming that the resolution in the resulting stability class or category is no better than one half a class. The Briggs (1973) dispersion parameter curves for σ_ϕ in rural areas contain a leading coefficient for each class that is essentially a mean σ_ϕ (in radians) for the category. If a linear trend is computed for these coefficients, from class B to class F, its slope is approximately .02 radians/class. Therefore, an uncertainty of half a class produces an uncertainty of approximately .01 radians, or 20 percent of the mean σ_ϕ for the entire range (class B to class F). Therefore, an uncertainty of about 20 percent would be associated with the use of surrogate methods (via the stability class) for σ_ϕ, if the variability in σ_ϕ within each class were ignored. But Luna and Church (1972), among others, show that the scatter in observed values of σ_ϕ associated with each stability class is so great, that any measured σ_ϕ could belong to any one of the stability classes selected on the basis of the surrogate methods.

B. NCAR Wind Representativeness Study

The literature review given above in Section A was concerned with data uncertainties for a single instrument at a point. However, even if that instrument has no errors, the resulting measurement may not be representative of a measurement at another nearby site. These differences are due to the presence of mesoscale eddies in the atmosphere. For example, Lockhart and Irwin (1980) found that the root-mean-square difference in hourly-averaged wind speed and direction between stations separated by about 20 km was about 1.2 m/s and 31°, respectively. Hanna et al. (1982) found that the wind direction differences were strong functions of wind speed, with larger differences at smaller wind speeds.

Because of a lack of adequate field data, a two week field experiment was conducted in Hereford, Colorado, in March 1990 under a cooperative agreement with the National Center for Atmospheric Research (NCAR). As shown in Figure 7-1, 13 wind monitors were set out along an "L-shaped" pattern with maximum station separation of 10 km. All monitors were part of NCAR's Portable Automated Meso network (PAM) system. A detailed discussion of the analyses of these data is attached as Appendix A. Some of the major conclusions are summarized below:

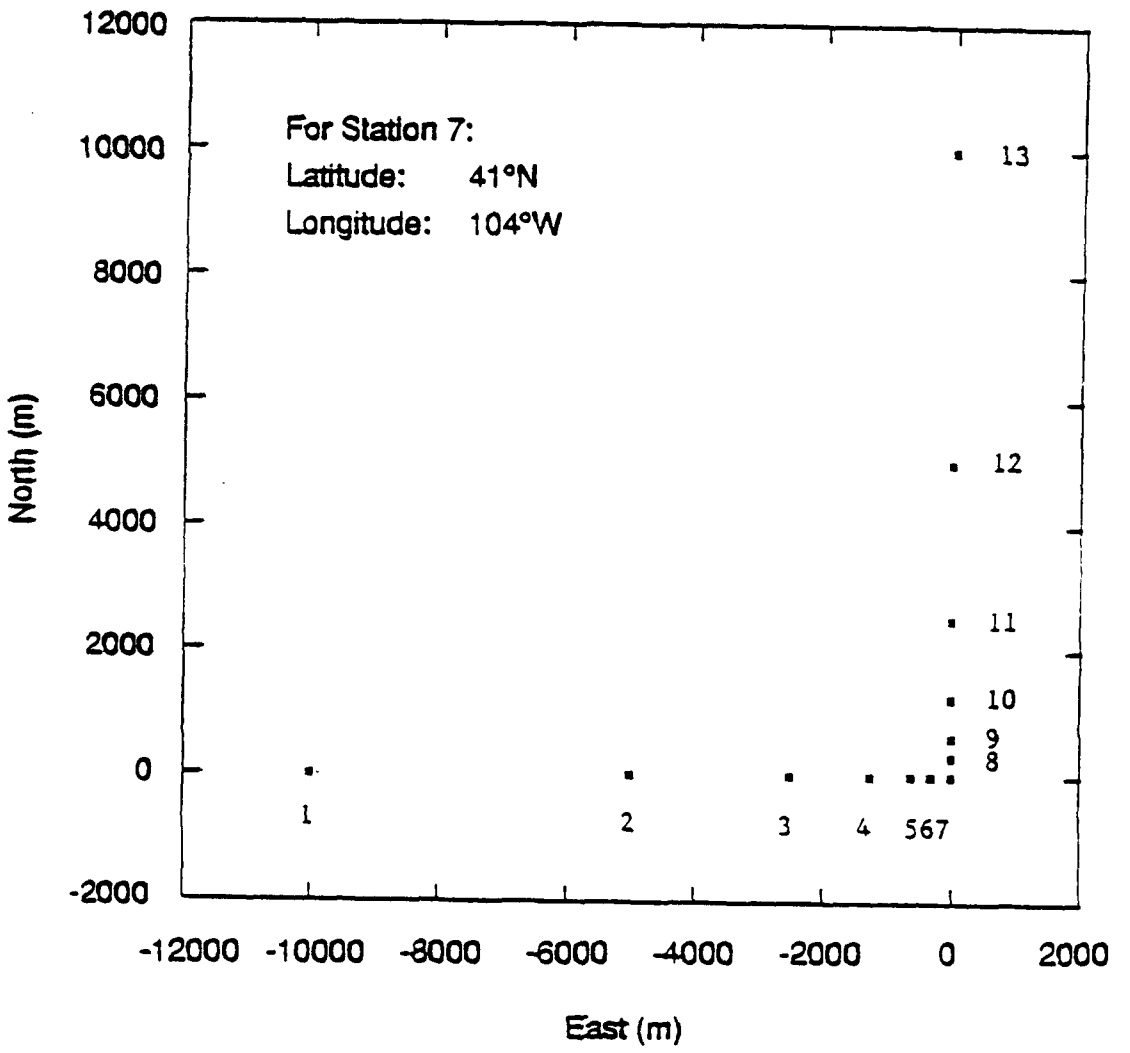

Figure 7-1. Schematic diagram of wind station locations at the Hereford site. Terrain sloped slightly downward from west to east with an average slope of 1%. North is towards the top of the figure and there is 10 km spacing between stations 1 and 7 or stations 7 and 13.

- The turbulent energy, σ^2, at any monitoring station decreases with averaging time, T_a, according to the formula

$$\sigma^2(T_a)/\sigma^2(0) = (1 + T_a/2T_I)^{-1} \qquad (7\text{-}1)$$

where the integral time scale, T_I, is on the order of 1000 s for these data. Thus at an averaging time of about 30 minutes, the turbulent energy is reduced to one-half of its value at much shorter averaging times.

- The correlation coefficient between wind speed or direction fluctuations for short averaging times at two stations separated by distance Δx has the form:

$$R(\Delta x) = e^{-\Delta x/\Lambda}$$

where the integral time distance scale, Λ, is on the order of 1000 m for these data. Thus, at a separation, Δx, of about 700 m, the correlation coefficient drops to about 0.5.

- A general formula for the mean square difference in wind speed fluctuations at two stations has the form:

$$\frac{\sigma^2_{\Delta u}(\Delta x,\ T_a)}{2\sigma^2_u(T_a = 0)} = \left[\frac{0.5}{1 + T_a/2T_{I1}} + \frac{0.5}{1 + T_a/2T_{I2}}\right] \cdot$$

$$\left[1 - e^{-\Delta x/\Lambda_2} + 0.5\,\frac{(e^{-\Delta x/\Lambda_2} - e^{-\Delta x/\Lambda_1})}{(1 + (T_a u/a\Lambda_1)^2)}\right] \qquad (7\text{-}2)$$

where $T_{I1} \sim 300$ s $\qquad T_{I2} \sim 1800$ s

$\Lambda_1 \sim 300$ m $\qquad \Lambda_2 \sim 1200$ m

a (Lagrangian-Eulerian scale) ~ 5

There are two time and distance scales in this equation because the Hereford field data show that there are two relevant mesoscale eddy scales--one that affects correlations at small separations and one that represents a "background" mesoscale variance. This equation should be tested with independent data from a different site. Slightly different values of the time and distance scales may be appropriate at a different site.

C. Source Emission Rate Uncertainties

Emission rate uncertainties were investigated for two types of sources: smoke munitions and the fog-oil smoke generator. The full analyses are presented in Appendix B; the results are summarized below.

The first type of emission rate data to be investigated was from smoke munitions. The issue of estimating the emission rate of obscurant munitions is complex, aside from the issue of estimating the associated uncertainty. There are several reasons for this. First, the critical property which provides the obscurant effect is not directly emitted by the munition; it results from an interaction of the active ingredient, e.g., red phosphorus, and moisture in the ambient atmosphere to form a dense smoke cloud. Second, munitions contain other materials which burn simultaneously but do not contribute directly to the obscurant effect; thus measuring total weight loss over burn time only indirectly measures the amount of active ingredient which has been released. Third, to experimentally determine the amount of active ingredient released, the mass of the active ingredient in the entire smoke cloud must be determined and this measurement can only be carried out in a wind tunnel. Thus, data from the wind tunnel experiments must be extrapolated to the field setting.

Appendix B-1 contains an in-depth discussion of the methods and results of this uncertainty analysis. The topics covered include: how emissions are measured in both wind tunnel and field experiments, the model used for estimating emission rates, a technique for estimating uncertainty (using existing data as an example), and conclusions and recommendations for the collection of additional data which would enhance the uncertainty analysis. Several reports were reviewed for this analysis, but the information on the

method of measuring and modeling emission rates is based on two reports: *Basic Smoke Characterization Test* (DPG-FR-77-311) (DPG, 1978) and *Methodology Investigation Final Report Validation of a Transport and Dispersion Model for Smoke* (DPG-FR-702) (Carter et al., 1979). These reports contain data on three different types of smoke obscurant munitions: white phosphorus, red phosphorus, and zinc oxide-hexachloroethane-aluminum. Because only limited amounts of appropriate data are available for the uncertainty analysis, the conclusions drawn from this analysis are considered tentative. The results of this analysis are summarized below.

Emission rate data from the following types of smoke munitions were analyzed:

155mm HC M1 Canister (zinc)
155mm HC M2 Canister (zinc)
105mm HC M1 Canister (zinc)
6 inch WP Wick (white phosphorus)
2.75 inch Rocket WP Wick (white phosphorus)
81mm Navy RP Wedge (red phosphorus)
155mm Navy RP Wedge (red phosphorus)
81mm German RP Wedge (red phosphorus).

Experiments with these munitions were conducted in two settings: the wind tunnel and the field (Horizontal Grid): One purpose of the wind tunnel experiments was to measure the total amount of active ingredient aerosolized. In the field, the emission rate of active ingredient cannot be directly measured and is estimated from the following expression:

$$Q_t = M_o \, MYF \, YF(A/t_b + 2Bt/t_b^2 + 3Ct^2/t_b^3 + 4Dt^3/t_b^4) \qquad (7\text{-}3)$$

where: Q_t = mass emission rate
M_o = initial mass
MYF = munition yield factor
YF = yield factor
A, B, C, D = coefficients which are determined by fitting the observed data in the wind tunnel experiments to a curve. They are constrained to sum to unity.

The munition yield factor, MYF, is the ratio of the mass of zinc or phosphorus burned, M_x, to the initial mass of the munition, M_o. M_x is determined from the wind tunnel experiments and is calculated by summing the mass of zinc or phosphorus collected by all the impingers. These wind tunnel values of M_x are used to predict the emission rate, Q_t, for field experiments, as M_x cannot be measured in the field setting. The yield factor takes into account the hydroscopic growth of the aerosolized zinc or phosphorus and is a function of ambient relative humidity. The mass emission rate, Q_t, is used as input to the atmospheric dispersion models.

There is no direct way of determining emission rate uncertainty values (such as comparing modeled versus measured emission rates). Thus the uncertainty is modeled based on uncertainty values for the input parameters and on the uncertainty inherent in the emissions rate model.

Two factors limit the uncertainty analysis of the smoke munitions data. First, too few experiments were conducted for each type of munition to determine robust probability density functions for the various parameters. For both wind tunnel and field experiments, only two burns were conducted for each type of submunition; thus means or variances will not be stable or robust. Therefore the quantitative uncertainty analysis presented in Appendix B-1 is neither a precise nor an accurate measure of uncertainty, but the method would be valid for a larger data set (i.e., $n > 5$). Second, some of the munition yield factor data from the wind tunnel experiments are suspect. Appendix B-1 contains a complete discussion of how these data were identified. Because of this second item only the following munitions were used in the analysis:

155mm HC M1 Canister (zinc)
155 HC M2 Canister (zinc)
105 HC Canister (zinc)
81mm Navy RP Wedge (red phosphorus)

It is assumed that the input variables to the emission rate model are dependent and the uncertainty, expressed as the variance, is computed according to Goodman (1960):

$$\sigma^2_{xy} = \bar{x}^2\sigma^2_y + \bar{y}^2\sigma^2_x + 2\,\overline{xy}\,(COV_{xy}) \qquad (7\text{-}4)$$

where σ^2_{xy} = variance of the product xy

$\bar{x}$ = mean of X

σ^2_x = variance of X

$\bar{y}$ = mean of Y

σ^2_y = variance of Y

$$COV_{xy} = \sigma_x\sigma_y = \frac{1}{N}\sum_{i=1}^{N}(x-\bar{x})(y-\bar{y})$$

The variance of the quantity Q_t/M_o was computed for each munition by integrating over the burn time and by assuming the load cell was accurate. Thus equation (7-3) simplifies to:

$$Q_t/M_o = (MYF)\,(YF) \qquad (7\text{-}5)$$

The variance estimates of Q_t/M_o are presented in Table B-2 of Appendix B-1. Interpretation of the variance estimates is limited by the potential error in the munition yield fraction (YF) values and the limited amount of data (n = 2) for each type of munition. However, some summary comments can be made about these data and this approach to calculating variance. The variance of the 81mm Navy red phosphorus wedge is larger than the three zinc based munitions (zinc oxide-hexachloroethane-aluminum). The cause of this difference could be due to the type of munition. For example, the red phosphorus Munition Yield Factor (MYF) is larger than the MYF for zinc munitions.

Further review of these results revealed an interesting comparison to the modeling results presented in *Methodology Investigation Final Report, Validation of Transport and Dispersion Model for Smoke* (DPG, 1979). The red phosphorus munitions showed a greater deviation between the measured and modeled concentration line integrated dose, whereas the zinc munitions showed less deviation. It is hypothesized that a portion of the difference between measured and modeled concentrations could be attributed to variability in the emission rate.

It is concluded from this analysis that although the available data are limited, the approach to variance estimation is applicable to larger data sets. Two recommendations are made. First, the munition yield factor should be determined in an accurate and precise manner. This variable is critical, as it is applied to all the field test data. Second, to assess meaningfully the uncertainty in the emission rate values, more than two sets of data must be available for the results to be more stable, and thus reliable.

The second type of emissions evaluated for uncertainty was from the fog-oil smoke generator. Emission rate data were taken from the experiments reported in Liljegren et al. (1988). Details of this analysis are presented in Appendix B-2; only the results are summarized here. The objectives of this analysis were three-fold: (1) to assess the variability in the emission rate of the fog-oil generator, (2) to compare two methods of computing emission rate, and (3) to evaluate the influence of averaging time on emission rate variability.

As opposed to the smoke munitions, the emission of fog-oil could be measured directly. The weight loss of the oil drum and the exit velocity were measured almost continuously during the experiment. The emission rate data were digitized from the original data which were presented in plots versus time. The first objective was evaluated by computing the coefficient of variation ($sd/\bar{x}$), which normalizes the standard deviation by the mean. It also can be interpreted as what percentage of the mean is the standard deviation. In these data the CV values ranged from 10% to 50%.

In the second objective the two methods of computing emission rate were that of Liljegren et al. (1988) who calculated the time integrated average emission rate by dividing the mass of oil burned by the duration of the smoke generator operation. Our approach averaged the 1-minute "instantaneous" emission rates obtained from the digitized data. The differences between the two methods ranged from -12% to +33%. However, four of the experiments only differed by -4% to +6%. The greatest discrepancies are associated with the experiments when the smoke generator operated unevenly.

The third objective focused on evaluating the variability in the emission rate with averaging times up to 510 seconds. Sufficient data were available

from only five experiments. A plot of the data are shown in Appendix B-2 along with a theoretical curve representing the equation:

$$\frac{\sigma^2(T_a)}{\sigma^2(30\ \text{sec})} = \frac{1 + 30\ \text{sec}/2\ T_I}{1 + T_a/2\ T_I} \qquad (7\text{-}6)$$

where T_a is the variance of the i-th averaging time and T_I is the integral time scale of the physical process. Figure B-1 in Appendix B-2 shows that an integral time scale of 150 seconds provides the best fit of the data.

D. Methods for Estimating the Effects of Data Uncertainties on Model Predictions

As a result of the research conducted and reported in the first part of this section, estimates of the magnitude of data uncertainties are available. These estimates can then be used to calculate the resulting uncertainties in model predictions. Either analytical or Monte Carlo methods can be employed, as described below.

Analytical Model Sensitivity Studies

An analytical formula for assuming the effects of data uncertainties was suggested by Freeman et al. (1986), and has been applied by Hanna (1986) to a simplified air quality model. If concentration, C, is an analytical function of the variables x_i (i = 1 to n), then the uncertainty or variance $V_c = \sigma_c^2$ is given by the equation

$$V_c = \sum_{i=1}^{n} \left(\partial C/\partial x_i\right)^2 V_{xi} + \sum_{i=1}^{n} \sum_{j=1}^{n} \left(\partial^2 C/\partial x_i \partial x_i\right)^2 V_{xi}\ V_{xj} \qquad (7\text{-}7)$$

$$+\ 0.5 \sum_{i=1}^{n} \left(\partial^2 C/\partial x_i^2\right) V_{xi}^2$$

where V_{xi} is the uncertainty or variance in input variable x_i. This equation is a Taylor expansion and implicitly assumes that the individual uncertainties are much less than one. This analytical method is useful only when data uncertainties are small and when the functional form of the model is relatively simple.

Monte Carlo Sensitivity Studies

Monte Carlo error analysis has become a popular exercise with environmental models since it was first described by O'Neill and Gardner (1979). In this method a given model is run many times for sets of input data randomly selected (by a Monte Carlo method) from distributions with assumed means and standard deviations. The resulting standard deviation of the model output is then compared with the standard deviations of the model input. Examples of applications of this procedure are listed below:

- Irwin et al. (1987) studied a Gaussian plume model for atmospheric dispersion with up-to-date algorithms for boundary layer turbulence. They assumed a log-normal distribution for input parameters such as wind speed, turbulence intensity, and mixing depth. They found that the standard deviation in the variability of predicted maximum concentrations was about double the standard deviation in the variability of individual input parameters. When the predicted areas enclosed by given isopleths were considered, their variability was about triple that of the input parameters.

- Lewellen and Sykes (1989) also studied an atmospheric plume model, but incorporated predictions of the distribution function of concentration fluctuations in their model. The effects of variations of ± 20% in wind speed, σ_w, and mixing depth were considered. They concluded that the observed concentration fields included the effects of mesoscale wind fluctuations that were not accounted for by the model.

- Freeman et al. (1986) applied Monte Carlo techniques to the ISC model, and compared the resulting uncertainties with those calculated by the analytical formula discussed in Subsection 1 above. It was found that the two methods agreed fairly well for input data uncertainties less than ± 30%.

Examples of applications of Monte Carlo procedures to water quality models and to other environmental models are given by Chahuneau et al. (1983), Fedra (1983), Gardner and O'Neill (1983), Gardner (1988), Karmeshu and

Lara-Rosano (1987), Keesman and van Straten (1989), McLaughlin (1983), McLaughlin and Wood (1988), O'Neill et al. (1982), Smolyody (1983), and Warwick and Gale (1988). A major concern of these studies is the optimum number of Monte Carlo samples to be used to calculate the variance in the mode output. It appears that a few hundred samples are sufficient.

Our software also includes a Monte Carlo algorithm. All that is needed is the identification of a basic prediction formula, in the general form:

$$y = f(x_1, x_2, x_3 \ldots)$$

Then means and variances of one or more of the input parameters, x_1 through x_n, must be stated. (It is assumed that variations in any of these parameters are independent of variations in the others). Then the formula is solved several hundred times and a mean and variance of y is calculated from these results. For simple formulas the solution to equation (7-7) and the Monte Carlo solution should agree.

E. Similarity Approach to Reducing Variance in a Data Analysis System

There are many external and internal forces and parameters influencing any physical system. However, only a few of these parameters have a dominant effect on the system. Any given analytical formula attempts to incorporate only the most dominant parameters, while ignoring those parameters that have little or no influence on the system. This section provides an example of an exercise in which the important governing parameters are identified for the Prairie Grass field experiment.

1. Identification of Dominant Parameters

If the modeler has sufficient knowledge he may immediately know the dominant parameters of his system. This result is more likely if he is working with a "hard" system, which is characterized by well-known equations.

If data are available, the dominant parameters can be identified through statistical analysis. As an example, the Prairie Grass field data (Barad, 1958) were considered, where a tracer gas was released from a

continuous point source near the ground over flat farmland. The following parameters were analyzed:

C: Observed maximum concentration on a monitoring arc located at a distance x from the source

x: Distance of monitoring arc from source

Q: Continuous tracer gas source strength

u: Wind speed

σ_w: Vertical component of turbulent velocity fluctuation

σ_v: Lateral component of turbulent velocity fluctuation

The total relative variance of the observed concentration, defined as $\sigma_C^2/\bar{C}^2$, was calculated as 2.20. The relative variances of various scaled observed concentrations (e.g., C/Q or Cxu) were then calculated, with the following results:

Scaled Variable	Relative Variance	Percent Reduction of Variance
C	2.20	
$Cx^2\sigma_w\sigma_v/u$	0.51	77%
Cxu	0.67	70%
$Cx\sigma_q\sigma_v/u$	0.75	66%
$Cx^2\sigma_w\sigma_v/uQ$	1.03	53%
Cx	1.36	38%
Cu	1.65	25%
Cux^2	1.80	18%
$C\sigma_w/u$	1.86	15%

$C\sigma_v/u$	1.88	14%
C/Q	2.98	-35%
Cx^2	4.67	-112%

It is seen that, just by combining the variables judiciously, the total variance can be reduced by about 77%. The best performing combination, $Cx^2\sigma_w\sigma_v/u$, is based on the functional form of the Gaussian equation ($C \propto (u\sigma_y\sigma_z)^{-1}$, where $\sigma_y \propto (\sigma_v/u)x$ and $\sigma_z \propto (\sigma_w/u)x$). Even the simple hypothesis $C \propto (xu)^{-1}$ produces a 70% reduction in variance. It is concluded that it would be difficult for more complex models to significantly improve upon these simple scaling relations.

The lack of dependence of C upon source strength, Q, is surprising--in fact, the variance is <u>increased</u> by 35% when Q is included. This unexpected result is due to the fact that Q was controlled by the Prairie Grass experimenters so that it was twice as high during the day than during the night, with the intention of maintaining a nearly constant C. Consequently, there is little correlation between Q and C.

Intentionally Blank

SECTION VIII

ASSESSMENT OF STOCHASTIC UNCERTAINTIES

A. Background

The work summarized in this section emphasizes development of a quantitative method to estimate the magnitude of the stochastic uncertainties component of the total uncertainty. We can control the other two components of total uncertainty (model physics errors and data input errors) to some extent, but cannot harness the stochastic uncertainty component. It will always be there due to the randomness in atmospheric processes, in the same way that variability in wind speed can never be eliminated. Our goal is therefore to estimate the stochastic component, not to control it. In Phase I, we tested a few formulas for this component that were developed as a result of an Army Research Office (ARO) contract on concentration fluctuations. Concentration data recorded in time series form had been studied during the course of the ARO project, and estimates of the time scale of fluctuations observed under conditions similar to those experienced during many of the DPG smoke/obscurant effectiveness tests facilitated our estimate of the stochastic uncertainty. Several other time series records have been studied during Phase II of this project and are discussed in Sections C and D.

Some models grossly characterize concentration fluctuations by assuming that the ratio of the peak (fluctuating) concentration to the model predicted mean concentration is about two. Chatwin (1982) pointed out that in many cases involving accidental releases of hazardous gases, the maximum short term (~1 sec) concentration is the most important variable to predict. Similarly, one-second averages of smoke obscuration are of primary importance in DPG applications. According to Chatwin the mean concentration predicted by the model can be irrelevant in these cases, since the probability distribution function (pdf) of concentration fluctuations in the atmosphere is characterized by a standard deviation at least as large as the mean. The relative magnitude of short term concentration fluctuations (characterized as $\sigma_c/\bar{C}$) is the same order as the relative magnitude of short term velocity fluctuations ($\sigma_u/\bar{U}$) in the atmosphere. The parameters σ_c and σ_u are the standard deviations of

turbulent fluctuations in concentration and wind speed, respectively. It is assumed that averaging times are about one second and sampling times are about ten minutes.

There are a few papers that deal with the general topic of stochastic uncertainty as it relates to atmospheric dispersion models. For example, summaries of workshops on this topic are given by Fox (1984) and Carson (1986), both of whom recommend that predictions of stochastic uncertainty should be given along with predictions of ensemble mean concentrations. In this manner, decision-makers can see the confidence intervals associated with any model prediction.

Venkatram (1984) and Benarie (1987) discuss stochastic uncertainty as it relates to the limits of air quality modeling. For example, Venkatram points out that there are large turbulent eddies in the convective boundary layer with distance scales of about 1000 m and time scales of 5 to 10 minutes that cause broad fluctuations in concentrations. If a plume is caught in a convective updraft, it can rise to the top of the boundary layer for several minutes at a time.

Weil et al. (1988) provide an overview of current methods of addressing this problem, and suggest that Lewellen et al. (1984) are on the right track, since they currently possess the only dispersion model that predicts variances as well as means. For example, their model might predict $\bar{C}_p$ = 100 $\mu g/m^3$ and σ_{cp} = 50 $\mu g/m^3$. These predictions would imply that there is a 2 1/2 % probability that C_p would exceed $\bar{C}_p + 2\,\sigma_{cp}$, or 200 $\mu g/m^3$. However, we point out that current methods of predicting σ_{cp} are highly uncertain in themselves.

Several references were reviewed on the subject of observations of concentration fluctuations, σ_c, for a wide range of averaging times, ranging from 0.01 sec to 1 hour. Jones (1983) has developed an instrument with very fast response (0.01 sec or less) and has demonstrated that there are large turbulent fluctuations in concentration even in the center of plumes. Wilson and Simms (1985) and Chatwin and Sullivan (1989) emphasize the importance of intermittency, generally caused by plume meandering, which leads to long periods of zeros in the concentration time series, and complicates the derivation of analytical formulas for the probability density function (pdf).

It is generally agreed that the pdf for plumes from point sources has a long positive tail and can be approximated by an exponential, log-normal, or clipped-normal function with $\sigma_c/\bar{C}$ approximately equal to unity. In addition, the references emphasize that there are special problems in analyzing instantaneous puffs, since large numbers of them are required in order to define an ensemble mean.

Another interesting and innovative line of research relates to the use of fractals to analyze the stochastic component of atmospheric phenomena. Lovejoy et al. (1985, 1986) and Schertzer and Lovejoy (1985, 1990) discuss many geophysical phenomena, including clouds, and demonstrate that they can be analyzed from the viewpoint of fractals. For example, the fractal dimension can be determined from the ratio of the perimeter to the area of a cloud as observed by radar and by satellites. Gifford (1989) extends this theory to smoke plumes and calculates their fractal dimension from mesoscale and larger scale observations. He points out that plumes are "torn-apart" by synoptic systems, such that their perimeter is always quite jagged.

Predictions of models such as VSDM can be thought of as ensemble means for certain averaging times. An ensemble mean is defined as the mean over an infinite number of realizations of a given experiment. The averaging time is usually implicit in the data used by the model and in its formulations for treating the input data - for example, if hourly-averaged wind and turbulence observations are used, then the predictions represent a one hour average. If the Pasquill-Gifford-Turner dispersion curves are used, then the predictions represent a 10 minute average, since data from 10 minute periods were used to derive the curves. In the case of instantaneous (puff) models, the predictions represent an ensemble mean only to the extent that a large enough set of experiments (20 or more) was used to derive the model. These experiments should be conducted under the same external conditions (i.e., wind speed, stability, source term). For example, if it were possible to run a set of DPG experiments long enough that 100 independent time periods (e.g., of ten-minute duration) could be found which all satisfy the following meteorological conditions:

$4.8 < u < 5.2$ m/s, $\qquad 65\% < RH < 70\%$

$10^{\circ} < T < 12^{\circ}C$, $-2 <$ net radiation flux < 2 watts/m^2

then the observed concentration field averaged over these 100 experiments would approach an ensemble average. The reader quickly sees that it is difficult operationally and financially to generate ensemble averages from atmospheric field experiments.

Thus the results of a single experiment, or even three or four experiments conducted under similar external conditions will likely differ (perhaps by as much as an order of magnitude) from the ensemble mean predictions of the model. If this happens, it is not an indictment of the model but may be a manifestation of the inherent stochastic variability of the atmosphere.

Wind tunnel experiments can be used to study variability, since it is easier to insure repeatability of experiments and thus create a large ensemble of data. On the negative side, the wind tunnel cannot simulate larger scale eddies and other phenomena that contribute to variability in the atmosphere. Furthermore, the laboratory Reynolds number is not high enough to permit the establishment of an inertial subrange like there is in the atmosphere. Meroney and Lohmeyer (1984) conducted extensive studies of tracer clouds released in a wind tunnel and calculated the stochastic or random concentration fluctuation intensity, $\sigma_c/\bar{C}$, for various source volumes, wind speeds and downwind distances. They find that the average $\sigma_c/\bar{C}$ is about 0.3 in this wind tunnel. The value of $\sigma_c/\bar{C}$ in individual experiments range from 0.1 to 0.7. In contrast, Hanna (1984) reports observed values of $\sigma_c/\bar{C}$ of 1.5 on the plume centerline and $\sigma_c/\bar{C}$ of 5.0 on the plume edges for one second observations a smoke plume released in the atmospheric boundary layer.

B. Estimating Stochastic Uncertainties

Generic methods are needed for estimating σ_c, the stochastic component of concentration fluctuations. These methods should be robust and should be based on easily-defined input parameters. In a study funded by ARO, Hanna (1984) suggests the following equations for σ_c, based on the review of a number of articles in the literature. These assume that concentrations are measured at a fixed point at downwind distances small enough that lateral plume meandering is

still significant. This is true at $x \lesssim 10$ km for plumes released in the boundary layer and is therefore applicable for most problems concerned with maximum concentrations due to point source releases.

It must be understood that what is really needed is a probability density function (pdf) for concentrations, C. The standard deviation, σ_c, is always an important parameter and is sometimes sufficient for describing this pdf. The value of $\sigma_c/\overline{C}$ is a function of:

- x or t — downwind distance or travel time
- $x-x_o$ — along-wind distance from cloud centerline
- $x-y_o$ — cross-wind distance from cloud centerline
- $z-h_e$ — vertical distance from cloud centerline
- T_c — integral time scale of concentration fluctuations--usually parameterized through the two components of the Lagrangian time scale, T_{Ly} and T_{Lz}
- T_a — averaging time for observations
- Λ_a — averaging distance scale for observations
- σ_o — initial distance scale of source

Hanna et al. (1991) assume that the exponential pdf is valid for observations of concentration at a point and that

$$\sigma_c/\overline{C} = \left((2/I) - 1\right)^{1/2} \qquad (8\text{-}1)$$

where I is intermittency (i.e., fraction of time that plume is present). Note that I must be between 0 and 1.0, so the minimum value of $\sigma_c/\overline{C}$ is 1. Hanna (1984) proposes that

$$I = (\sigma_{yI}\sigma_{zI}/\sigma_{yT}\sigma_{zT})\exp(-(h_e-z)^2/2\sigma_{zT}^2 - (y-y_o)^2/2\sigma_{yT}^2) \qquad (8\text{-}2)$$

where subscripts I and T refer to "instantaneous" and "total", respectively. In the derivation of Equation (8-2), it is assumed that averaging time, T_a, equals 0.0. The parameter h_e is the initial plume height and y and z are the lateral and vertical positions of the receptor.

As suggested by Gifford (1959), the "meandering" component, σ_{ym}, can be expressed by the formula:

$$\sigma_{ym}^2 = \sigma_{yT}^2 - \sigma_{yI}^2 \qquad (8\text{-}3)$$

At small travel times, $\sigma_{ym} > \sigma_{yI}$, and at large travel times, $\sigma_{yI} > \sigma_{ym}$. The ratio σ_I/σ_T can be given by a formula suggested by Gifford (1982) and Lee and Stone (1983):

$$\frac{\sigma_I^2}{\sigma_T^2} = \frac{\hat{\sigma}_o^{\,2} + T' - (1 - e^{-T'}) - 0.5(1 - e^{-T'})^2}{\hat{\sigma}_o^{\,2} + T' - (1 - e^{-T'})} \qquad (8\text{-}4)$$

where $T' = t/T_L$ and $\hat{\sigma}_o = \sigma_o/\sqrt{2}\sigma_v T_L$. The parameter σ_v is the lateral turbulence (in general, $\sigma_v \sim 2u_*$) and the product $\sqrt{2}\sigma_v T_L$ is the approximate size of the plume after a travel time of T_L.

Csanady (1973) and others show that the cross-wind variation of $\sigma_c\sqrt{C}$ is given by the formula:

$$\left[\sigma_c\sqrt{C}\ (\text{at } y - y_o)\right] = \left[\sigma_c\sqrt{C}\ (\text{at } y = y_o)\right] e^{(y - y_o)^2/4\sigma_{yT}^2} \qquad (8\text{-}5)$$

It can be assumed that similar functional relations hold for the vertical and along-wind variations, with $(z - h_e)^2/4\sigma_{zT}^2$ and $(x - x_o)^2/4\sigma_{xT}^2$, respectively, substituted into the exponential term in Equation (8-5).

The formulas above are valid for "instantaneous" averaging times--in practice, for time series of C observations at a point at time intervals of a few seconds. For longer averaging time, σ_c will decrease. The following correction for averaging time is based on Taylor's formula:

$$\frac{\sigma_c^2(T_a)}{\sigma_c^2(0)} = 2\frac{T_c}{T_a}\left[1 - \frac{T_c}{T_a}\left(1 - e^{-\frac{T_a}{T_c}}\right)\right] \qquad (8\text{-}6)$$

which can be fairly accurately approximated by the simpler formula:

$$\frac{\sigma_c^2(T_a)}{\sigma_c^2(0)} = (1 + T_a/2T_c)^{-1} \quad , \qquad (8\text{-}7)$$

where T_a is the averaging time and T_c is the integral time scale for concentration fluctuations.

If concentration data are not available, T_c can be estimated by making an analogy with the turbulence time scale: $T_c = T_{Ly}$, and T_{Ly}. However, in all cases, T_c should be capped by the value $T_s/5$, since it is not possible to have an integral scale larger than 0.2 times the sampling time, T_s.

The theoretical equations discussed above work fine during short-term, specialized experiments. However, the general procedures must be capable of being applied to the entire range of possible meteorological and source conditions. The problem is that the theoretical equations are not robust; i.e., they do not consistently yield results in a reasonable range. Under certain combinations of h, u, h_e, etc., they can "blow up" and yield unreasonable results. Furthermore, formulas for T_{Ly} and T_{Lz} are not well-validated, and are the subject for much current discussion.

Available observations of $\sigma_c/\overline{C}$ consistently demonstrate that $\sigma_c/\overline{C} \sim 1$ near the plume centerline, and $\sigma_c/\overline{C}$ grows to about 5 near the plume edge. This variation with cross-wind distance, $y - y_o$, is consistent with the concept that the "plume edge" is defined as a value of $(y - y_o)$ approximately equal to $2\sigma_{yT}$. Observations also show that, if concentrations are considered only when the plume is over the monitor (i.e., conditional data), then $\sigma_c/\overline{C}$ (conditional) $\sim$ 0.5 to 1.0. (Mylne and Mason, 1991, Sawford et al., 1985, Peterson et al. 1988, Hanna 1984a and 1984b). These results are all valid for short averaging times ($T_a \sim 1$ sec) and for sources near the ground surface. Deardorff and Willis' (1984) data for tall stack sources suggest that $\sigma_c/\overline{C}$ can be as high as 5 to 10 for ground-level receptors at small downwind distances, where the plume only occasionally strikes the ground. This situation could be treated by assuming that $\sigma_c/\overline{C} \sim 1$ on the plume centerline aloft, and that $h_e/\sigma_z \sim 2$ to 3.

Consequently, Hanna et al. (1991) propose that actual calculations be carried out with simple robust default parameters. They propose the following:

- Input for $\sigma_c\sqrt{C}$ calculation

x:	downwind distance
$z-h_e$:	vertical distance
$y-y_o$:	crosswind distance
T_c:	integral time scale of concentration fluctuations
T_{Ly}:	y component of Lagrangian turbulent scale
T_{Lz}:	z component of Lagrangian turbulent scale
T_a:	averaging time for observations of C
Λ_a:	averaging distance for observations of C
σ_o:	initial size of source

Default Values:

x:	(not needed, but set = 100 m)
$z-h_e$:	(must be input)
$y-y_o$:	(must be input)
T_c:	(100 seconds)
T_{Ly}:	(not needed, but set = T_c)
T_{Lz}:	(not needed, but set = T_c)
T_a:	(must be input)
Λ_a:	(not needed, but set = 1 m)
σ_o:	(not needed, but set = 0.1 m)

In addition, it is assumed that σ_{yT} and σ_{zT} can be estimated, possibly from typical dispersion curves. If no information is available on σ_{yT} or σ_{zT}, then set $z-h_e$ and $y-y_o = 0$ and assume all calculations are on the plume centerline.

- Part 1 of calculation:

  $\sigma_c\sqrt{C}$ calculation for $T_a = 0$:

  Default: $$\sigma_c\sqrt{C} = \left[e^{(y-y_o)^2/4\sigma_{yT}^2}\right]\left[e^{(z-h_e)^2/4\sigma_{zT}^2}\right] \qquad (8\text{-}8)$$

  where it is assumed that $\sigma_c\sqrt{C}$ on the plume centerline equals 1.0.

  Note: do not let $(y-y_o)/\sigma_{yT}$ or $(z-h_e)/\sigma_{zT}$ exceed 2.0

- Part 2 of calculation:

  Correction to $\sigma_c/\overline{C}$ for averaging time T_a

  Default:

$$\frac{\sigma_c^2(T_a)}{\sigma_c^2(0)} = (1 + T_a/2T_c)^{-1} \qquad (8\text{-}9)$$

  where the default value for T_c is 100 seconds.

We note that much of the data collected to assess the screening effectiveness of smoke munitions and generators is obtained from transmissometers. These instruments provide line-of-sight, integrated concentrations (C_y or CL) rather than concentrations at a specific point. Therefore, information on the lateral distribution of material in the smoke-clouds is "lost." Furthermore, because these smoke releases are near the ground surface, they tend to "hug the ground" and do not often lift off the ground. When the trials are conducted during ideal conditions, $\sigma_{CL}/\overline{CL}$ is typically uninfluenced by meandering and is related to in-plume fluctuations, unless the entire cloud is displaced in the vertical by convective motions. As a result, typical values of $\sigma_{CL}/\overline{CL}$ are observed to fall in the range 0.5 to 1.0. Therefore, the part 1 calculation for the line-of-sight integrated concentrations should be replaced by the assumption that $\sigma_{CL}/\overline{CL}$ equals 0.75.

The recommended value of 100s for the integral time scale T_C ought to be revised as well when CL measurements are obtained. If the line-of-sight has integrated over all lateral meanders of the smoke-plume, then T_C for near-surface releases is expected to be on the order of 10s rather than 100s. However, if the plume meanders outside the range of the line-of-sight, the effects of meander must be recognized, which will require assumptions similar to those for point-measurements of concentration.

Estimates of the stochastic uncertainty in line-of-sight average concentrations derived from transmissometer measurements of smoke-clouds have been made for two representative U.S. Army datasets and are discussed in the next two sections. The first dataset involves data pertaining to smoke-clouds

produced by smoke munitions, which typically provide time series data for a period of several minutes. The second dataset involves smoke-plumes produced by a fogger, which provides time series data for periods of about one hour. In both cases, the concentrations derived from the transmissometer data are "concentration-lengths" (CL) along a path that lies across the transport direction, and the end-points of each path lie outside of the smoke-cloud. Therefore, lateral meanders of the clouds as they pass through the line-of-sight are not documented in these data.

C. Analysis of Data from Development Test 1 (XM819 Munition)

This dataset was obtained from the Atmospheric Aerosol and Optics Data Library (AAODL), which sent us a data tape and excerpts from an unidentified report that describes the trials. From this report, it is clear that the trials included both the XM819 and the M375A2 smoke projectiles, and that the trials were designed to evalute the performance of the developmental device (XM819) relative to the standard device. The configuration of measuring systems, and descriptions of general operations during the trials are reviewed, and estimates of the accuracy of the instruments are reported. A table gives the location (x,y,z) of each of the instruments. The trials were conducted at the Dugway Proving Ground (DPG).

A second report provided by AAODL (Davis and Farmer, 1986) casts considerable doubt on the estimates of line-integrated concentrations obtained from some of the transmittance data. Optical depth plots, in which -ln(transmittance) from one band of wavelengths is plotted against that for a second band, showed a distinct departure from the expected linear relationship, thereby indicating that Beer's law is not applicable to these data (although it should be applicable). There is a "large area void of data points at relatively high values of transmission", in addition to a strongly curved appearance with a greater degree of scatter than expected. Much of this is shown to be related to what is termed a premature threshold problem. In essence, they find that scattering of sunlight into the transmissometer receiver results in an abnormal setting for the threshold of detection for the visible bandpass. The IR band is not affected to such an extent, so that the relationship between the optical depths obtained from the two wavelengths becomes nonlinear. The nonlinearity could also be caused by pushing the

electronics into a nonlinear range (by having an abnormally high background signal). The study points out that the signature of the problem is seen in almost half of the trials along lines-of-sight (LOS) 1 and 2, but in only 6% of the trials along LOS 4, 5, and 6. The orientaion of LOS 1 and 2 places the transmissometer receiver so that it points WSW, while the recievers for LOS 4, 5, and 6 point NNW. Only four of the 22 trials were completed before noon (MST). This suggests that data obtained in the visible band from LOS 1, and 2 should not be used in this analysis.

The trials consisted of releases of smoke from firing either 1 or 3 munitions at a time. The XM819 munition is made up of red phosphorous (RP) wedges, and is fired in the "Series A" trials. The M375A2 munition contains white phosphorous, packed as an unconsolidated powder (refered to as "bulk WP"), and is fired in the "Series B" trials. The bulk WP is said to burn hot, which tends to produce some rise in the cloud during light-wind conditions due to its buoyancy. Transmissometer data were obtained along 5 lines of sight (LOS). Figure 8-1 shows the locations of the points of release of the clouds from the munitions, relative to the LOS's. Because the predominant wind directions during the trials carried the clouds across LOS 1 and LOS 2, these provide the most useful data for our analyses. From the figure, we see that the projectiles tended to be fired near LOS 1 if the wind was blowing from LOS 1 toward LOS 2, and they tended to be fired near LOS 2 if the winds were from the other direction. As a result of this configuration, transmissometer data across the cloud (approximately perpendicular to the transport direction) are usually available at only 1 LOS, and at a distance of 100 to 200 m from the location of the burst.

These data had been analyzed by Saterlie et al. (1981). The problems identified later by Davis and Farmer (1986), while not recognized in detail, were nonetheless being studied from the point of view of developing an effective way to "remove the noise" in the transmissometer data. As a first cut, Saterlie et al. calculated average background concentrations, CL, for each LOS. They also noted a drift in the baseline of the signal in that concentrations did not return to zero after the passage of the cloud. This appears to have been noticed on very few occasions (T305A:LOS2; T307A:LOS2; T401A:LOS1,2; T901A:LOS2,5). Also called out in the report, visual observations of the smoke clouds indicated that the cloud from the M375A2 munitions passed above a given LOS in many instances, reflecting the reality

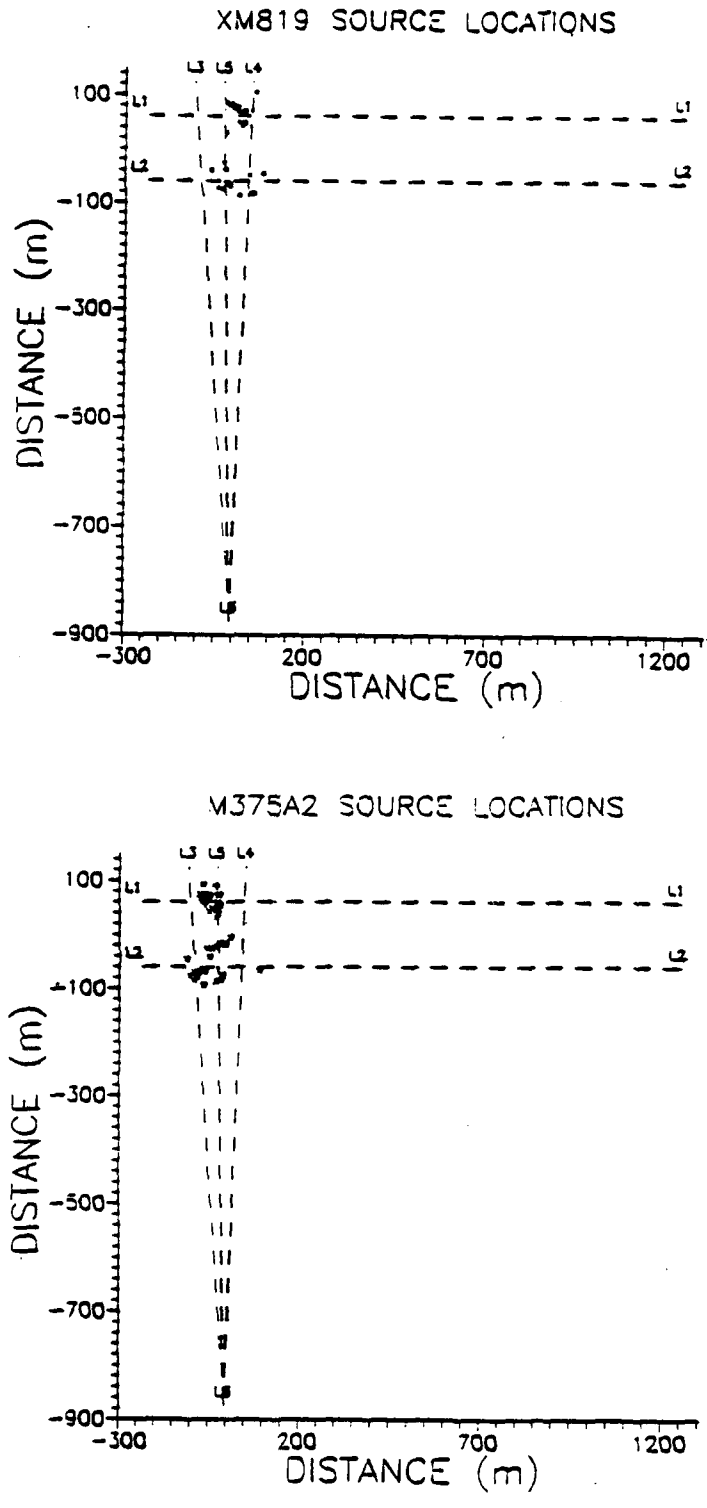

Figure 8-1. Location of sources of smoke relative to the lines-of-site (LOS) of transmissometers used to measure concentrations during Development Test 1 of the XM819 smoke munition.

that they are air-burst smoke munitions. After neglecting data from a particular LOS if it was upwind of the burst region, or if the collection of data from the LOS was terminated before all of the smoke had travelled across it, or if more than half of the smoke passed outside the range of the LOS, cross-wind line-integrated dosages CLIDS were calculated from the time series of CL values. LOS 1 and LOS 2 were positioned best to record the smoke clouds during these trials. The CL data processed and contained in the dataset are derived from measurements made in the IR band, rather than the visible band.

The time series of CL included among the data in the AAODL dataset appear to be the values calculated by Saterlie et al. We checked this by converting the transmissometer data contained in the AAODL dataset to CL, making use of the same extinction coefficient. Our results match the CL data in the dataset. Saterlie et al. (1981) obtained dosages from these time series by integrating in time over the record. They adjusted the resulting CLID values for what was called "background". A background value was set for each LOS, for each munition (either the XM819 or the M375A2):

Background Values for CLID ($g\text{-}s/m^2$)

LOS	1	2	3	4	5
XM819	60	50	19	42	32
M375A2	16	4	6	6	9

Record lengths for the XM819 trials were typically 500 to 600 s, while those for the M375A2 trials were typically 150 to 250 s. If we assume periods of 550 s and 200 s, respectively, the CLID background values used by Saterlie et al. imply CL background values of order:

Background Values for CL (g/m^2)

LOS	1	2	3	4	5
XM819	.11	.09	.03	.08	.06
M375A2	.08	.02	.03	.03	.05

An almost linear trend in time series of CL had been noted for a few of the LOS records. Saterlie et al. removed this trend by simply subtracting out a linear trend between the CL values at the start of the record, and the end of the record.

Figures 8-2 through 8-5 contain time series of the CL data, denoted as CLEN, from the "best" LOS downwind of the burst, for the trials that do not exhibit anomalous behavior. The four figures distinguish between the two types of munition, and they further distinguish between trials in which a single munition was fired, and trials in which three munitions were fired. Comparing these time series with the approximate "background" values of CL listed above, most of the signal contained in the time series appears to result from the munition. However, two distinct patterns describe the time series. The pattern that we will call A contains a single, well-defined group of pulses of smoke. The pattern that we will call B displays a broader signal in which fluctuations dominate any underlying pulse-like pattern.

These time series of CL have been used to calculate properties of the fluctuations in the concentrations. These fluctuations are characterized in terms of $\sigma_{CL} / \overline{CL}$, where σ_{CL} is the standard deviation of CL, and $\overline{CL}$ is the mean value of CL in the time series record. Furthermore, we estimate an integral time scale by comparing σ_{CL} calculated for two averaging times. This estimate is based on Equation (8-6), which is repeated below:

$$\frac{\sigma^2_{CL}(T_a)}{\sigma^2_{CL}(0)} = 2\,(T_c/T_a)\,\left(1 - \frac{T_c}{T_a}\,[1 - e^{-T_a/T_c}]\right)$$

where T_a is the averaging time, and T_c is the integral timescale. This equation is based on Taylor's (1921) analysis of the statistical theory of diffusion. With two averaging times (say T_{a1} and T_{a2}), the standard deviation $\sigma_{CL}(0)$ for the time series of "instantaneous" concentrations can be eliminated, and the resulting equation can be inverted to find T_c.

Properties of the fluctuations in CL are summarized in Table 8-1, along with calculated values of L (Monin-Obukhov length) and u_* (friction velocity). These were calculated from profiles of wind speed and temperature by assuming that surface-layer similarity results apply to this site. All values of L are less than zero, indicating that all of the trials were conducted during daytime convective conditions. The intermittency (I) listed in the table is

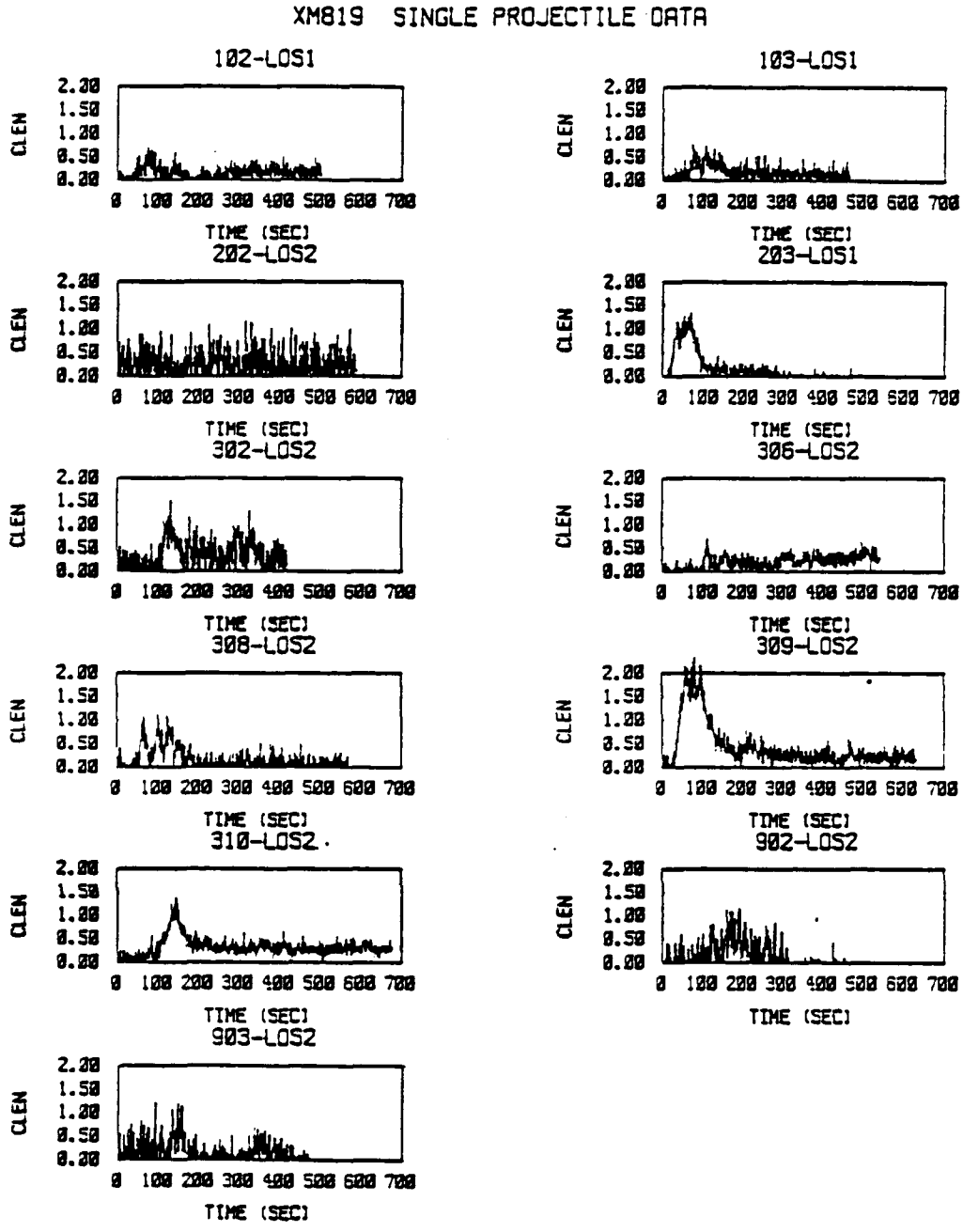

Figure 8-2. Time series of smoke concentration-length (CLEN) data calculated from transmissometer measurements made along the line-of-sight (LOS) downwind from the source of the smoke. The source of the smoke is a single XM819 munition.

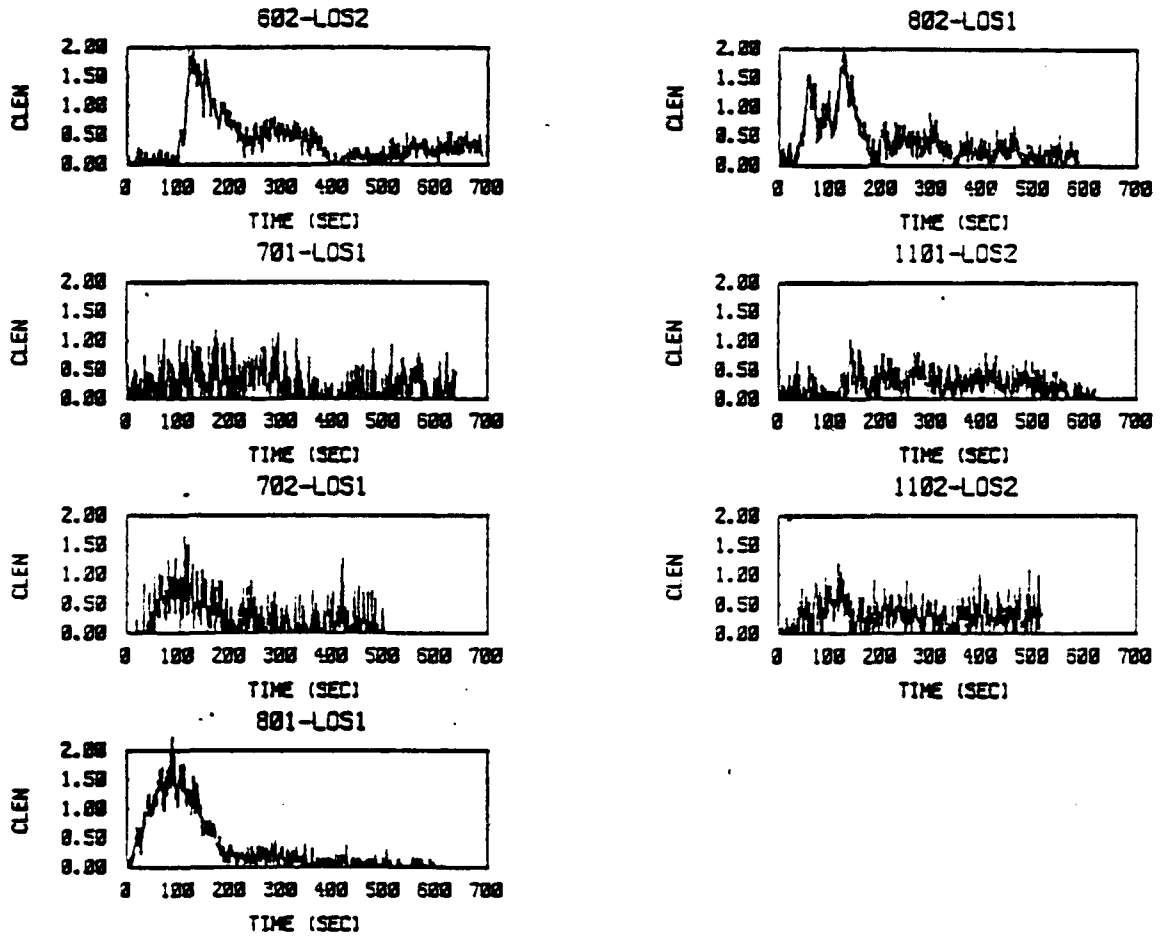

Figure 8-3. Time series of smoke concentration-length (CLEN) data calculated from transmissometer measurements made along the line-of-sight (LOS) downwind from the source of the smoke. The source of the smoke is a group of three XM819 munitions.

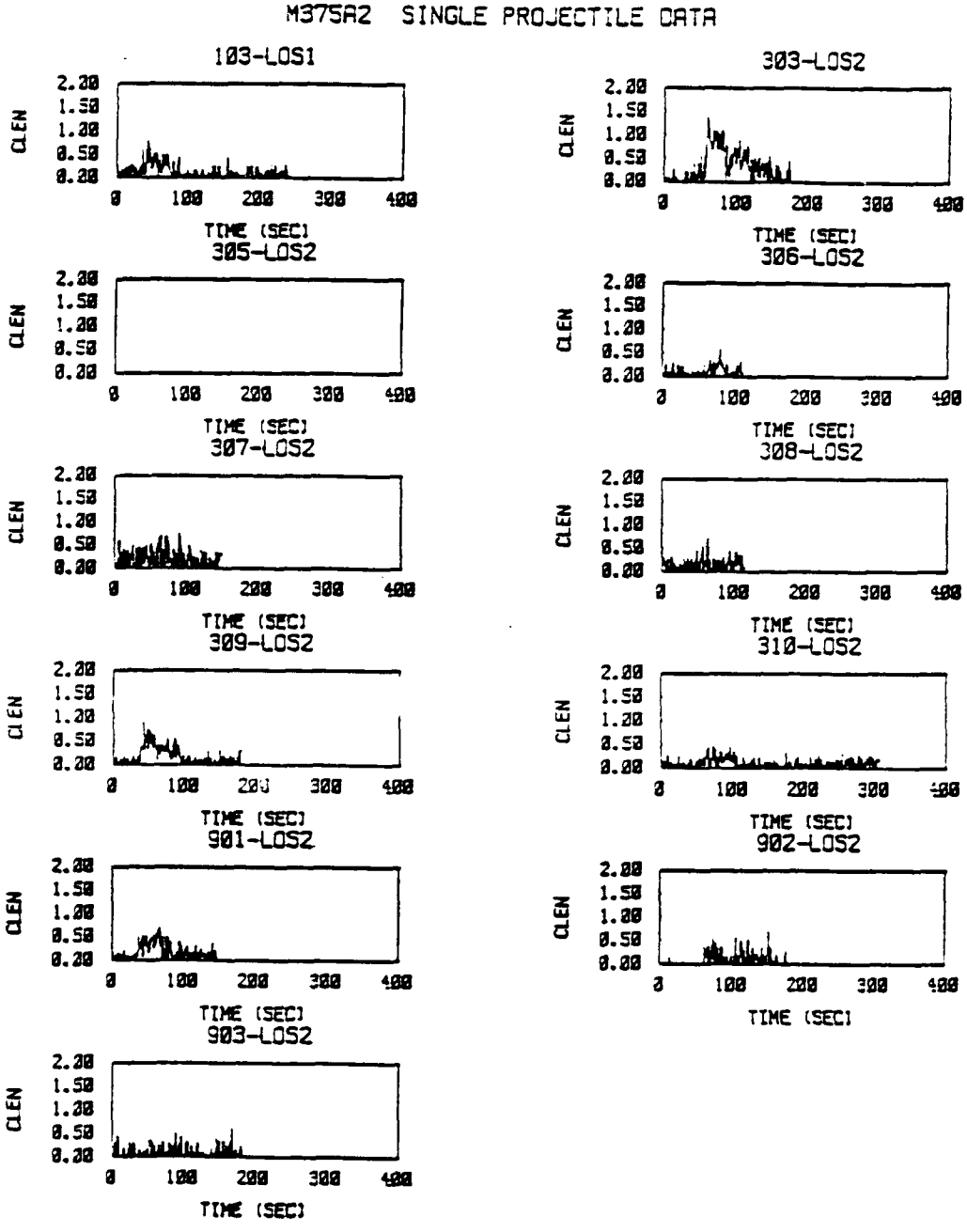

Figure 8-4. Time series of smoke concentration-length (CLEN) data calculated from transmissometer measurements made along the line-of-sight (LOS) downwind from the source of the smoke. The source of the smoke is a single M375A2 munition.

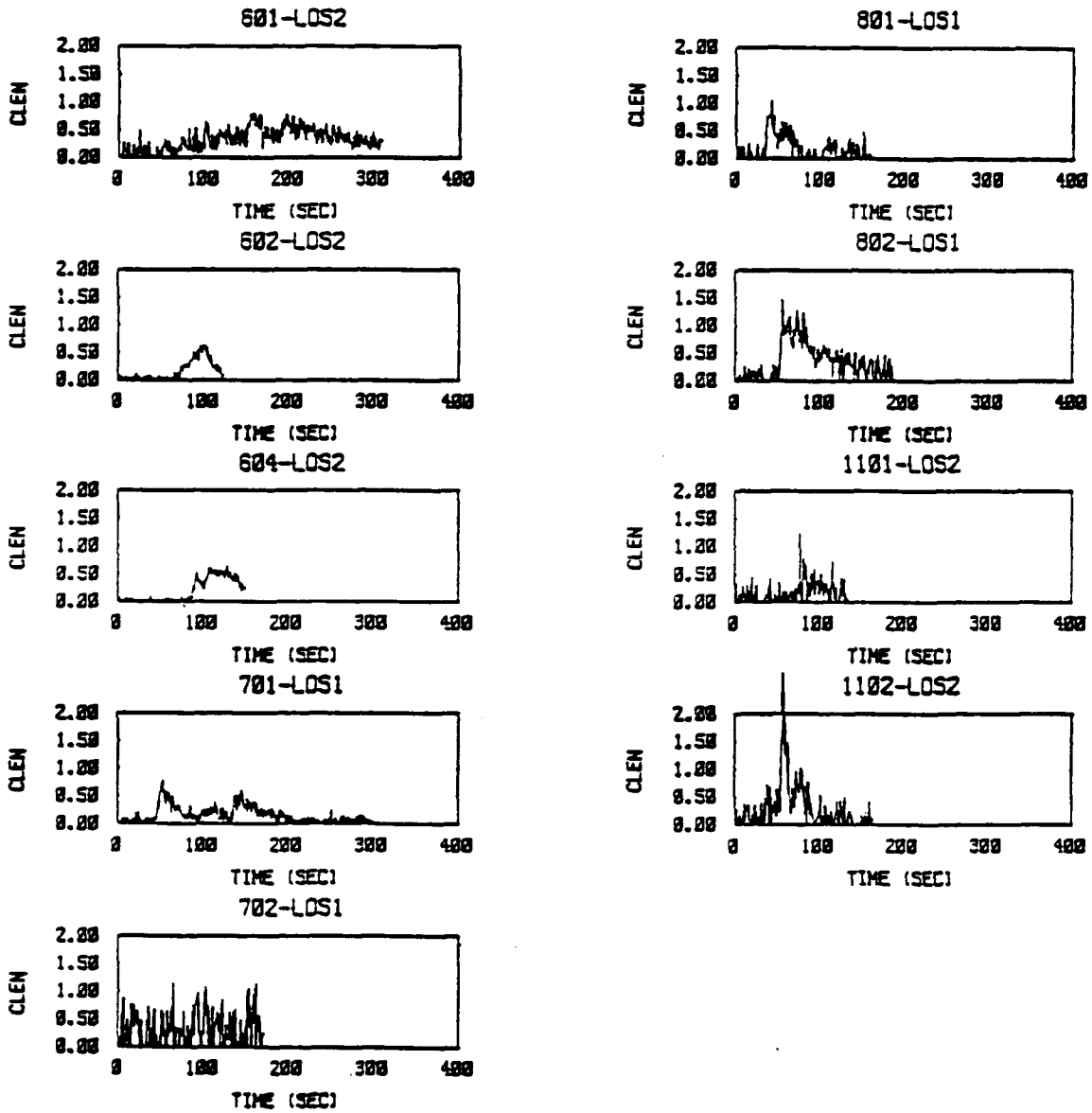

Figure 8-5. Time series of smoke concentration-length (CLEN) data calculated from transmissometer measurements made along the line-of-sight (LOS) downwind from the source of the smoke. The source of the smoke is a group of three M375A2 munitions.

the fraction of the time that the concentration is greater than zero.

Variations in the estimated integral time scale appear to be controlled by the "pattern" displayed by the time series, rather than changes in meteorology, the number of projectiles, or the type of projectile. We see that the larger integral time scales are associated with pattern A, which exhibits a clear "pulse" of smoke. T_c is typically 20% to 25% of the duration of these pulses. When such a pulse is absent (pattern B), T_c is typically 3 to 4 s for the XM819 munition, and it varies between 2 and 8 s for the M375A2 munition, with several values estimated to be less than 1 s. Because the time series are comprised of 1-s data, time scales of order 1 s and less are interpreted to be noise.

These results might be anticipated. CL are line-of-sight-integrated concentrations, obtained from a cloud of smoke resulting from munitions with a typical burn-time of a few minutes. This duration is too short to mark significant fluctuations associated with lateral "meandering" of the wind, and furthermore, integration of the concentration along the LOS would tend to "contain" any such meanders, so these meanders would be invisible to the transmissometer. Therefore, the variability seen in the CL time series would be expected to arise from "in-plume" fluctuations in the concentration of the smoke. These fluctuations would result from unsteadiness in the initial concentration of the smoke, and also from fluctuations in the vertical dispersion processes. When a single, well-defined cloud of smoke is produced, the time it takes to pass across the LOS will dominate the time series (pattern A). When such a dominant signal is absent (pattern B), the fluctuations may be related to "patchiness", with a much shorter timescale. Wind speed measured at 2 m during those trials with the XM819 munition in which pattern B dominates, varies between 2 and 3 m/s. Therefore the estimated timescale of 3 to 4 seconds can be associated with an advective length-scale of 6 to 12 m, which is consistent with the scale of puff-like structures frequently observed in smoke plumes released at the surface.

From the perspective of assessing the uncertainty in estimating emission strength (emission rates or total mass released) of a munition, as derived from measurements of dosages, or CLID values, an integral time scale on the

Table 8-1

Summary of Measures of Concentration Fluctuations and Boundary Layer Parameters for Development Test 1, XM819 and M375A2 Munitions

TRIAL	# PROJ.	u_*	L	I	T_i (s)	$\sigma_{CL} / \overline{CL}$ (1-sec)	LOS	TIME-SERIES PATTERN
XM819 MUNITION:								
309.1	1	0.19	-17.6	0.954	34.62	1.101	2	A
308.1	1	0.15	-17.5	0.667	2.54	1.357	2	A
203.1	1	0.30	-49.8	0.527	34.39	1.821	1	A
310.1	1	0.14	-23.2	0.962	15.19	0.643	2	A
802.1	3	0.25	-23.6	0.934	19.51	0.935	1	A
801.1	3	0.29	-30.5	0.774	41.40	1.365	1	A
702.1	3	0.12	-4.0	0.675	3.40	1.110	1	A
602.1	3	0.08	-32.9	0.900	31.42	0.987	2	A
902.1	1	0.14	-10.5	0.465	3.39	1.504	2	B
103.1	1	0.16	-10.2	0.893	3.28	0.818	1	B
102.1	1	0.16	-8.0	0.827	2.82	0.866	1	B
903.1	1	0.13	-8.1	0.622	2.80	1.339	2	B
202.1	1	0.15	-7.1	0.764	0.03	0.968	2	B
306.1	1	0.11	-23.5	0.865	4.81	0.697	2	B
302.1	1	0.10	-7.4	0.835	3.47	0.821	2	B
701.1	3	0.12	-2.9	0.702	1.48	1.057	1	B
1101.1	3	0.22	-0.5	0.826	2.90	0.824	2	B
1102.1	3	0.19	-5.7	0.876	2.03	0.769	2	B
M375A2 MUNITION:								
309.2	1	0.18	-13.3	0.711	7.98	1.163	2	A
303.2	1	0.10	-4.6	0.701	7.43	1.060	2	A
103.2	1	0.18	-10.4	0.714	3.14	1.213	1	A
901.2	1	0.27	-14.7	0.792	3.68	0.998	2	A
802.2	3	0.17	-8.6	0.836	7.34	0.929	1	A
604.2	3	0.09	16.6	0.603	47.77	1.174	2	A
801.2	3	0.31	-40.3	0.671	4.04	1.247	1	A
1102.2	3	0.18	-4.6	0.747	3.43	1.390	2	A
602.2	3	0.11	-994.7	0.744	31.34	1.199	2	A
903.2	1	0.18	-11.3	0.482	0.43	1.523	2	B
306.2	1	0.11	-27.8	0.750	1.39	1.130	2	B
307.2	1	0.14	-8.4	0.807	0.50	0.917	2	B
308.2	1	0.15	-9.0	0.800	0.00	0.922	2	B
310.2	1	0.14	-14.6	0.709	1.76	1.096	2	B
902.2	1	0.12	-6.0	0.422	1.24	1.694	2	B
601.2	3	0.11	-0.5	0.929	7.53	0.605	2	B
701.2	3	0.19	-36.5	0.846	8.70	1.001	1	B
702.2	3	0.13	-3.8	0.764	0.38	0.946	1	B
1101.2	3	0.22	-9.3	0.669	1.15	1.157	2	B

order of 4 seconds implies that the ratio $\sigma_{CL}(T_a)/\sigma_{CL}(0)$ is equal to 0.16 for an averaging time (T_a) of 300 s, which is approximately equal to the length of the record from which the dosage for the XM819 munition would be calculated. Table 8-1 lists the ratio of $\sigma_{CL}(1)/\overline{CL}$ for these trials, and the average value for the group of XM819 trials characterized as pattern B is equal to 0.97, which is essentially unity. Assuming that $\sigma_{CL}(1)$ represents the standard deviation of the instantaneous concentrations, $\sigma_{CL}(0)$, we can estimate the expected stochastic uncertainty as $\sigma_{CL}(300s)/\overline{CL} = 0.16$. This uncertainty in the measured CL values carries directly over to estimates of the emission strength, and may be used to evaluate the significance of differences in estimated emission strengths.

D. Analysis of Data from Screening Effectiveness Trials of the M3A3E2 Smoke Generator

Among a long series of tests of the M3A3E2 smoke generator performed during August and September, 1984, six screening effectiveness trials were successfully performed. These tests produced a dataset containing time series of concentration-length or cross-wind integrated concentration data and the associated meteorological data, over continuous periods of approximately one hour. Bowers and Black (1985) describe these trials, and provide summaries of the meteorological data averaged during each one.

Two lines-of-sight were set up for transmissometer measurements for the screening effectiveness trials, as plotted in Figure 8-6. The lines were set at a right-angle, and the 32-m meteorological tower which was used to obtain the primary meteorological data during the trials was located near their intersection. The asterisks in Figure 8-6 mark the locations from which fog-oil was released during the six trials. Their placement was determined by the direction of the wind, and for these trials, LOS1 is the preferred source of data for this analysis because it lies across the trajectory of the smoke-plumes. The approximate distance from the generator to LOS1 varies between 55 m and 75 m.

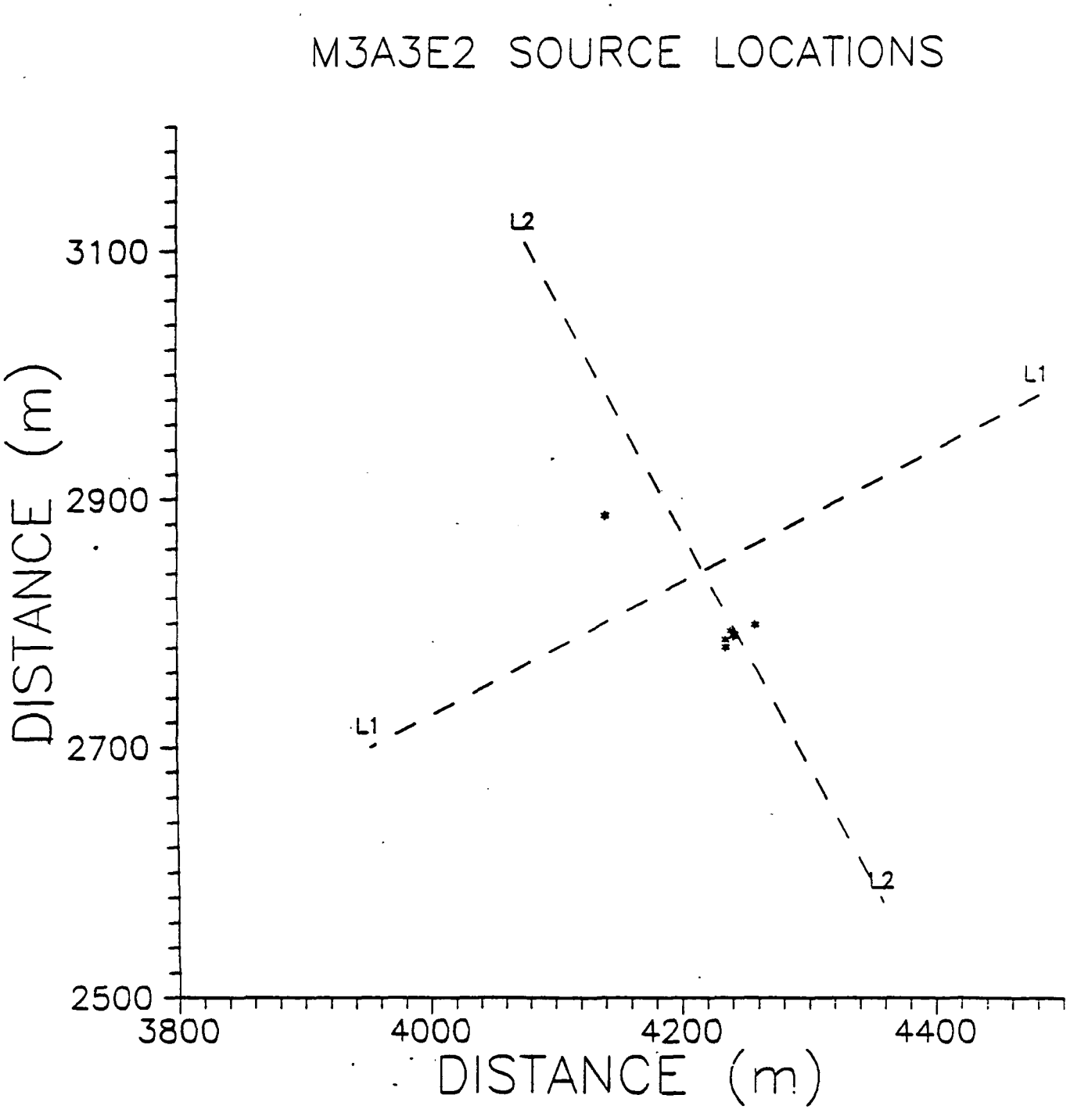

Figure 8-6. Location of sources of smoke relative to the lines-of-site (LOS) of transmissometers used to measure concentrations during the screening effectiveness trials of the M3A3E2 smoke generator.

Although the smoke generator was tested with both diesel oil and fog-oil, the screening effectiveness trials employed only the fog-oil. The smoke was released at a height of 0.9 m above the surface, at a mean rate that ranged from 34.54 g/s during trial T0091, to 38.06 g/s during trial T0031. The mean rate was determined by averaging the rate at which the oil was consumed during the period of the release.

Time series data from the transmissometers are stored on tape at a rate of 1 Hz, providing approximately 3600 points for each LOS during each trial, for each of two wavelengths (visible: 0.4-0.7 μm; IR: 1.06 μm). We converted the transmissometer data from LOS1 to "concentration-length" (CL) data by using average extinction coefficients for fog-oil reported by Saterlie et al. (1981). Denote the transmission measurement as TR, and the extinction coefficient as α, then Beer's Law leads to:

$$CL = \frac{-1}{\alpha} \ln (TR)$$

where $\alpha = 6.76\ m^2/g$ for $\lambda = 0.4\text{-}0.7\ \mu m$

$\alpha = 3.55\ m^2/g$ for $\lambda = 1.06\ \mu m$

No filtering or smoothing of the transmissometer data was performed. The time series of CL values derived from both wavelengths were characterized in terms of the mean, standard deviation, maximum value, and $\sigma_{CL} / \overline{CL}$.

It was immediately evident that the maximum value obtained at each wavelength corresponds to an imposed detection threshold for transmittance of 0.003. Plots of transmittance illustrate the presence of this threshold as well. Because of the smaller extinction coefficient of the IR beam, the threshold in the IR data corresponds to a larger value of CL, so that more of the denser portions of the cloud are resolved in the IR data. As a result, we have chosen to use the IR data to characterize fluctuations in CL.

Because these trials provide a long record of values of CL, an integral time scale T_c can be estimated. Rather than using the result obtained from Taylor's formula for the effect of averaging time T_c on σ_{CL}, which had been used in analyzing the CL data from the smoke munitions in Section C, the simpler approximate formula was used:

$$\frac{\sigma_c^2(T_a)}{\sigma_c^2(0)} = (1 + \frac{T_a}{2\,T_c})^{-1}$$

We assume once again that the standard deviation obtained from the series of 1-second values represents "zero" averaging time in the equation, so that several estimates of T_c can be obtained as T_a is increased.

Table 8-2 summarizes the mean meteorological data, the mean and standard deviation of the CL values, and the range in estimates of the integral time scale for each of the trials. All trials were conducted during the daytime, half within a neutral boundary layer flow (Pasquill Stability Class D), and the rest within a convective boundary layer (Pasquill Stability Classes of C and B). The mean values of CL display little variation, and the measure of the fluctuations in Cl, $\sigma_{CL} / \overline{CL}$, varies between 0.5 and 0.7. It is noted that the intensity of fluctuations appears to be weakly dependent on the inverse of the wind speed. This may be related to effects of convective motions , because the light wind speeds are associated with the more convective conditions (stability classes C and B). Estimates of the integral time scales range from about 4 to 13 seconds, and there is a pronounced trend with the shorter time scales being associated with the larger wind speeds, and neutral stability class conditions. Note that the intermittency (fraction of the record in which CL is greater than zero) is unity for averaging times in excess of 6 s, and range between 0.989 and 1.0 for an averaging time of 1 s. This indicates the presence of a smoke screen with virtually no "holes". However, DPG personnel suggest that this is a misleading result, since the experiments were shut down if holes began to appear in the smoke screen.

Comparing these results with those obtained for the smoke munitions evaluated in Section C, we surmise that the smoke screen produced by the fogger is less "patchy" than that produced by the smoke munitions. For example, the intermittency indicates fewer "holes". And although short, the time scales tend to be longer than those found for the smoke munitions. In fact, the wind speeds reported during the trials characterized as pattern B varied between 2 and 3 m/s (at 2 m above the ground), while those for the trials with the smoke generator varied from 2.5 to 6.5 m/s (at 2 m above the ground). With the inverse relationship just noted between the wind speed and

Table 8-2

Summary of Meteorological Data[1] and Concentration-Length Data for the Screening Effectiveness Trials of the M3A3E2 Smoke Generator

Trial	U(m/s)	σ_w(m/s)	Stability Class	$\overline{CL}$(g/m^2)	σ_{CL} / $\overline{CL}$	T_c(s)
T0031	2.9	0.37	C	0.850	0.69	11-13
T0061	5.9	0.59	D	0.835	0.54	3-4
T0081	6.4	0.69	D	0.892	0.50	3-5
T0091	7.5	0.80	D	0.811	0.52	3-7
T1011	3.2	0.46	B	0.956	0.58	8-11
T1071	4.8	0.60	C	0.903	0.54	5-7

note: [1] Meteorological data are those reported at 4 m above the surface.

the time scale, we might expect the time scales for the smoke munition trials to be greater than those for the smoke generator! The difference in integral time scales between the two sources can be characterized by looking at the advective length-scale. When we take the product of u(2 m)*T_c to estimate an advective length-scale, we find length-scales of 6 to 12 m for the smoke munitions (pattern B), and 18 to 33 m for the smoke generator. One could argue that this difference is related to the steadiness of the source of the smoke.

Of greater importance is the magnitude of σ_{CL} / $\overline{CL}$ for these trials compared with the trials involving the individual smoke munitions. Recall that the magnitude of σ_{CL} / $\overline{CL}$ for the individual smoke munitions averaged nearly 1.0, whereas σ_{CL} / $\overline{CL}$ for the continuous oil-fog clouds average 0.56. This measure indicates that variations in the cross-wind integrated concentration (CL) are more pronounced in the clouds of smoke produced by the smoke munitions, than in the clouds produced by the smoke generator.

As discussed in Section C, this information can be used to evaluate the significance of different estimates of emission strength (emission rates or total mass released) of two smoke generators, as derived from measurements of dosages, or CLID values. An integral timescale on the order of 7 seconds implies that the ratio $\sigma_{CL}(T_a)/\sigma_{CL}(0)$ is equal to 0.06 for an averaging time (T_a) of 3600 s, which is the duration of the tests that were analyzed. If we take the average ratio of $\sigma_{CL}(1)/\overline{CL}$ for these trials, 0.56, and assume that $\sigma_{CL}(1)$ represents the standard deviation of the instantaneous concentrations, $\sigma_{CL}(0)$, we can estimate the expected stochastic uncertainty as $\sigma_{CL}(3600s)/\overline{CL}$ = 0.03, which is very small. This uncertainty in the measured CL values carries directly over to estimates of the emission strength, so we see that if the source strength can be maintained at a constant level for a full hour, as it was in these trials, then an estimate of the emission strength made on the basis of measured values of CL is likely to be more accurate, from the standpoint of errors associated with stochastic fluctuations, than estimates made for munitions that produce smoke for periods of about 5 minutes.

E. Summary

The field data analyzed in this section suggest that there is so much variability in the results that it would be unwise to set specific formulas for stochastic fluctuations at this time. Some formulas may be valid for certain special conditions, but lead to unrealistic predictions during other conditions. Consequently, until well-validated practical formulas are available, it is best to make simple assumptions such as $\sigma_c/\overline{C} = 1$.

SECTION IX

DESCRIPTION AND USER'S GUIDES FOR SOFTWARE PACKAGES CONTAINING QUANTITATIVE METHODS TO ACCOUNT FOR METEOROLOGICAL INFLUENCE ON SMOKE/OBSCURANT EFFECTIVENESS

A. Introduction

A software package, ASSEMBLE, was written for the purpose of establishing quantitative methods to account for meteorological influences on the effectiveness of smoke/obscurants. The ASSEMBLE software package is coded in such a way that it also acts like a simple database management system. As mentioned in Section VI, a separate software package (DDAMC) generates one ASCII file for the results of one dispersion formula for one Dugway Data Archive (DDA). The ASSEMBLE software package integrates all the individual ASCII files into one composite *binary* file. The user then has the freedom of comparing, say, the predicted total mass emitted for a certain DDA (the DDA may represent the trials when munition A was used) based on any dispersion formula with the values from the same formula for another DDA (the DDA may represent the trials when munition B was used) to see whether or not there is any significant difference. To illustrate, this is like creating a large two-dimensional master table containing results from all the dispersion formulas for all the data archives (DDA's). The rows of the table represent the individual data archives, and the columns of the table represent the dispersion formulas. A "cell" is defined as the application of a certain dispersion formula to a certain data archive. The user specifies any two "cells" on the table, and forms the null hypothesis: "the information stored in cell A is not significantly different from the information stored in cell B." The ASSEMBLE software package then tests the null hypothesis using a standard statistical procedure. Note that the information stored at each cell includes values of concentration and source strength for all the trials, concentric arcs, and lines-of-sight (LOS) for one DDA; therefore, the user can not only test the hypothesis concerning the source strength (i.e. emission rate or total mass emitted), but also the hypothesis concerning obscuring ability (i.e. concentrations).

The ASSEMBLE software package is mainly used to estimate the effectiveness of smoke/obscurants after removal of meteorological influences

using dispersion formulas. On the other hand, one can also estimate the probability density functions (pdf's) for the concentration or source predictions resulting from the uncertainties in the meteorological input data. To accomplish this, The DDAMC software package, already described in part in Section VI, includes an additional feature that allows the uncertainty due to data input errors to be assessed using the Monte Carlo method.

The ASSEMBLE software package uses the Student-t test (explained in any basic statistics text, e.g. Panofsky and Brier, 1958) to analyze the significance of an observed difference of two means. Suppose two samples, with size N_1 and N_2, respectively, are randomly drawn from a population. Assume μ_1 and μ_2 are the sample means, and σ_1 and σ_2 are the sample standard deviations. The ratio

$$t = \frac{\mu_1 - \mu_2}{\left[\frac{N_1\sigma_1^2 + N_2\sigma_2^2}{N_1 + N_2 - 2}\left(\frac{1}{N_1} + \frac{1}{N_2}\right)\right]^{1/2}} \qquad (9\text{-}1)$$

is distributed as the t distribution, with the degrees of freedom of N_1+N_2-2. An important assumption of the Student-t test is that all of the samples are independent.

The ASSEMBLE software package also has the option of generating an input file to be used by the distribution analysis software package, ANADISTR (see Appendix D). The ANADISTR package analyzes the distribution of one variable as a function of another variable, and generates a data file that can be used to create a so-called "box plot", using the SIGPLOT plotting package (see Appendix E). Therefore, by using this program option, the user can investigate whether there is a systematic deterioration of the performance of a dispersion formula as downwind distance increases, as wind speed decreases, or as the atmosphere becomes more unstable. Note that this option mainly focuses on the issue of "evaluation", whereas the option described in the previous paragraph mainly emphasizes the issue of "uncertainty".

Each composite binary file is like a database file. We recommend that only those results from similar trials be included in a composite binary file.

From Section IV, it is natural to include the results for the historical datasets in one binary file, and the results for the smoke/obscurant datasets in another binary file.

The advantages of a binary file include smallness in size and faster I/O. However, the most severe drawback of a binary file is that it is not only system-dependent, but also compiler-dependent. In other words, a binary file created by a program compiled using a certain compiler can only be easily read by another program compiled using the same compiler.

In the following, the user's guides for the ASSEMBLE and DDAMC (Monte Carlo mode only) packages will be described in detail.

B. User's Guide for ASSEMBLE

In the following, we will 1) discuss in detail the use of the package, 2) provide guidelines for analyses of data that are not independent, 3) describe the format of the composite binary file, 4) discuss the maximum limits of the package, and 5) provide some general programming information concerning the package. In addition to the detailed description of the use of the package, hard copies of the screen images during the execution of the ASSEMBLE package will also be provided in order to further assist the user. More examples of application of the ASSEMBLE package are discussed in Section X.

Before going into details, it is useful to mention first that the ASSEMBLE software package is able to handle the following list of 13 variables.

Variable	Definition
C	centerline concentration (mg/m^3) for each arc
C^y	cross-wind integrated concentration (mg/m^2) for each arc
σ_y	plume standard deviation (m) for each arc
CL	LOS-integrated concentration (mg/m^2) for each LOS
CLID	LOS-integrated dosage ($mg*s/m^2$) for each LOS
Q(C)	emission rate (g/s) based on C for each arc
$Q(C^y)$	emission rate (g/s) based on C^y for each arc

Q(CL)	emission rate (g/s) based on CL for each LOS
Q(CLID)	emission rate (g/s) based on CLID for each LOS
M(C)	total mass emitted (kg) based on C for each arc
M(C^y)	total mass emitted (kg) based on C^y for each arc
M(CL)	total mass emitted (kg) based on CL for each LOS
M(CLID)	total mass emitted (kg) based on CLID for each LOS

Execution of ASSEMBLE

The ASSEMBLE software package has the following five major options:

Option 1: Update or expand the composite binary file.

Option 2: View the records in the composite binary file on screen.

Option 3: Tabulate a subset of the records in the composite binary file so that a good-quality hard copy can be generated.

Option 4: Generate an input file for the distribution analysis software package, ANADISTR.

Option 5: Perform the Student-t test to see whether the values (e.g. source emission rate or total mass emitted) for one group (e.g. munition A) are significantly different from the values for another group (e.g. munition B).

Options (4) and (5) are the most important ones among the five options. During the execution of the ASSEMBLE package, the user is first asked to provide the name of the composite binary file. If the binary file does not already exist, Option 1 will be automatically selected. The user can select one of the above five options only if the binary file already exists. The user's guide for each program option is described below.

Option 1: In this option, individual ASCII files generated by the DDAMC software package will be incorporated into the composite binary file. Remember that each ASCII file contains both 1) the results from

one dispersion formula and 2) the observations for one DDA. A list of questions that the user will be asked under Option 1 is described below. The user is referred to Figure 9-1 for a hard copy of the screen image during the execution of ASSEMBLE under Option 1.

Q1: The user is asked to specify the key letters (at most three letters are allowed) of the dispersion formula whose results will be incorporated into the binary file. At present, the following key letters are used to represent the dispersion formulas.

key letters	Formulas
VS	VSDM
GP	GPM
OB	OBDG (C/Q)
RE	Regression (C/Q)
SI	Similarity (C/Q)
REY	Regression (C^y/Q)
SIY	Similarity (C^y/Q)
NV	Nieuwstadt/Venkatram (C^y/Q)
BR	Briggs (C^y/Q)

Q2: The user is asked whether to incorporate the observed values as well. Recall that each DDA file contains both the predicted values from the dispersion formula and the observed values for one DDA. Since the ASSEMBLE software package also treats the observation as one "formula" (under the key letters "OBS"), the user, therefore, actually has the opportunity of integrating the values from *two* formulas into the binary file. The default answer (by typing the RETURN key) is "n". Suppose we have applied nine dispersion formulas to the same DDA, thus creating nine ASCII files. Then the same observed values are duplicated in all of the nine ASCII files. However, we obviously only need to incorporate the observed values from one of the ASCII files.

Q3: The user is asked to specify the name of the DDA (at most five letters are allowed).

Q4: The user is asked to specify the DOS-path name where the ASCII file resides. The ASCII files and the binary file do not have to be in

```
assemble

Enter the name of the composite binary file: (default is assemble.bin)
***** USER INPUT --->  181.bin

Select one of the following five main program options:

1) Update or expand 181.bin, i.e., incorporate additional DDA's or scaling
   results into the binary file,
2) View the contents of 181.bin on screen,
3) Tabulate the concentration or source data (to be defined later) for a
   subset of 181.bin,
4) Generate the input files to be used by the distribution analysis
   software package, ANADISTR, for the concentration or source data for a
   subset of 181.bin,
5) Summarize comparisons between two source-groups and characterize
   significance by performing the Student-t test.  The two groups can
   be either from the same dispersion formula but different DDA, or
   different dispersion formula but the same DDA.

Because the binary file 181.bin does not exist, Option 1 is
automatically selected.

Press Enter to Continue.


The update or expand option has been selected.  In the following, results from
one formula for one DDA will be incorporated into the binary file at a time.
The user will be prompted for the DDA and formula names.  Note that the *.out
file can be generated by the DDAMC package or created by the user using a
text editor.

Furthermore, since both the formula-predicted and observed concentrations and
source data are stored in the *.out file, and the program also treats the
observations as another formula, the user will also be asked whether or not to
incorporate the observed values into the binary file as another formula (under
the name 'OBS').  This should be done once for each DDA.

Press Enter to Continue.

Enter key letters for the dispersion formula (3 LETTERS AT MOST):
Example:
VS: VSDM,                    GP: GPM,
OB: OBDG,                    RE: Regression, C only,
SI: Similarity, C only,      REY: Regression, Cy only,
SIY: Similarity, Cy only,
NV: Nieuwstadt/Venkatram, Cy only
BR: Briggs, Cy only
***** USER INPUT --->  vs

Want to incorporate the observed values too (y/<N>) ?
Do this only once for each DDA included in the binary file
***** USER INPUT --->  y
```

Figure 9-1. Screen image during the execution of the ASSEMBLE software package under Option 1, where the results from the VSDM dispersion formula for the L81A1, L81B1, L81C1, and L81D1 datasets (see Section IV) are integrated into a composite binary file named L81.BIN.

```
Enter key letters for the DDA (5 LETTERS AT MOST):
Examples:
OB_*:  Ocean Breeze,          DGB_*: Dry Gulch, Course B
DGD_*: Dry Gulch, Course D,   GG_*:  Green Glow
PG_*:  Prairie Grass,         AT*: Atterbury-87
INVHC: Inventory smoke munition test
DT1??: DT I  of 155mm projectiles
DT2??: DT II of 155mm projectiles
L81*:  Evaluation of L8A1 grenades
L83*:  Evaluation of L8A3 grenades
DT1?:  DT I of 81mm projectiles
INT??: Evaluation of international smoke pots/generators
PO*:   Evaluation of man-portable smoke generators
***** USER INPUT --->  181a1

Enter the path where the input file (*.OUT) resides:
(default is \a135\ddamc\runs, a . means the current directory):
***** USER INPUT --->

The program assumes the name of the *.out file to be: VSL81A1.out
Is this correct (<Y>/n) ?
***** USER INPUT --->  y

Reading VSL81A1.out  ...
Want to import all trials in this DDA (<Y>/n) ?
***** USER INPUT --->  y

Updating 181.bin...
Writing 181.bin...
Incorporating observed values...
Reading 181.bin...
Updating 181.bin...
Writing 181.bin...
Ready to do more updates (y/<N>) ?
***** USER INPUT --->  y

Enter key letters for the dispersion formula (3 LETTERS AT MOST):
Example:
VS: VSDM,                   GP: GPM,
OB: OBDG,                   RE: Regression, C only,
SI: Similarity, C only,     REY: Regression, Cy only,
SIY: Similarity, Cy only,
NV: Nieuwstadt/Venkatram, Cy only
BR: Briggs, Cy only
***** USER INPUT --->  vs

Want to incorporate the observed values too (y/<N>) ?
Do this only once for each DDA included in the binary file
***** USER INPUT --->  y

Enter key letters for the DDA (5 LETTERS AT MOST):
Examples:
OB_*:  Ocean Breeze,          DGB_*: Dry Gulch, Course B
DGD_*: Dry Gulch, Course D,   GG_*:  Green Glow
PG_*:  Prairie Grass,         AT*: Atterbury-87
INVHC: Inventory smoke munition test
DT1??: DT I  of 155mm projectiles
DT2??: DT II of 155mm projectiles
L81*:  Evaluation of L8A1 grenades
L83*:  Evaluation of L8A3 grenades
DT1?:  DT I of 81mm projectiles
INT??: Evaluation of international smoke pots/generators
PO*:   Evaluation of man-portable smoke generators
***** USER INPUT --->  181b1
```

Figure 9-1. Screen image during the execution of the ASSEMBLE software package under Option 1, where the results from the VSDM dispersion formula for the L81A1, L81B1, L81C1, and L81D1 datasets (see Section IV) are integrated into a composite binary file named L81.BIN. (Continued)

```
Enter the path where the input file (*.OUT) resides:
(default is \a135\ddamc\runs, a . means the current directory):
***** USER INPUT --->

The program assumes the name of the *.out file to be: VSL81B1.out
Is this correct (<Y>/n) ?
***** USER INPUT --->  y

Reading VSL81B1.out  ...
Want to import all trials in this DDA (<Y>/n) ?
***** USER INPUT --->  y

Reading 181.bin...
Updating 181.bin...
Writing 181.bin...
Incorporating observed values...
Reading 181.bin...
Updating 181.bin...
Writing 181.bin...
Ready to do more updates (y/<N>) ?
***** USER INPUT --->  y

Enter key letters for the dispersion formula (3 LETTERS AT MOST):
Example:
VS: VSDM,                    GP: GPM,
OB: OBDG,                    RE: Regression, C only,
SI: Similarity, C only,      REY: Regression, Cy only,
SIY: Similarity, Cy only,
NV: Nieuwstadt/Venkatram, Cy only
BR: Briggs, Cy only
***** USER INPUT --->  vs

Want to incorporate the observed values too (y/<N>) ?
Do this only once for each DDA included in the binary file
***** USER INPUT --->  y

Enter key letters for the DDA (5 LETTERS AT MOST):
Examples:
OB_*:  Ocean Breeze,          DGB_*: Dry Gulch, Course B
DGD_*: Dry Gulch, Course D,   GG_*:  Green Glow
PG_*:  Prairie Grass,         AT*: Atterbury-87
INVHC: Inventory smoke munition test
DT1??: DT I  of 155mm projectiles
DT2??: DT II of 155mm projectiles
L81*:  Evaluation of L8A1 grenades
L83*:  Evaluation of L8A3 grenades
DT1?:  DT I of 81mm projectiles
INT??: Evaluation of international smoke pots/generators
PO*:   Evaluation of man-portable smoke generators
***** USER INPUT --->  181c1

Enter the path where the input file (*.OUT) resides:
(default is \a135\ddamc\runs, a . means the current directory):
***** USER INPUT --->

The program assumes the name of the *.out file to be: VSL81C1.out
Is this correct (<Y>/n) ?
***** USER INPUT --->  y

Reading VSL81C1.out  ...
Want to import all trials in this DDA (<Y>/n) ?
***** USER INPUT --->  y
```

Figure 9-1. Screen image during the execution of the ASSEMBLE software package under Option 1, where the results from the VSDM dispersion formula for the L81A1, L81B1, L81C1, and L81D1 datasets (see Section IV) are integrated into a composite binary file named L81.BIN. (Continued)

```
Reading 181.bin...
Updating 181.bin...
Writing 181.bin...
Incorporating observed values...
Reading 181.bin...
Updating 181.bin...
Writing 181.bin...
Ready to do more updates (y/<N>) ?
***** USER INPUT ---> y

Enter key letters for the dispersion formula (3 LETTERS AT MOST):
Example:
VS: VSDM,                    GP: GPM,
OB: OBDG,                    RE: Regression, C only,
SI: Similarity, C only,      REY: Regression, Cy only,
SIY: Similarity, Cy only,
NV: Nieuwstadt/Venkatram, Cy only
BR: Briggs, Cy only
***** USER INPUT ---> vs

Want to incorporate the observed values too (y/<N>) ?
Do this only once for each DDA included in the binary file
***** USER INPUT ---> y

Enter key letters for the DDA (5 LETTERS AT MOST):
Examples:
OB_*:  Ocean Breeze,          DGB_*: Dry Gulch, Course B
DGD_*: Dry Gulch, Course D,   GG_*:  Green Glow
PG_*:  Prairie Grass,         AT*: Atterbury-87
INVHC: Inventory smoke munition test
DT1??: DT I  of 155mm projectiles
DT2??: DT II of 155mm projectiles
L81*:  Evaluation of L8A1 grenades
L83*:  Evaluation of L8A3 grenades
DT1?:  DT I of 81mm projectiles
INT??: Evaluation of international smoke pots/generators
PO*:   Evaluation of man-portable smoke generators
***** USER INPUT ---> 181d1

Enter the path where the input file (*.OUT) resides:
(default is \a135\ddamo\runs, a . means the current directory):
***** USER INPUT --->

The program assumes the name of the *.out file to be: VSL81D1.out
Is this correct (<Y>/n) ?
***** USER INPUT ---> y

Reading VSL81D1.out  ...
Want to import all trials in this DDA (<Y>/n) ?
***** USER INPUT ---> y

Reading 181.bin...
Updating 181.bin...
Writing 181.bin...
Incorporating observed values...
Reading 181.bin...
Updating 181.bin...
Writing 181.bin...
Ready to do more updates (y/<N>) ?
***** USER INPUT ---> n
```

Figure 9-1. Screen image during the execution of the ASSEMBLE software package under Option 1, where the results from the VSDM dispersion formula for the L81A1, L81B1, L81C1, and L81D1 datasets (see Section IV) are integrated into a composite binary file named L81.BIN. (Concluded)

the same directory. The current default answer is "\a135\ddamc\runs", which is defined in the main program but can be easily changed by the user. By typing a ".", it is indicated that the current directory will be assumed.

Q5: The ASSEMBLE software package automatically constructs the name of the ASCII file, with an extension of ".OUT", according to the key letters of the dispersion formula and DDA just specified. For example, if the results from the GPM dispersion formula (key letter "GP") for the DDA of the Green Glow experiments (key letter "GG") were to be incorporated, the ASSEMBLE software package assumes the name of the ASCII file to be "GPGG.OUT". The user is asked to validate this information. The default answer is "y". If "n", the user should specify the *full* name of the ASCII file (do not include the path name) at this point.

Q6: The user is asked whether all the trials should be included in the DDA. The default answer is "y". If "y", all the trials in the DDA will be automatically incorporated into the binary file. If "n", the user will be prompted, one trial at a time, whether to include that trial.

Q7: During the process of updating the binary file, the ASSEMBLE software package checks whether there is any conflict between the existing information and the information to be brought in; i.e., results for a certain dispersion formula for a certain trial may already exist in the binary file. If this is the case, the user is asked whether to overwrite the existing information. The default answer is "y". If "n", the user is asked to enter a new set of key letters (at most three letters) representing a new dispersion formula. The results in the ASCII file will be "filed" under that new dispersion formula, and the original information in the binary file is left intact.

Q8: Finally, the user is asked whether to do more updates. The default answer is "n". If "n", the program terminates. If "y", the user is directed back to the first question (Q1) regarding the key letters of the dispersion formula, and the whole process repeats.

Note that currently the ASSEMBLE software package is not able to delete any information from the binary file. To protect the original binary file from any possible damage due to incorrect user inputs, the ASSEMBLE software package writes or saves the updated binary file to the storage media (e.g., a hard disk) only if no errors were encountered during the entire updating process. Finally, duplicate trial names are not allowed in the binary file, although the trials might be from different DDA's.

Option 2: In this option, the user can view the contents of the composite binary file on the screen. This option is necessary because the data stored in the binary file cannot be displayed by any text editor. In the composite binary file, the header records are used to describe general information such as the names of the dispersion formulas and DDA's, the names of the trials in each DDA, and the source and meteorological data for each trial. For the remaining data records, two records are used to store the results from one dispersion formula for one trial. The reader is referred to a separate sub-section below for a more detailed description or the format of the composite binary file. The user is referred to Figure 9-2 for a hard copy of the screen image during the execution of ASSEMBLE under Option 2.

By default, Option 2 always displays the header records on screen. The user needs only to specify the starting and ending data records, and all the data in between will be displayed on the screen. For example, if the user wants to see the whole content of the binary file, then "1" (for the starting record) and a very large integer, such as "9999" (for the ending record), should be entered.

Because large amounts of information will be scrolled across the screen very quickly, the user should be prepared to use Control-S (pressing the Control and S keys simultaneously) any time to temporarily stop the scrolling. Or the user can simply redirect the output to a disk file instead.

```
D:\A135\DDAMC\ASSEMBLE\assemble

Enter the name of the composite binary file: (default is assemble.bin)
***** USER INPUT --->  181.bin
Select one of the following five main program options:

1) Update or expand 181.bin, i.e., incorporate additional DDA's or scaling
   results into the binary file,
2) View the contents of 181.bin on screen,
3) Tabulate the concentration or source data (to be defined later) for a
   subset of 181.bin,
4) Generate the input files to be used by the distribution analysis
   software package, ANADISTR, for the concentration or source data for a
   subset of 181.bin,
5) Summarize comparisons between two source-groups and characterize
   significance by performing the Student-t test.  The two groups can
   be either from the same dispersion formula but different DDA, or
   different dispersion formula but the same DDA.

Now enter 1, 2, 3, 4, or 5
***** USER INPUT --->  2
A brief description of the format of 181.bin:

The first record contains the names of the formulas included in 181.bin.
The second record contains the names of the DDA's included in 181.bin.
The next IDDA records contain the names of the trials for each DDA,
  where IDDA = the total no. of DDA's included.
The next ITRL records contain the met. and source data for each trial,
  where ITRL = the total no. of trials included.
The remaining records make up the main data section.  The results from one
formula for one trial are stored in TWO records, and these include various
concentration and source predictions.  Note that the program also treats
the observations as one formula.

The first 2+IDDA+ITRL records of 181.bin will always be printed out.
For the main data section, you need to specify the starting and ending records
that you wish to view.  If you want to view all records in 181.bin, please
specify 1 and a very large number, such as 9999, in the following.

Now enter two integer record numbers:
***** USER INPUT --->  1 4

Note that large amount of information will be scrolled very quickly on screen.
Be prepared to use Ctrl-S to stop the scrolling.

Press Enter to Continue.

The following dispersion formulas are in the file:
VS  OBS
The following DDA's are in the file:
     L81A1     L81B1     L81C1     L81D1
Each DDA has the following trials:
L81A1: bb2       bb3       bb4       bb5       bb6       bb7       bb9

L81B1: bb11      bb12      bb14      bb15      bb16      bb18
L81C1: bb21      bb22      bb25      bb26      bb28      bb30
L81D1: bb32      bb35      bb36      bb38      bb40
```

Figure 9-2. Screen image during the execution of the ASSEMBLE software package under Option 2, where the contents of the L81.BIN (see Figure 9-1) is listed.

```
Characteristics of each trial:
    u          q          mass       sigd       sigp       ustar      z0         onebyl
  wstar      wpl        dtl62        pg
  ndist      nlos         x
Trial: bb2
 3.10E+00 3.57E+00 8.97E-01 1.37E+01 6.55E+00 2.95E-01 3.00E-02 0.00E+00
-9.99E+01 4.80E-02-1.37E-01  4
  0  2
Trial: bb3
 3.80E+00 3.42E+00 8.59E-01 1.07E+01 6.55E+00 3.62E-01 3.00E-02 0.00E+00
-9.99E+01 4.70E-02-1.37E-01  4
  0  2
Trial: bb4
 2.80E+00 3.35E+00 8.40E-01 2.88E+01 7.51E+00 3.06E-01 3.00E-02-1.28E-01
 2.09E+00 7.90E-02-1.35E+00  1
  0  2
Trial: bb5
 3.60E+00 3.35E+00 8.40E-01 2.81E+01 7.24E+00 3.79E-01 3.00E-02-8.17E-02
 2.23E+00 7.30E-02-1.59E+00  2
  0  2
Trial: bb6
 3.20E+00 3.35E+00 8.40E-01 1.64E+01 6.91E+00 3.22E-01 3.00E-02-3.56E-02
 1.43E+00 1.06E-01-7.67E-01  3
  0  2
    u          q          mass       sigd       sigp       ustar      z0         onebyl
  wstar      wpl        dtl62        pg
  ndist      nlos         x
Trial: bb7
 2.20E+00 3.50E+00 8.78E-01 2.43E+01 6.91E+00 2.21E-01 3.00E-02-3.56E-02
 9.87E-01 4.90E-02-4.35E-01  3
  0  2
Trial: bb9
 5.60E+00 3.42E+00 8.59E-01 1.01E+01 6.55E+00 5.33E-01 3.00E-02 0.00E+00
-9.99E+01 4.20E-02-1.37E-01  4
  0  2
Trial: bb11
 3.10E+00 4.22E+00 8.40E-01 2.15E+01 6.91E+00 3.11E-01 3.00E-02-3.56E-02
 1.39E+00 1.02E-01-7.29E-01  3
  0  2
Trial: bb12
 2.70E+00 4.51E+00 8.97E-01 1.67E+01 6.91E+00 2.71E-01 3.00E-02-3.56E-02
 1.21E+00 1.02E-01-5.86E-01  3
  0  2
Trial: bb14
 4.20E+00 4.32E+00 8.59E-01 1.31E+01 6.55E+00 4.00E-01 3.00E-02 0.00E+00
-9.99E+01 6.70E-02-1.37E-01  4
  0  2
    u          q          mass       sigd       sigp       ustar      z0         onebyl
  wstar      wpl        dtl62        pg
  ndist      nlos         x
Trial: bb15
 3.80E+00 4.22E+00 8.40E-01 2.00E+01 6.91E+00 3.82E-01 3.00E-02-3.56E-02
 1.70E+00 9.40E-02-1.03E+00  3
  0  2
Trial: bb16
 4.20E+00 4.22E+00 8.40E-01 1.00E+01 6.55E+00 4.00E-01 3.00E-02 0.00E+00
-9.99E+01 6.70E-02-1.37E-01  4
  0  2
Trial: bb18
 7.00E+00 3.83E+00 7.63E-01 1.23E+01 6.55E+00 6.67E-01 3.00E-02 0.00E+00
-9.99E+01 9.70E-02-1.37E-01  4
  0  2
Trial: bb21
 3.90E+00 6.51E+00 8.20E-01 1.60E+01 6.91E+00 3.92E-01 3.00E-02-3.56E-02
 1.75E+00 8.00E-02-1.07E+00  3
  0  2
```

Figure 9-2. Screen image during the execution of the ASSEMBLE software package under Option 2, where the contents of the L81.BIN (see Figure 9-1) is listed. (Continued)

```
Trial: bb22
 3.60E+00 7.12E+00 8.97E-01 1.79E+01 6.55E+00 3.43E-01 3.00E-02 0.00E+00
-9.99E+01 2.00E-02-1.37E-01  4
  0  2
    u         q        mass      sigd      sigp      ustar      z0       onebyl
  wstar      wpl      dt162      pg
  ndist      nlos       x
Trial: bb25
 4.00E+00 6.67E+00 8.40E-01 1.15E+01 6.55E+00 3.81E-01 3.00E-02 0.00E+00
-9.99E+01 6.70E-02-1.37E-01  4
  0  2
Trial: bb26
 5.10E+00 6.82E+00 8.59E-01 6.50E+00 6.55E+00 4.86E-01 3.00E-02 0.00E+00
-9.99E+01 7.50E-02-1.37E-01  4
  0  2
Trial: bb28
 7.30E+00 6.06E+00 7.63E-01 6.70E+00 6.55E+00 6.95E-01 3.00E-02 0.00E+00
-9.99E+01 8.30E-02-1.37E-01  4
  0  2
Trial: bb30
 3.30E+00 6.82E+00 8.59E-01 2.04E+01 6.91E+00 3.31E-01 3.00E-02-3.56E-02
 1.48E+00 1.16E-01-8.08E-01  3
  0  2
Trial: bb32
 2.30E+00 7.80E+00 8.97E-01 1.39E+01 6.55E+00 2.19E-01 3.00E-02 0.00E+00
-9.99E+01 9.40E-02-1.37E-01  4
  0  2
    u         q        mass      sigd      sigp      ustar      z0       onebyl
  wstar      wpl      dt162      pg
  ndist      nlos       x
Trial: bb35
 1.30E+00 7.30E+00 8.40E-01 1.57E+01 6.55E+00 1.24E-01 3.00E-02 0.00E+00
-9.99E+01 0.00E+00-1.37E-01  4
  0  2
Trial: bb36
 4.50E+00 7.30E+00 8.40E-01 1.72E+01 6.55E+00 4.29E-01 3.00E-02 0.00E+00
-9.99E+01 4.00E-02-1.37E-01  4
  0  2
Trial: bb38
 6.80E+00 6.80E+00 7.82E-01 1.36E+01 6.55E+00 6.48E-01 3.00E-02 0.00E+00
-9.99E+01 8.00E-02-1.37E-01  4
  0  2
Trial: bb40
 6.50E+00 7.47E+00 8.59E-01 9.60E+00 6.55E+00 6.19E-01 3.00E-02 0.00E+00
-9.99E+01 4.20E-02-1.37E-01  4
  0  2
```

Figure 9-2. Screen image during the execution of the ASSEMBLE software package under Option 2, where the contents of the L81.BIN (see Figure 9-1) is listed. (Continued)

```
Dispersion formula: VS , trial: bb2
chi:
chiy:
sigy:
qc:
qcy:
cl:       2.40E+02  48.
clid:     6.01E+04 1.20E+04
qcl:     -9.99E+01-9.99E+01
qcld:      1.5       1.9
Dispersion formula: OBS, trial: bb2
chi:
chiy:
sigy:
qc:
qcy:
cl:      -9.99E+01-9.99E+01
clid:     2.51E+04 6.50E+03
qcl:       3.6       3.6
qcld:      3.6       3.6
Dispersion formula: VS , trial: bb3
chi:
chiy:
sigy:
qc:
qcy:
cl:       2.19E+02  34.
clid:     5.49E+04 8.51E+03
qcl:     -9.99E+01-9.99E+01
qcld:      3.3     -9.99E+01
Dispersion formula: OBS, trial: bb3
chi:
chiy:
sigy:
qc:
qcy:
cl:      -9.99E+01-9.99E+01
clid:     5.30E+04-9.99E+01
qcl:       3.4       3.4
qcld:      3.4       3.4
```

Figure 9-2. Screen image during the execution of the ASSEMBLE software package under Option 2, where the contents of the L81.BIN (see Figure 9-1) is listed. (Concluded)

Option 3: In this option, the user can instruct the ASSEMBLE software package to tabulate any subset of the data contained in the binary file, which can then be printed out. Option 3 has many built-in formatting features to improve the appearance of the table, so that it can be included in the report with very little modification. These features include inserting the line-feed character to start a new page whenever is appropriate, adding necessary spacing to delineate different groups of data, and optimally deciding the format for the data depending on their values. Described below is a list of questions that will be asked under Option 3. The user is referred to Figure 9-3 for a hard copy of the screen image during the execution of ASSEMBLE under Option 3.

Q1: The ASSEMBLE software package first prints out all the dispersion formulas available in the composite binary file. The user is asked whether to include data for all of the dispersion formulas in the table. The default answer is "y". If "y", all the dispersion formulas will be rearranged so that they will appear in the table in alphabetical order, except that the observations (under the dispersion formula name "OBS"), if available, will always appear first. If "n", then the user is asked to specify the desired sequence that each of the dispersion formulas should appear in the table. By entering a negative integer, zero, or simply a carriage return for the sequence of a dispersion formula, it is indicated that the results for that formula are not to be included in the table. For example, if the program shows that the results from three dispersion formulas, "VS", "PG", and "RE", are available in the binary file, and the user does not want "VS" to be included, but desires "PG" to appear second and "RE" to appear first, then "RETURN", "2", and "1" should be entered, in that order. The user can restart the whole process of specifying the sequence anytime by entering a "*" as the dispersion formula sequence. This provides the user with the opportunity to recover from a situation where mistakes might have been made. Note that internally the program also validates all the sequence numbers entered by the user to ensure that they start from 1, and are continuous. In other words, the program will ask the user to try again if "RETURN", "3", and "1" were entered for the previous example.

```
D:\A135\DDAMC\ASSEMBLE>assemble

Enter the name of the composite binary file: (default is assemble.bin)
xxxxx USER INPUT --->  181.bin

Select one of the following five main program options:

1) Update or expand 181.bin, i.e., incorporate additional DDA's or scaling
   results into the binary file,
2) View the contents of 181.bin on screen,
3) Tabulate the concentration or source data (to be defined later) for a
   subset of 181.bin,
4) Generate the input files to be used by the distribution analysis
   software package, ANADISTR, for the concentration or source data for a
   subset of 181.bin,
5) Summarize comparisons between two source-groups and characterize
   significance by performing the Student-t test.  The two groups can
   be either from the same dispersion formula but different DDA, or
   different dispersion formula but the same DDA.

Now enter 1, 2, 3, 4, or 5
xxxxx USER INPUT --->  3

Reading 181.bin...
The following dispersion formulas are found in 181.bin.
  1:VS      2:OBS
Want to include them all ? (<Y>/n)
If yes, all formulas will be arranged in alphabetic order,
except that formula OBS, if present, will be the first
xxxxx USER INPUT --->  y

The following DDA's are found in 181.bin.
  1:L81A1   2:L81B1   3:L81C1   4:L81D1
Want to include them all ? (<Y>/n)
If yes, all DDA's will be arranged in alphabetic order.
xxxxx USER INPUT --->  y

Want to review the selections just made (y/<N>) ?
xxxxx USER INPUT --->  n


Want to discard the current selections and select again (y/<N>) ?
xxxxx USER INPUT --->  n

First, some definitions of the variables that may appear in the following:
(1)  CHI:     centerline conc. (mg/m**3) for each arc
(2)  CHIY:    cross-wind integrated conc. (mg/m**2) for each arc
(3)  SIGY:    plume width(m) for each arc
(4)  Q(CHI):  emission rate (g/s) based on CHI for each arc
(5)  Q(CHIY): emission rate (g/s) based on CHIY for each arc
(6)  CL:      LOS-integrated conc. (mg/m**2) for each LOS
(7)  CLID:    LOS-integrated dosage (mg*s/m**2) for each LOS
(8)  Q(CL):   emission rate (g/s) based on CL for each LOS
(9)  Q(CLID): emission rate (g/s) based on CLID for each LOS
(10) M(CHI):  total mass emitted (kg) based on CHI for each arc
(11) M(CHIY): total mass emitted (kg) based on CHIY for each arc
(12) M(CL):   total mass emitted (kg) based on CL for each LOS
(13) M(CLID): total mass emitted (kg) based on CLID for each LOS
```

Figure 9-3. Screen image during the execution of the ASSEMBLE software package under Option 3, where values of the LOS-integrated dosage ($mg*s/m^2$) are tabulated.

```
In the following, the user will be asked to choose any combination from
a subset of the above 13 variables for tabulation.  Because some of these
variables may not be included in the DDA's you have selected, the program
has already screened these choices.
During the following choosing session, the user can restart the whole
process anytime, possibly because mistakes have been made, by typing a 'z'
(no need to type the quotes).

Press Enter to Continue.

Want to generate results for CL       (y/<N>) ?
zzzzz USER INPUT ---> n

Want to generate results for CLID     (y/<N>) ?
zzzzz USER INPUT ---> y

Want to generate results for Q(CL)    (y/<N>) ?
zzzzz USER INPUT ---> n

Want to generate results for Q(CLID) (y/<N>) ?
zzzzz USER INPUT ---> n

Want to generate results for M(CL)    (y/<N>) ?
zzzzz USER INPUT ---> n

Want to generate results for M(CLID) (y/<N>) ?
zzzzz USER INPUT ---> n

Enter name (NO EXTENSION) of the tabular ASCII output files:
Proper extensions, 1 - 13, corresponding to the 13 variables listed
previously, will be added by the program
zzzzz USER INPUT ---> test

Print out records even when the OBSERVED is missing (y/<N>) ?
The answer to this question matters only if the observed values
(or formula 'OBS') are to appear first in the table
zzzzz USER INPUT ---> n
```

Figure 9-3. Screen image during the execution of the ASSEMBLE software package under Option 3, where values of the LOS-integrated dosage ($mg*s/m^2$) are tabulated. (Concluded)

Q2: This question is identical to the previous question (Q1), except that it relates to the DDA's

Q3: The user is asked whether to review the selections just made under the previous two questions (Q1 and Q2). The default answer is "n".

Q4: The user is asked whether to discard all the selections made so far and start all over again. The default answer is "n". If "y", the user will be directed back to the first question (Q1).

Q5: The ASSEMBLE software package prints out the list of the 13 variables (refer to the beginning of Section B), together with their definitions, that the user can analyze. Then the user needs to specify, one variable at a time, whether to include that variable. The default answer is "n". Separate tables will be created for each variable. The user can select as many variables as he desires. The user can start this selection process all over again (i.e. go back to Q5) by entering a "*" anytime during this session. This provides the user with an opportunity to recover from a situation where mistakes might have been made. Note that depending on the nature of the DDA's chosen under the second question (Q2), there might be some variables that are simply not relevant. The user does not need not to be concerned with these variables. Take for example the DDA's from all the historical datasets. Since there were no line-of-sight (LOS)-related data, the user will not be asked whether to consider variables such as CL, CLID, Q(CL), Q(CLID), M(CL), and M(CLID).

Q6: The user is asked to specify only the name (not including extension) of the files to which the tables of various variables will be written. As just mentioned, separate tables will be created for each variable. The DDAMC software package automatically adds to the name specified by the user the appropriate extensions to construct complete names for all the files that need to be opened to contain the tables. As currently implemented, the extensions ".1", ".2", ".3", ".4", ".5", ".6", ".7", ".8", ".9", ".10", ".11", ".12", and ".13" are used for the variables C, C^y, σ_y, Q(C), $Q(C^y)$, CL, CLID, Q(CL), Q(CLID), M(C), $M(C^y)$, M(CL), and M(CLID), respectively. For example, if the user just entered

the name "TEST", and under the previous question (Q5), the user indicated that only the tables for CLID and Q(CLID) were to be created, then the ASSEMBLE software package will write the CLID table to a file called "TEST.7", and the Q(CLID) table to a file called "TEST.9".

Q7: The user is asked whether he still wants to print out the results from the dispersion formulas even if the observed value for that trial is missing. The default answer is "n", i.e., not to print out all the results for that trial if the observed value is missing. This filtering process is sometimes necessary, since there is nothing against which the predicted values by the dispersion formulas can be compared if the observed value is missing,. However, note that the filtering process only works if the observations (under the dispersion formula name "OBS") were to appear first (see the first question, Q1, above).

A missing value is flagged using "*****" in the table. Figure 9-4 is an example of the tables generated by the ASSEMBLE software package.

Option 4: Sometimes the user may want to investigate the distribution of variable A (e.g., predicted concentration, observed concentration, or the ratio of the two) as a function as variable B (e.g. downwind distance, atmospheric stability condition, or wind speed). The most straightforward approach is to plot one variable versus the other using scatter plots. However, scatter plots are only useful when the number of data points is small. One way of displaying large number of data is through the use of "box" plots, where 1) all the data points in variable A are first grouped according to the ranges of variable B, 2) within each group, the distribution (represented by the 2th, 16th, 50th, 84th, and 98th percentiles) of variable A is calculated, and 3) the distribution for each group is plotted using the box pattern. A generic distribution analysis software package, ANADISTR, see Appendix D, is used to accomplish tasks 1) and 2) just described. ANADISTR creates a output file containing the distribution information from an input file containing basically just columns of data where each column represents one variable. The SIGPLOT plotting package (see Appendix E) is used to make box plots using the distribution information file generated by ANADISTR. The purpose of Option 4 of the ASSEMBLE software package is to prepare the input files that can be accepted by the ANADISTR software

Integrated dosage (mg*s/m**2) along various LOS's

DDA	TRIAL	LOS	OBS.	VSDM
L81A1	bb2	1	2.51E+04	6.01E+04
		2	6.50E+03	1.20E+04
L81A1	bb3	1	5.30E+04	5.49E+04
L81A1	bb4	1	2.84E+04	5.39E+04
		2	7.60E+03	1.01E+04
L81A1	bb5	1	3.49E+04	4.35E+04
L81A1	bb6	1	5.14E+04	5.49E+04
L81A1	bb7	1	1.70E+04	7.89E+04
		2	6.40E+03	1.57E+04
L81A1	bb9	1	5.07E+04	3.45E+04
		2	2.49E+04	6.50E+03
L81B1	bb11	1	1.53E+04	9.52E+03
L81B1	bb12	1	4.19E+04	6.96E+04
L81B1	bb14	1	3.00E+04	4.27E+04
		2	1.72E+04	8.14E+03
L81B1	bb15	1	3.59E+04	4.45E+04
		2	1.20E+04	7.94E+03
L81B1	bb16	1	3.52E+04	4.35E+04
		2	9.70E+03	7.95E+03
L81B1	bb18	1	1.89E+04	4.07E+03
		2	3.19E+04	2.17E+04
L81C1	bb21	1	6.70E+03	7.71E+03
		2	3.89E+04	4.19E+04
L81C1	bb22	1	3.66E+04	5.41E+04
		2	1.77E+04	1.10E+04
L81C1	bb25	1	2.85E+04	4.31E+04
		2	1.10E+04	8.35E+03
L81C1	bb26	1	4.65E+04	3.47E+04
		2	2.23E+04	6.55E+03
L81C1	bb28	1	1.82E+04	4.07E+03
		2	3.17E+04	2.12E+04
L81C1	bb30	1	3.67E+04	4.98E+04
		2	1.11E+04	8.73E+03
L81D1	bb32	1	1.21E+04	7.91E+04
L81D1	bb35	1	3.91E+04	1.43E+05
		2	1.43E+04	2.98E+04
L81D1	bb36	1	3.96E+04	4.11E+04
L81D1	bb38	2	4.41E+04	2.50E+04
L81D1	bb40	1	1.71E+04	3.18E+04

Figure 9-4. An example of the tabular output of the LOS-integrated dosage ($mg*s/m^2$) for Option 3 of the ASSEMBLE software package.

package. The user is referred to Figure 9-5 for a hard copy of the screen image during the execution of ASSEMBLE under Option 4.

The first six questions (Q1 through Q6) asked under Option 4 are identical to those asked under Option 3, and will not be repeated here. Like Option 3, separate input files will be generated for each of the variables chosen by the user. The last question that will be asked is described below.

Q7: Under this option, after selecting the dispersion formulas and the DDA's (i.e. through Q1 and Q2), the user has the option to further instruct the program to consider only a subset of the data, such as the high wind cases, the stable cases, or the cases when the arcs were sufficiently close to the source. Here the user is first asked whether to consider only a subset of the data. The default answer is "n". If "n", the program proceeds to generate the input files and then terminates. If "y", the user will be further asked to develop subsets of data according to one of the following choices: 1) downwind distance or line-of-sight (depending on the variable, such as Q(C) or Q(CLID), under consideration), 2) wind speed, 3) Pasquill-Gifford stability class, 4) surface roughness, and 5) combination of 1) and 3). The user can only enter an integer between 1 and 5. The user is then asked to specify the lower and upper bounds for the subset variable just chosen. For example, if the user decides to divide up the data according to the wind speed, then by entering 0.0 and 6.0 for the lower and upper bounds, the ASSEMBLE software package will consider the trials only when the wind speeds were between 0.0 and 6.0 m/s.

Figure 9-6 shows an example of the input file generated by the ASSEMBLE software package for the values of CLID for the L81A1, L81B1, L81C1, and L81D1 datasets (see Section IV). The format of this input file is described in Appendix D. Figure 9-7 shows an example of the box plot displaying the distribution of the ratio of the values of CLID predicted by the VSDM dispersion formula to the observed values as a function of wind speeds. Note that the user needs to run both the ANADISTR and SIGPLOT packages in order to generate a plot like Figure 9-7.

```
D:\A135\DDAMC\ASSEMBLE>assemble

Enter the name of the composite binary file: (default is assemble.bin)
***** USER INPUT --->  181.bin

Select one of the following five main program options:

1) Update or expand 181.bin, i.e., incorporate additional DDA's or scaling
   results into the binary file,
2) View the contents of 181.bin on screen,
3) Tabulate the concentration or source data (to be defined later) for a
   subset of 181.bin,
4) Generate the input files to be used by the distribution analysis
   software package, ANADISTR, for the concentration or source data for a
   subset of 181.bin,
5) Summarize comparisons between two source-groups and characterize
   significance by performing the Student-t test.  The two groups can
   be either from the same dispersion formula but different DDA, or
   different dispersion formula but the same DDA.

Now enter 1, 2, 3, 4, or 5
***** USER INPUT --->  4

Reading 181.bin...
The following dispersion formulas are found in 181.bin.
  1:VS      2:OBS
Want to include them all ? (<Y>/n)
If yes, all formulas will be arranged in alphabetic order,
except that formula OBS, if present, will be the first
***** USER INPUT --->  y

The following DDA's are found in 181.bin.
  1:L81A1   2:L81B1   3:L81C1   4:L81D1
Want to include them all ? (<Y>/n)
If yes, all DDA's will be arranged in alphabetic order.
***** USER INPUT --->  y

Want to review the selections just made (y/<N>) ?
***** USER INPUT --->  n


Want to discard the current selections and select again (y/<N>) ?
***** USER INPUT --->  n

First, some definitions of the variables that may appear in the following:
(1)  CHI:     centerline conc. (mg/m**3) for each arc
(2)  CHIY:    cross-wind integrated conc. (mg/m**2) for each arc
(3)  SIGY:    plume width(m) for each arc
(4)  Q(CHI):  emission rate (g/s) based on CHI for each arc
(5)  Q(CHIY): emission rate (g/s) based on CHIY for each arc
(6)  CL:      LOS-integrated conc. (mg/m**2) for each LOS
(7)  CLID:    LOS-integrated dosage (mg*s/m**2) for each LOS
(8)  Q(CL):   emission rate (g/s) based on CL for each LOS
(9)  Q(CLID): emission rate (g/s) based on CLID for each LOS
(10) M(CHI):  total mass emitted (kg) based on CHI for each arc
(11) M(CHIY): total mass emitted (kg) based on CHIY for each arc
(12) M(CL):   total mass emitted (kg) based on CL for each LOS
(13) M(CLID): total mass emitted (kg) based on CLID for each LOS
```

Figure 9-5. Screen image during the execution of the ASSEMBLE software package under Option 4, where the input file, to be read by the ANADISTR software package, containing the values of the LOS-integrated dosage ($mg*s/m^2$) is created.

```
In the following, the user will be asked to choose any combination from
a subset of the above 13 variables for tabulation.  Because some of these
variables may not be included in the DDA's you have selected, the program
has already screened these choices.
During the following choosing session, the user can restart the whole
process anytime, possibly because mistakes have been made, by typing a 'r'
(no need to type the quotes).

Press Enter to Continue.

Want to generate results for CL      (y/<N>) ?
xxxxx USER INPUT ---> n

Want to generate results for CLID    (y/<N>) ?
xxxxx USER INPUT ---> y

Want to generate results for Q(CL)   (y/<N>) ?
xxxxx USER INPUT ---> n

Want to generate results for Q(CLID) (y/<N>) ?
xxxxx USER INPUT ---> n

Want to generate results for M(CL)   (y/<N>) ?
xxxxx USER INPUT ---> n

Want to generate results for M(CLID) (y/<N>) ?
xxxxx USER INPUT ---> n

Enter name (NO EXTENSION) of the ASCII output files that will serve
as the input to the evaluation software:
Proper extensions, 1 - 13, corresponding to the 13 variables listed
previously, will be added by the program
xxxxx USER INPUT ---> test1

Want to consider only a subset of CLID (y/<N>) ?
xxxxx USER INPUT ---> y

The following subsetting options are possible:
 1) downwind distance (m) (for the arc data like CHI) or
    LOS (for the LOS data like CLID),
 2) wind speed (m/s),
 3) P-G stability class (1-6),
 4) surface roughness, z0 (m), or
 5) combination of 1) and 3),
Please enter 1-5:
xxxxx USER INPUT ---> 2

Please specify lower and upper bounds for the parameter just chosen,
only those trials which fall into this interval will be considered.
Example: If 1 (downwind distance) is selected above, and the user enters
0. and 300. as the lower and upper bounds for downwind distance, this will
cause the program to process only those records with downwind distance
between 0 and 300 m
Note that lower bound must be < upper bound
xxxxx USER INPUT ---> 0.0 8.0
```

Figure 9-5. Screen image during the execution of the ASSEMBLE software package under Option 4, where the input file, to be read by the ANADISTR software package, containing the values of the LOS-integrated dosage ($mg*s/m^2$) is created. (Concluded)

```
  39   2   4   5
  11  10  12   6
'OBS.     ' 'VSDM     ' '
'L81A1    ' 'L81B1    ' 'L81C1    ' 'L81D1    ' '
 2.510E+04 6.012E+04  1.00       3.10       4.00       1.00       3.000E-02
 6.500E+03 1.202E+04  2.00       3.10       4.00       1.00       3.000E-02
 5.300E+04 5.487E+04  1.00       3.80       4.00       1.00       3.000E-02
 2.840E+04 5.392E+04  1.00       2.80       1.00       1.00       3.000E-02
 7.600E+03 1.010E+04  2.00       2.80       1.00       1.00       3.000E-02
 3.490E+04 4.348E+04  1.00       3.60       2.00       1.00       3.000E-02
 5.140E+04 5.486E+04  1.00       3.20       3.00       1.00       3.000E-02
 1.700E+04 7.892E+04  1.00       2.20       3.00       1.00       3.000E-02
 6.400E+03 1.568E+04  2.00       2.20       3.00       1.00       3.000E-02
 5.070E+04 3.448E+04  1.00       5.60       4.00       1.00       3.000E-02
 2.490E+04 6.502E+03  2.00       5.60       4.00       1.00       3.000E-02
 1.530E+04 9.523E+03  1.00       3.10       3.00       2.00       3.000E-02
 4.190E+04 6.959E+04  1.00       2.70       3.00       2.00       3.000E-02
 3.000E+04 4.271E+04  1.00       4.20       4.00       2.00       3.000E-02
 1.720E+04 8.139E+03  2.00       4.20       4.00       2.00       3.000E-02
 3.590E+04 4.447E+04  1.00       3.80       3.00       2.00       3.000E-02
 1.200E+04 7.944E+03  2.00       3.80       3.00       2.00       3.000E-02
 3.520E+04 4.355E+04  1.00       4.20       4.00       2.00       3.000E-02
 9.700E+03 7.951E+03  2.00       4.20       4.00       2.00       3.000E-02
 1.890E+04 4.070E+03  1.00       7.00       4.00       2.00       3.000E-02
 3.190E+04 2.169E+04  2.00       7.00       4.00       2.00       3.000E-02
 6.700E+03 7.713E+03  1.00       3.90       3.00       3.00       3.000E-02
 3.890E+04 4.187E+04  2.00       3.90       3.00       3.00       3.000E-02
 3.660E+04 5.412E+04  1.00       3.60       4.00       3.00       3.000E-02
 1.770E+04 1.103E+04  2.00       3.60       4.00       3.00       3.000E-02
 2.850E+04 4.307E+04  1.00       4.00       4.00       3.00       3.000E-02
 1.100E+04 8.353E+03  2.00       4.00       4.00       3.00       3.000E-02
 4.650E+04 3.468E+04  1.00       5.10       4.00       3.00       3.000E-02
 2.230E+04 6.549E+03  2.00       5.10       4.00       3.00       3.000E-02
 1.820E+04 4.073E+03  1.00       7.30       4.00       3.00       3.000E-02
 3.170E+04 2.124E+04  2.00       7.30       4.00       3.00       3.000E-02
 3.670E+04 4.978E+04  1.00       3.30       3.00       3.00       3.000E-02
 1.110E+04 8.726E+03  2.00       3.30       3.00       3.00       3.000E-02
 1.210E+04 7.906E+04  1.00       2.30       4.00       4.00       3.000E-02
 3.910E+04 1.426E+05  1.00       1.30       4.00       4.00       3.000E-02
 1.430E+04 2.984E+04  2.00       1.30       4.00       4.00       3.000E-02
 3.960E+04 4.115E+04  1.00       4.50       4.00       4.00       3.000E-02
 4.410E+04 2.500E+04  2.00       6.80       4.00       4.00       3.000E-02
 1.710E+04 3.176E+04  1.00       6.50       4.00       4.00       3.000E-02
7,'LOS',0.5,1.5,2.5,3.5,4.5,5.5,6.5,7.5
10,'u (m/s)',0.,2.,4.,6.,8.,10.,12.,14.,16.,18.,20.
3,'pg class',0.999,3.999,4.001,6.001
11,'experiment',0.5,1.5,2.5,3.5,4.5,5.5,6.5,7.5,8.5,9.5,10.5,11.5
5,'z0 (m)',0.0001,0.001,0.01,0.1,1.,10.
```

Figure 9-6. An example of the input file, to be read by the ANADISTR software package, generated by the ASSEMBLE software package under Option 4 for the values of the LOS-integrated dosage ($mg*s/m^2$) for the L81A1, L81B1, L81C1, and L81D1 datasets (see Section IV).

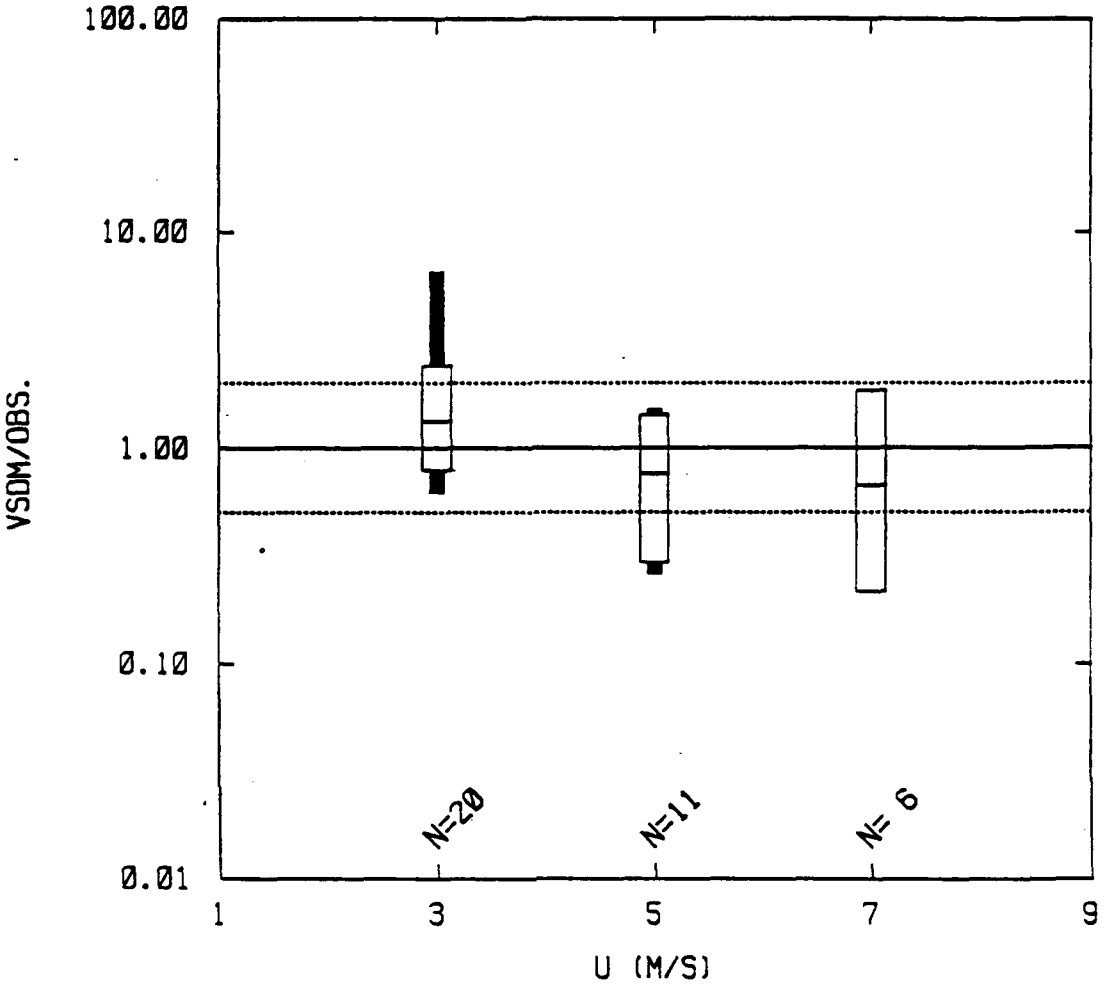

Figure 9-7. An example of the box plot created by the SIGPLOT plotting package, using the information originally given by the ASSEMBLE software package under Option 4 and then analyzed by the ANADISTR software package. The box plot describes the distribution of the ratio of the values of the LOS-integrated dosage ($mg*s/m^2$) predicted by the VSDM dispersion formula to the observed as a function of wind speeds for the L81A1, L81B1, L81C1, and L81D1 datasets (see Section IV).

Option 5: In this option, the user can compare any one of the 13 variables (described at the beginning of Section B) calculated by one dispersion formula for one DDA with the values calculated by another dispersion formula for another DDA. To illustrate, we again use the analog of the large two-dimensional master table where the rows represent the DDA's, the columns represent the dispersion formulas, and each cell of the table represents the results of the 13 variables for all the trials, arcs, and LOS's. By using this option, the user can test the general null hypothesis, "the mean of any variable at cell A is not significantly different from the mean of the same variable at cell B," using the Student-t test.

Although, as described above, we can compare information from any two "cells" within this large master table, we do not want to do this comparison blindly. As a result, under Option 5, the user is allowed only to select two "cells" that are on the same row or on the same column. In other words, statistical comparisons can be made only for the results that are 1) from the same dispersion formula for two DDA's, or 2) from two dispersion formulas for one DDA. The appropriate null hypothesis to be tested for case 1) can be: "the predicted total mass emitted by munition A based on the GPM dispersion formula is not significantly different from the predicted total mass emitted by munition B based on the same dispersion formula," or "the observed concentrations for munition A are not significantly different from the observed concentrations for munition B." (Recall that the ASSEMBLE software also treats the observations as a separate formula.) The appropriate null hypothesis to be tested for case 2) can be: "the concentrations predicted by the GPM dispersion formula for munition A is not significantly different from the concentrations predicted by the VSDM dispersion formula for the same munition."

The following is a list of questions that the user will encounter under Option 5. Most of the questions are for selecting the two cells just mentioned above. The user is referred to Figure 9-8 for a hard copy of the screen image during the execution of ASSEMBLE under Option 5.

```
D:\A135\DDAMC\ASSEMBLE>assemble

Enter the name of the composite binary file: (default is assemble.bin)
***** USER INPUT --->  181.bin

Select one of the following five main program options:

1) Update or expand 181.bin, i.e., incorporate additional DDA's or scaling
   results into the binary file,
2) View the contents of 181.bin on screen,
3) Tabulate the concentration or source data (to be defined later) for a
   subset of 181.bin,
4) Generate the input files to be used by the distribution analysis
   software package, ANADISTR, for the concentration or source data for a
   subset of 181.bin,
5) Summarize comparisons between two source-groups and characterize
   significance by performing the Student-t test.  The two groups can
   be either from the same dispersion formula but different DDA, or
   different dispersion formula but the same DDA.

Now enter 1, 2, 3, 4, or 5
***** USER INPUT --->  5

Reading 181.bin...
*****  ATTENTION  *****
Because of the option chosen at the beginning of the program, in the following
the user is allowed only to choose either one dispersion formula and
two DDA's or two dispersion formulas and one DDA.

The following dispersion formulas are found in 181.bin.
  1:VS      2:OBS
Want to include how many formulas ? (enter 1 or 2)
***** USER INPUT --->  1

Enter the formula NUMBER (not name) to be included first
***** USER INPUT --->  1

The following DDA's are found in 181.bin.
  1:L81A1   2:L81B1   3:L81C1   4:L81D1
Want to include how many DDA's ? (enter 1 or 2)
***** USER INPUT --->  2

Enter the DDA NUMBER (not name) to be included first
***** USER INPUT --->  1

Enter the DDA NUMBER (not name) to be included second
***** USER INPUT --->  2

Want to review the selections just made (y/<N>) ?
***** USER INPUT --->  n

Want to discard the current selections and select again (y/<N>) ?
***** USER INPUT --->  n
```

Figure 9-8. Screen image during the execution of the ASSEMBLE software package under Option 5, where the Student-t test is performed for the total mass emitted (kg) for the L81A1 and L81B1 datasets (see Section IV). The VSDM dispersion formula was used to remove the meteorological influences.

```
First, some definitions of the variables that may appear in the following:
(1)  CHI:      centerline conc. (mg/m**3) for each arc
(2)  CHIY:     cross-wind integrated conc. (mg/m**2) for each arc
(3)  SIGY:     plume width(m) for each arc
(4)  Q(CHI):   emission rate (g/s) based on CHI for each arc
(5)  Q(CHIY):  emission rate (g/s) based on CHIY for each arc
(6)  CL:       LOS-integrated conc. (mg/m**2) for each LOS
(7)  CLID:     LOS-integrated dosage (mg*s/m**2) for each LOS
(8)  Q(CL):    emission rate (g/s) based on CL for each LOS
(9)  Q(CLID):  emission rate (g/s) based on CLID for each LOS
(10) M(CHI):   total mass emitted (kg) based on CHI for each arc
(11) M(CHIY):  total mass emitted (kg) based on CHIY for each arc
(12) M(CL):    total mass emitted (kg) based on CL for each LOS
(13) M(CLID):  total mass emitted (kg) based on CLID for each LOS

In the following, the user will be asked to choose any combination from
a subset of the above 13 variables for tabulation.  Because some of these
variables may not be included in the DDA's you have selected, the program
has already screened these choices.
During the following choosing session, the user can restart the whole
process anytime, possibly because mistakes have been made, by typing a 'z'
(no need to type the quotes).

Press Enter to Continue.

Want to generate results for CL      (y/<N>) ?
***** USER INPUT --->  n

Want to generate results for CLID    (y/<N>) ?
***** USER INPUT --->  n

Want to generate results for Q(CL)   (y/<N>) ?
***** USER INPUT --->  n

Want to generate results for Q(CLID) (y/<N>) ?
***** USER INPUT --->  n

Want to generate results for M(CL)   (y/<N>) ?
***** USER INPUT --->  n

Want to generate results for M(CLID) (y/<N>) ?
***** USER INPUT --->  y

Enter name of the output file containing the Student-t test results:
***** USER INPUT --->  test.out

Ready to do more Student-t test (y/<N>) ?
***** USER INPUT --->  n


D:\A135\DDAMC\ASSEMBLE>
```

Figure 9-8. Screen image during the execution of the ASSEMBLE software package under Option 5, where the Student-t test is performed for the total mass emitted (kg) for the L81A1 and L81B1 datasets (see Section IV). The VSDM dispersion formula was used to remove the meteorological influences. (Concluded)

Q1: The ASSEMBLE software package first prints out all the dispersion formulas available in the composite binary file. The user needs to specify how many dispersion formulas are to be considered. Enter only "1" or "2" at this point. Selecting "1" means that the two cells will be chosen along a certain column of the large master table (i.e. two data sets are analyzed with one formula), and selecting "2" means that the two cells will be chosen along a certain row of the large master table (i.e. one data set is analyzed with two formulas).

Q2: The user is asked to specify the dispersion formula by entering the corresponding formula number. For example, if there are three dispersion formulas: (1) VSDM, (2) GPM and (3) OBS, that are available, and the user decides to use only the GPM dispersion formula only (i.e., "1" has been entered for the previous question, Q1), then the GPM dispersion formula will be selected by entering "2".

Q3: The ASSEMBLE software package then prints out all the DDA's available in the composite binary file. The user needs to specify how many DDA's that are to be considered. If the user answered "1" to the first question (Q1), then he enters "2" here; if the user answered "2" to the first question (Q1), then he enters "1" here. This procedure insures that only two cells will be selected.

Q4: The user is asked to specify the DDA by entering the corresponding DDA number. For example, if there are four DDA's: (1) OBLO, (2) OBHI, (3) GGLO, and (4) GGHI, that are available, and the user decides to consider GGLO and GGHI (i.e., "2" has been entered for the previous question, Q3), the "3" and "4" should be entered, one at a time

Q5: The user is asked whether to review the selections just made concerning dispersion formulas and DDA's. The default answer is "n".

Q6: The user is asked whether to discard all the selections just made and start all over again. The default answer is "n". This question provides the user with an opportunity to recover from a situation where mistakes might have been made. If "y", the user will be redirected back to the first question (Q1).

Q7: The ASSEMBLE software package prints out the list of the 13 variables (refer to the beginning of Section B), together with their definitions, that the user can analyze. Then the user needs to specify, one variable at a time, whether to include that variable. The default answer is "n". The user can select as many variables as he desires. This selecting process can start all over again (i.e., go back to Q7) by entering a "*" anytime during this session. This provides the user with an opportunity to recover from a situation where mistakes might have been made. Note that, depending on the nature of the DDA's chosen under the fourth question (Q4), there might be some variables that are simply not relevant. In the case of the DDA's from all the historical datasets, for example, there were no LOS-related data. Therefore, the user will not be asked whether to consider variables such as CL, CLID, Q(CL), Q(CLID), M(CL), and M(CLID).

Q8: The user is asked to specify the name of the output file to which the ASSEMBLE software package will write its results. Unlike Options 3 and 4, only one file will be created to contain the results.

Q9: Finally, the user is asked whether to make more analyses using other dispersion formulas and DDA's. The default answer is "n". If "n", the program terminates. If "y", the user is directed back to the first question (Q1) and the whole process repeats.

The ASSEMBLE software package uses the Student-t test to test the difference of two means. An important assumption is that all the data are independent. The user is cautioned not to apply Option 5 blindly if the requirement of data independence is not guaranteed. Guidelines concerning data independence are discussed in a separate sub-section below.

The output file generated by the ASSEMBLE software package under this option is concise and self-explanatory (see Figure 9-9). It is divided into sections, each section corresponds to the Student-t test results for one variable. Recall that the same variables from two groups will be compared to each other. These two groups represent data from one dispersion formula for two DDA's, or data from two dispersion formulas

```
**********************************************************************
Summary of the Student-t Test for Two Source Groups.
These two source groups can make use of the same scaling
formula with different datasets, or different formulas
with the same dataset.
**********************************************************************

Predicted M (kg) based on CLID
----------------------------------------------------------------------

Group 1 (Q1):   VSDM     ,  L81A1     (Formula,DDA)
Group 2 (Q2):   VSDM     ,  L81B1     (Formula,DDA)

'PROB' is the probability that |T| could be this large or
  larger just by chance for distributions with equal means.
  Therefore, a small numerical value of the probability
  (e.g. 0.05 or 0.01) means that the observed difference
  is "very significant."


Statistics for source group 1 :
     LOS    AVG        SD        N
       1 0.651     0.329        7.
       2  1.19      1.22        4.

Statistics for source group 2 :
     LOS    AVG        SD        N
       1  1.23      1.07        6.
       2  1.31     0.306        4.

Cross comparison between two source groups:

If two source groups made use of the same source position
  and sampling array, compare the values from the same arc
  or LOS, with the most confidence given to the results
  based on the arc or LOS that is closest to the source.

If two source groups made use of different source or
  sampler locations, compare the values based on the arc or
  LOS that is closest to the source for group 1 with the
  values based on the arc or LOS that is closest to the
  source for group 2

The results for all possible combinations are presented
  in the following.

 LOS(Q1)    LOS(Q2)      T       PROB   DF
       1          1  -1.256    0.235 11.0
       1          2  -2.952    0.016  9.0
       2          1  -0.050    0.962  8.0
       2          2  -0.161    0.878  6.0
```

Figure 9-9. An example of the output file generated by the ASSEMBLE software package under Option 5, containing summary information for the Student-t test.

for one DDA's. Within each group, there are data for all the trials, arcs, and LOS's.

For each section, the variable under investigation and the definition of the two groups are first identified in the output listing. Means, standard deviations, and sample sizes for the data for *each arc/LOS* and each group are listed. Note that the data from different arcs/LOS's during the same trial are not lumped together because they are not really independent of each other. If we conduct an experiment only one time but using 100 instruments to measure the outcome, it is likely that the 100 data points obtained are highly dependent. On the other hand, if we conduct an experiment 100 times but only one instrument, then the 100 data points obtained can be treated as independent samples.

The Student-t test is performed for all possible combinations of arcs/LOS's between two groups. Suppose both groups have data available at two arcs, this means that the following comparisons will be made:

arc 1 of group 1	vs.	arc 1 of group 2
arc 1 of group 1	vs.	arc 2 of group 2
arc 2 of group 1	vs.	arc 1 of group 2
arc 2 of group 1	vs.	arc 2 of group 2

It is obvious that conflicting results of the significance tests may be obtained from all of the above cross-comparisons. The user should have some prior knowledge concerning which arc/LOS from each group should be given the highest relevance. For a typical application, the arcs or LOS's that are closest to the source should be given the highest priority.

Note that rather than specifying a fixed significance level against which the t statistic is checked, the ASSEMBLE software package prints out "PROB", the probability that |t| could be this large or larger just by chance for two samples from the same population. Therefore, a small numerical value of the probability (like 0.05 or 0.01) means that the observed difference in means is "very significant". The user can then test the significance of the t statistics based on any desired significance level.

Analysis of Data That Are Not Independent

A basic assumption in all statistical analysis procedures is that all of the data points are independent (i.e. they are completely random samples drawn from some underlying distribution). Because of the costs and practical difficulties of conducting field experiments in the atmosphere, the data independence principle is always violated to some degree. For example, weather conditions during a one-hour sampling period are not independent of those during the preceding one-hour period. Nevertheless, the correlations from one hour to the next are sufficiently small that a *reasonably* independent set of data points can be constructed from a series of hourly experiments.

We start running into serious problems with the independence principle if we consider, say, concentration observations at several spatial positions during each of the hours in question. If the concentration at one location is higher than usual, then the concentrations during that same time period at other locations are also likely to be higher than usual.

Consider the example where N independent field tests are conducted, and concentrations are observed at M locations during each test. Assume that these M locations do not move from test to test. There are two conclusions:

(1) For any location, there are N independent data points, and these data can be analyzed using standard statistical procedures, with N-1 degrees of freedom.

(2) If we construct a dataset of size N*M, these data are *not* independent, there are *not* N*M-1 degrees of freedom, and standard statistical procedures should not be used.

We could start making arbitrary assumptions about reduced degrees of freedom for the N*M dataset, but we are on shaky grounds which would generate much criticism from statisticians.

The issue is also complicated by the fact that dispersion model accuracy deteriorates as distance from the source increases. Consequently, the

relative variance (σ_Q / $\bar{Q}$) is likely to be larger for the locations at large x, which also violates the requirements for independence.

Thus we recommend that the significance tests for munitions use only a single location from each field test, and that the location that is selected should be the closest available monitor to the source. The monitor should be near the plume centerline (if a point measurement is made) or should sample the entire plume cross-section at nearly right angles to the plume centerline (if a cross-wind integrated measurement is made).

If the user wants to use the data from all M positions, they should be first combined, e.g.

$$\bar{Q}_j = \frac{1}{M} \sum_{i=1}^{M} Q_{i,j} , \qquad \text{where } j = 1,N \qquad (9\text{-}2)$$

and then the N values of $\bar{Q}$ analyzed.

To conclude, in atmospheric dispersion field experiments, as in everything else, the user cannot get something for nothing. There is no substitute for conducting more field experiments in order to improve the size of the dataset and the degrees of freedom.

Format of the Composite Binary File

- Record 1: Contains the number (IMOD, INTEGER) of dispersion formulas whose results are included in the binary file, and the names (CHARACTER*3) of the dispersion formulas. Note that the observations (under the name "OBS") are also treated as one.

- Record 2: Contains the number (IDDA, INTEGER) of the DDA's included in the binary, and the names (CHARACTER*5) of the DDA's.

- Next IDDA records: There is one record for each DDA. Each record contains the number (INTEGER) of the trials available for that DDA, and the names (CHARACTER*10) of the trials.

• Next ITRL (the total number of trials in the binary file) records: Each record contains, for each trial, the trial name (CHARACTER*10), wind speed (REAL), total emission rate (REAL), total mass emitted (REAL), standard deviation of the wind azimuth angle fluctuations (REAL), standard deviation of the wind elevation angle fluctuations (REAL), friction velocity (REAL), surface roughness (REAL), inverse of the Monin-Obukhov length (REAL), convective velocity scale (REAL), wind speed power-law exponent (REAL), temperature difference between 16 m and 2 m (REAL), Pasquill-Gifford stability class (INTEGER), number of concentric arcs (INTEGER), number of LOS's (INTEGER), and downwind distances for all the arcs. These records are used to store the characteristics of each trial.

• Remaining records: Two records are used to store the results from one dispersion formula (including observations as one) for each trial. The first record contains all arc-related data, including the name of the dispersion formula (CHARACTER*3), the name of the trial (CHARACTER*10), the number of arcs (INTEGER), the predicted values (REAL) of centerline concentration for each arc, the predicted values (REAL) of cross-wind integrated concentration for each arc, the predicted values (REAL) of plume width for each arc, the predicted values of emission rate (REAL) based on centerline concentration for each arc, and the predicted values of emission rate (REAL) based on cross-wind integrated concentration for each arc. The second record contains all LOS-related data, including the name of the dispersion formula (CHARACTER*3), the name of the trial (CHARACTER*10), the number of LOS's (INTEGER), the predicted values (REAL) of LOS-integrated concentration for each LOS, the predicted values of LOS-integrated dosage for each LOS, the predicted values of total emission rate (REAL) based on LOS-integrated concentration for each LOS, and the predicted values of total emission rate (REAL) based on LOS-integrated dosage for each LOS.

As an example, suppose there are two DDA's with 12 and 19 trials each, and three dispersion formulas were used. Then the composite binary file should contain:

```
        1 (header record for dispersion formulas)
        1 (header record for DDA's)
        2 (2 DDA's)
       31 (12 + 19 = 31 trials)
+     248 [31 * 4 (3 dispersion formulas + observations) * 2
            (2 records for each formula and trial)]
-------------------------------------------------------------
=     283 records.
```

Maximum Limits

The ASSEMBLE software package is very memory-intensive because it uses a simple flat structure (i.e. two-dimensional table) to store the information. At present, the ASSEMBLE software package has the following limits imposed:

	Generic version	For Historical Datasets	For Smoke/Obscurant Datasets
• maximum number of total trials	100	200	420
• maximum number of DDA's	50	10	50
• maximum number of trials per DDA	70	70	70
• maximum number of dispersion formulas	10	10	3
• maximum number of arcs	6	6	1
• maximum number of LOS's	6	1	6
Required memory (KB)	480	535	405

Note that the historical and smoke/obscurant datasets are distinctly different. In the historical datasets, there are results from many dispersion formulas, only point concentrations (no LOS's), and only a moderate number of trials. In the smoke/obscurant datasets, there are results from only two dispersion formulas (VSDM and GPM), only LOS-related data (no point data), and a large number of trials. It is impossible to have a version of the program that accommodates the requirements for both of these datasets without exceeding the DOS 640 KB limit. As a result, we have also generated specific versions of the ASSEMBLE software package for the historical datasets and smoke/obscurant datasets, respectively. All the above limits are specified in the "ASPARAMS.CMN" Fortran INCLUDE file using the PARAMETER statements. The user can easily modify the limits depending on the particular application at hand. However, it is not required to, say, bring results for all the smoke/obscurant datasets (i.e., all 47 DDA's listed in Table 4-2) into a *single* composite binary file. The user can, instead, create many smaller composite binary files, each one including only the DDA's where the same munition was used. In this case, the generic version should be sufficient for

most typical applications.

Programming Information

The ASSEMBLE software package was developed on a 80386/7-based PC using Version 4.1 of the Lahey Fortran Compiler. Because the extension "call system (command)" was used (a subroutine that passes a CHARACTER expression "command" to DOS to be executed as if it had been typed at the console), porting the package to other platforms can be achieved only if a similar extension is also supported on that platform. As previously mentioned, a binary file is not only system-dependent, but also compiler-dependent. Therefore, the composite binary file needs to be recreated if the ASSEMBLE software package is re-compiled on other platforms.

The ASSEMBLE software package consists of 18 Fortran programs and 4 INCLUDE files. Because a relatively large number of programs are involved, the MAKE utility, part of the Lahey Fortran program development tools, was used to develop the package. The use of the MAKE utility is not essential, but is very useful in keeping track of the updates of the programs.

C. User's Guide for DDAMC - Monte Carlo Sensitivity Analysis

The DDAMC software package, already described in part in Section VI, can also assess sensitivity of any analysis procedure to input data errors using the Monte Carlo method. Currently, the user is allowed to perturb the following ten parameters: wind speed (u), wind direction (θ), standard deviation of the wind azimuth angle fluctuations (σ_θ), standard deviation of the of wind elevation angle fluctuations (σ_ϕ), temperature difference between two levels (ΔT), surface roughness (z_0), emission rate (Q), source duration (T_d), source dimensions (σ_{x0}, σ_{y0} and σ_{z0}), and source location (x_0, y_0, and z_0).

Execution of DDAMC (Monte Carlo Mode)

The DDAMC software package is switched to Monte-Carlo mode if the user answers "y" to the fourth question described in Section VI.D. In this application, the DDAMC software package assesses the sensitivity of a dispersion formula to input data error using the Monte-Carlo method. In the

following, the procedure for implementing the Monte-Carlo method will be first described, followed by instructions for using the DDAMC package.

The input parameters accepted by the dispersion formulas can be classified as either primary or secondary. The primary input parameters refer to those input variables that can be directly measured. The secondary input parameters refer to those input variables that can be derived from the primary input parameters based on known physical relationships.

The DDAMC software package currently treats the following ten primary input parameters:

- wind speed (u)
- wind direction (θ)
- temperature difference between two levels (ΔT)
- standard deviation of the wind azimuth angle fluctuations (σ_θ)
- standard deviation of the wind elevation angle fluctuations (σ_ϕ)
- surface roughness (z_0)
- source emission rate scaling factor (SRSF)
- source duration scaling factor (SDSF)
- source size scaling factor (SSSF)
- source location scaling factor (SLSF)

The reason for using SRSF, SDSF, SSSF, and SLSF rather than dealing directly with the values of emission rate (Q), source duration (T_d), source size (σ_{x0}, σ_{y0}, and σ_{z0}), and source location (x_0, y_0, and z_0) for each source is mainly due to the fact that there can be multiple sources involved in any given trial. Suppose there were N sources involved in a given trial. Instead of defining the individual variation of each of the N emission rates, SRSF defines the simultaneous variation of all the source emission rates. Examples of the use of SRSF, SDSF, SSSF, and SLSF will be given later.

Examples of secondary input parameters are the wind speed power-law exponent (WPL), friction velocity (u_*), Monin-Obukhov length (L), and Pasquill-Gifford stability class (PG). Their values will be derived from the updated primary input parameters by the DDAMC software during each simulation. A primary input parameter will be automatically "degraded" to a secondary input parameter if it is missing. The user is referred to Section VI.D regarding the derivation of these secondary input parameters.

Perhaps the most difficult problem encountered in the Monte Carlo sensitivity analysis is the specification of the probability distributions functions (pdf) of the primary input parameters. Gaussian and log-normal pdf's are commonly assumed for many ambient measurements (e.g. Lewellen and Sykes, 1989; Irwin et al., 1987). However, there is a lack of knowledge about the distributions of other parameters. Moreover, the need for a detailed description of the pdf's for parameters such as surface roughness is not so clear. Therefore, is was decided that a simple uniform pdf, defined by a lower and upper bound, would be used for all the primary input parameters in the DDAMC software package. The upper and lower bounds of the uniform pdf's usually are determined either by instrument accuracy or by some ad hoc assumptions.

The following default ranges of uncertainties for the primary input parameters are assumed; however, the user always has the option of altering the default values.

u: the original value ± larger of 0.5 m/s and σ_u
θ: the original value ± 10°
ΔT: the original value ± 0.2 °C
σ_θ: the original value ± 10%
σ_ϕ: the original value ± 30%
z_0: the original value ± 1/2 order of magnitude
SRSF: the original value ± 1/2 order of magnitude
SDSF: the original value ± 10%
SSSF: the original value ± 1/2 order of magnitude
SLSF: the original value ± 25 m

The following five examples are used to demonstrate the use of the default ranges of uncertainties for some of the variables. Example 1: if the observed value of θ is 178°, then during each Monte Carlo simulation, a new value of θ will be randomly sampled from a uniform distribution between 168° and 188°. Example 2: If the reported value of z_0 is 10 cm, the during each Monte Carlo simulation, a new value of z_0 will be randomly sampled from a uniform distribution between 3.14 cm and 31.4 cm. Example 3: If there are two sources whose observed emission rates (Q_1 and Q_2) are 500 g/s and 80 g/s, respectively, then during each Monte Carlo simulation, new values of Q_1 and Q_2

will be randomly sampled from uniform distributions between 157 g/s and 1570 g/s, and 25.12 g/s and 251.2 g/s, respectively. Example 4: If the initial dimensions of the source (σ_{x0}, σ_{y0}, and σ_{z0}) are 4.5 m, 2.3 m, and 0.12 m, respectively, then during each Monte Carlo simulation, new values of σ_{x0}, σ_{y0}, and σ_{z0} will be randomly sampled from uniform distributions between 1.413 m and 14.13 m, 0.722 m and 7.22 m, and 0.0387 m and 0.387 m, respectively. Example 5: If the source coordinates (x_0 and y_0) are 68 m and -156 m, respectively, then during each Monte Carlo simulation, new values of x_0 and y_0 will be randomly sampled from uniform distributions between 43 m and 93 m, and -181 m and -131 m, respectively.

The following is a list of six questions that will be posed to the user when the DDAMC software package is run. The questions regarding the name of the DDA, the path name for the DDA file, the choice of dispersion formula, and whether to use the Dugway method to relate σ_θ and σ_ϕ have been discussed in Section VI.D and will not be repeated here. The user is referred to Figure 9-10 for a hard copy of the screen image during the execution of DDAMC (Monte Carlo mode).

Q1: The user is asked to specify the name of the output file. There is no default answer to this question.

Q2: The user is asked whether detailed output (i.e., the listing of the values of all the primary input parameters, some secondary input parameters (L, u_*, PG, and WPL) and concentration and emission rate predictions) for each Monte-Carlo simulation is desired. The default answer is "n".

Q3: The user is asked whether to generate an output file containing the probability density functions (pdf) for the concentration and emission rate predictions. Because of its columnar format, this file can be easily plotted using the SIGPLOT (see Appendix E) or other plotting packages. The default answer to this questioh is "y". If "y", the user also has to specify the name of this output file.

Q4: The user is asked to select a trial from the current DDA as the "base" case for application of the Monte Carlo procedure. There is no default answer to this answer.

```
ddamc

Enter key letters for the DDA (5 letters at most):
Examples:
OB_*:  Ocean Breeze,          DGB_*: Dry Gulch, Course B
DGD_*: Dry Gulch, Course D,   GG_*:  Green Glow
PG_*:  Prairie Grass,         AT*: Atterbury-87
INVHC: Inventory smoke munition test
DT1??: DT I  of 155mm projectiles
DT2??: DT II of 155mm projectiles
L81*:  Evaluation of L8A1 grenades
L83*:  Evaluation of L8A3 grenades
DT1?:  DT I of 81mm projectiles
INT??: Evaluation of international smoke pots/generators
PO*:   Evaluation of man-portable smoke generators
***** USER INPUT --->  athc

Enter the full path name where DDA resides
(default is \a135\ddamc\dda, a . means current directory):
***** USER INPUT --->

Choose one dispersion formula to run from the following list:
1)  VSDM
2)  GPM
Formulas for C only:
3)  OB/DG
4)  Regression (dataset specific)
5)  Similarity
Formulas for Cy only:
6)  Regression (dataset specific)
7)  Similarity
8)  Nieuwstadt/Venkatram
9)  Briggs
Enter 1-9:
***** USER INPUT --->  2

Perform Monte Carlo sensitivity analysis? (y/<N>):
***** USER INPUT --->  y

Use the Dugway scheme to relate sigma-phi and sigma-theta,
if necessary? (y/<N>):
***** USER INPUT --->  n

Reading DDA...
Enter name of the listing output file:
testmc.out

Generate detailed output, including results for each sample? (y/<N>):
***** USER INPUT --->  y

Want to plot pdf? (<Y>/n):
***** USER INPUT --->  n
```

Figure 9-10. Screen image during the execution of the DDAMC software package (Monte Carlo mode), where 20 Monte Carlo simulations were carried out for the trial AT5 of the Atterbury-87 dataset using the GPM dispersion formula. Default ranges of uncertainties (see text) were used.

```
Following trials are available :
 1)             at5
 2)             at6
 3)             at7
 4)             at8
 5)             at9
Now enter the integer value corresponding to the trial to be run:
zzzzz USER INPUT ---> 1

Enter the no. of simulations to be made:
zzzzz USER INPUT ---> 20

The default ranges for each variable are:
1)  u:     original value q max(0.5 m/s, sigu)
2)  wd:    original value q 10x
3)  dT:    original value q 0.20xC
4)  sigt:  original value q 10%
5)  sigp:  original value q 30%
6)  z0:    original value q 1/2 order of magnitude
7)  SRSF:  original value q 1/2 order of magnitude
8)  SDSF:  original value q 10%
9)  SSSF:  original value q 1/2 order of magnitude
10) SLSF:  original value q 25m

where SRSF: source rate scaling factor
      SDSF: source duration scaling factor
      SSSF: source size scaling factor
      SLSF: source location scaling factor

No resampling will be made for some of the variables, including
dt, sigt, sigp, source emission rate, source duration, and source
size, if they were missing in the first place!

Accept all defaults? (<Y>/n)
zzzzz USER INPUT ---> y

Running dispersion formula...
          10 iterations...
          20 iterations...
Writing results...

D:\A135\DDAMC\PROG>
```

Figure 9-10. Screen image during the execution of the DDAMC software package (Monte Carlo mode), where 20 Monte Carlo simulations were carried out for the trial AT5 of the Atterbury-87 dataset using the GPM dispersion formula. Default ranges of uncertainties (see text) were used. (Concluded)

Q5: The user is asked to specify the number of Monte Carlo simulations to be made. There is no default answer to this answer. The maximum number of simulations allowed is 400.

Q6: The user is asked whether to accept the default ranges of uncertainties for all the primary input parameters. The default answer is "y". If "n", then the user is asked to specify, one parameter at time, the desired lower and upper bounds between which the parameter will be randomly sampled.

The user is cautioned that the DDAMC software package only addresses the issue of uncertainties associated with primary input data error. No attempts were made to estimate the uncertainties associated with the procedures (refer to Section VI.D) used to derive the secondary input parameters from the primary input parameters.

Format of the Mandatory ASCII Output File Generated by DDAMC (Monte Carlo Mode)

When the DDAMC software package is run in Monte Carlo mode, one output file will always be created summarizing the results of the Monte Carlo sensitivity analyses. As an option, another output file will also be created containing the pdf information for the concentration data.

The mandatory output file (see Figure 9-11 for an example) starts with the name of trial under investigation, and the number of simulations made. The file then lists, for each one of the primary input parameters, the original value, lower and upper bounds used to define the range of uncertainties and the uniform distribution, the *theoretical* values of the mean (μ) and standard deviation (σ) for the uniform distribution, and finally the ratio of σ/μ. The file then documents the dispersion formula used, and whether the Dugway method is used to relate σ_θ and σ_ϕ. Next, the file lists the numbers of concentric arcs and lines-of-sight (LOS) employed, together with appropriate information regarding geometric positions.

If the user chooses to generate detailed output, the mandatory file lists the values of all the primary input parameters and some secondary input

```
Trial name: at5
No. of simulation:          20
Orig. value, lower bound, upper bound, mean, sigma, and sigma/mean for each variable:
Note that the means and sigmas here are based on the THEORETICAL UNIFORM distribution

          Orig. value lower bnd. upper bnd.     mean       sigma     sigma/mean

  u         4.400E+00  3.370E+00  5.430E+00  4.400E+00  5.947E-01  1.352E-01
  wd        2.500E+01  1.500E+01  3.500E+01  2.500E+01  5.774E+00  2.309E-01
  dT       -6.800E-01 -8.800E-01 -4.800E-01 -6.800E-01  1.155E-01 -1.698E-01
  sigd      1.100E+01  9.900E+00  1.210E+01  1.100E+01  6.351E-01  5.774E-02
  sigp      8.000E+00  5.600E+00  1.040E+01  8.000E+00  1.386E+00  1.732E-01
  z0        2.000E-01  6.320E-02  6.320E-01  3.476E-01  1.642E-01  4.724E-01
  SRSF      1.000E+00  3.160E-01  3.160E+00  1.738E+00  8.210E-01  4.724E-01
  SDSF      1.000E+00  9.000E-01  1.100E+00  1.000E+00  5.773E-02  5.773E-02
  SSSF      1.000E+00  3.160E-01  3.160E+00  1.738E+00  8.210E-01  4.724E-01
  SLSF      0.000E+00 -2.500E+01  2.500E+01  0.000E+00  1.443E+01  9.990E+02

GPM model, both C and Cy
The HPDM scheme is used to calculate sigma-phi and/or sigma-theta
NDIST =  0
And the downwind arc distances (m) are:

NLOS  =  4
And the locations of lines-of-sight (LOS) are:
     (  -282.,   -390.), to (  -190.,   -482.)
     (  -312.,   -282.), to (   -92.,   -520.)
     (  -270.,   -123.), to (    67.,   -459.)
     (  -196.,     73.), to (   256.,   -376.)


Following are the values for each simulation:

     u         wd         dT         sigd       sigp       z0         SRSF       SDSF       SSSF       SLSF
 4.173E+00 1.842E+01-6.230E-01 1.181E+01 6.419E+00 4.576E-01 1.000E+00 1.034E+00 3.131E+00 3.112E+00
 4.761E+00 3.176E+01-5.360E-01 1.145E+01 6.562E+00 5.708E-01 2.436E+00 1.067E+00 2.157E+00 2.697E+00
 4.137E+00 2.792E+01-4.819E-01 1.203E+01 8.216E+00 5.525E-01 8.221E-01 9.756E-01 1.320E+00 1.787E+01
 4.103E+00 2.121E+01-7.441E-01 1.146E+01 7.878E+00 5.746E-01 3.612E-01 1.096E+00 7.815E-01 1.000E+01
 4.947E+00 2.440E+01-5.786E-01 1.102E+01 6.058E+00 2.816E-01 2.161E+00 9.727E-01 1.395E+00 2.185E-01
 5.242E+00 2.659E+01-5.073E-01 1.054E+01 5.970E+00 4.915E-01 1.199E+00 9.253E-01 1.664E+00 1.110E+01
 5.009E+00 2.271E+01-8.775E-01 1.025E+01 9.705E+00 2.082E-01 1.575E+00 1.040E+00 2.938E+00-2.585E+00
 4.893E+00 2.819E+01-6.642E-01 1.163E+01 9.872E+00 3.411E-01 3.040E+00 1.090E+00 1.878E+00-2.308E+01
 4.253E+00 3.400E+01-8.567E-01 1.115E+01 7.898E+00 7.398E-02 2.002E+00 1.003E+00 2.862E+00-1.776E+01
 3.975E+00 2.385E+01-6.354E-01 1.125E+01 6.036E+00 3.386E-01 3.073E+00 1.016E+00 1.629E+00 1.650E+01
 5.189E+00 2.273E+01-7.276E-01 1.365E+01 1.027E+01 1.222E-01 2.132E+00 1.056E+00 2.050E+00-1.982E+01
 4.276E+00 2.176E+01-6.154E-01 1.190E+01 1.028E+01 5.083E-01 1.150E+00 9.963E-01 7.023E-01 2.587E+00
 4.862E+00 2.305E+01-4.987E-01 1.043E+01 5.725E+00 3.112E-01 1.292E+00 1.004E+00 1.547E+00 9.617E+00
 4.031E+00 2.656E+01-7.120E-01 1.191E+01 6.972E+00 4.313E-01 2.363E+00 9.939E-01 1.927E+00 1.360E+01
 4.557E+00 2.818E+01-5.963E-01 1.187E+01 8.613E+00 5.348E-01 2.305E+00 1.081E+00 3.119E+00 2.313E+01
 3.745E+00 2.146E+01-7.382E-01 1.141E+01 8.487E+00 1.655E-01 1.495E+00 9.745E-01 1.691E+00 8.619E+00
 4.036E+00 2.197E+01-8.077E-01 1.136E+01 6.535E+00 2.606E-01 1.114E+00 1.025E+00 9.315E-01 1.865E+01
 4.719E+00 2.965E+01-5.808E-01 1.022E+01 6.084E+00 2.506E-01 4.473E-01 1.037E+00 3.342E-01-1.029E+01
 4.481E+00 2.542E+01-7.179E-01 1.132E+01 7.474E+00 6.029E-01 3.100E+00 1.012E+00 5.347E-01-8.305E+00
 3.661E+00 2.631E+01-7.277E-01 1.045E+01 8.809E+00 3.147E-01 2.940E+00 1.083E+00 9.668E-01-1.628E+01

     L      PG   ustar      wpl

-1.390E+02  3 5.828E-01 5.797E-01
-2.581E+02  4 6.372E-01 6.396E-01
-2.146E+02  4 6.036E-01 6.783E-01
-1.294E+02  3 6.254E-01 6.994E-01
-1.567E+02  4 5.872E-01 4.333E-01
-3.015E+02  4 7.236E-01 6.187E-01
-8.012E+01  3 5.662E-01 3.663E-01
-1.466E+02  4 6.179E-01 4.798E-01
-3.083E+01  3 3.972E-01 2.355E-01
-9.875E+01  3 5.130E-01 4.724E-01
-7.397E+01  3 5.100E-01 2.969E-01
-1.605E+02  4 6.145E-01 6.300E-01
-1.935E+02  4 5.890E-01 4.591E-01
-1.055E+02  3 5.617E-01 5.324E-01
-1.976E+02  4 6.598E-01 6.589E-01
-4.480E+01  3 4.154E-01 3.221E-01
-6.367E+01  3 4.959E-01 4.032E-01
-1.310E+02  4 5.462E-01 4.068E-01
-1.682E+02  4 6.842E-01 7.344E-01
-6.655E+01  3 4.757E-01 4.468E-01
```

Figure 9-11 An example of the mandatory output file generated by the DDAMC software package summarizing the results of the Monte Carlo sensitivity analysis for the trial AT5 of the Atterbury-87 dataset. Note that the GPM dispersion formula was used, default ranges of uncertainties (see text) were used, and only 20 simulations were carried out.

Following are the values for each simulation:

cl(mg/m**2)... clid(mg-s/m**2)... for each LOS

8.561E+01	2.234E+02	4.677E+02	1.416E+03	1.328E+05	3.466E+05	7.255E+05	2.197E+06
4.244E+02	9.436E+02	1.551E+03	4.425E+03	6.791E+05	1.510E+06	2.481E+06	7.082E+06
1.731E+02	3.756E+02	6.093E+02	1.775E+03	2.534E+05	5.496E+05	8.917E+05	2.598E+06
3.500E+01	9.000E+01	1.867E+02	6.477E+02	5.756E+04	1.480E+05	3.070E+05	1.065E+06
1.587E+03	2.603E+03	3.645E+03	9.767E+03	2.316E+06	3.799E+06	5.318E+06	1.425E+07
1.937E+02	4.244E+02	6.888E+02	1.933E+03	2.688E+05	5.890E+05	9.560E+05	2.683E+06
5.228E+02	1.117E+03	1.807E+03	6.371E+03	8.155E+05	1.743E+06	2.819E+06	9.937E+06
5.309E+02	1.182E+03	1.964E+03	6.128E+03	8.681E+05	1.933E+06	3.211E+06	1.002E+07
6.898E+02	1.605E+03	2.629E+03	8.653E+03	1.038E+06	2.415E+06	3.955E+06	1.302E+07
3.009E+02	7.625E+02	1.486E+03	4.161E+03	4.586E+05	1.162E+06	2.265E+06	6.341E+06
7.908E+02	1.538E+03	2.457E+03	9.667E+03	1.252E+06	2.436E+06	3.891E+06	1.531E+07
2.063E+02	4.860E+02	8.550E+02	2.698E+03	3.082E+05	7.263E+05	1.278E+06	4.032E+06
1.761E+02	4.317E+02	7.746E+02	2.065E+03	2.651E+05	6.500E+05	1.166E+06	3.109E+06
2.392E+02	6.002E+02	1.143E+03	3.217E+03	3.566E+05	8.949E+05	1.704E+06	4.796E+06
4.398E+02	9.557E+02	1.558E+03	4.587E+03	7.130E+05	1.549E+06	2.526E+06	7.437E+06
5.618E+02	1.279E+03	2.059E+03	5.703E+03	8.211E+05	1.870E+06	3.009E+06	8.335E+06
3.634E+02	8.639E+02	1.409E+03	3.835E+03	5.587E+05	1.328E+06	2.166E+06	5.896E+06
3.952E+02	5.806E+02	8.245E+02	2.482E+03	6.150E+05	9.036E+05	1.283E+06	3.863E+06
6.024E+02	1.318E+03	2.148E+03	6.407E+03	9.146E+05	2.001E+06	3.261E+06	9.727E+06
3.794E+02	9.442E+02	1.816E+03	6.935E+03	6.161E+05	1.533E+06	2.949E+06	1.126E+07

qpred-cl(g/s)... qpred-clid(g/s)... for each LOS

3.204E+01	5.376E+01	2.888E+01	5.907E+02	3.098E+01	5.196E+01	2.793E+01	5.711E+02
1.575E+01	3.101E+01	2.122E+01	4.605E+02	1.476E+01	2.905E+01	1.989E+01	4.316E+02
1.302E+01	2.629E+01	1.822E+01	3.874E+02	1.335E+01	2.694E+01	1.868E+01	3.971E+02
2.831E+01	4.820E+01	2.613E+01	4.665E+02	2.582E+01	4.395E+01	2.383E+01	4.255E+02
3.734E+00	9.967E+00	8.007E+00	1.851E+02	3.838E+00	1.024E+01	8.232E+00	1.902E+02
1.698E+01	3.393E+01	2.351E+01	5.187E+02	1.835E+01	3.666E+01	2.541E+01	5.606E+02
8.262E+00	1.692E+01	1.177E+01	2.068E+02	7.945E+00	1.627E+01	1.132E+01	1.988E+02
1.570E+01	3.088E+01	2.090E+01	4.149E+02	1.441E+01	2.832E+01	1.918E+01	3.907E+02
7.960E+00	1.498E+01	1.028E+01	1.935E+02	7.938E+00	1.493E+01	1.026E+01	1.930E+02
2.800E+01	4.839E+01	2.792E+01	6.176E+02	2.756E+01	4.762E+01	2.748E+01	6.080E+02
7.394E+00	1.665E+01	1.172E+01	1.845E+02	7.003E+00	1.576E+01	1.110E+01	1.747E+02
1.530E+01	2.842E+01	1.817E+01	3.566E+02	1.535E+01	2.852E+01	1.824E+01	3.579E+02
2.013E+01	3.594E+01	2.253E+01	5.234E+02	2.005E+01	3.580E+01	2.244E+01	5.214E+02
2.709E+01	4.727E+01	2.792E+01	6.143E+02	2.726E+01	4.755E+01	2.809E+01	6.181E+02
1.437E+01	2.896E+01	1.998E+01	4.202E+02	1.330E+01	2.679E+01	1.848E+01	3.888E+02
7.301E+00	1.404E+01	9.810E+00	2.193E+02	7.492E+00	1.440E+01	1.007E+01	2.251E+02
8.406E+00	1.548E+01	1.068E+01	2.429E+02	8.201E+00	1.510E+01	1.042E+01	2.370E+02
3.104E+00	9.251E+00	7.327E+00	1.507E+02	2.992E+00	8.914E+00	7.063E+00	1.453E+02
1.412E+01	2.825E+01	1.949E+01	4.048E+02	1.395E+01	2.790E+01	1.926E+01	3.999E+02
2.125E+01	3.739E+01	2.186E+01	3.546E+02	1.963E+01	3.453E+01	2.020E+01	3.276E+02

Following are min., max., mean, sigma and sigma/mean in all simulations:

	u	wd	dT	siqd	siqp	z0	SRSF	SDSF	SSSF	SLSF
min.	3.661E+00	1.842E+01	-8.775E-01	1.022E+01	5.725E+00	7.398E-02	3.612E-01	9.252E-01	3.342E-01	-2.308E+01
max.	5.242E+00	3.400E+01	-4.819E-01	1.203E+01	1.028E+01	6.029E-01	3.100E+00	1.096E+00	3.131E+00	2.313E+01
mean	4.453E+00	2.516E+01	-6.613E-01	1.121E+01	7.693E+00	3.696E-01	1.800E+00	1.024E+00	1.678E+00	1.979E+00
sigma	4.657E-01	3.935E+00	1.126E-01	5.782E-01	1.498E+00	1.584E-01	8.531E-01	4.447E-02	8.308E-01	1.357E+01
sig/mean	1.046E-01	1.564E-01	-1.702E-01	5.160E-02	1.947E-01	4.284E-01	4.739E-01	4.343E-02	4.951E-01	6.858E+00

	L	PG	ustar	wpl
min.	-3.015E+02		3.972E-01	2.355E-01
max.	-3.083E+01		7.236E-01	7.344E-01
mean	-1.383E+02		5.733E-01	5.087E-01
sigma	6.918E+01		8.532E-02	1.448E-01
sig/mean	-5.001E-01		1.488E-01	2.846E-01

Following are min., max., mean, sigma and sigma/mean in all simulations:

cl(mg/m**2)... clid(mg-s/m**2)... for each LOS

min.	3.500E+01	9.000E+01	1.867E+02	6.477E+02	5.756E+04	1.480E+05	3.070E+05	1.065E+06
max.	1.587E+03	2.603E+03	3.645E+03	9.767E+03	2.316E+06	3.799E+06	5.318E+06	1.531E+07
mean	4.349E+02	9.163E+02	1.504E+03	4.644E+03	6.654E+05	1.404E+06	2.308E+06	7.148E+06
sigma	3.298E+02	5.688E+02	8.280E+02	2.667E+03	4.890E+05	8.523E+05	1.253E+06	4.119E+06
sig/mean	7.582E-01	6.208E-01	5.506E-01	5.743E-01	7.349E-01	6.069E-01	5.427E-01	5.762E-01

qpred-cl(g/s)... qpred-clid(g/s)... for each LOS

min.	3.104E+00	9.251E+00	7.327E+00	1.507E+02	2.992E+00	8.914E+00	7.063E+00	1.453E+02
max.	3.204E+01	5.376E+01	2.888E+01	6.176E+02	3.098E+01	5.196E+01	2.809E+01	6.181E+02
mean	1.541E+01	2.880E+01	1.832E+01	3.757E+02	1.501E+01	2.806E+01	1.788E+01	3.676E+02
sigma	8.303E+00	1.324E+01	6.864E+00	1.503E+02	8.003E+00	1.278E+01	5.703E+00	1.498E+02
sig/mean	5.388E-01	4.596E-01	3.748E-01	4.002E-01	5.332E-01	4.555E-01	3.749E-01	4.076E-01

Figure 9-11 An example of the mandatory output file generated by the DDAMC software package summarizing the results of the Monte Carlo sensitivity analysis for the trial AT5 of the Atterbury-87 dataset. Note that the GPM dispersion formula was used, default ranges of uncertainties (see text) were used, and only 20 simulations were carried out. (Concluded)

parameters (L, u_s, PG, WPL) for each Monte Carlo simulation. This detailed output is useful in 1) verifying that the random sampling from the uniform distributions was performed correctly, and 2) investigating the dependence of the secondary input parameters on the primary input parameters. For each arc, values of the centerline concentration (denoted as "conc" in the file), cross-wind integrated concentration ("conc-y"), plume width ("sigy"), predicted emission rate based on centerline concentration ("qpred-conc"), and predicted emission rate based on cross-wind integrated concentration ("qpred-conc-y") can be listed for each Monte Carlo simulation. In addition, for each LOS, values the LOS-integrated concentration ("cl"), LOS-integrated dosage ("clid"), predicted *total* (explained later) emission rate based on LOS-integrated concentration ("qpred-cl") and predicted *total* emission rate based on LOS-integrated dosage ("qpred-clid") can also be listed in the file for each Monte Carlo simulation. Note that as mentioned in Section IV, only single sources are allowed if concentric arcs are employed, and both single and multiple sources are allowed if LOS's are employed. This is the reason why the word *total* was used for all the LOS-related emission rate predictions, since if there is more than one source, then the emission rate predictions would refer the combined values from all sources.

The last part of the mandatory output contains the summary for the Monte Carlo sensitivity analyses. It includes the minimums, maximums, means, standard deviations, and the ratios of the standard deviation to the mean for all the primary input parameters, some secondary parameters, and all predicted concentrations and emission rates based on all the simulations. The user can use this information to analyze the relationship of input data errors to dispersion formula uncertainty.

Format of the Optional ASCII Output File Generated by DDAMC (Monte Carlo Mode)

As an option, the DDAMC software package also generates an ASCII output file (see Figure 9-12 for an example) containing the probability density functions for the concentration and source predictions by a dispersion formula as a result of the Monte Carlo simulations. This file can be easily plotted (see Figure 9-13 for an example) using the SIGPLOT plotting package (see Appendix E), and the format of the file is described in Table E-2.

```
transect  1
ci (mg/m**2)
pdf (percent)
          31 1
    27.9125        0.250000
    79.8920         8.50000
    131.871         10.0000
    183.850         10.5000
    235.829         11.2500
    287.808         12.0000
    339.788         6.50000
    391.767         6.75000
    443.746         4.00000
    495.725         4.25000
    547.704         3.50000
    599.683         3.50000
    651.662         2.25000
    703.641         1.50000
    755.621        0.500000
    807.600         1.25000
    859.579         1.75000
    911.558         1.25000
    963.537         1.00000
    1015.52         1.25000
    1067.50         1.25000
    1119.47        0.750000
    1171.45         1.25000
    1223.43         1.50000
    1275.41        0.250000
    1327.39        0.250000
    1379.37        0.750000
    1431.35        0.750000
    1483.33        0.500000
    1535.31        0.000000
    1587.30         1.00000
transect  1
clid (mg-s/m**2)
pdf (percent)
          31 1
    38752.0        0.250000
    121703.         8.50000
    204654.         11.2500
    287604.         11.7500
    370555.         12.0000
    453506.         11.5000
    536457.         7.00000
    619407.         5.25000
    702358.         5.25000
    785309.         3.75000
    868259.         3.00000
    951210.         2.75000
  0.103416E+07      1.75000
  0.111711E+07      1.00000
  0.120006E+07      1.50000
  0.128301E+07      1.50000
  0.136596E+07      1.75000
  0.144891E+07      1.00000
  0.153186E+07     0.750000
  0.161482E+07      1.50000
  0.169777E+07      1.75000
  0.178072E+07     0.250000
  0.186367E+07      1.00000
  0.194662E+07      1.25000
  0.202957E+07      1.00000
  0.211252E+07     0.000000
  0.219547E+07     0.750000
  0.227842E+07     0.250000
  0.236137E+07     0.500000
  0.244432E+07     0.000000
  0.252730E+07     0.250000
```

Figure 9-12. An example of the optional output file (partial listing only) generated by the DDAMC software package (Monte Carlo mode) containing the probability density functions (pdf) of the LOS-integrated concentrations and dosages for the first LOS predicted by the GPM dispersion formula as a result of the Monte Carlo sensitivity analysis for the trial AT5 of the Atterbury-87 dataset. The results were based on the default ranges of uncertainties (see text) and 400 simulations.

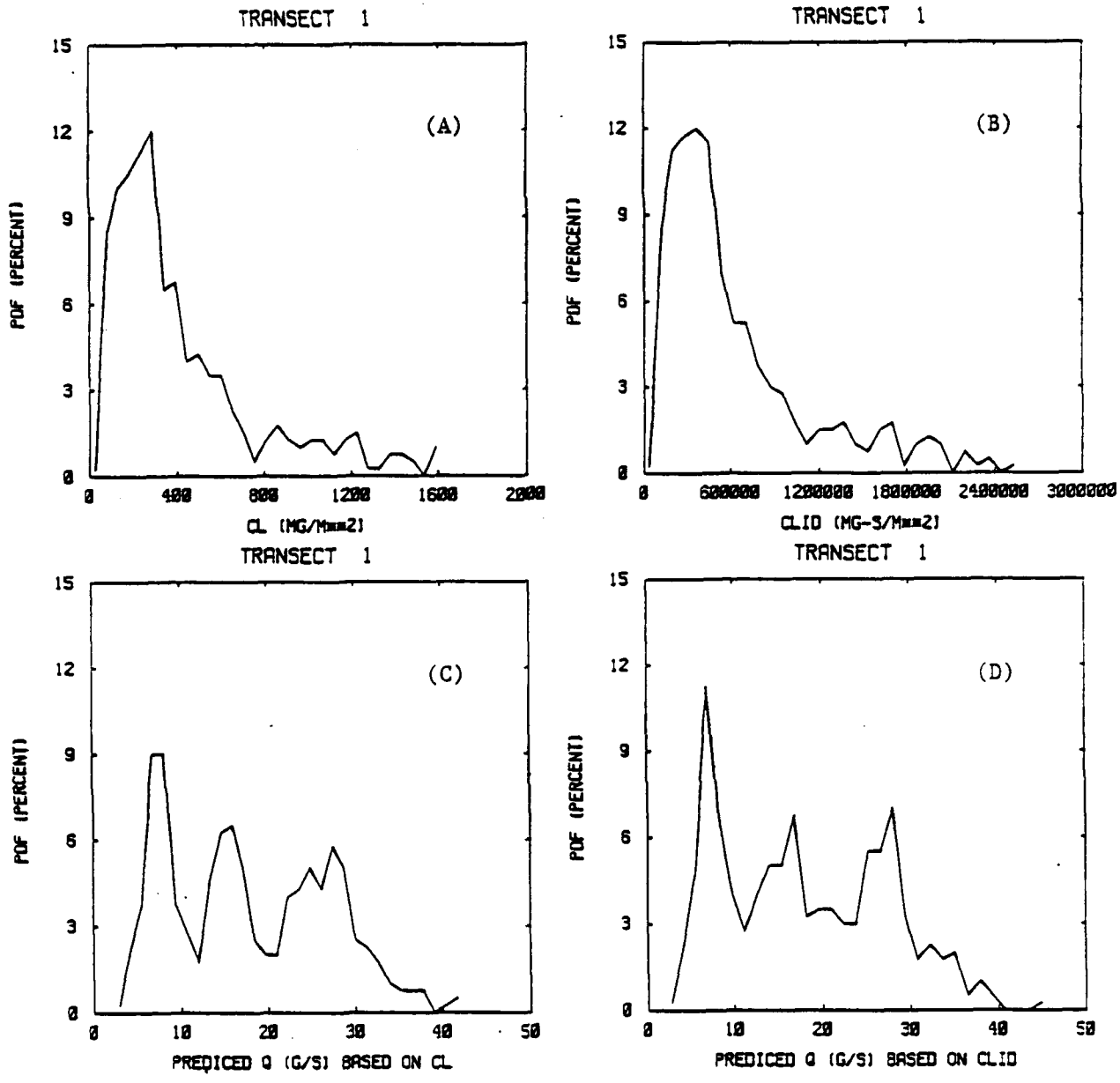

Figure 9-13. A display of the information listed in Figure 9-7 using the SIGPLOT plotting package, (A) the pdf of the LOS-integrated concentrations (CL, mg/m^2), (B) the pdf of the LOS-integrated dosages (CLID, $mg*s/m^2$), (C) the pdf of the emission rate (g/s) based on CL, (D), the pdf of the emission rate (g/s) based on CLID.

Intentionally Blank

SECTION X

EXAMPLES OF APPLICATION OF METEOROLOGICAL ASSESSMENT SOFTWARE

A primary objective of this research is the development of methods for estimating whether there is a significant difference in the source emission rate or the obscuring capability of similar types of munitions from one experiment to another, as determined by observations of point concentration or cross-wind integrated concentrations.

The meteorological assessment software is designed to "remove" the influences of meteorological factors from the concentration observations. It uses regression formulas, scaling laws, and dispersion models to remove the effects of variations in meteorological parameters and downwind position of the concentration monitor. For example, it is expected that the observed concentration due to ground-level releases will be inversely related to the wind speed, for all other conditions the same. The resulting normalized concentrations or emission estimates for one set of trials can then be compared to those for another set of trials to determine if there is a significant difference. Although there may be thought to be a difference on the basis of the magnitude of the measured concentrations alone, differences in the dispersive action of the atmosphere might fully account for the perceived differences. In this section, we demonstrate the use of this software by identifying groups of field data that might be compared in this way, and by carrying out the procedure.

The database constructed during the project contains several types of sources, scenarios, and concentration measurements. The so-called "historical datasets" (Prairie Grass, Ocean Breeze, Dry Gulch, and Green Glow) are characterized by known source strengths, and by concentration dosages measured at fixed locations along arcs at several distances from the point of release. Because the release duration was long compared to the time of travel to the monitoring arcs, mean concentrations determined from the dosages are typically analyzed and the largest is reported at each arc. In addition, other researchers have reported estimates of the crosswind integrated concentration along each arc for the Prairie Grass experiments. The so-called "smoke" datasets are derived from measurements of smoke-plumes

and are characterized by less precise information about the source strengths. Furthermore, concentrations or dosages obtained from transmissometer data are obtained along one or more lines-of-sight through the cloud. Many of the smoke datasets have been previously analyzed to assess differences in emissions.

Datasets chosen to illustrate the procedure reflect these differences. In the sections that follow, we describe the application of the software to one "historical" dataset, and one "smoke" dataset. Procedures for avoiding selection of non-independent datasets are discussed. Results for all of the datasets contained in the database are summarized at the end of this section.

A. Example Application to One Historical Dataset (Prairie Grass)

Characteristics: The source strength is well known, and there are at least two distinctly different source groups in the dataset.

For the Prairie Grass experiments, the source strength is well-known for all trials. Furthermore, the emission rates used during the daytime trials are greater than the emission rates used during the nighttime trials by roughly a factor two. There are, therefore, two natural source groups whose average source strength differs so that the Prairie Grass dataset provides an opportunity to test the ability of the system to discern differences in source emissions. The assessment software is used to estimate the source strengths by removing meteorological influences from the measured concentrations, and these source strengths are then evaluated to determine if they are indeed significantly different (as they should be). This exercise is more fully described in Appendix A and has been published in the journal Atmospheric Environment by Hanna et al. (1990). The statistical evaluation is framed by the following question -

> Question: Can the null hypothesis that there is no difference between the average source strength inferred from concentration measurements for the daytime group and the average source strength inferred from concentration measurements for the nighttime group be rejected with 95% confidence?

During the Prairie Grass experiment the nighttime emissions, Q, of tracer gas were controlled so that Q averaged 45.6 g/s with a range from

about 38 to 58 g/s and a standard deviation of 6.57 g/s, and the daytime emissions were controlled so that Q averaged 98.4 g/s with a range from about 90 to 104 g/s and a standard deviation of 4.45 g/s. The observed source emissions, Q, are plotted in Figure 10-1 as a function of the stability parameter 1/L (the point for run 46 has been excluded, since it was an evening transition period when Q was still high although 1/L had just become positive). The experimentalists deliberately maintained this factor of 2 difference in day-night Q's so that the magnitude of concentrations at the monitors would not vary so much from day to night. With 22 stable runs and 21 unstable runs, the calculated student-t parameter (see equation 10-3) is 30.04 for the difference between the mean nighttime and daytime emission rates, which implies that the difference is significant at far greater than the 95% confidence level (for which t = 2.04).

These emission rate statistics can be generated by the Meteorological Assessment Software, when applied to the binary data base file for the Prairie Grass trials. Option 3 can be used to obtain a listing of the observed emission rates for each trial, and Option 5 can be selected to obtain the means, standard deviations, and the Student-t test parameters. The series of answers to questions within the program that are associated with options 3 and 5 are discussed in Section IX. For the Prairie Grass application, the daytime and nighttime trials are contained in separate DDA's.

Scaling formulas are used to predict emission rates by expressing them in the following manner:

$$Q_p = C_o/(C/Q)_p \qquad (10\text{-}1)$$

$$\text{or} \quad Q_p = C_o^y/(C^y/Q)_p \qquad (10\text{-}2)$$

where C_o is the observed maximum concentration and C_o^y is the observed cross-wind integrated concentration at any downwind distance, and Q_p is the estimated source emission rate. The null hypothesis istested using the following formulas to compensate for differences in meteorology and receptor distances among the trials:

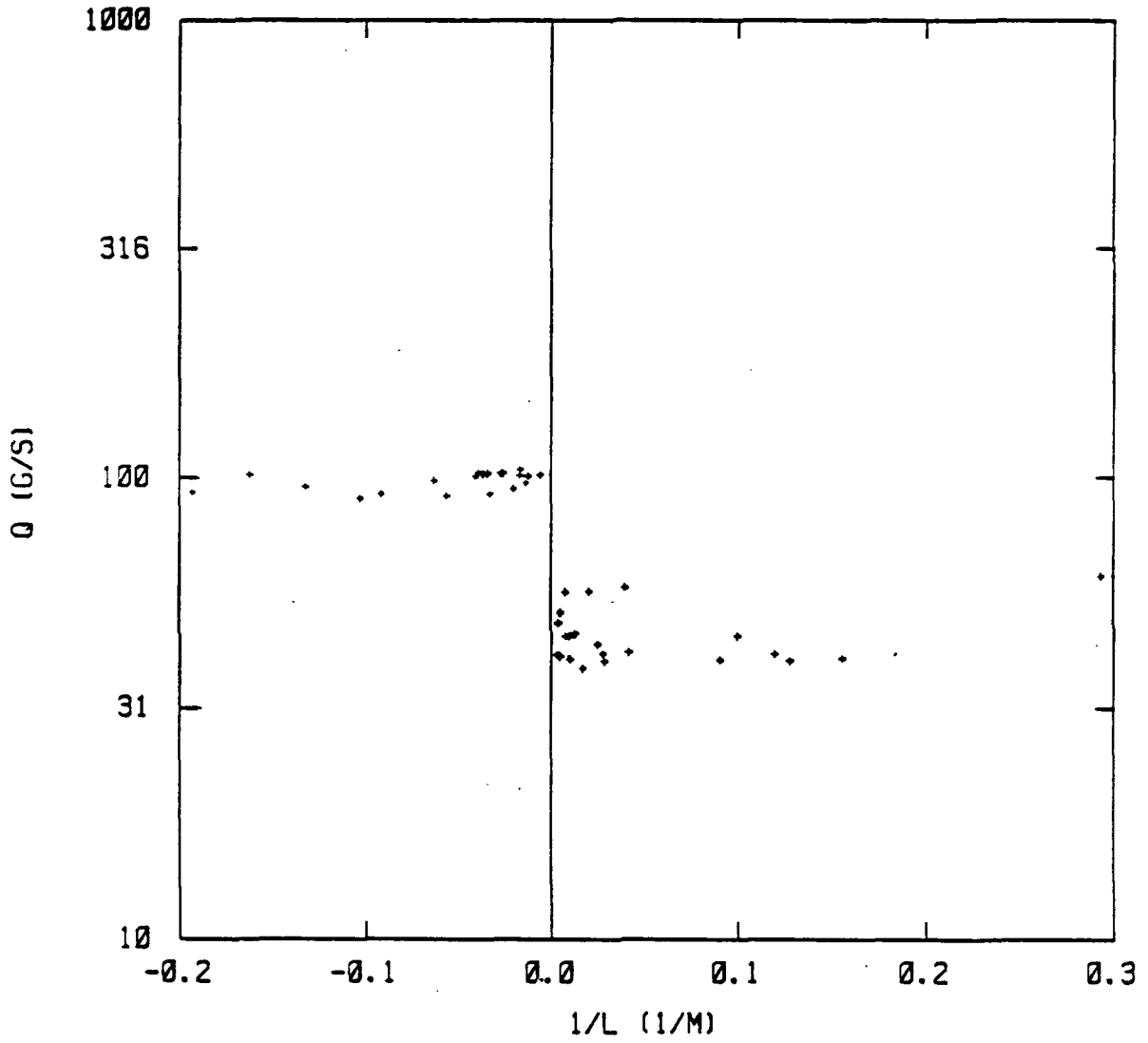

Figure 10-1. Observed tracer gas source emission rates, Q, as a function of inverse Monin-Obukhov length, 1/L, for the Prairie Grass data (Run 46 excluded).

Scaling Procedures for C : OB/DG, REGRESSION-C, SIMILARITY-C, GPM, VSDM
Scaling Procedures for C^y: REGRESSION-C^y, SIMILARITY-C^y, Nieuwstadt/Venkatram, Briggs, GPM, and VSDM

The observed C_o values are available from monitoring arcs at downwind distances of 50, 100, 200, 400, and 800 m, and the observed C_o^y values are available (for all stability classes) from monitoring arcs at downwind distances of 50, 200, and 800 m. Source emission rate predictions, Q_p, are made for each downwind distance, for each scaling model listed above, using both C_o and C_o^y where appropriate. Option 5 of the Meteorological Assessment Software is used to summarize the predicted emission rates for each group (day, night), and to calculate the Student-t parameter for assessing the null hypothesis. These results are summarized in Tables 10-1 and 10-2. The value of Student-t is calculated from the formula (Panofsky and Brier, 1968, p 63):

$$t = \left(\bar{Q}_{pd} - \bar{Q}_{pn} \right) \Big/ \left(\frac{N_d \sigma_{Q_{pd}}^2 + N_n \sigma_{Q_{pn}}^2}{N_d + N_n - 2} \left(\frac{1}{N_d} + \frac{1}{N_n} \right) \right)^{1/2} \qquad (10\text{-}3)$$

where subscripts d and n indicate day and night. If $|t|$ is less than 2.04 for datasets of this size, then the difference $(\bar{Q}_{pd} - \bar{Q}_{pn})$ is not significantly different from zero, at the 95% confidence level.

The selection of monitoring arcs for analysis must be considered from the viewpoint of data independence. In equation (10-3) it is assumed that all points in the set of size N_d or the set of size N_n are <u>independent</u>. This condition is satisfied if data from a <u>single</u> monitoring arc from each experiment are considered, but is not satisfied if data from two or more monitoring arcs are included. It is preferable to use the data only from the <u>closest</u> monitoring arc (50 m in this case) in the statistical analysis, since the procedures are the most accurate at close distances.

The software produces a student-t value for comparing emission rates estimated from concentrations observed at each arc-distance. This includes a comparison of the emission rate obtained for the 800 m arc of the day-group with that obtained for the 50 m arc of the night-group. However, because all

Table 10-1

Predictions of Source Emission Rate, Q_p(g/s), for Nighttime and Daytime Prairie Grass Runs, using Observed Maximum Concentrations, C_o, on Monitoring Arcs at Distances of 50, 100, 200, 400, and 800 m, as well as the Average Q_p over All Monitoring Arcs. Five Different Scaling Procedures are Used to Calculate $Q_p = C_o/(C/Q)_p$. The Average, $\bar{Q}_p$, and Standard Deviation, σ_{Qp}, for Nighttime and Daytime Conditions is Listed. Student-t is calculated using Equation (10-3).

Model	Monitoring Distance (m)	Student t	Night (N=19) $\bar{Q}_p$ (g/s)	Night (N=19) σ_{Qp} (g/s)	Day (N=20) $\bar{Q}_p$ (g/s)	Day (N=20) σ_{Qp} (g/s)
Observed Q		30.86	45.2	5.9	98.2	4.5
OB/DG	50	7.23	25.0	10.2	131.6	61.8
	100	5.49	40.0	17.9	139.7	75.1
	200	4.38	52.3	23.1	142.1	84.0
	400	2.54	67.7	30.1	113.9	71.5
	800	-0.74	102.3	61.7	86.6	67.8
	All*	3.80	57.5	27.1	122.8	68.1
REGRESSION-C (Regression)	50	7.40	30.1	12.0	144.6	64.7
	100	5.47	43.8	19.4	139.1	71.6
	200	4.27	52.0	23.0	128.3	72.5
	400	2.20	61.2	27.3	93.4	56.2
	800	-1.19	84.2	51.6	64.5	48.9
	All*	3.96	54.3	25.1	114.0	59.2
SIMILARITY-C (Similarity)	50	5.68	39.9	14.1	70.8	18.5
	100	4.62	49.2	16.2	84.0	27.9
	200	5.51	48.7	16.2	101.1	37.1
	400	5.52	45.8	15.6	105.4	43.2
	800	4.80	46.3	14.6	116.2	60.1
	All*	5.56	46.0	14.3	95.5	35.1
GPM	50	2.40	55.2	45.5	115.5	96.9
	100	1.07	76.3	94.9	109.2	92.2
	200	0.05	98.1	150.9	100.2	70.1
	400	-0.88	118.8	196.3	76.8	62.7
	800	-1.67	150.1	264.1	48.0	30.1
	All*	-0.26	99.7	149.9	90.0	67.4
VSDM	50	6.40	21.3	3.8	56.6	23.1
	100	8.16	25.9	6.9	53.7	12.8
	200	6.50	29.2	10.5	52.8	11.6
	400	2.07	33.1	15.3	42.6	12.7
	800	-1.53	41.3	20.6	32.1	15.8
	All*	5.26	30.1	10.8	47.6	9.3

*The results given for "All" arcs are not strictly correct, because the observations on arcs during the same experiment are not independent.

Table 10-2

Predictions of Source Emission Rate, Q_p(g/s), for Nighttime and Daytime Prairie Grass Runs, using Observed Cross-Wind Integrated Concentrations, C_o^y, on Monitoring Arcs at Distances of 50, 200, and 800 m, as well as the Average Q_p over All Monitoring Arcs. Six Different Scaling Procedures are Used to Calculate $Q_p = C_o^y/(C/Q)_p$. The Average, $\bar{Q}_p$, and Standard Deviation, σ_{Qp}, for Nighttime and Daytime Conditions Listed. Student-t is calculated using Equation (10-3).

Model	Monitoring Distance (m)	Student t	Night (N=19) $\bar{Q}_p$ (g/s)	Night (N=19) σ_{Qp} (g/s)	Day (N=15) $\bar{Q}_p$ (g/s)	Day (N=15) σ_{Qp} (g/s)
Observed Q		27.27	45.2	5.9	97.8	4.7
REGRESSION-C^y (Regression)	50	17.19	29.7	9.8	140.1	24.8
	200	7.43	46.9	16.9	124.8	40.1
	800	-0.58	69.4	34.3	62.1	36.4
	All*	7.13	48.7	18.7	109.0	28.9
SIMILARITY-C^y (Similarity)	50	16.24	39.7	8.3	89.6	9.0
	200	9.54	49.0	9.0	100.1	20.3
	800	4.38	45.2	13.8	99.6	50.2
	All*	9.09	44.6	9.8	96.4	21.4
Nieuwstadt/ Venkatram	50	11.85	39.6	9.1	87.4	13.6
	200	4.51	46.7	10.1	119.5	67.2
	800	4.43	53.7	31.6	189.3	124.5
	All*	5.71	46.7	14.8	132.0	60.9
Briggs	50	18.64	43.8	8.8	106.7	10.3
	200	11.35	58.8	11.1	133.2	24.7
	800	4.13	66.2	28.1	160.7	91.5
	All*	8.25	56.3	14.6	133.5	36.0
GPM	50	6.18	61.7	30.9	161.0	58.4
	200	2.83	65.5	60.3	116.6	34.9
	800	-0.99	85.5	145.1	46.9	20.3
	All*	1.70	70.9	77.9	108.2	30.4
VSDM	50	12.73	51.4	9.3	138.3	26.9
	200	7.17	49.7	11.7	115.9	36.8
	800	0.51	55.9	27.9	62.1	40.5
	All*	6.72	52.3	14.8	105.5	29.0

*The results given for "All" arcs are not strictly correct, because the observations on arcs during the same experiment are not independent.

of the trials made use of the same grid of receptors and the same point of releases, we need only consider comparisons made for the same arc-distance (results for the 50 m arc for the day-group are compared with results for the 50 m arc for the night-group). The results are also given for "all arcs," but there are clearly problems with data independence in that analysis and those conclusions are probably not correct. These are the results reported in Tables 10-1 and 10-2.

The ability of the scaling procedure to arrive at the proper answer (i.e., that the daytime $\bar{Q}$ is significantly larger than the nighttime $\bar{Q}$, with at least 95% confidence) can be seen by identifying cases where $t \geq 2.04$ in Tables 10-1 and 10-2. It is seen that most scaling formulas are able to reproduce this conclusion at most arc distances. However, false conclusions ($t < 2.04$) are reached for the following arcs and scaling formulas:

C_o:	100 m arc:	GPM
	200 m arc:	GPM
	400 m arc:	GPM
	800 m arc:	OB/DG, REGRESSION-C, GPM, and VSDM
C_o^y:	800 m arc:	REGRESSION-C^y, GPM, and VSDM

It is seen that the use of C_o or C_o^y from the closest arc (50 m) leads to no false conclusions, with a median value for Student-t of about 7 for C_o and 16 for C_o^y. Furthermore, since t is larger for the cross-wind integrated observations, it is evident that those data are better able to discern differences in Q than the point concentration data. However, the number of false conclusions increases rapidly as downwind distance increases. At the 800 m arc, only the SIMILARITY-C scaling procedure yields the proper conclusion for the C_o data, and only the three similarity scaling procedures (SIMILARITY-C^y, Nieuwstadt/Venkatram, and Briggs) yield the proper conclusion for the C_o^y data.

Figures 10-2 and 10-3 are given as examples of mediocre and good estimates of Q_p. In both figures, Q_p is plotted as a function of the stability parameter, 1/L. There is seen to be much scatter in Figure 10-1,

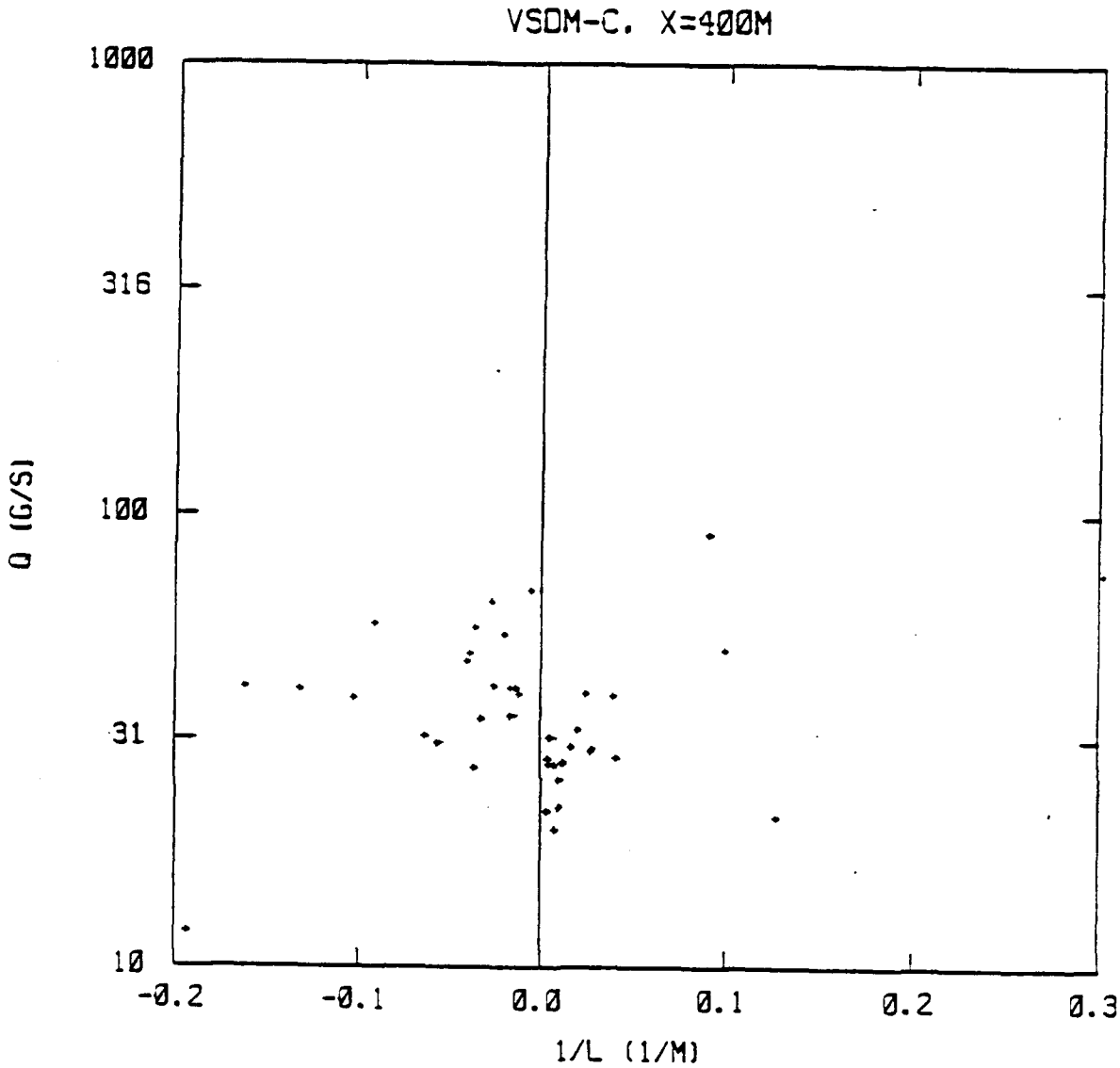

Figure 10-2. Tracer gas source emission rates, Q_p, calculated by the VSDM model using C_o observations on the 400 m arc at Prairie Grass, plotted as a function of inverse Monin-Obukhov length, 1/L.

which employs the VSDM model and observed concentrations on the 400 m arc. In contrast, relatively good predictions of Q_p are seen in Figure 10-3 by the SIMILARITY-C^y model, using C_o^y observations on the 50 m arc. The relative positions of the clouds of points for $1/L < 0$ and $1/L > 0$ are similar in Figures 10-1 and 10-3. The $\bar{Q}_p$ predictions of SIMILARITY-C^y are 39.7 g/s for nighttime conditions (the observed $\bar{Q}$ was 45.2 g/s) and 89.6 g/s for daytime conditions (the observed $\bar{Q}$ was 97.8 g/s). The value of Student-t is 16.2, which greatly exceeds the value of 2.04 that indicates significant difference at the 95% confidence level, but is still less than the observed value of 30.9. Consequently, the proper conclusion is reached regarding the day-night difference in Q.

Table 10-2 shows that the predicted standard deviation, σ_{Qp}, exceeds the observed value, σ_{Qo}, by about 50% to a factor of 2. The ratio $\sigma_{Qp}/\bar{Q}_p$ (i.e., the uncertainty in the source term estimation) is seen to equal about 0.1 to 0.2 for these data, suggesting that this procedure may not be able to discern differences in source emission rates of about $\pm$ 20% or less.

B. Example Application to One Smoke Dataset

Characteristics: The source strength is not precisely known, and there are two or more source groups made up of the same type of munition.

During the Comparison Test of L8A1 Screening Smoke Grenades (Rafferty and Dumbauld, 1983), single grenades, taken from one of four grenade lots (A, B, C, or D), were fired in 24 trials. Although only a single type of grenade was used, differences between lots might foster differences in burn time and mass yield fraction, which would have an effect on screening effectiveness. The observed effectiveness also depends on the range from the impact point to the LOS used by the transmissometer, the impact pattern dimensions, and meteorological conditions. The meteorological assessment software is used to estimate the source strength of each grenade on the basis of the concentrations obtained from transmissometer measurements, and the significance of differences in source strength among the four lots is quantified. The statistical analysis is framed by the following question -

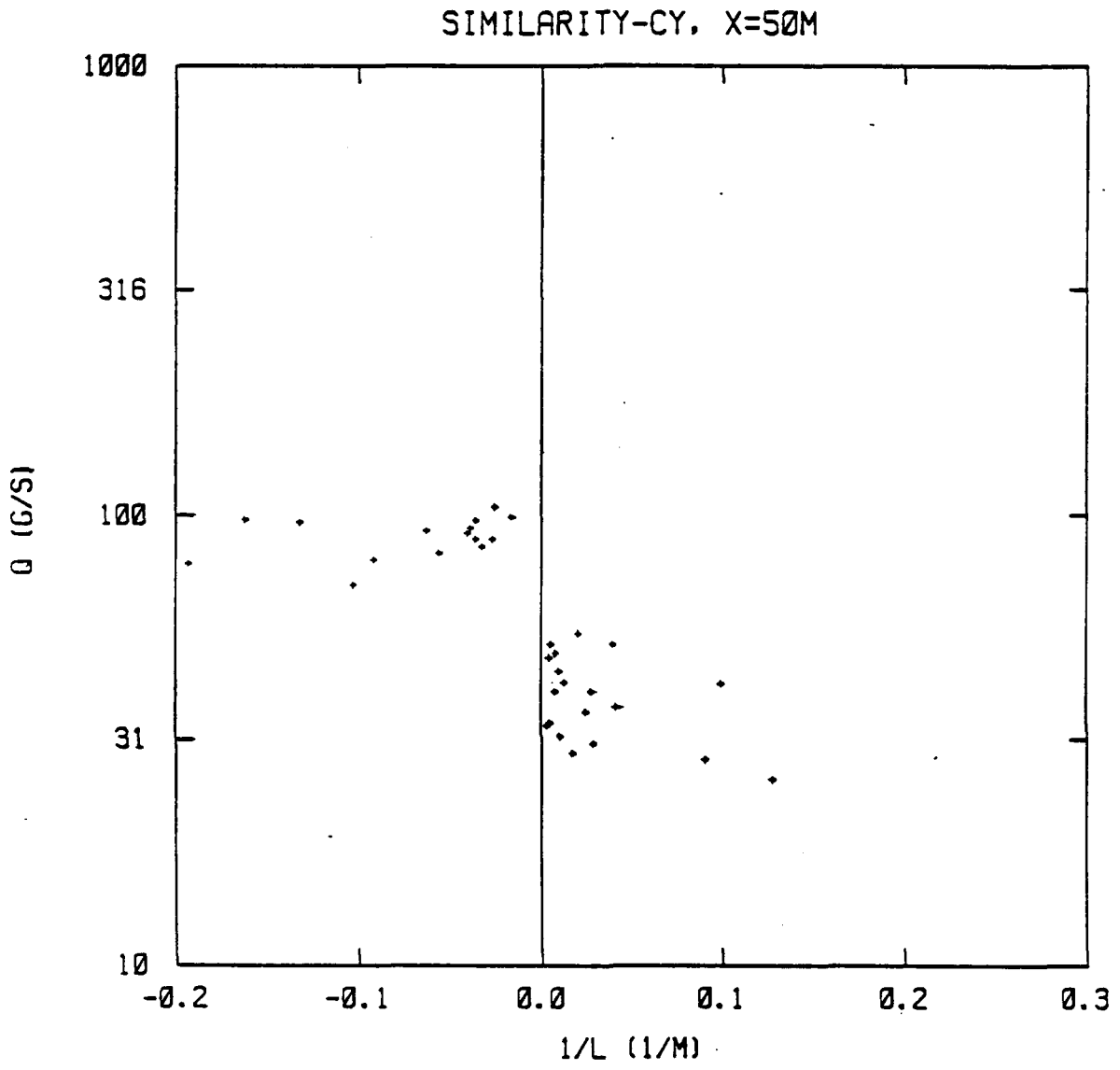

Figure 10-3. Tracer gas source emission rates, Q_p, calculated by the SIMILARITY-C^y model using $C_o{}^y$ observations on the 50 m arc at Prairie Grass, plotted as a function of inverse Monin-Obukhov length, 1/L.

Question: Can the null hypothesis that there is no difference among the average source strengths inferred from transmissometer measurements for the four lots be rejected with 95% confidence?

Rafferty and Dumbauld (1983) had analyzed data from this test, and had identified a subset of the data as suitable for estimating the emission strength of the munitions. They do not use either line-of-sight (LOS) 2N or 2S, because these usually pass through the source region. Furthermore, they make use of LOS 1N or LOS 1S only when the smoke-cloud is considered to be contained within the LOS more than 85% of the time. We use only those data selected by Rafferty and Dumbauld (1983).

The data for this test are organized within the DDA's named L81A1, L81B1, L81C1, L81D1, and L8112. The first four are single grenade tests using lots A, B, C, and D respectively. The last contains the six trials in which salvos of 12 grenades were fired. Option 5 of the software package is used once again to perform the analyses needed to evaluate the null hypothesis. The sample application described in Section IX actually makes use of these DDA's, and so may be followed to "work through" the details reported below.

The first issue addressed is the effect of burn time, yield fraction, and mass fill weight on the strength of the emission. This can be assessed by characterizing differences among lots in both the mean emission rate (Q), and the total mass released (M), as computed from the fill weight, burn time, relative humidity and yield factor for each trial. The results are listed in Table 10-3. The average mass of smoke expected from grenades in each lot is nearly the same, but differences in burn times between lots produce mean emission rates that can differ by a factor of two. Significance tests (Student-t) indicate that the null hypothesis that there are no differences among the calculated values of M for the four lots cannot be rejected with 95% confidence. In fact, there is a 30% to 99% chance that the differences would result from chance. This is not the case for the values of Q. The null hypothesis that there are no differences among the calculated values of Q can be rejected with at least 98% confidence. The implication of this is that the potential screening effectiveness of the smoke produced by grenades

Table 10-3

Emission Rates (Q) and Total Mass Released (M)
for Lots A, B, C, and D of the L8A1 RP Grenade.
These Calculations are Based on Fill Weights, Burn
Time, Yield Factors, and Relative Humidities

	Average Q (g/s)	σ_Q	Average M (kg)	σ_M
Lot A	3.42	0.08	0.859	0.020
Lot B	4.22	0.20	0.840	0.040
Lot C	6.66	0.33	0.840	0.041
Lot D	7.34	0.32	0.844	0.037

in the four different lots is significantly different, because the mass of smoke produced per unit volume is proportional to Q.

These conclusions are based upon average properties of the L8A1 grenade, not on direct measurements of Q. We must look to predicted values of Q that are based on the transmissometer measurements to demonstrate these differences in Q, if they really exist. We have done this for two scaling procedures, VSDM and the Gaussian Plume Model (GPM), and the results are listed in Table 10-4.

Here, we have calculated means and standard deviations of the predicted values of emission rate using CLID observations divided by burn time over the trials performed for each lot. But note that no more than one value is included from each trial. As discussed in Section A, data obtained from more than one line-of-sight during a single trial should <u>not</u> be considered independent. For example, a total of six trials were performed with grenades from lot C, and concentration data from each of these trials were obtained at two lines-of-sight. But even though a total of twelve concentrations were obtained, and twelve values of emission rate were predicted from these, we only have six independent values, one for each trial. When comparing mean emission rates between different lots, the significance of differences between means must include a proper estimate of the number of degrees of freedom, and this is properly specified when all values used in the means are independent.

In Table 10-4, we assure that no more than one predicted value of the emission rate per trials is included in an average for each lot by including data from only one of the two lines-of-sight in an average. Hence, means and standard deviations are reported for LOS 1N and LOS 1S for each of the four lots. Other ways of selecting one value per trial may be used as well, by setting a different order for entering the concentrations in the DDA file. For example, we could have placed the larger concentrations first, thereby grouping together emission rates predicted from the largest concentrations measured during each trial. Or we could have determined the order by the distance of the LOS from the source region (an individual LOS is fixed, but the source locations vary from trial to trial). In any application of this procedure, an analyst must determine the appropriate way to select one "observation" from each trial in a test.

Table 10-4

Predicted Emission Rates (Q, in g/s) Derived from Crosswind Integrated Dosages (CLID) Measured by Transmissometer for Lots A, B, C, and D of the L8A1 Grenade

Lot	LOS	Expected Q (from Table 10-3)	Predicted (VSDM) $\overline{Q}$	Predicted (VSDM) σ_Q	Predicted (GPM) $\overline{Q}$	Predicted (GPM) σ_Q	N
A	1N	3.42	2.60	1.31	1.86	0.81	7
	1S	3.42	4.75	4.84	2.63	2.00	4
B	1N	4.22	6.19	5.36	3.02	1.85	6
	1S	4.22	6.57	1.54	3.08	0.62	4
C	1N	6.66	9.35	8.07	4.57	2.96	6
	1S	6.66	11.20	5.59	5.24	1.91	6
D	1N	7.34	3.56	2.25	2.00	1.27	4
	1S	7.34	7.75	4.25	4.10	2.43	2

Note: N denotes the number of trials used in each average.

Although neither scaling procedure produces predicted emission rates for each LOS that are equal to those expected, we do see that the increase in emission rates from lots A to B to C is suggested by the scaling procedures. The expected increase in rate for lot D is not apparent in the predicted emission rates, however. We should now ask if the differences in emission rate between the four lots are significant. To answer this question in the form of the null hypothesis posed at the start of this section, we compute the Student-t value for each LOS and each scaling procedure, for each pair of lots (A:B, A:C, A:D, B:C, B:D, and C:D). Table 10-5 lists the results.

As discussed in Section A, the null hypothesis can be rejected with approximately 95% confidence or greater if the Student-t value is greater in absolute magnitude than approximately 2. The actual t-value corresponding to 95% depends on the number of degrees of freedom. For example, we see that the Student-t value for comparing emission rates for Lots A and C, predicted by applying the GPM scaling procedure to CLID values (divided by burn time) measured along LOS 1N, is -2.14. For 11 degrees of freedom (7 + 6 - 2), the probability that (t) could be greater than or equal to 2.14 by chance, for distributions with equal means, is only 5.6%. Therefore, the null hypothesis that there is no difference in the emission rate between lots A and C can be rejected with 94.6% confidence. The other t-values in Table 10-5 suggest that differences in the emission rate are most significant between lots A and C, and lots B and C.

The same analysis has been completed for the total mass released (M). Although the screening effectiveness is proportional to M only when the burn duration is constant, which is not the case here, we may still ask if the measured values of CLID support our expectation that M is constant for these four lots of grenades. The results are listed in Tables 10-6 and 10-7.

Results for M obtained from both scaling procedures appear fairly consistent for lots A, B, and C, but not for Lot D. In Table 10-6, the predicted mass for lot D appears substantially smaller than that for the other lots, especially for the four trials in which data from LOS 1N are available. Therefore, we would like to know if the relatively small differences between the amount of mass burned in lots A, B, and C are

Table 10-5

Student-t Values Calculated for Comparing Mean Emission Rates, Q, for Four Lots of the L8A1 Grenade Predicted from Scaling Measured CLID Values (Divided by Burn Time) by the VSDM and GPM Procedures

	VSDM		GPM	
Lot 1: Lot 2	LOS 1N	LOS 1S	LOS 1N	LOS 1S
A:B	-1.58	-0.62	-1.39	-0.37
A:C	-2.01	-1.68	-2.14	-1.86
A:D	-0.81	-0.61	-0.20	-0.64
B:C	-0.73	-1.44	-0.99	-1.96
B:D	0.83	-0.40	0.87	-0.64
C:D	1.25	0.69	1.47	0.59

Note: LOS 1N denotes emission rates derived from CLID values (divided by burn time) obtained from the transmissometer located at Line-of-Sight 1N for both lots being compared.

Table 10-6

Predicted Total Mass (M, in kg) Released as Derived from Crosswind Integrated Dosages (CLID) Measured by Transmissometer for Lots A, B, C, and D of the L8A1 Grenade

Lot	LOS	Expected M(kg)	Predicted (VSDM) M(kg)	Predicted (VSDM) σ_M(kg)	Predicted (GPM) M(kg)	Predicted (GPM) σ_M(kg)	N
A	1N	0.86	0.65	0.33	0.47	0.20	7
	1S	0.86	1.19	1.22	0.66	0.50	4
B	1N	0.84	1.23	1.07	0.60	0.37	6
	1S	0.84	1.31	0.31	0.61	0.12	4
C	1N	0.84	1.18	1.02	0.58	0.37	6
	1S	0.84	1.41	0.71	0.66	0.24	6
D	1N	0.84	0.41	0.26	0.23	0.15	4
	1S	0.84	0.89	0.49	0.47	0.28	2

Note: N denotes the number of trials used in each average

Table 10-7

Student-t Values Calculated for Comparing Mean Mass Emitted for Four Lots of the L8A1 Grenade, as Predicted from Scaling Measured CLID Values by the VSDM and GPM Procedures

	VSDM		GPM	
Lot 1: Lot 2	LOS 1N	LOS 1S	LOS 1N	LOS 1S
A:B	-1.26	-0.16	-0.77	0.16
A:C	-1.19	-0.32	-0.62	0.01
A:D	1.14	0.27	1.85	0.41
B:C	0.08	-0.25	0.11	-0.32
B:D	1.35	1.04	1.73	0.70
C:D	1.32	0.84	1.58	0.80

Note: LOS 1N denotes the predicted mass released as derived from CLID values obtained from the transmissometer located at Line-of-Sight 1N for both lots being compared.

significant, and if the larger difference between these and lot D is significant.

Table 10-7 lists the Student-t values for comparisons between each of the lots, taken in pairs. Not one of the values suggests that the null hypothesis can be rejected with 95% confidence. That is, we cannot reject the hypothesis that the masses released from grenades in each of the four lots are not different. However, we do see that the differences in predicted masses obtained for LOS 1N appear larger than the differences obtained for LOS 1S. For example, when M is obtained by means of the GPM scaling procedure, t-values of 1.6 and greater are found when lot D is compared to lots A, B, and C. The probability that t-values as large as those listed for LOS 1N could be the result of chance range from 10% to 15%. In contrast, the probability that t-values as large as those corresponding values listed for LOS 1S could be caused by chance range from 45% to 70%.

All of the analyses reported in this section were prepared using the meteorological assessment software in a manner similar to that described in Section IX. Output from the system includes the mean emission rates and corresponding standard deviations of the emission rates for each line-of-sight (LOS 1 = LOS 1N; LOS 2 = LOS 1S) and source group (lot). In the cross-comparison table, the t-values are listed along with the number of degrees of freedom and the corresponding probability that the t-value could have resulted by chance (i.e., that the mean Q for each lot is the same).

C. Summary of Results of Application to All Datasets

Datasets included in the meteorological assessment software in the form of DDA's were listed in Tables 4-1 and 4-2. The historical datasets in Table 4-1 include Ocean Breeze (OB), Dry Gulch (DG), and Green Glow (GG) as well as the Prairie Grass dataset already addressed in Section A. The smoke datasets listed in Table 4-2 include a variety of smoke grenades, smoke projectiles, smoke pots, and smoke generators. Each of these datasets can be processed by means of the software package to remove the influence of meteorological factors (and downwind distance) from measured concentrations in order to produce estimates of the mean source strength of various groups or classes of sources, and to assess the significance of differences in these strengths.

Methods for doing these analyses have already been illustrated in Sections A and B. Overall results obtained for several of the other datasets are summarized here.

Historical Datasets

The Ocean Breeze, Dry Gulch, and Green Glow databases are used to test the ability of the scaling procedures to distinguish mean emission rates that are known to be significantly different. First, within each field experiment, the 10 highest observed Q values and the 10 lowest observed Q values are selected. Then, the observed C's during these periods are used to make predictions of Q using the OB/DG, Regression, and GPM scaling procedures. The results are given in Table 10-8, which includes the calculated student-t variable (from Equation 10-3). If $t \geq 2.23$ (for $N = 10$), then the difference $\bar{Q}_{max} - \bar{Q}_{min}$ is significant at the 95% confidence level.

The observed values of $\bar{Q}_{min}$ and $\bar{Q}_{max}$ differ by about 30% at Ocean Breeze and by about a factor of 2.2 at the other three experiments. This observed difference is definitely significant, since the calculated t's are in the range from 7.06 to 26.82. Note that an asterisk is given in the table next to t values that exceed 2.23, which is the 95% confidence level.

The t values in the table for the four models are averaged over the various monitoring arcs, since there was little variation with distances. It is seen that the scaling procedures do not do a very good job discerning the difference between $\bar{Q}_{min}$ and $\bar{Q}_{max}$ for these experiments when $N = 10$. None of the procedures can resolve the observed 30% differences at the Ocean Breeze site, probably because the difference is a factor of four smaller here than at the other sites. Only the OB/DG and VSDM procedures can detect a significant difference for the Dry Gulch Course B experiment, while only the GPM procedure can detect a difference for the Dry Gulch Course D experiment. The results are more encouraging for the Green Glow experiment, where the use of OB/DG, VSDM, and GPM indicate a significant difference between $\bar{Q}_{max}$ and $\bar{Q}_{min}$.

The four databases were also used to investigate the converse question--if two sets of 10 field experiments with nearly the same observed $\bar{Q}$ are

Table 10-8. Analysis of datasets consisting of maximum 10 observed Q's and minimum, 10 observed Q's for four data bases. Observations and predictions of the averaged $\bar{Q}_{max}$ and $\bar{Q}_{min}$ for the maximum 10 and minimum 10 datasets are compared. Units of all Q values are g/s. Observed values and predicted values from three scaling procedures are considered. For each procedure, the $\bar{Q}$ and σ_Q values from the several monitoring arcs are averaged, since the results do not vary with downwind distance. Student-t values exceeding 2.23 (the criterion for 95% confidence) are marked with an asterisk.

	Ocean Breeze	Dry Gulch B	Dry Gulch D	Green Glow
Observed				
$\bar{Q}_{min}$ (g/s)	1.30	0.69	0.70	0.87
$\bar{Q}_{max}$ (g/s)	1.68	1.62	1.63	1.88
t	7.06*	26.82*	18.50*	10.32*
OB/DG Formula				
$\bar{Q}_{min}$ (g/s)	1.92	0.78	0.60	0.73
$\bar{Q}_{max}$ (g/s)	2.33	2.34	0.97	1.47
t	0.68	2.72*	2.07	2.79*
Regression Formula				
$\bar{Q}_{min}$ (g/s)	1.90	0.94	1.27	1.33
$\bar{Q}_{max}$ (g/s)	1.99	1.54	1.75	1.76
t	0.16	1.52	1.31	1.58
GPM Formula				
$\bar{Q}_{min}$ (g/s)	0.97	0.57	0.25	0.44
$\bar{Q}_{max}$ (g/s)	1.38	1.09	0.70	1.19
t	1.38	1.41	2.44*	3.06*
VSDM Formula				
$\bar{Q}_{min}$ (g/s)	1 28	0.74	0.88	7.10
$\bar{Q}_{max}$ (g/s)	1.31	1.94	1.30	17.93
t	0.05	2.77*	1.01	2.98*

chosen, will application of any of the scaling procedures predict that $\bar{Q}_1 - \bar{Q}_2$ is significantly different at the 95% confidence level? This exercise was carried out, and the answer is "no," since in no case did the calculated t exceed 2.23. A few values of t in the range from 1.0 to 2.0 were calculated, which would correspond to significant differences at relatively low confidence levels (70 to 90%). Thus, it is unlikely that a significant difference in $\bar{Q}_1 - \bar{Q}_2$ will be predicted if, in fact, this difference does not occur.

Smoke Datasets

The meteorological assessment software has been applied to six of the smoke datasets listed in Table 4-2. For most datasets, we selected DDA's for two munitions, and calculated the mean emission rate, Q(CLID), from measurements of CLID obtained from transmissometer measurements. Q(CLID) is chosen rather than M(CLID) in order to characterize differences in the potential screening effectiveness of each munition. We then posed the question:

> Can the null hypothesis that there is no difference in the mean emission rate (between two groups of munitions) be rejected with 95% confidence?

Mean values of Q(CLID) were obtained for each LOS contained in each dataset, and the Student-t value for each pair of munitions compared was computed on the basis of a single LOS for each group. This constraint is imposed by the requirement that the data used in the procedure be independent.

The specific munitions compared, the corresponding mean values and standard deviation of Q(CLID), the Student-t value and the probability that the t-value could have been this large or larger just by chance, and the resulting conclusion regarding the null hypothesis are summarized in Table 10-9 for Q(CLID) obtained by means of the VSDM scaling procedure. Table 10-10 reports the results when the GPM scaling procedure is used. Results for just one LOS are presented in these tables, and we must point out that these data can be analyzed in several ways, while still satisfying the data independence requirement. Here, we have grouped the data in the DDA by

Table 10-9

Summary of Assessments Made of Differences in Mean Emission Rates of Several Smoke Munitions Made on the Basis of Q(CLID) Predictions from the VSDM Scaling Procedure

Database	Munition	$\overline{Q(CLID)}$ (g/s)	σ_Q (g/s)	N	Paired Comparison Pair	Student-t	Prob(%)	Reject Null ?
Foreign Smoke Pots (1 LOS)	Britain (BR)	11.4	3.1	18	BR:CA	-2.01	5.3	Yes
					BR:JA	-0.65	52	No
	Canada (CA)	13.4	2.7	17	BR:US	-1.02	32	No
	Japan (JA)	12.3	3.3	7	CA:JA	0.80	43	No
	U.S. (US)	12.5	3.3	17	CA:US	0.86	40	No
					JA:US	-0.11	92	No
Smoke Generators (Fog-oil) (LOS 2)	XM49 (X)	64.5	28.5	12	X:M	1.46	16	No
	M3A3 (M)	43.5	24.2	6				
Dev. Test I 81 mm Projectiles (LOS 2)	XM819 (X)	35.2	27.3	11	X:M	3.02	0.7	Yes
	M375A2 (M)	8.9	4.2	11				
L8A Series Smoke Grenades (LOS 3)	L8A1 (1)	87.9	14.9	6	1:1R	0.26	80	No
	L8A1R (1R)	85.5	15.9	6	1:3	-0.72	49	No
	L8A3 (3)	100.0	35.7	6	1R:3	-0.85	41	No

Table 10-9 (Concluded)

Summary of Assessments Made of Differences in Mean Emission Rates of Several Smoke Munitions Made on the Basis of Q(CLID) Predictions from the VSDM Scaling Procedure

Database	Munition	$\overline{Q(CLID)}$ (g/s)	σ_Q (g/s)	N	Paired Comparison			
					Pair	Student-t	Prob(%)	Reject Null ?
Dev. Test I 155 mm Projectiles (LOS 1)	M116 (M)	36.2	57.3	15	M:MA1	-0.99	33	No
Dev. Test II 155 mm Projectiles (LOS 2)	M116 A1 (MA1)	56.6	31.7	10				
Dev. Test I 155 mm Projectiles (LOS 1)	XM825 (I)	40.7	22.9	14	I:II	1.54	14	No
Dev. Test II 155 mm Projectiles (LOS 3)	XM825 (II)	28.7	17.3	15				

Table 10-10

Summary of Assessments Made of Differences in Mean Emission Rates of Several Smoke Munitions Made on the Basis of Q(CLID) Predictions from the GPM Scaling Procedure

Database	Munition	$\overline{Q(CLID)}$ (g/s)	σ_Q (g/s)	N	Paired Comparison Pair	Student-t	Prob(%)	Reject Null ?
Foreign Smoke Pots	Britain (BR)	7.1	2.3	18	BR:CA	-2.43	2.1	Yes
					BR:JA	-2.02	5.5	Yes
(1 LOS)	Canada (CA)	9.0	2.2	17	BR:US	-1.37	18	No
	Japan (JA)	9.4	2.7	7	CA:JA	-0.34	74	No
	U.S. (US)	8.4	2.9	17	CA:US	0.71	48	No
					JA:US	0.77	45	No
Smoke Generators (Fog-oil) (LOS 2)	XM49 (X)	25.8	11.0	12	X:M	1.37	19	No
	M3A3 (M)	18.0	10.2	6				
Dev. Test I 81 mm Projectiles (LOS 2)	XM819 (X)	14.6	11.3	11	X:M	2.86	1.0	Yes
	M375A2 (M)	4.3	1.9	11				
L8A Series Smoke Grenades (LOS 3)	L8A1 (1)	95.3	21.0	6	1:1R	-0.12	90	No
	L8A1R (1R)	98.4	51.5	6	1:3	2.02	7.1	No
	L8A3 (3)	74.8	8.7	6	1R:3	1.01	34	No

Table 10-10 (Concluded)

Summary of Assessments Made of Differences in Mean Emission Rates of Several Smoke Munitions Made on the Basis of Q(CLID) Predictions from the GPM Scaling Procedure

Database	Munition	$\overline{Q(CLID)}$ (g/s)	σ_Q (g/s)	N	Paired Comparison Pair	Student-t	Prob(%)	Reject Null ?
Dev. Test I 155 mm Projectiles (LOS 1)	M116 (M)	14.5	17.5	15	M:MA1	-1.59	12.5	No
Dev. Test II 155 mm Projectiles (LOS 2)	M116 A1 (MA1)	24.8	11.0	10				
Dev. Test I 155 mm Projectiles (LOS 1)	XM825 (I)	18.1	9.54	14	I:II	2.28	5.7	Yes
Dev. Test II 155 mm Projectiles (LOS 3)	XM825 (II)	10.9	6.56	15				

an LOS at a specific position, and reported results for that LOS which produced good estimates of Q(CLID) for the greatest number of trials in the dataset. Had we, for example, organized the DDA in such a way that the data for the LOS with the largest CLID for each trial were grouped together, our results might be altered for some of the comparisons.

Although the results for individual munitions are of interest, we are more concerned with illustrating the use of the assessment software when data from a number of trials for each munition are available. These trials need not be conducted during the same test-series, and the munitions need not be similar. However, it is apparent from all of the applications reviewed here that it is not often that the null hypothesis can be rejected. Field evaluations ought to be performed under very similar conditions, with as many trials as is feasible if small differences in the screening capacity of various sources of smoke must be resolved.

Furthermore, the use of more than one scaling procedure in these applications points up the potential sensitivity of the results obtained to the scaling procedure selected. Most of the conclusions reached are equivalent, whether VSDM or GPM is used to predict Q(CLID). However, we find that the emission rates produced by the British smoke pot and the Japanese smoke pot do not appear significantly different when VSDM is used (there is a 52% probability that the difference is caused by chance), but they do appear significantly different (there is only a 5.5% probability that the difference is caused by chance) when GPM is used.

D. Example Application of DDAMC - Monte Carlo Sensitivity Analysis

In the following example, the use of the DDAMC software package to estimate the sensitivity of an analysis procedure to input data errors using the Monte Carlo method is demonstrated with the BB2 trial (where a single L8A1 smoke grenade was fired) from the Comparison Test of L8A1 Screening Smoke Grenades (Rafferty and Dumbauld, 1983; Sutton, 1981) and the Gaussian Plume Model (GPM) dispersion formula. The following observed values are listed in the data archive for the BB2 trial: wind speed (u) = 3.1 m/s, wind direction (θ) = 335°, temperature difference between two levels (ΔT) was missing, standard deviation of the wind azimuth angle fluctuations (σ_θ) = 13.7°,

standard deviation of the wind elevation angle fluctuations (σ_ϕ) was missing, surface roughness (z_0) = 0.03 m, source duration (T_d) = 251 s, total mass emitted (M) = 0.897 kg, source emission rate (Q) = 3.57 g/s (based on M/T_d), initial source dimensions (σ_{x0}, σ_{y0}, and σ_{x0}) = 9.389, 13.758, and 0.12 m, respectively, and the source locations (x_0 and y_0) = -62.9 and 68.0 m, respectively (where x_0 is positive eastward, y_0 is positive northward, and the origin is located at the center of the measuring grid, see Figure 4-9). The following default uncertainty ranges for the eight primary input parameters (previously described in Section IX.C) are used.

u: the original value ± 0.5 m/s
θ: the original value ± 10°
σ_θ: the original value ± 10°
z_0: the original value ± 1/2 order of magnitude
SRSF: the original value ± 1/2 order of magnitude
SDSF: the original value ± 10%
SSSF: the original value ± 1/2 order of magnitude
SLSF: the original value ± 25 m

The parameters SRSF (source emission rate scaling factor), SDSF (source duration scaling factor), SSSF (source size scaling factor), and SLSF (source location scaling factor) serve as surrogates for source emission rate, source duration, initial source dimensions, and source locations, respectively. (See Section IX.C for more detailed descriptions). ΔT and σ_ϕ were missing from the above list because their observed values were not available in the data archive and were degraded to "secondary" input parameters. For a uniform distribution with the indicated default ranges of uncertainty, the ratios of standard deviation to mean for u, θ, σ_θ, z_0, SRSF, SDSF, and SSSF are 0.0931, 0.0172, 0.0577, 0.472, 0.472, 0.0577, 0.472, respectively. In order to derive these ratios, it is assumed that the standard deviation of a uniform distribution equals 0.29 times the total range of the distribution. The corresponding ratio for SLSF is not mentioned here since its value depends on the origin of the coordinate system.

The GPM dispersion formula that is being applied here does not make use of values of σ_θ and z_0 directly. However, the value of σ_θ influences the value of the Pasquill-Gifford stability class, and the value of z_0 influences whether the "urban" or "rural" set of dispersion coefficients is used in the calculation.

The DDAMC software package was first run with all eight primary input parameters perturbed simultaneously and independently. In order to isolate the influence of each parameter, DDAMC was run eight more times, each time varying only one of the primary input parameters. Figure 10-4 shows the probability density functions (pdf) of the predicted LOS-integrated concentrations (CLID, in $mg*s/m^2$) and the predicted emission rate (Q(CLID), in g/s) based on CLID for LOS 2 only. LOS 1 is not included because when we perturbed the source locations, there were some simulations when LOS 1 was too close to the source or was even partially upwind. The spacing between LOS 1 and LOS 2 employed during the BB2 trial was 120 m (see Figure 4-9). Table 10-11 summarizes the results for CLID. Table 10-12 summarizes the results for Q(CLID). The results of the dispersion formula using the original input data listed in the data archive, without any perturbation, are also included and are referred to as the "reference value."

Tables 10-11 and 10-12 show that there is no variation in the values of CLID and Q(CLID) when perturbing only the the values of σ_θ. This is because the range of perturbation for σ_θ is not large enough to cause a change in the stability class when the Irwin (1980) relations are used. Table 10-12 also shows that there is no variation in the values of Q(CLID) when only the values of SRSF are perturbed. This is because Q(CLID) is obtained using the ratio of the observed CLID to the predicted CLID based on *unit* emission rate. Since neither term depends on SRSF, there is no subsequent variation in the values of Q(CLID). In this case, it is more appropriate to study uncertainties in the observed concentration values.. From Figure 10-4 it is clear that even though all the primary input parameters were given a uniform distribution, the distributions of CLID and Q(CLID) are far from being uniform. Furthermore, the distribution of CLID is found to be very different from that of Q(CLID). This is due to the fact for the values of CLID, SRSF is one of the more important parameters, while for the values of Q(CLID), as just described, the influence of SRSF is removed completely.

Table 10-13 summarizes the ratios of the relative dispersion formula uncertainties, $\sigma_{CLID} / \overline{CLID}$ and $\sigma_{Q(CLID)} / \overline{Q(CLID)}$, to the relative data uncertainties, $\sigma_I / \bar{I}$, for this particular example of Monte Carlo sensitivity analysis, where σ = standard deviation, overbar = mean, and I = input parameter. Note that, as expected, the values of CLID are most sensitive to

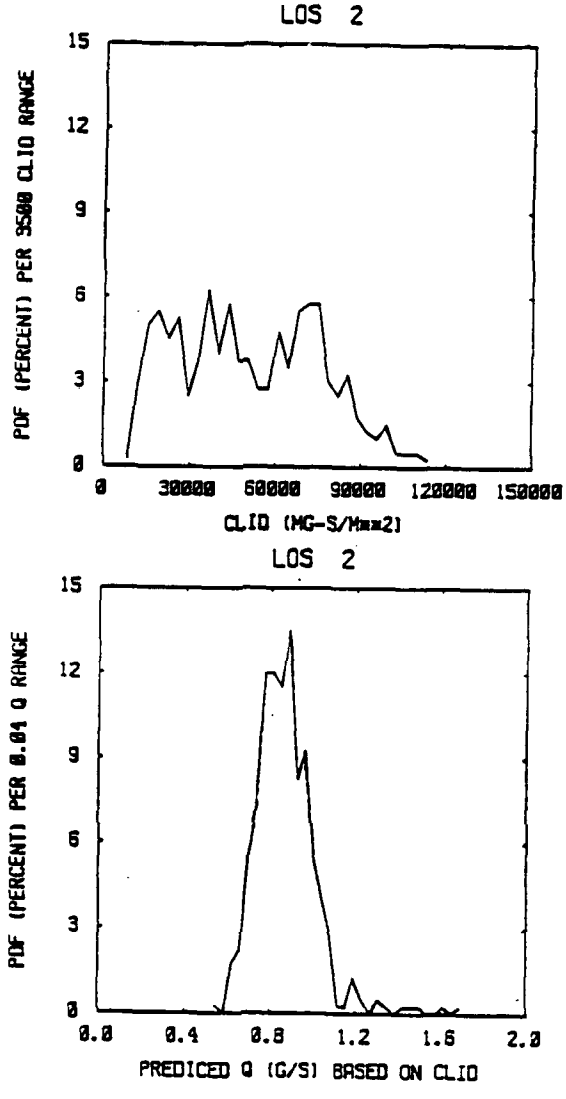

Figure 10-4. The probability density functions (pdf) of the predicted LOS-integrated dosages (CLID, $mg*s/m^2$) and the predicted emission rate (g/s) based on CLID for LOS 2 of the BB2 trial from the Comparison Test of L8A1 Screening Smoke Grenades (Rafferty and Dumbauld, 1983; Sutton, 1981) for the GPM dispersion formula in 400 Monte Carlo simulations.

Table 10-11

Uncertainties in the predicted CLID's, or LOS-integrated dosages ($mg*s/m^2$), for LOS 2 of the BB2 trial from the Comparison Test of L8A1 Screening Smoke Grenades (Rafferty and Dumbauld, 1983; Sutton, 1981) for the Gaussian Plume Model (GPM) dispersion formula using 400 Monte Carlo simulations. Run 1: when all eight primary input parameters (see text) were perturbed simultaneously, Run 2: when only u was perturbed, Run 3: when only θ was perturbed, Run 4: when only σ_θ was perturbed, Run 5: when only z_0 was perturbed, Run 6: when only SRSF was perturbed, Run 7: when only SDSF was perturbed, Run 8: when only SSSF was perturbed, and Run 9: when only SLSF was perturbed. The reference value is the dispersion formula result using the original input data listed in the data archive.

	Run 1	Run 2	Run 3	Run 4	Run 5	Run 6	Run 7	Run 8	Run 9
Reference Value	27860	27860	27860	27860	27860	27860	27860	27860	27860
Minimum	8371	24010	27850	27860	19270	9119	25090	27170	23560
Maximum	113300	33200	27960	27860	27860	87660	30640	28090	34490
Mean	49280	28200	27880	27860	27470	49320	28020	27630	27990
S.D.	24730	2623	31	0	1780	23330	1521	270	2433
S.D. / Mean	0.502	0.0930	0.00111	0	0.0648	0.473	0.0543	0.00978	0.0869

Table 10-12

Same as Table 10-11, Except for the Predicted Emission Rate (g/s) Based on the LOS-Integrated Dosages

	Run 1	Run 2	Run 3	Run 4	Run 5	Run 6	Run 7	Run 8	Run 9
Reference Value	0.834	0.834	0.834	0.834	0.834	0.834	0.834	0.834	0.834
Minimum	0.545	0.700	0.831	0.834	0.834	0.834	0.758	0.827	0.674
Maximum	1.687	0.968	0.834	0.834	1.205	0.834	0.926	0.855	0.986
Mean	0.856	0.831	0.833	0.834	0.851	0.834	0.832	0.841	0.836
S.D.	0.144	0.0766	0.00093	0	0.077	0	0.0457	0.00823	0.0715
S.D. / Mean	0.168	0.0922	0.00111	0	0.0905	0	0.0549	0.00979	0.0856

Table 10-13

Ratios of the relative dispersion formula uncertainties, $\sigma_{CLID} / \overline{CLID}$ and $\sigma_{Q(CLID)} / \overline{Q(CLID)}$, to the relative input data uncertainties, $\sigma_I / \overline{I}$, when the seven primary input parameters (see text) were perturbed one at a time in 400 Monte Carlo simulations for LOS 2 of the BB2 trial from the Comparison Test of L8A1 Screening Smoke Grenades (Rafferty and Dumbauld, 1983; Sutton, 1981) for the GPM dispersion formula. (σ = standard deviation, overbar = mean, CLID = LOS-integrated dosage, Q(CLID) = emission rate based on CLID, and I = input parameter)

	u	θ	σ_θ	z_0	SRSF	SDSF	SSSF
$\sigma_I / \overline{I}$	0.0931	0.0172	0.0577	0.472	0.472	0.0577	0.472
$\dfrac{\sigma_{CLID} / \overline{CLID}}{\sigma_I / \overline{I}}$	1.00	0.065[1]	0	0.14	1.00	0.94	0.021
$\dfrac{\sigma_{Q(CLID)} / \overline{Q(CLID)}}{\sigma_I / \overline{I}}$	0.99	0.065[1]	0	0.19	0	0.95	0.021

[1]The reason why these two numbers are the same is that for small perturbation, ε, the mathematical identity, $1 / (1 + \varepsilon) = 1 - \varepsilon$, is valid.

variations in wind speed, source emission rate and source duration. The values of Q(CLID) are most sensitive to variations in wind speed and source duration. Uncertainties in wind direction and initial source dimensions, on the other hand, are found to be less important.

Intentionally Blank

SECTION XI

RECOMMENDATIONS

In the course of this research, it has become clear that future analyses of the meteorological influences on smoke/obscurant effectiveness could be improved if the following recommendations are followed:

1) Because statistically-significant results can be achieved only if a sufficient number of independent data are available, it is best if there are at least ten independent experiments.

2) In order to minimize uncertainties, concentration-observing monitors should be located at downwind distances of about 50 to 100 m.

3) Because confidence in the results decreases as the source configuration becomes more complex, an attempt should be made to simplify the source scenarios as much as possible, and to pinpoint the locations of multiple sources.

4) The meteorological instruments should be located as close to the smoke plume as possible.

5) If it is expected that the difference in average source emissions in two sets of munitions is less than about 10-20%, then these statistical procedures will not be able to detect these differences due to the random noise in the data. For munitions with complicated release scenarios (e.g., multiple bursts of grenades at unknown scattered locations), these procedures cannot detect factor of two differences.

6) Uncertainties in source emissions of smoke/obscurant munitions have been found to be very poorly known. It is recommended that field and laboratory experiments be conducted to quantify the random variations in the "yield factor" and other parameterizations.

7) Monte Carlo procedures should be applied to a number of source scenarios and dispersion formulas in order to estimate the influence of data uncertainties on point measurements or cross-wind integrated measurements of concentrations.

8) Further research is needed on the best ways to apply statistics to datasets that are weakly dependent.

9) Preliminary formulas are available for the stochastic (random) fluctuations, but cannot be confidently applied to all types of scenarios. Future field experiments and data analyses should permit these formulas to be improved.

SECTION XII

REFERENCES

Barad, M.L., (Ed.), 1958: Project Prairie Grass, A Field Program in Diffusion, Vol. 1, Geophysical Research Papers No. 59, AFCRC-TR-58-235(I), Air Force Cambridge Research Center, Bedford, MA.

Barad, M.L., and J.J. Fuquay, (Eds.), 1962: "The Green Glow Diffusion Program," Geophysical Research Papers, 73, Vols. I and II. USAEC Report HW-71400, Air Force Cambridge Research Laboratories.

Benarie, M.M., 1987: "The Limits of Air Pollution Modeling." Atmos. Environ., 21, pp. 1-5.

Bjorklund, J.R. and R.K. Dumbauld, 1981: User's Instructions for the Volume Source Diffusion Models Program and the Volume/Line Source Graphs Computer Program, H.E. Cramer Company, Inc., Technical Report TR-81-321-08, prepared for US Army Dugway Proving Ground, Dugway, UT.

Bowers, J.F., 1990: Private communication.

Bowers, J.F. and R.B. Black, 1985: Test Report - Product improved M3A3 (M3A3R2) smoke generator (mobile applications), DPG Report No. DPG-FR-85-205. U.S. Army Dugway Proving Ground, Dugway, UT 84022.

Bowers, J.F., R.K. Dumbauld, T.M. Kincaid and R.S. Wentsel, 1985: "IR-2 Deposition and Dosage Measurements at Dugway Proving Ground and Comparison with Model Predictions," In Proceedings Smoke/Obscurants Symposium IX. Project Manager Smoke/Obscurants, Aberdeen Proving Ground, MD 21005.

Bowman, C.R., S.F. Saterlie and R.K. Dumbauld, 1982: Effective Source Strengths, Line-of-Sight Integrated Concentrations and Transmittances for Projectiles Tested During DT II of 155MM Smoke Projectile, XM825, H.E. Cramer Co. Report No. TR-82-321-01, U.S. Army Dugway Proving Ground, Dugway, UT 84022.

Box, G.E.P. and G.M. Jenkins, 1976: Time Series Analysis, Forecasting, and Control, Holden-Day, San Francisco, CA.

Briggs, G.A., 1973: Diffusion Estimation for Small Emissions, ATDL Contribution File No. 79, Atmospheric Turbulence and Diffusion Laboratory, Oak Ridge, TN.

Briggs, G.A. and K.R. MacDonald, 1978: Prairie Grass revisited: Optimum indicators of vertical spread, Proc. NATO/CCMS Meeting, Toronto, 31 pp.

Briggs, G.A., 1982: "Similarity forms for ground source surface layer diffusion," Bound-Lay. Meteorol., 23, 489-502.

Carter, F.L., R.K. Dumbauld and J.E. Rafferty, 1979: Methodology Investigation, Final Report, Validation of a Transport and Dispersion Model for Smoke. AD No. B044 868. U.S. Army Dugway Proving Ground, Dugway, UT 84022.

Chahuneau, F., S. des Clers, and J.A. Meyer, 1983: "Analysis of Prediction Uncertainty: Monte Carlo Simulation and Nonlinear Least-Squares Estimation of a Vertical Transport Submodel for Lake Nantua," Uncertainty and Forecasting of Water Quality. (M.B. Beck and G. van Straten, eds.), Springer-Verlag, Berlin, pp. 183-203.

Chatwin, P.C., 1982: "The Use of Statistics in Describing and Predicting the Effects of Dispersing Gas Clouds," Dense Gas Dispersion, (Ed. by Britter and Griffiths), Elsevier, New York, NY, pp. 213-230.

Chatwin, P.C. and P.J. Sullivan, 1989: "The Intermittency Factor of Scalars in Turbulence," Phys. Fluids A , 1, pp. 761-763.

Chintawongvanich, P., R. Olsen and C.A. Biltoft, 1989: "Intercomparison of Wind Measurements from Two Acoustic Doppler Sodars, a Laser Doppler Lidar, and in situ Sensors," J. Atm. and Ocean Technol., 6, pp. 785-797.

Cramer, H.E., 1957: A Practical Method for Estimating the Dispersal of Atmospheric Contaminants, Proceedings of the First National Conference on Applied Meteorology, American Meteorological Society, C-33 to C-55.

Cramer, H.E., Co., 1983: Review of Meteorological Safety Methodologies for Testing of Toxic Chemical Agents at Dugway Proving Ground. Prepared for Battelle, RTP Office by H.E. Cramer Co., Salt Lake City.

Csanady, G.T., 1973: Turbulent Diffusion in the Environment, D. Reidel Publ. Co., Dordrecht, Holland, pp. 222-248.

Davis, R.E. and W.M. Farmer, 1986: Effects of background light on transmissometry measurements: The XM819 development trials, Aberdeen Proving Ground, MD 21005-5001.

DeVaull, G.E., W.D. Dunn, J.C. Liljegren and A.J. Policastro, 1989: Analysis methods and results of hexachloroethane smoke dispersion experiments conducted as part of Atterbury-87 field studies. Prepared for U.S. Army Biomedical Res. and Dev. Lab., Fort Detrick, Frederick, MD 21701.

Deardorff, J.W. and G.E. Willis, 1984: "Ground-level concentration fluctuations from a buoyant and non-buoyant source within a laboratory convectively mixed layer," Atmos. Environ., 18, 1297-1310.

DPG, 1978: Basic smoke characterization test, Final Report, TECOM Project No. 7-CO-RD7-DPI-001, U.S. Army Dugway Proving Ground, Dugway, UT.

Draxler, R.R., 1984: Diffusion and transport experiments. Chapter 9 in Atmospheric Science and Power Production, Chapter 9 (edited by D. Randerson), pp. 367-422, DOE/TIC-27601, USDOE.

Dumbauld, R.K. and F.L. Carter, 1986: "A Review of Smoke/Obscurant Model Verification Studies for Dugway Proving Ground."

EPA, 1987: Guideline on air quality models (revised) with Supplement A. EPA-450/2-78-027R, Environmental Protection Agency, Research Triangle Park, NC.

Fedra, K., 1983: "A Monte Carlo Approach to Estimation and Prediction," Uncertainty and Forecasting of Water Quality. (M.B. Beck and G. van Straten, eds.), Springer-Verlag, Berlin, pp. 259-291.

Freeman, D.L., R.T. Egami, N.F. Robinson and J.G. Watson, 1986: "A Method for Propagating Measurement Uncertainties Through Dispersion Models," J.Air Poll. Control Assoc., 36, pp. 246-253.

Gardner, R.H., 1988: "A Unified Approach to Sensitivity and Uncertainty Analysis," Applied Simulation and Modeling, ISBN 0-88986-061-0, Acta Press, pp. 155-157.

Gifford, F.A., 1959: "Statistical properties of a plume dispersion model," Advances Geophys., 6, 117-138.

Gifford, F.A., 1982: "Horizontal diffusion in the atmosphere: A Lagrangian-dynamical theory," Atmos. Environ., 16, 505-512.

Gifford, F.A., 1989: "The Shape of Large Tropospheric Clouds, or "Very Like a Whale," Bull. Am. Meteorol. Soc., 70, pp. 468-475.

Golder, D., 1972: Relations among stability parameters in the surface layer. Boundary Layer Meteorol., 3, 47-58.

Goodman, L.A., 1960: "On the exact variance of products," J. of the American Statistical Assoc., 55, 708-713.

Hanna, S.R., 1984a: "Concentration fluctuations in a smoke plume," Atmos. Environ., 18, 1091-1106.

Hanna, S.R., 1984b: "The exponential probability density function and concentration fluctuations in smoke plumes," Bound. Lay. Meteorol., 29, 361-375.

Hanna, S.R., 1986: "A review of air quality model evaluation procedures," WMO Int. Conf. on Air Poll. Modeling and Its Applic., Leningrad, USSR.

Hanna, S.R., 1988: Air quality model evaluation and uncertainty. J. Air Poll. Control Assoc., 38, pp. 406-412.

Hanna, S.R., G.A. Briggs and R.P. Hosker, Jr., 1982: Handbook on Atmospheric Diffusion. Technical Information Center, U.S. Department of Energy, 102 pp.

Hanna, S.R. and J.C. Chang, 1990: Modification of the hybrid plume dispersion model (HPDM) for urban conditions and its evaluation using the Indianapolis data set. Prepared for EPRI, Palo Alto, CA 94303.

Hanna, S.R., J.C. Chang and D.G. Strimaitis, 1990: Uncertainties in source emissions estimates using dispersion models. Atmos. Environ., 24A, 2971-2980.

Hanna, S.R., L.L. Schulman, R.J. Paine, J.E. Pleim and B. Baer, 1985: Development and Evaluation of the Offshore and Coastal Diffusion Model. J. Air Poll. Control Assoc., 35, 1039-1047.

Hanna, S.R., D.G. Strimaitis and J.C. Chang, 1991: Hazard response modeling uncertainty (A Quantitative Method), 3 volumes, Prepared for AFESC, Tyndall AFB, FL 32403.

Hanna, S.R., J.C. Weil and R.J. Paine, 1986: Plume Model Development and Evaluation: Hybrid Approach, Final Report to EPRI, 3412 Hillview Ave., Palo Alto, CA 94303.

Hanna, S.R., J.C. Weil and R.J. Paine, 1987: Testing of a New Plume Dispersion Model with the Kincaid and Bull Run Data. Paper 87-73.4, Air Poll. Cont. Assoc. Ann. Meeting.

Hansen, F.V., 1979: Engineering Estimates for the Calculation of Atmospheric Dispersion Coefficients, Internal Report, US Army Atmospheric Sciences Laboratory, White Sands Missile Range, NM.

Haugen, D.A. and J.J. Fuquay (Eds.), 1963: The Ocean Breeze and Dry Gulch Diffusion Programs, Vol. I, USAEC Report HW-78435 [Report AFCRL-63-791(I)], Air Force Cambridge Research Laboratories and Hanford Atomic Products Operation.

Hicks, B.B., 1985: "Behavior of turbulence statistics in the convective boundary layer," J. Clim. and Appl. Meteorol., 24, 607-614.

Holtslag, A.A.M. and F.T.M. Nieuwstadt, 1986: "Scaling the Atmospheric Boundary Layer," Bound. Lay. Meteorol., 36, 201-209.

Horst, T.W., 1979: "Lagrangian similarity modeling of vertical diffusion from a ground-level source," J. Appl. Met., 18, 733-740.

Irwin, J.S., 1980: Dispersion estimate suggestion #8: Estimation of Pasquill stability categories. Environmental Protection Agency, Research Triangle Park, NC. (Docket Reference No. II-B-10).

Irwin, J.S., S.T. Rao, W.B. Petersen and D.B. Turner, 1987: "Relating error bounds for maximum concentration estimates to diffusion meteorology uncertainty," Atmos. Environ., 21, 1927-1937.

Jones, C.D., 1983: "On the structure of instantaneous plumes in the atmosphere," J. Haz. Mat., 7, pp. 87-112.

Kaimal, J.C., J.C. Wyngaard, D.A. Haugen, O.R. Cote, Y. Izumi, S.J. Caughey and C.J. Readings, 1976: "Turbulence Structure in the Convective Boundary Layer," J. Atmos. Sci., 33, 2152-2169

Kaimal, J.C., J.E. Gaynor, P.L. Finkelstein, M.E. Groves and T.J. Lockhart, 1984: A Field Comparison of In Site Meteorological Sensors, Boulder Atmospheric Observatory Report No. 6, NOAA/ERL, Boulder, CO, 80303.
Karmeshu and Lara-Rosano, F., 1987: "Modeling data uncertainty in growth forecasts," Appl. Math. Modeling, 11, pp. 62-70.

Keesman, K. and G. van Straten, 1989: "Identification and prediction propagation of uncertainty in models with bounded noise," Int. J. Control, 49, pp. 2259-2269.

Kunkel, B.A., 1988: User's Guide for the Air Force Toxic Chemical Dispersion Model (AFTOX), Report no. AFGL-TR-88-0009, Air Force Geophysics Laboratory, Hanscom AFB, MA.

Lee, J.T. and J.L. Stone, 1983: "The use of Eulerian initial conditions in a Lagrangian model of turbulent diffusion," Atmos. Environ., 17, 2477-2481.

Lewellen, W.S. and R.I. Sykes, 1989: "Meteorological data needs for modeling air quality uncertainties," J. Atmos. and Oceanic Tech., 6, 759-768.

Lewellen, W.S., R.I. Sykes and S.F. Parker, 1984: An evaluation technique which uses the prediction of both concentration mean and variance, Proceedings of the DOE/AMS Model Evaluation Workshop. A.H. Weber and A.J. Garrett, eds.), DP-1701-1, Sec. 2, Savannah River Lab., Aiken, SC 29808.

Liljegren, J.C., W.E. Dunn, G.E. DeVaull and A.J. Policastro, 1988: Field Study of Fog-Oil Smokes, Supported by U.S. Army Medical Research and Development Command, Fort Detrick, MD.

Lockhart, T.J. and J.S. Irwin, 1980: Methods for calculating the Representativeness of Data: Proceedings DOE Symposium on Intermediate Range Atmospheric Transport Processes and Technology Assessment, CONF801064, NTIS, 169-176.

Lovejoy, S. and D. Schertzer, 1985: "Generalized scale invariance in the atmosphere and fractal models of rain," Water Resources Research, 21, pp. 1233-1250.

Lovejoy, S. and D. Schertzer, 1986: "Scale invariance, symmetries fractals, and stochastic simulations of atmospheric phenomena," Bull. Am. Meteorol. Soc., 67, pp. 21-32.

Ludwig, F.L., 1977: A Theoretical Dispersal Model for Aerosols, Stanford Research Institute International, Report TR-T-CR-78-3, Menlo Park, CA 94025.

Luna, R.E. and H.W. Church, 1972: "A Comparison of Turbulence Intensity and Stability Ratio Measurements to Pasquill Stability Classes," Journal of Applied Meteorology, 11, pp 663-669.

McLaughlin, D.B., 1983: Statistical analysis of uncertainty propagation and model accuracy, Uncertainty and Forecasting of Water Quality. (M.B. Beck and G. van Straten, eds.), Springer-Verlag, Berlin, 305-319.

McLaughlin, D. and E.F. Wood, 1988: "A distributed parameter approach for evaluating the accuracy of groundwater model predictions," Water Resources Research, 24, pp. 1037-1060.

Meroney, R.N. and A. Lohmeyer, 1984: "Prediction of Propane Cloud Dispersion by a Wind-Tunnel Data Calibrated Box Model," J. Haz. Mat., 8, pp. 205-221.

Milly, George H., 1958: Atmospheric Diffusion and Generalized Munitions Expenditures, Operations Research Group Study No. 17, US Army Chemical Corps., Operations Research Group, Army Chemical Center, MD.

Monin, A.S. and A.M. Obukhov, 1953: "Dimensionless characteristics of turbulence in the layer of atmosphere near the ground," Dokl. Akad. Nauk. SSSR, 93, 256-267.

Mylne, K.R. and P.J. Mason, 1991: "Concentration fluctuation measurements in a dispersing plume at a range of up to 1000 m," Q.J. Royal Meteorol. Soc., 115.

Nieuwstadt, F.T.M., 1980: "Application of mixed-layer similarity to the observed dispersion from a ground-level source," J. Appl. Meteorol., 19, 157-162.

Nou, J.V., 1963: The ocean breeze and dry gulch diffusion programs, AFCRL, Hanscom AFB, MA.

Ohmstede, W.D., 1984: DOD Applied Diffusion Models Proceedings, Short Course on Atmospheric Transport and Diffusion, Published by IFAORS, P.O. Box P, Hampton, VA 23666.

O'Neill, R.V. and R.H. Gardner, 1979: "Sources of uncertainty in ecological models," Methodology in Systems Modeling and Simulation. (B.P. Zeigler, M.S. Elzas, G.J. Klir and T.I. Oren, eds.), North Holland Publishing Co., Amsterdam, pp. 447-463.

O'Neill, R.V., R.H. Gardner and J.H. Carney, 1982: "Parameter constraints in a stream ecosystem model: incorporation of a priori information in Monte Carlo error analysis," Ecological Modeling, pp. 51-65.

Panofsky, H.A. and G.W. Brier, 1968: Some Applications of Statistics to Meteorology. The Penn State Univ. Press, University Park, PA, 22479.

Panofsky, H.A., H. Tennekes, D.H. Lenschow and J.C. Wyngaard, 1977: "The characteristics of turbulent velocity components in the surface layer under convective conditions," Boundary Layer Meteorol., 11, 355-361.

Panofsky, H.A. and J.A. Dutton, 1984: Atmospheric Turbulence, Models and Methods for Engineering Applications, John Wiley & Sons, 397 pp.

Pasquill, F., 1961: "The estimation of dispersion of windborne material," Met. Mag., 90, 33-49.

Pennsyle, R.O., 1979: Methodology for Estimating Smoke/Obscurants Munition Expenditure Requirements, ARCSL-TR-79022, Chemical Systems Laboratory, Aberdeen Proving Ground, MD.

Peterson, H.G., B.K. Lamb and D.E. Stock, 1988: "Plume concentration and velocity fluctuations during convective and stable conditions," Eighth Symp. on Turb. and Diff., AMS, 341-344.

Policastro, A.J. and W.E. Dunn, 1984: Survey and Evaluation of Field Data Suitable for Smoke Hazard Model Evaluation. US Army Medical Bioengineering Research and Development Laboratory, Fort Detrick, Frederick, MD 21701.

Rafferty, J.E., and R.K. Dumbauld, 1983: Analysis of Transmissometer Data for Smoke Grenades Tested During the Comparison Test of Grenade, Smoke: Screening, RP, LA81. Dugway Proving Ground Technical Report TR-83-342-01.

Saterlie, S.F., C.R. Bowman, J.E. Rafferty and R.K. Dumbauld, 1981a: Effective Source Strengths for Projectiles Tested During Development Test I, 81MM Smoke Cartridges. H.E. Cramer Co. Report No. TR-81-321-04, U.S. Army Dugway Proving Ground, Dugway, UT 84022.

Saterlie, S.F., C.R. Bowman, R.K. Dumbauld and J.E. Rafferty, 1981b: Effective Source Strengths and Obscuration Calculations for Smoke Generators Tested During Development Test I (ADVT-G) of the Man-Portable Smoke Generator (MPSG), XM49. H.E. Cramer Co. Report No. TR-81-321-10, U.S. Army Dugway Proving Ground, UT 84022.

Saterlie, S.F. and R.K. Dumbauld, 1982a: Analysis of Transmissometer Data for Smoke Grenades Tested During the Evaluation of Reworked L8A1 and Product Improved L8A3 Screening Smoke Grenade Trials. H.E. Cramer Co. Report No. TR-82-321-04, U.S. Army Dugway Proving Ground, UT 84022.

Saterlie, S.F. and R.K. Dumbauld, 1982b: Analysis of Transmissometer Data for Smokepots Tested During Phase II, International Material Evaluation of Foreign Smoke Pots/Generators. H.E. Cramer Co. Technical Report Submitted to U.S. Army Dugway Proving Ground, Dugway, UT 84022.

Sawford, B.L., C.C. Frost and T.C. Allan, 1985: "Atmospheric boundary-layer measurements of concentration statistics from isolated and multiple sources," Bound. Lay. Meteorol., 31, 249-268.

Schertzer, D. and S. Lovejoy, 1985: "Generalized scale invariance in turbulent phenomena," Physic. Chemical Hydrodynamics, 6, pp. 623-635.

Schertzer, D. and S. Lovejoy, 1990: "Nonlinear variability in geophysics: multifractal simulations and analysis," Fractals, (L. Pietronero, ed.), Plenum Press, pp. 1-29.

Smith, F.B., 1972: A Scheme for Estimating the vertical dispersion of a plume from a source near ground level. Proceedings of the Third Meeting of the Expert Panel on Air Pollution Modeling, NATO/CCMS Report No. 14.

Smolyody, L., 1983: Input data uncertainty and parameter sensitivity in a lake hydrodynamic model. Uncertainty and Forecasting of Water Quality. (M.B. Beck and G. van Straten, eds.), Springer-Verlag, Berlin, pp. 129-155.

Strimaitis, D.G., G.F. Hoffnagle and A. Bass, 1980: On-Site Meteorological Instrumentation Requirements to Characterize Diffusion from Point Sources - A Workshop, U.S. EPA, Research Triangle Park, NC 27711.

Sutton, G.L., 1981: Comparison test of grenade, smoke: screening, RP, L8A1, U.S. Army Dugway Proving Ground, Dugway, UT 84022.

Taylor, G.I., 1921: Diffusion by continuous movements, Proc. London Math. Soc., 20, 196-200.

van Ulden, A.P., 1978: "Simple estimates for vertical diffusion from sources near the ground," Atmospheric Environment, 12, 2125-2129.

Venkatram, A., 1981: "A semi-empirical method to compute concentrations associated with surface releases in the stable boundary layer," Atmos. Environ., 15,

Venkatram, A., 1984: "The uncertainty in estimating dispersion in the convective boundary layer," Atmos. Environ., 18, pp. 307-310.

Warwick, J.J. and W.G. Gale, 1988: "Estimating model reliability using data with uncertainty," Ecol. Model, 41, pp. 169-181.

Weil, J.C., R.I. Sykes, A. Venkatram and J.C. Wyngaard, 1988: The role of inherent uncertainty in evaluating dispersion models. Report of a Special Working Group of the AMS/EPA Steering Committee on Air Quality Modeling. 55 pp.

White, J., R. Ewald and C. Biltoft, 1986: Site Influences on the XM76 Grid. DPG Doc. No. DPG-FR-86-701, U.S. Army Dugway Proving Ground, Dugway, UT 84022.

Wilson, D.J. and B.W. Simms, 1985: Exposure time effects on concentration fluctuations in plumes. Cont. No. 830990, prepared for Alberta Environment, 9820-106 St., Edmonton, Alberta, Canada T5K 2J6.

Wyngaard, J.C., 1985: "Structure of the Planetary Boundary Layer and Implications for Its Modeling," J. Clim. and Appl. Meteorol., 24, 1111-1130.